

Carla Patrícia Rodrigues Paiva

# HUMAN SPERM MOTILITY: PROTEINS AND METABOLITES TOWARDS THE SAME JOURNEY'S END

Tese de doutoramento em Biologia Experimental e Biomedicina, Ramo de Biologia Molecular, Celular e do Desenvolvimento  
orientada pelo Professor Doutor João Ramalho-Santos e pela Doutora Maria Alexandra Barreto Amaral  
e apresentada ao Instituto de Investigação Interdisciplinar da Universidade de Coimbra (IIIUC)

Fevereiro de 2015



UNIVERSIDADE DE COIMBRA



INSTITUTO DE INVESTIGAÇÃO INTERDISCIPLINAR (III-UC)



## **HUMAN SPERM MOTILITY: PROTEINS AND METABOLITES**

### **TOWARDS THE SAME JOURNEY'S END**

Tese de Doutoramento em Biologia Experimental e Biomedicina,  
Ramo de Biologia Molecular, Celular e do Desenvolvimento

**Carla Patrícia Rodrigues Paiva**

**Fevereiro de 2015**

Tese de Doutoramento apresentada ao Instituto de Investigação Interdisciplinar da Universidade de Coimbra (III-UC), para cumprimento dos requisitos necessários à obtenção do grau de Doutor em Biologia Experimental e Biomedicina (Especialidade em Biologia Molecular, Celular e do Desenvolvimento), realizada sob a orientação científica do Professor Doutor João Ramalho-Santos (Departamento de Ciências da Vida, Faculdade de Ciências e Tecnologia da Universidade de Coimbra e Centro de Neurociências e Biologia Celular da Universidade de Coimbra) e da Doutora Maria Alexandra Barreto Amaral (Centro de Neurociências e Biologia Celular da Universidade de Coimbra). O trabalho foi efectuado ao abrigo de uma bolsa de doutoramento financiada pela Fundação para a Ciência e Tecnologia (FCT; SFRH/BD/51193/2010) e atribuída pelo programa doutoral em Biologia Experimental e Biomedicina (PDBEB) do Centro de Neurociências e Biologia Celular da Universidade de Coimbra.

PhD thesis presented to the Institute for Interdisciplinary Research of the University of Coimbra (III-UC) in partial fulfilment of the requirements for the degree of Doctor of Philosophy in Experimental Biology and Biomedicine (Speciality Molecular, Cellular and Developmental Biology), under supervision of Professor João Ramalho-Santos (Department of Life Sciences of the Faculty of Sciences and Technology of University of Coimbra and Center for Neurosciences and Cell Biology of University of Coimbra) and of Maria Alexandra Barreto Amaral (Center for Neurosciences and Cell Biology of University of Coimbra). This study was supported by a PhD Studentship from the Portuguese Foundation for Science and Technology (FCT; SFRH/BD/51193/2010), attributed by the PhD Programme in Experimental Biology and Biomedicine (PDBEB) from the Center for Neurosciences and Cell Biology of University of Coimbra.



*“Apenas sei que caminho como quem  
É olhado amado e conhecido  
E por isso em cada gesto ponho  
Solenidade e risco.”*

(Sophia de Mello Breyner Andresen)

**A Ti.**



*“You raise me up, so I can stand on mountains  
You raise me up, to walk on stormy seas  
I am strong, when I am on your shoulders  
You raise me up... To more than I can be.”*

Brendan Graham

**Ao João Pedro.**  
O meu porto seguro!





**Aos meus pais,**  
os meus Heróis!

**Ao meu irmão,**  
o meu eterno amigo  
e companheiro!

**À Cati,**  
a minha irmã!

**À Sofia Raposo,**  
**à Sofia Paiva**  
**e à Leonor Raposo,**  
os meus pequenos anjos!



## ACKNOWLEDGEMENTS

Porque estou convencida de que um dos maiores dons que recebemos é poder agradecer, ainda que muitas vezes as palavras fiquem aquém da enorme gratidão que sentimos, o meu muito obrigada a todos os que fazem parte da minha vida e do meu percurso!

Um especial obrigada...

Ao Programa Doutoral em Biologia Experimental e Biomedicina (PDBEB) pela enorme oportunidade, e aos meus colegas e amigos da 9ª edição pelos muitos momentos e experiências partilhadas.

À Fundação para a Ciência e Tecnologia (FCT) pelo financiamento sem o qual este trabalho não teria sido possível.

Ao meu mentor e orientador Professor Doutor João Ramalho Santos. Por me ter desafiado a seguir este caminho. Pelos desafios profissionais e pessoais que me fizeram crescer ao longo de todos estes anos. Obrigada pela voz mais crítica, pela frontalidade e franqueza, bem como pela paciência e compreensão.

À minha orientadora Doutora Alexandra Amaral. Pela confiança, conselhos e críticas construtivas que me ajudam a evoluir e a tentar fazer melhor. Pela enorme paciência e compreensão. Por acreditar. Obrigada!

Al Profesor Doctor Rafael Oliva por haberme recibido tan bien en su laboratorio que acabé quedándome todos estos años. Por apoyarme, ayudarme y por su entusiasmo con mis proyectos. Muchas gracias por tu dedicación y constante disponibilidad. Y sobretodo gracias por haberme permitido el privilegio de ser parte de este fantástico grupo que es el “Human Genetics Lab”.

Ao grupo de reprodução humana e células estaminais (CNC-UC). Obrigada a todos por todos estes anos de trabalho, colaboração e discussões científicas. Em especial o meu muito obrigada à Sandra, Ana Sofia, Marta, Renata, Paula e Maria Inês pelo apoio e motivação constantes ao longo desta caminhada, mas acima de tudo pela vossa amizade. Por apesar de fisicamente distantes estarem sempre presentes e disponíveis. Pelos tantos abraços, sorrisos e lágrimas partilhadas ao longo do caminho. Por contribuírem para que eu seja melhor, cada dia.

A todo el grupo del Human Genetics Lab: Moltíssimes gracies! Us estimo molt a tots i mai us oblidaré!!

À Xana por acreditar e me fazer acreditar. Pelos abraços e pelas cañas nos momentos certos. Pela amizade. Obrigada pelo enorme desafio e por teres feito parte dele. Pela companhia em horas intermináveis de trabalho (“we work all night to get lucky”), pelas partilhas, pelos “viernes de cañas” e pelas “magic nights” que tornaram este caminho mais sorridente. Obrigada!!

A ti Judit, creo que “obrigada” tampoco llega para agradecerte. Eres una de las personas que mejor conoce todo este trayecto. Gracias por ser parte de cada momento, de cada paso de este camino. Por tantas horas en el lab y discusiones científicas. Por tantos momentos que fueron “la caña”. Pero sobretodo gracias por la amistad y complicidad. Por tantos “5 minutos”, alegrías y locuras. We will always be young!

A ti Rubén, muchas gracias por ayudarme a simplificar, tantas veces. Por tu amistad, tu cariño y tantos viernes de cañas, que fueron haciendo este recorrido mucho mas sonriente y feliz.

Al Claudio, gracias por impulsar mi crecimiento, a nivel profesional y personal. Por los desafíos y conquistas. A la Montse, la super-mujer, gracias por tu paciencia, disponibilidad y por compartir tu experiencia científica (como se nota que eres madre-doctora-posdoc-project manager). My dear Orleigh, thank you, for your contagious joy, for your immense strength and huge heart. Thanks for your big smile, your hugs and complicity. And for reminding me that humility is the key for everything. Thank you for your friendship and comprehension. And for instinctively protect me (from our nocturne friend Luis)!

Al Antoni Riera, por tantos detalles y sonrisas. A Ferran por su enorme pasión por la ciencia y ganas de aprender e saber mas. Tienes un gran potencial pequé! Gracias a la Meri, Ingrid, Eva por su alegría en el laboratorio. Thanks also to the Reprotrain fellows Kishlay, Hitoshi and Afsaneh for being so good lab mates.

A la Unitat de Proteomica de la Universidate de Barcelona, al Doctor Josep Maria Estanyol y a la Doctora Maria Jose Fidalgo por su gran ayuda durante los experimentos de proteómica, por su simpatía y buen humor. En especial, gracias al Dr Josep Maria por enseñarme con enorme paciencia. Gracias por reconocer mi trabajo, porque tu sabes la dedicación y hasta cariño que hay detrás de cada celda de Excel, de cada tabla.

A la unitat de RMN de la Universitat de Barcelona, por el apoyo y simpatía durante los experimentos de RMN. Al Centro de Investigación Biomédica en Red de Diabetes y Enfermedades Metabólicas Asociadas (CIBERDEM), Institut d'Investigació Sanitària Pere Virgili (IISPV) y Universitat Rovira i Virgili, en especial, al Doctor Xavier Correig, Dr Miguel, Dr Nicolau por la colaboración en la identificación de los metabolitos en los espectros de RMN y al Doctor Oscar Yanes, por el apoyo y ayuda con los experimentos de GC-TOF/MS.

Aos os meus amigos o meu muito obrigada pela vossa presença mesmo quando ausentes! Pelos esforços constantes para criar a oportunidade de um café, um brinde, um jantar, um abraço ou dois dedos (ou linhas) de conversa, superando qualquer barreira geográficas! A todos aqueles cujos olhos brilham com a palavra "Colmeosa", por todos os brindes, abraços e sorrisos!

A todos aqueles que pela sua presença e/ou ausência, pelas suas histórias e percursos, me vão relembrando que a vida é demasiado efémera para não nos centrarmos no que verdadeiramente importa. E a todos os que ao longo desta caminhada testaram os meus limites, pondo à prova a minha resistência, o meu sincero obrigada por me fazerem superar, evoluir, crescer!

Não posso acabar esta secção sem agradecer às pessoas mais importantes para mim, a minha família. A todos vós o meu muito obrigado por serem sempre a minha base mais sólida e a minha força! Por me apoiarem em cada passo e por me fazerem sentir verdadeiramente amada. Sem vós este trabalho teria sido infinitamente mais difícil e a vida também. É um verdadeiro privilégio fazer parte desta família!!

Em especial, um grande obrigada ao João Pedro, por seres o meu porto de abrigo, sempre! Sem ti não teria metade da piada. Obrigada por todos os votos, principalmente os de confiança! Pelo compromisso, pela coragem, pelos sorrisos e pela partilha, pela dedicação, pelos abraços e pela cumplicidade, pelos silêncios, brindes e cocktails perfeitos no momento certo! Pelo teu amor, carinho, amizade e enorme paciência! Obrigada pela caminhada e por me recordares amiúde que "no hay camino, se hace el camino al andar... Golpe a golpe, verso a verso!" (Manuel Machado) e lado a lado! A dois é bem melhor. Obrigada!

Aos meus Pais, os meus Heróis! As palavras nunca chegarão para vos agradecer... Obrigada pela dedicação, apoio e amor incondicionais! Obrigada por serdes os melhores pais que alguém pode desejar. Os primeiros a acreditar e a apoiar cada um dos meus passos. A vós devo grande parte do que sou hoje. Obrigada! Tenho imenso orgulho em vós! Quando for grande quero ser como vós!

Ao meu irmão, o meu cúmplice, modelo e refúgio (e também o meu irmão preferido!). As palavras também não chegam para te agradecer. És uma verdadeira bênção na minha vida. Obrigada por seres tão genuinamente bom, e por me ajudares a ser melhor cada dia. Por seres o primeiro a apoiar cada passo meu e a amparar cada queda ao longo da vida. Obrigada pelo apoio incondicional, por seres a minha luzinha e um porto seguro, sempre! É um enorme orgulho e privilégio ser tua irmã!

À Cati. Obrigada por seres uma irmã! Pelo teu apoio, carinho e amizade ao longo de todos estes anos. Pela paciência, conselhos, abraços e tantos sorrisos. Pela tua força e determinação contagiantes. Obrigada pela tua inspiração, criatividade, amor e dedicação! É um privilégio ser tua irmã mais nova!

Às minhas sobrinhas, os meus pequenos anjos, Sofia R, Sofia P e Leonor R. Obrigada por me mostrarem uma nova forma de amor incondicional. Por me fazerem sentir todos os dias a beleza e o encanto da inocência! Por me inspirarem e me darem uma enorme força. Por serem a minha maior fonte de sorrisos genuínos e lágrimas de pura felicidade. Obrigada pela ternura de cada gesto, cada sorriso e cada mini-abraço!

I would like to finish acknowledging the financial support that made this work possible. Specially thanks to the Portuguese National Science Foundation (FCT) for my studentship (SFRH/BD/51193/2010) and for the bench fees provided to Dr Rafael Oliva's Group in the University of Barcelona (Human Genetics Lab Group; Hospital Clinic Foundation / IDIBAPS). Also the Spanish Ministry of Economy and Competitiveness (Ministerio de Economía y Competitividad FEDER BFU 2009-07118 and PI13/00699), Fundación Salud 2000 (SERONO 13-015), and European Union (EU-FP7-PEOPLE-2011-ITN289880) for the grants to Dr Rafael that support this work.





## ABSTRACT

Mammalian sperm motility is a prerequisite for *in vivo* fertilization and alterations in this parameter are commonly observed in infertile males. However, we still do not have a complete understanding of the molecular mechanisms controlling it. The first aim of this study was to identify proteins involved in human sperm motility deficiency, by using TMT protein labeling and LC-MS/MS to compare proteins of sperm samples differing in motility (asthenozoospermic *versus* normozoospermic). LC-MS/MS resulted in the identification of 1157 proteins, of which 80 proteins were found differentially abundant between the two groups of samples. The differential proteins were analyzed by GO, cellular pathways and clustering analyses and resulted in the identification of core deregulated proteins and pathways associated with sperm motility dysfunction. These included proteins associated with energetic metabolism, protein folding/degradation, vesicle trafficking and the cytoskeleton. Contrary to what is usually accepted, these outcomes support the hypothesis that several metabolic pathways (notably mitochondrial-related ones) contribute towards regulating sperm motility. Moreover, this work considerably contributes to the increase of the compiled list (185 proteins) of differentially expressed proteins in asthenozoospermic samples.

Additionally, the second objective of this study was to contribute to the first comprehensive metabolomic characterization of human sperm cell extracts through the application of two untargeted metabolomics platforms based on proton nuclear magnetic resonance ( $^1\text{H-NMR}$ ) spectroscopy and gas chromatography coupled to mass spectrometry (GC-MS). Using these two complementary strategies we were able to identify a total of 69 metabolites, of which 42 were identified using NMR, 27 using GC-MS and 4 by both techniques. The identity of some of these metabolites was further confirmed by two-dimensional  $^1\text{H-}^1\text{H}$  homonuclear correlation spectroscopy (COSY) and  $^1\text{H-}^{13}\text{C}$  heteronuclear single-quantum correlation (HSQC) spectroscopy. Most of the metabolites identified are reported here for the first time as present in mature human sperm. The relationship between the metabolites identified and the previously reported sperm proteome was also explored. Interestingly, overrepresented pathways included not only the metabolism of carbohydrates, but also of lipids and lipoproteins. Of note, a large number of the metabolites identified belonged to the “amino acids, peptides and analogues” super class. The identification of this initial set of metabolites represents an important first step to further study their function in male gamete physiology and to explore potential reasons for dysfunction in future studies. We also demonstrate that the application of NMR and MS provides complementary results,

thus constituting a promising strategy towards the completion of the human sperm cell metabolome.

Furthermore, we have performed the first combined analysis of the human sperm identified metabolites and human sperm compiled proteome, using bioinformatic tools. This resulted in interesting outcomes, with metabolism as a most significant pathway, but also reinforcing the importance of fatty acids oxidation and lipids metabolism, among others. Alltogether, our study show the importance of performing an integrated analysis (proteomics and metabolomics) to biologicaly better understand human sperm cells. We have also preformed the preliminary comparison between the metabolic fingerprints of extracts of human sperm samples with different motility. As very preliminary outcomes, we observed a general lower concentration of the identified metabolites in asthenozoospermic samples when compared to normozoospermic ones.

In conclusion, our work aimed to contribute to better understand human sperm motility (at protein and metabolite level) and also to iniciate the analysis of human sperm metabolome. These will hopefully contribute to increase our knowledge about the molecular basis of male gametes and also to better understand human sperm (dys)function and male (in)fertility.



## RESUMO

A mobilidade dos espermatozoides é um pré-requisito para a fertilização *in vivo* em mamíferos e alterações neste parâmetro são frequentemente observadas em machos inférteis. Em humanos esta patologia (percentagem de espermatozoides móveis reduzida) é definida como asthenozoospermia. Contudo, os mecanismos moleculares que controlam a mobilidade dos espermatozoides não estão completamente descodificados. Assim, o primeiro objectivo deste trabalho foi identificar proteínas envolvidas na mobilidade de espermatozoides humanos através de proteómica diferencial utilizando amostras normozoospermicas e astenozoospermicas. As proteínas das diferentes amostras foram marcadas com marcadores isobáricos (TMT) e posteriormente identificadas e quantificadas por cromatografia líquida e espectrometria de massa em tandem (LC-MS/MS). Esta estratégia resultou na identificação de 1157 proteínas, das quais 80 estavam presentes em quantidades significativamente diferentes em espermatozoides menos móveis. As proteínas diferenciais foram analisadas relativamente à sua ontologia génica (GO), função biológica e participação em vias celulares. Esta análise resultou na identificação de uma série de proteínas e vias desreguladas, associadas à disfunção da mobilidade espermática. Entre elas incluem-se proteínas associadas ao metabolismo energético, à conformação e degradação de proteínas, transporte de vesículas e citoesqueleto. Ao contrário do que é normalmente aceite, estes resultados vêm suportar a hipótese de que várias vias metabólicas (entre elas as mitocondriais) contribuem para a regulação da mobilidade dos espermatozoides. Este trabalho também contribuiu consideravelmente para o enriquecimento da lista de proteínas (somando um total de 185) que estão descritas como diferencialmente expressas em amostras astenozoospermicas.

O segundo objectivo do presente estudo foi contribuir para a primeira caracterização metabólica de extractos de espermatozoides humanos através da utilização de duas técnicas frequentemente utilizadas para identificação não direccionada de metabolitos: espectroscopia de ressonância magnética nuclear de protão ( $^1\text{H}$ -RMN) e cromatografia gasosa acoplada a espectrometria de massa (GC-MS). Usando estas duas estratégias complementares identificámos um total de 69 metabolitos endógenos, dos quais 42 por RMN, 27 por GC-MS e 4 identificados por ambas técnicas. A identificação de alguns destes metabolitos foi ainda confirmada através de espectroscopia de duas dimensões: correlação homonuclear  $^1\text{H}$ - $^1\text{H}$  (COSY) e correlação heteronuclear  $^1\text{H}$ - $^{13}\text{C}$  (HSQC). Curiosamente, grande parte dos metabolitos descritos pertence à superclasse de “aminoácidos, péptidos e análogos”. Uma vez mais, através de análise

bioinformática das vias biológicas em que os metabolitos descritos estão envolvidos, volta a destacar-se o metabolismo de lípidos e a beta-oxidação de ácidos gordos. A identificação deste primeiro conjunto de metabolitos constitui assim um primeiro passo para futuros estudos metabolómicos, no sentido do melhor conhecimento dos gametas masculinos a nível molecular e fisiológico, e também da caracterização de diversas patologias. Neste trabalho mostrou-se também a importância do uso de técnicas complementares que poderão constituir ferramentas valiosas na descrição e compreensão do metaboloma humano.

Foi ainda explorada a relação entre a lista de metabolitos descritos com as proteínas descritas na compilação do proteoma de espermatozoides humanos, usando ferramentas bioinformáticas. Esta análise revelou a importância de vias não só como metabolismo de hidratos de carbono, mas também o metabolismo de lípidos e lipoproteínas, entre outros, constituindo assim a primeira análise integrada de proteínas e metabolitos de espermatozoides humanos. Por último, neste trabalho efetuámos a primeira comparação preliminar entre a quantidade de metabolitos identificados em extractos de amostras com diferentes mobilidades. Os resultados sugerem a presença em menor quantidade de quase todos os metabolitos em extractos de espermatozoides menos móveis, abrindo assim caminho a novos trabalhos futuros para caracterização metabólica da mobilidade de espermatozoides humanos.

Em conclusão, o nosso trabalho teve como principal objectivo contribuir para o melhor entendimento da mobilidade de espermatozoides humanos (a nível proteico e metabólico) e simultaneamente dar o primeiro passo na análise do metaboloma de espermatozoides humanos, contribuindo desta forma para um aumento do conhecimento sobre a base molecular dos gametas masculinos e a (dis)função dos mesmos associada à (in) fertilidade.

## Table of Contents

<b>ACKNOWLEDGEMENTS</b> .....	<b>I</b>
<b>ABSTRACT</b> .....	<b>V</b>
<b>RESUMO</b> .....	<b>VII</b>
<b>LIST OF FIGURES</b> .....	<b>XI</b>
<b>LIST OF TABLES</b> .....	<b>XII</b>
<b>LIST OF ABBREVIATIONS</b> .....	<b>XIII</b>
<b>PUBLICATIONS ARISING FROM THIS WORK</b> .....	<b>XVI</b>
<b>CHAPTER I. INTRODUCTION</b> .....	<b>3</b>
<b>1.1. The mammalian sperm cell</b> .....	<b>3</b>
1.1.1 Spermatogenesis.....	3
1.1.2 Mammalian sperm: a highly specialized cell .....	4
1.1.2.1 The Sperm Head .....	5
1.1.2.2 The Sperm Flagellum .....	7
1.1.3 Specific mammalian sperm features: maturation, capacitation and acrosome reaction .....	11
1.1.4 Mammalian sperm motility .....	12
1.1.4.1 Molecular mechanisms behind motility: cAMP and Ca <sub>2</sub> <sup>+</sup> signalling .....	14
1.1.4.2 Motility fuel: the so-called energy debate .....	17
1.1.5 Male infertility .....	20
<b>1.2 Human sperm proteomics</b> .....	<b>21</b>
1.2.1 Comparative human sperm proteomics.....	25
1.2.1.1 Comparative human sperm proteomics focused on sperm motility .....	26
<b>1.3 Reproductive metabolomics</b> .....	<b>28</b>
<b>1.4 Objectives</b> .....	<b>29</b>
<b>CHAPTER II. MATERIALS AND METHODS</b> .....	<b>33</b>
<b>2.1 Chemicals</b> .....	<b>33</b>
<b>2.2 Biological Material</b> .....	<b>33</b>
<b>2.3 Differential Proteomics</b> .....	<b>33</b>
2.3.1 Preparation and selection of sperm samples .....	33
2.3.2 Protein solubilization .....	34
2.3.3 Protein labeling with isobaric tags (TMT 6-Plex) .....	34
2.3.4 Sodium dodecyl sulphate-polyacrylamide gel electrophoresis (SDS-PAGE).....	36
2.3.5 Liquid Chromatography and Tandem Mass Spectrometry (LC-MS/MS) .....	36
2.3.6 Protein identification and quantification.....	37
2.3.7 Differential protein annotation and bioinformatics analyses.....	38
2.3.8 Clustering analysis.....	38
2.3.9 Determination of protamine 1 (P1)/protamine 2 (P2) ratio.....	38
2.3.10 Western blotting.....	39

2.3.11 Statistical analyses.....	39
<b>2.4 Metabolomics.....</b>	<b>40</b>
2.4.1 Biological material .....	40
2.4.2 Sperm samples preparation and purification.....	40
2.4.3 Sperm sample selection and metabolite extraction for <sup>1</sup> H-NMR.....	41
2.4.4 NMR analyses .....	42
2.4.5 Metabolite extraction and derivatization for GC-TOF/MS.....	43
2.4.6 GC-TOF/MS analysis .....	43
2.4.7 Metabolites annotation and bioinformatics analysis.....	43
2.4.8 Statistical analysis.....	44
<b>CHAPTER III. RESULTS.....</b>	<b>47</b>
<b>3.1 Human Sperm Differential Proteomics .....</b>	<b>47</b>
3.1.1 Motility, vitality and P1/P2 ratio of the selected samples .....	47
3.1.2 Protein identification and quantification .....	47
3.1.3 Differentially abundant proteins in asthenozoospermic samples .....	48
3.1.4 UniProt classification of the differentially abundant proteins in asthenozoospermic samples.....	52
3.1.5 Gene ontology terms analysis and cellular pathways enrichment analyses.....	53
3.1.6 Western blot analysis: Tektin 1 and WDR 16 .....	54
3.1.7 Compiled list of differentially abundant proteins in asthenozoospermic samples....	55
<b>3.2 Human Sperm Metabolomics .....</b>	<b>55</b>
3.2.1 Metabolites identified by nuclear magnetic resonance (NMR) spectroscopy .....	56
3.2.2 Metabolites identified by mass spectroscopy (MS) .....	65
3.2.3 Overall metabolite Super Class and enriched gene ontology term pathways .....	68
<b>3.3 Combined analysis of the human sperm proteome and metabolites.....</b>	<b>69</b>
<b>3.4 Comparison of metabolic signatures of normozoospermic and asthenozoospermic pool of samples.....</b>	<b>71</b>
<b>CHAPTER IV. DISCUSSION.....</b>	<b>75</b>
<b>4.1 Human sperm differential proteomics – insights about human sperm motility .....</b>	<b>75</b>
<b>4.2 Human sperm endogenous metabolites – the first little step towards human sperm metabolome .....</b>	<b>81</b>
<b>4.3 Combined analysis of human sperm endogenous metabolites and the human sperm compiled proteome – the importance of the integration of metabolomics and proteomics analysis.....</b>	<b>83</b>
<b>4.4 The comparison between the metabolic signatures of extracts of normozoospermic and asthenozoospermic pool of samples – a preliminary look to possible important metabolites to human sperm motility .....</b>	<b>84</b>
<b>CHAPTER V. CONCLUSIONS .....</b>	<b>89</b>
<b>CHAPTER VI. BIBLIOGRAPHY .....</b>	<b>93</b>
<b>SUPPLEMENTARY TABLES.....</b>	<b>119</b>

## LIST OF FIGURES

<b>Figure 1.1</b> – Spermatogenesis.....	3
<b>Figure 1.2</b> – Mammalian sperm cell structure.....	5
<b>Figure 1.3</b> – Chromatin changes during spermiogenesis. ....	6
<b>Figure 1.4</b> – Schematic representation of the ultrastructure of the human sperm. ....	8
<b>Figure 1.5</b> – A possible model for the oscillatory mechanism of flagellar bending. ....	13
<b>Figure 1.6</b> – Schematic representation of the signalling pathways known or believed to be involved in the regulation of mammalian sperm motility. ....	17
<b>Figure 1.7</b> – Human sperm proteomics strategies.....	24
<b>Figure 2.1</b> – Overall strategy used for the identification of proteomic alterations in sperm with low motility. ....	35
<b>Figure 2.2</b> – Overall untargeted metabolomics strategy used for the identification of metabolites in human sperm. ....	41
<b>Figure 3.1</b> – Motility, vitality and Protamine 1 to Protamine 2 (P1/P2) ratio of the selected samples for differential proteomic analysis.....	47
<b>Figure 3.2</b> – Representative example of a MS/MS spectrum of one peptide derived from one of the detected differential proteins (tektin-5). ....	48
<b>Figure 3.3</b> – Heat maps of the levels of the differentially expressed proteins detected in each individual sample. ....	51
<b>Figure 3.4</b> – Classification of the differential proteins according to their subcellular localization using the information available at the UniProtKB/Swiss-Prot web site. ....	52
<b>Figure 3.5</b> – Classification of the differential proteins according to their main cellular function using the information available at the UniProtKB/Swiss-Prot web site.....	53
<b>Figure 3.6</b> – Immunoblotting detection of tektin 1 (Tekt 1 – 55 kDa) and WD repeat-containing protein 16 (WDR 16 – 46 kDa). ....	54
<b>Figure 3.7</b> – Classification of the compiled list of 185 differentially abundant proteins in asthenozoospermic samples according to their main cellular function using the information available at the UniProtKB/Swiss-Prot web site.....	55
<b>Figure 3.8</b> – Total number of metabolites identified using the two untargeted metabolomics strategies (NMR and GC-MS).....	56
<b>Figure 3.9</b> – Representative NMR spectra (600 MHz) of extracts from human sperm cells. .	57
<b>Figure 3.10</b> – Number of metabolites identified per class with the two complementary techniques.....	68
<b>Figure 3.11</b> – Representative <sup>1</sup> H-NMR spectra (600 MHz) of extracts from human sperm cells.....	71
<b>Figure 3.12</b> – Metabolites identified in variable concentration in the asthenozoospermic pool of samples compared to the normozoospermic pool of samples. ....	72

## LIST OF TABLES

<b>Table 1.1</b> – Reference values for the evaluation of human sperm quality (WHO, 2010). .....	21
<b>Table 3.1</b> – List of proteins detected at significantly different amounts in asthenozoospermic and normozoospermic samples.....	49
<b>Table 3.2</b> – Enriched Gene Ontology terms and cellular pathways altered in low motility sperm. ....	54
<b>Table 3.3</b> – Metabolites identified in human sperm extracts by NMR spectroscopy (1D and 2D). ....	58
<b>Table 3.4</b> – Metabolites identified from human sperm extracts by GC-TOF/MS.....	66
<b>Table 3.5</b> – Overrepresented pathways using the metabolites identified in human sperm extracts. ....	69
<b>Table 3.6</b> – Combined analysis of the human sperm proteome and the identified metabolites. ....	70
<b>Supplementary Table S1</b> – Complete list of identified proteins (1157) in Asthenozoospermic vs. Normozoospermic samples differential proteomics experiment. ....	119
<b>Supplementary Table S2</b> – Complete list of identified proteins (1157) in Asthenozoospermic (A) vs. Normozoospermic (N) samples differential proteomics experiment. ....	148
<b>Supplementary Table S3</b> – Quantification values (means $\pm$ standard deviation; Mean $\pm$ SD) of each differential protein detected in Asthenozoospermic (Asthen) vs Normozoospermic (Normo) samples experiment, and associated P value. ....	176
<b>Supplementary Table S4</b> – Compiled list of proteins (185) differentially expressed in asthenozoospermic samples compared to normozoospermic samples. ....	179

## LIST OF ABBREVIATIONS

A – Asthenozoospermic sample

AKAP – cAMP-dependent protein kinase (PKA) anchoring proteins

ATP – Adenosine triphosphate

BSA – Bovine serum albumin

Ca<sup>2+</sup> – Calcium

CaM – Calmodulin

CaMK – Calmodulin kinase

cAMP – Cyclic adenosine monophosphate

CAND1 – Cullin-associated neddylation/NEDD8 - dissociated protein 1

CCDC11 – Coiled-coil domain-containing protein 11

CE – Collision energy

CHAPS – 3-[(3-Cholamidopropyl) dimethylammonio]-1-propanesulfonate

COSY – Homonuclear correlation spectroscopy

COXVIb-2 – Cytochrome c oxidase 2, subunit VIb

CP – Central pair

CT – Internal control

D<sub>2</sub>O – Deuterium oxide

DA – Dynein arms

DAVID – Database for Annotation, Visualization and Integrated Discovery

DNA – Deoxyribonucleic acid

DTT – Dithiothreitol

EI – Electron impact

ENO4 – Enolase 4

ETC – Electron transfer chain

FDR – False discovery rate

FS – Fibrous sheath

GAPDH-S – Glyceraldehyde 3-phosphate dehydrogenase, sperm-specific isoform

GC – Gas Chromatography

GO – Gene ontology

GSK – Glycogen synthase kinase

GSK3A – Glycogen synthase kinase 3A

GSK3B – Glycogen synthase kinase 3B

GSTM5 – Glutathione-S transferase mu 5  
GTPase – Guanosine triphosphate (GTP) hydrolase  
HCD – Higher energy collisional dissociation  
HCO<sup>3-</sup> – Bicarbonate  
HK-S – Hexokinase type 1, spermatogenic cell-specific isoform  
HMDB – Human Metabolome Database  
HSPA2 – Heat shock-related 70 kDa protein 2  
HSPA4L – Heat shock-related 70 kDa protein 4L  
HSQC – Heteronuclear single-quantum correlation  
IEF – Isoelectric focusing  
IMAC – Immobilized metal affinity chromatography  
IMPALA – Integrated Molecular Pathway-Level Analysis  
IVF – *in vitro* fertilization  
KIF3A – Heterotrimeric kinesin II subunit  
KLC3 – Kinesin light chain 3  
KO – Knockout  
LC – Liquid chromatography  
    1D-LC – one-dimensional liquid chromatography  
    2D-LC –two-dimensional liquid chromatography  
MALDI – matrix-assisted laser desorption/ionization  
MBRole – Metabolites Biological Role  
MMP – Mitochondrial membrane potential  
MS – Mass spectroscopy  
    MS/MS – Tandem mass spectroscopy  
mtDNA – mitochondrial DNA  
N – Normozoospermic sample  
NaHCO<sub>3</sub> – Sodium bicarbonate  
NMR – Nuclear magnetic resonance  
    <sup>1</sup>H-NMR – Proton nuclear magnetic resonance  
NSF – Vesicle-fusing ATPase  
ODF – Outer dense fibers  
OMDA – Outer microtubule doublets of the axoneme  
OXPHOS – Oxidative phosphorylation  
P1 – Protamine 1



P2 – Protamine 2

PAGE – Polyacrylamide gel electrophoresis

    1D-PAGE – one-dimensional polyacrylamide gel electrophoresis

    2D-PAGE –two-dimensional polyacrylamide gel electrophoresis

PDHB – Pyruvate dehydrogenase E1 subunit

PKA – Protein kinase A

PM – Plasma membrane

PMSF – Phenylmethylsulfonyl fluoride

PPP – Pentose phosphate pathway

RD – Recycling delay

ROS – Reactive oxygen species

RS – Radial spokes

sACY – Soluble adenylyl cyclase, spermatogenic cell-specific isoform

SCF – Skp, Cullin, F-box containing complex

SCOT-t – Succinyl CoA transferase, testicular isoform

SDS – Sodium dodecyl sulfate

SMPDB – Small Molecule Pathway Database

SPTRX-1 – sperm tioredoxin type 1

SPTRX-2 – sperm tioredoxin type 2

TBST – Tris-buffered saline with Tween 20

TCA – Tricarboxylic acid

TCEP – Tris (2-carboxyethyl) phosphine

TEAB - Triethylammonium hydrogen carbonate buffer

TEKT1 – Tektin 1

TMT – Tandem mass tag

TOF – Time-of-flight

TPI1 – Triosephosphate isomerase 1

TR – Transverse ribs

TSP – 3-(Trimethylsilyl) propionic-2,2,3,3-d<sub>4</sub> acid sodium salt

WDR16 – WD repeat-containing protein 16

WHO – World Health Organization

## PUBLICATIONS ARISING FROM THIS WORK

Amaral A\*, **Paiva C\***, Attardo Parrinello C\*, Estanyol JM, Ballescà JL, Ramalho-Santos J, Oliva R. (2014) *Identification of Proteins Involved in Human Sperm Motility Using High-Throughput Differential Proteomics*. Journal of Proteome Research. 13(12):5670-84.

\*These authors contributed equally to this work

**Paiva C**, Amaral A, Rodriguez M, Canyellas N, Correig X, Ballescà JL, Ramalho-Santos J, Oliva R. (2015) *Identification of endogenous metabolites in human sperm cells using 1H-NMR and GC-MS*. Andrology. In press.

# **CHAPTER I. INTRODUCTION**



## CHAPTER I. INTRODUCTION

### 1.1. The mammalian sperm cell

#### 1.1.1 Spermatogenesis

The mammalian spermatozoon is the end product of a differentiation process called spermatogenesis which consists of successive mitotic (spermatogoniogenesis), meiotic and post-meiotic (spermiogenesis) phases within the seminiferous tubules of the testis (Fig. 1.1; (de Kretser *et al.*, 1998). This process is highly controlled by hormonal regulation via the hypothalamic-pituitary axis (Holdcraft and Braun, 2004) and locally by the Leydig cells, responsible for the production of testosterone and oestradiol-17 $\beta$  (through a process called steroidogenesis; (Holstein *et al.*, 2003)).

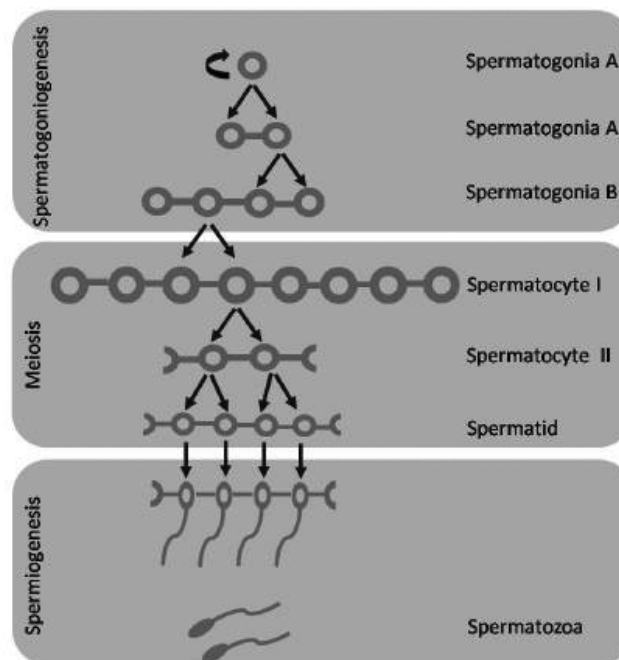


**Figure 1.1 – Spermatogenesis.**

Spermatogenesis is the differentiation process that culminates in the production of haploid sperm. It can be divided in three major phases. The spermatogoniogenesis is characterized by spermatogonial mitotic proliferation and formation of primary spermatocytes that then enter meiosis, a long phase characterized by changes in the chromatin. After two cell divisions, round spermatids are formed, which in turn undergo a final morphological differentiation step (spermiogenesis) that results in the production of spermatozoa. These, due to their unique shape and features, are able to leave the testis in the spermiation process.

(Reproduced from Amaral 2009)

During the first stage of spermatogenesis (the mitotic phase, or spermatogoniogenesis), germ line stem cells undergo a series of divisions to expand the spermatogonial population. Diploid

spermatogonial stem cells start to differentiate and undergo the second stage of the spermatogenesis, the meiotic phase, which begins with the last cell cycle S phase and culminates in two cell divisions without DNA replication, producing haploid spermatids. In the last phase, called spermiogenesis, spermatids undergo complex morphological modifications that give rise to sperm (de Kretser *et al.*, 1998). During this postmeiotic phase, the majority of the cellular components are reorganized and remodelled. Some of these remarkable alterations are: 1) the compaction of the nucleus; 2) the massive reduction of the cytoplasm, ending with the elimination of the majority of the typical somatic cell organelles, within residual bodies, which are phagocyted by Sertoli cells; 3) the Golgi apparatus undergoes conformational changes that result in the formation of a large secretory vesicle on the sperm head, the acrosome; 4) the formation of a highly specialized flagellum; 5) the rearrangement of the remaining mitochondria in elongated tubular structures, packed helically around the anterior portion of the flagellum (Otani *et al.*, 1988; Eddy, 2006; Ramalho-Santos *et al.*, 2009). All these events culminate in the formation of functional, hydrodynamic and highly differentiated cells, that are capable of crossing the female reproductive tract, reach and fertilize an oocyte, and undergo profound nuclear reorganization events essential for syngamy and early embryogenesis, and thus to begin the process that gives rise to the next generation.

### **1.1.2 Mammalian sperm: a highly specialized cell**

The mammalian sperm cell is composed of two main regions, the head and the flagellum, joined by the connecting piece (Fig. 1.2).

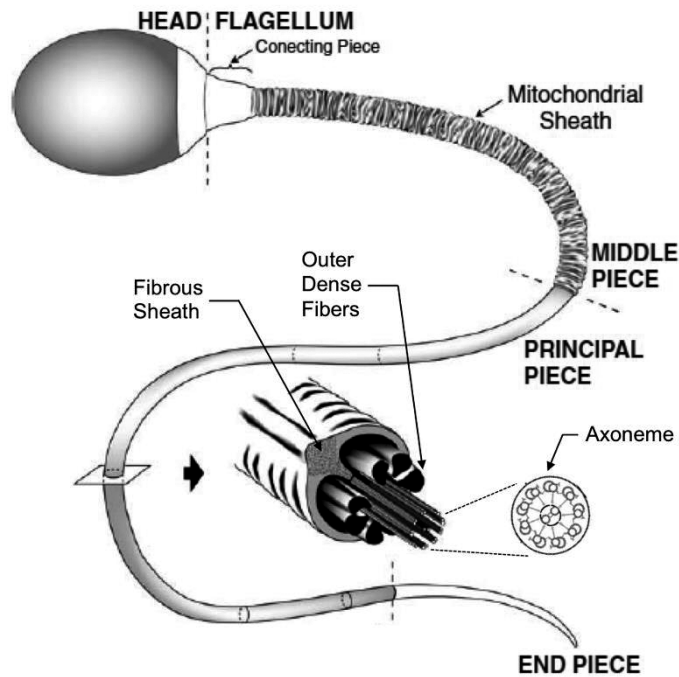


**Figure 1.2 – Mammalian sperm cell structure.**

The mammalian sperm cells are divided in two main parts, head and flagellum. The flagellum is divided in four regions: the connecting piece (which attaches the head to the flagellum); the middle piece (where mitochondria are localized); the principal piece; and the end piece. (Adapted from (Eddy, 2006)).

### **1.1.2.1 The Sperm Head**

The head of the sperm cell contains the acrosome, the haploid nucleus, cytoskeleton structures and a small amount of cytoplasm.

The acrosome is a unique sperm organelle that originates from the Golgi complex, and which covers the anterior part of the nucleus and contains multiple hydrolytic enzymes necessary for the sperm to penetrate through the oocyte vestments and achieve fertilization, in an event called acrosome reaction (Holstein *et al.*, 2003).

The main part of the sperm head is occupied by the nucleus where the sperm chromatin is highly condensed. This high level of compaction, a unique feature of the sperm nucleus, is due to the successive replacement of most histones (85-95%, depending on the species) firstly by nuclear transition proteins, and finally by protamines (the major nuclear proteins associated with

mammalian sperm DNA in its mature form), during the last stages of spermiogenesis (Fig. 1.3; (Oliva and Castillo, 2011; Castillo *et al.*, 2014b). These relatively small (27-65 amino acids) and highly basic proteins, extremely rich in arginine and cysteine, are grouped in two families in human sperm: Protamine type 1 (P1; protamine 1) and Protamine type 2 (P2; including protamines 2, 3 and 4) (Oliva and Dixon, 1991; Oliva and Castillo, 2011). Interestingly, both protamine families are essential for male fertility, and the alteration either of the amount of protamine content (Cho *et al.*, 2001, 2003) or of the relation between P1 and P2 (ratio P1/P2; (Oliva, 2006), can disrupt the stability of sperm DNA triggering DNA damage and male infertility. Some studies suggest that a higher prevalence of P2 may cause an increment of DNA damage susceptibility, since P2 contains fewer cysteine residues than P1 and consequently less disulphide cross-links (Corzett *et al.*, 2002). Moreover, altered levels of P2 expression were described in infertile patients (Carrell and Liu, 2001; Oliva, 2006; Torregrosa *et al.*, 2006). In conclusion the high level of DNA packaging contributes not only to the hydrodynamic shape of the sperm cell, but also to protect the DNA from oxidative stress and external aggressions, thus contributing to the integrity of the paternal genome. Furthermore, this highly compaction of the nucleus is one of the reasons whereby sperm cells are believed to be transcriptionally and translationally silent, at least for nuclear encoded genes (Miller *et al.*, 2010; Baker, 2011; Amaral and Ramalho-Santos, 2013).

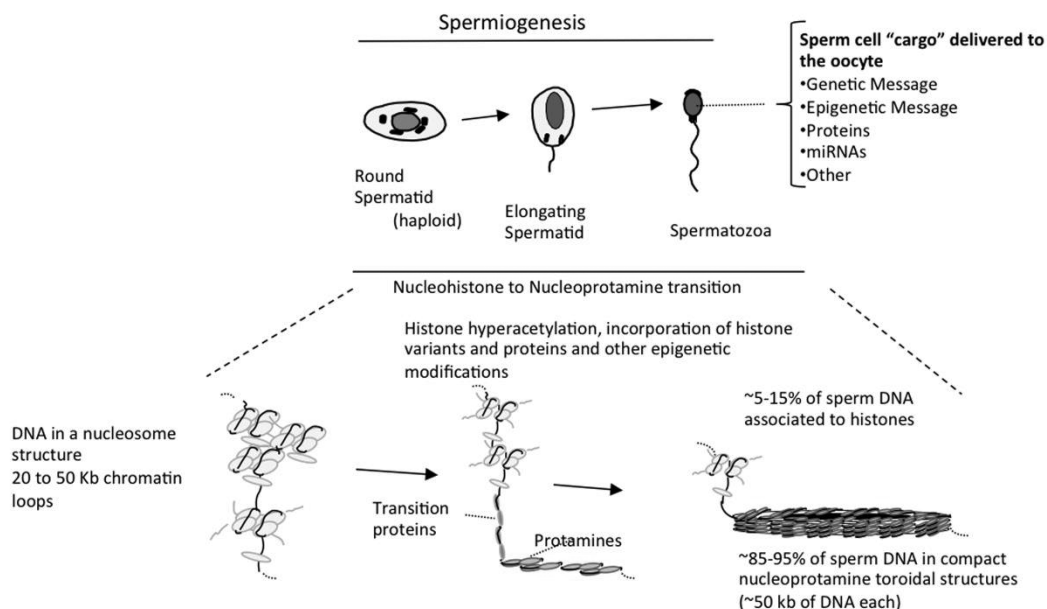


**Figure 1.3 – Chromatin changes during spermiogenesis.**

A chromatin model of the mammalian nucleohistone to nucleoprotamine transition is shown (Adapted from (Oliva and Castillo, 2011) ).

Concerning the 5-15% of DNA that remains packed by histones in the final conformation of the human sperm chromatin (Gatewood *et al.*, 1987; Bench *et al.*, 1996), and which remains less



tightly compacted than the remaining DNA, many studies have suggested that these clusters might be part of a sequence-specific component of the genome which is programmed for expression in early stages of embryonic development, by remaining less tightly compacted (Gatewood *et al.*, 1987; Hammoud *et al.*, 2009; Castillo *et al.*, 2014b). However, this subject is somehow controversial (Carone *et al.*, 2014; Samans *et al.*, 2014) and further studies will be needed to investigate the real role of these histones and DNA regions.

In addition to the inherited genetic information encoded in the DNA sequence, a growing body of evidence is suggesting that mammalian sperm may contain epigenetic information that might be crucial to the embryo (Carrell and Hammoud, 2010; Carone and Rando, 2012; Rando, 2012; Castillo *et al.*, 2014b; Hughes, 2014). This epigenetic information could be constituted among other markers by DNA methylation, modifications of histones, presence of chromatin-associated proteins and RNAs, chromatin structure and chromosome territories in the nucleus that may actively contribute to the regulation of the expression of some genes during development (Mercer and Mattick, 2013; Rivera and Ren, 2013; Brunner *et al.*, 2014).

### **1.1.2.2 The Sperm Flagellum**

The flagellum (tail) is the largest part of the mammalian spermatozoon and is responsible for its movement. Structurally, it is divided in four distinct and well-defined segments: 1) the connecting piece (neck), 2) the middle piece, 3) the principal piece and 4) the end piece (Fig. 1.4; (Fawcett, 1975)).

The connecting piece (or neck region) is the short, most proximal portion of the flagellum that attaches it to the sperm head and contains the sperm centriole (responsible for organizing the aster that brings together the male and female pronuclei after fertilization in most mammals) (Navara *et al.*, 1994; Sutovsky *et al.*, 1996; Terada *et al.*, 2000). The axoneme extends throughout the length of all four subdivisions of the flagellum, and contains the typical cilium conformation: nine outer microtubule doublets of the axoneme (OMDA) and a central pair (CP) of microtubules (9+2) (Fawcett, 1975). In addition, inner and outer dynein arms project from each of OMDA, whereas nine radial spokes (RS), one for each OMDA, project inwards the central pair in a helical fashion, being responsible for transmitting regulatory signals to the dynein arms (Fawcett, 1975; Porter and Sale, 2000) and also for regulating the size and shape of axonemal bending through calcium-dependent process (Wargo and Smith, 2003). The motor protein dyneins bind tubulin and

are responsible for converting the chemical energy derived from ATP hydrolysis into mechanical force and thus for propelling the flagellum movement (Lin *et al.*, 2014).

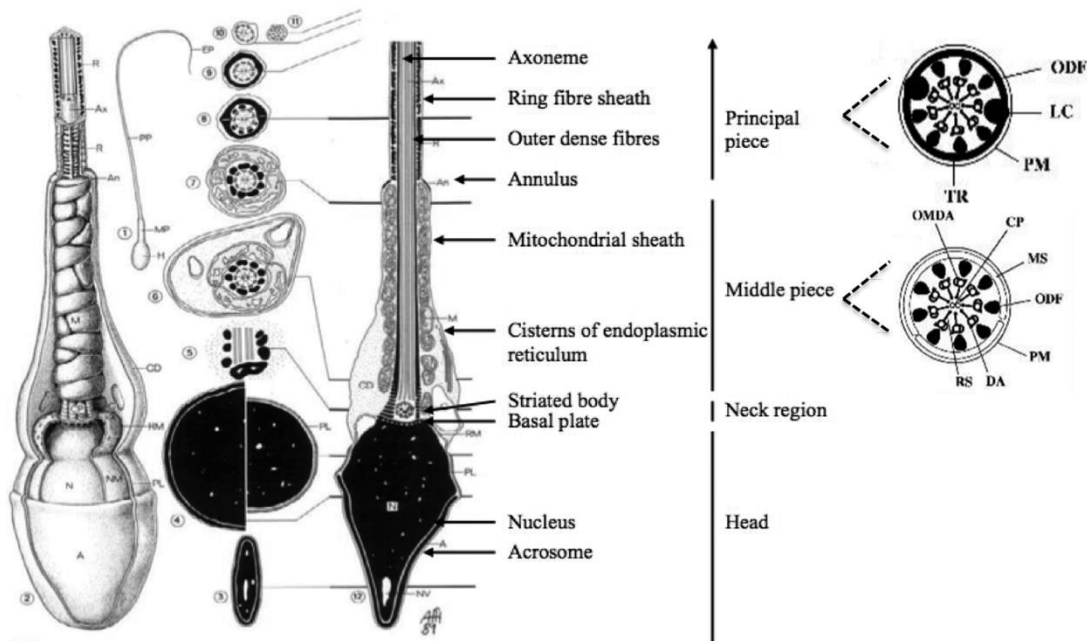


**Figure 1.4 – Schematic representation of the ultrastructure of the human sperm.**

Sperm flagella are structurally divided into four areas: the connecting piece (or neck region), middle piece, principal piece, and end piece. The schematic cross-section of the middle piece shows the plasma membrane (PM) and mitochondrial sheath (MS) surrounding the nine outer dense fibres (ODFs). Within the ODFs are the axoneme components: the nine outer microtubule doublets of the axoneme (OMDA) with associated dynein arms (DA) and radial spokes (RS) and the central pair (CP) of singlet microtubule. The schematic cross-section of the principal piece shows the PM surrounding seven ODFs, because two ODFs are replaced by the two longitudinal columns (LC) of the fibrous sheath (FS), a unique structure that is restricted to the principal piece. The two columns are connected by transverse ribs (TR) and the axonemal components are unchanged. (Adapted from (Holstein *et al.*, 2003; Turner, 2003) )

The middle piece comprises approximately one-quarter to one-third of the length of the flagellum, and is characterized by the presence of the mitochondrial sheath (MS). It is also constituted by nine outer dense fibers (ODFs) that extend into the principal piece and surround each of the nine outer axonemal microtubule doublets (Fig. 1.4). The annulus marks the end of the middle piece and the start of the principal piece where two ODFs are replaced by two longitudinal columns of the fibrous sheath (FS), a unique structure that is restricted to the principal piece. The last portion of the sperm flagellum is the end-piece, a short terminal section containing only the axoneme surrounded by the plasma membrane. These features make the sperm a highly specialized and physically well-compartmentalized cell. It is also important to note that although axonemes are highly conserved in all ciliated and flagellated eukaryotic cells, the MS, ODFs and FS

are accessory structures that are exclusive to the mammalian sperm flagellum (Fawcett, 1975; Turner, 2003).

### ***Outer dense fibres (ODF)***

The role of the ODFs has been proposed as merely structural, providing support for and passive elasticity to the long sperm tail (Fawcett, 1975). In fact, in the last few decades, some authors have isolated and characterized several ODF proteins in different species, including humans (Gastmann *et al.*, 1993; Morales *et al.*, 1994; Hoyer-Fender *et al.*, 1995; Schalles *et al.*, 1998; Zarsky *et al.*, 2003; Eddy, 2006), and the majority of them are keratin-like intermediate proteins (Kierszenbaum *et al.*, 1996; Tres and Kierszenbaum, 1996; Kierszenbaum, 2002). In addition, some of the genes encoding ODF proteins were successfully cloned of (Brohmann *et al.*, 1997; Shao *et al.*, 1997; Petersen *et al.*, 1999; O'Bryan *et al.*, 2001; Yang *et al.*, 2012) and the outcomes reinforce the hypothesis of the structural function of the ODFs. However, due to the lack of available ODF-defective sperm models, the true role of ODFs in sperm motility is not completely clear, remaining largely speculative.

### ***Mitochondrial sheath (MS)***

Sperm mitochondria are located exclusively in the MS of the middle piece. During spermatogenesis, germ cell mitochondria change their conformation, converting the orthodox forms in more condensed and metabolically more efficient ones (Ramalho-Santos *et al.*, 2009). These are rearranged in elongated tubular structures (Ho and Wey, 2007) that are packed helically around the anterior portion of the sperm flagellum. At the end of this process, mature mammalian sperm possess 22-75 mitochondria arranged end-to-end in the middle piece (Otani *et al.*, 1988). The sub-mitochondrial reticulum, a complex of filaments, seems to be the structure that sustains mitochondria and anchor them to the MS (Olson and Winfrey, 1990). This structure seems to depend on the expression of kinesin light chain 3 (KLC3), a protein that may bind both ODF1 and a mitochondrial outer membrane porin, creating a connection between them, and whose mutation has been proven to affect middle piece formation and sperm quality (Zhang *et al.*, 2012b; Lehti *et al.*, 2013). Moreover, the sperm mitochondria are encapsulated inside a keratinous structure formed by disulphide bonds between cysteine- and proline-rich selenoproteins (Calvin *et al.*, 1981;

Ursini *et al.*, 1999). This structure seems not only to confer mechanical stability, but also to be responsible for some distinctive properties of sperm mitochondria, namely the resistance to hypo-osmotic stress, and the unfeasibility of completely isolating these organelles (Ramalho-Santos *et al.*, 2009; Amaral *et al.*, 2013b). The fact that some mitochondria are evolutionarily retained in a very specialized sperm region, unlike what happens in few non-mammalian animal species living in habitats with very low oxygen levels and which lack sperm mitochondria (Balsamo *et al.*, 2007), suggests that these organelles have a crucial role in mammalian sperm function.

As in other cells sperm mitochondria produce ATP by aerobic respiration through oxidative phosphorylation (OXPHOS; (Ramalho-Santos *et al.*, 2009; Amaral *et al.*, 2013b)). Although these organelles might have similar roles to those in somatic cells, sperm mitochondria have several unique proteins or protein isoforms (testis- or sperm-specific), such as cytochrome C (Goldberg *et al.*, 1977; Hess *et al.*, 1993) and subunit VIb of the cytochrome c oxidase 2 (COXVIb-2) (Hüttemann *et al.*, 2003) among others (Blanco and Zinkham, 1963; Burgos *et al.*, 1995; Travis *et al.*, 1998), which functionally differentiate sperm mitochondria from the somatic counterparts. Any alteration in the sperm mitochondria that compromises their normal functionality may potentially affect male gamete function, including motility, highlighting the importance of these organelles in male reproduction (Piomboni *et al.*, 2012; Amaral *et al.*, 2013b). However, their physiological significance is still unclear and needs more investigation.

### ***Fibrous sheath***

The FS consists of two longitudinal columns (LCs) connected by closely arrayed circumferential ribs, which surround the axoneme and the ODF. This highly resistant structure, which includes many proteins cross-linked by disulphide bonds, provides mechanical support and modulates flagellar bending, thus defining the shape of the flagellar beat (Fawcett, 1975; Olson *et al.*, 1976). It also serves as a scaffold for proteins with indispensable roles in sperm motility, such as different signalling pathways and metabolism related proteins, namely glycolytic enzymes (Fig. 1.4) (Turner, 2006; Eddy, 2007). Some of the fibrous sheath proteins are cAMP-dependent protein kinase (PKA) anchoring proteins (AKAP), which are probably exclusive of spermatogenic cells (Eddy, 2007). The most abundant AKAP protein, and also one of the major structural component of the fibrous sheath, is AKAP4 (Carrera *et al.*, 1994; Fulcher *et al.*, 1995a). This protein has been proven through gene targeting disruption to be involved in triggering of progressive sperm motility in mice, and consequently in fertility (Brown *et al.*, 2003).

There are also many testis-specific isozymes or proteins associated with enzymatic activity in the FS including multiple glycolytic enzymes (Krisfalusi *et al.*, 2006) – namely Hexokinase 1-S (HK-S; (Mori *et al.*, 1993, 1998; Travis *et al.*, 1998; Nakamura *et al.*, 2010)), Glyceraldehyde 3-phosphate dehydrogenase-S (GAPDH-S; (Fenderson *et al.*, 1988; Welch *et al.*, 1992; Miki *et al.*, 2004)), Enolase 4 (ENO4; (Nakamura *et al.*, 2013)), Triosephosphate isomerase 1 (TPI1; (Ijiri *et al.*, 2013) –, a glutathione-S transferase (GSTM5; (Fulcher *et al.*, 1995b)), two thioredoxins – sperm thioredoxin-1 and 2 (SPTRX-1 and SPTRX-2; (Yu *et al.*, 2002; Miranda-Vizuetete *et al.*, 2003)) –, and a pyruvate dehydrogenase E1 subunit (PDHB; (Fujinoki *et al.*, 2004)).

Moreover, as scaffold for components involved in signal transduction and signalling pathways, the fibrous sheath contains for example some proteins of the Rho-GTPase signalling pathway, such as ropporin (Fujita *et al.*, 2000). Ropporin is a spermatogenic cell-specific protein that binds rhopilin (Nakamura *et al.*, 1999), which in turn interacts with Rho GTPase, important regulators of cellular processes associated with cell movement and adhesion and also with sperm motility (Fujita *et al.*, 2000; Fiedler *et al.*, 2013).

### **1.1.3 Specific mammalian sperm features: maturation, capacitation and acrosome reaction**

The human testes produce approximately 1000 spermatozoa per second (Amann and Howards, 1980). All these sperm cells, after released from seminiferous tubules, are transferred to the epididymis, where they finish their maturation process, which includes the acquisition of various proteins, probably in part through a structure called epididymosome (Frenette *et al.*, 2010). Although at this point sperm cells are considered mature, they are still immotile and unable to fertilize the oocyte, as the sperm plasma membrane remains ‘biologically frozen’ until sperm leave the male’s body and begin the ‘defrosting’ process. This consists on a series of poorly understood maturation steps known as capacitation, which occurs in the female reproductive tract, and is mandatory for spermatozoa to become fertilization-competent (Chang, 1951; Abou-haila and Tulsiani, 2009; Okabe, 2013). This fertilizing competence acquisition includes molecular, physical and biochemical events such as an increase in plasma membrane permeability and fluidity due to cholesterol efflux, influx of ions (specially  $\text{Ca}^{2+}$  and bicarbonate ( $\text{HCO}^{3-}$ )) that activate signalling cascades, internal pH rise and activation of protein kinases that promote protein phosphorylation, typically on tyrosine residues (Visconti and Kopf, 1998; Abou-haila and Tulsiani, 2009; Okabe, 2013). The capacitation process seems to be reversible, so that sperm cells can adapt their

fertilizing ability to the external conditions (Fraser, 2010). This process also leads to profound structural and functional changes in the male gamete, namely in motility pattern (hyperactivation), preparing it for acrosome reaction and egg fertilization (Okabe, 2013).

The acrosome reaction, a  $\text{Ca}^{2+}$ -dependent exocytotic event, consists on the release of the hydrolytic enzymes contained in the acrosome, such as acrosin, which facilitate sperm penetration through the oocyte zona pellucida (Ramalho-Santos *et al.*, 2007). Interestingly, progesterone, released by the cumulus cells, is one of the factors that triggers this reaction by the direct activation of a cation channel named CatSper, thus promoting  $\text{Ca}^{2+}$  influx apparently without the involvement of any metabotropic receptor (Lishko *et al.*, 2011; Strünker *et al.*, 2011). Another important factor seems to be membranar lipids, which are apparently involved in the modulation of calcium flux trough other calcium channels and participate in the regulation of acrosome exocytosis and fertilization (Cohen *et al.*, 2014).

After the penetration of the first oocyte vestments, specific molecules involved in the sperm-oocyte recognition are exposed and promote the interaction between the male and female gametes. For instance, the Izumo-Juno interaction (Inoue *et al.*, 2005; Bianchi *et al.*, 2014; Wassarman, 2014), seems to increase cell membrane fluidity and to facilitate fusion-related events, contributing to the fertilization of the oocyte (Primakoff and Myles, 2002; Okabe, 2013).

#### **1.1.4 Mammalian sperm motility**

Although sperm motility is one of the most important features of these special cells, being absolutely crucial to accomplish their main goal, i.e., reach and fertilize an oocyte, the molecular mechanisms behind sperm motility and its activation and regulation are not fully understood (Turner, 2006; Inaba, 2011). These cells acquire the capacity to move forward during epididymal maturation, but do not become motile until released from the epididymis (Vadnais *et al.*, 2013).

Mammalian sperm display two types of physiological motility: 1) activated progressive motility (typical from freshly ejaculated sperm) and 2) hyperactivated motility (characteristic from most sperm recovered from the site of fertilization) (Katz and Vanagimachi, 1980; Suárez and Osman, 1987; Turner, 2006). The first type of motility is characterized by strenuous and relatively symmetrical flagellar motion that results in a rapid forward movement. The second one starts after a period of time in the female reproductive tract or after *in vitro* incubation in appropriate medium,

and is characterized by asymmetrical flagellar bends, high amplitude and whip-like beating of the flagellum and a circular swimming trajectory. The hyperactivation of motility occurs during the process of capacitation, however it is not clear if this is a consequence of capacitation or a parallel independent event (Suarez, 2008).

The driving force for the flagellar motility is the result of the sliding of outer doublet microtubules by axonemal dyneins through a mechanochemical cycle of ATP hydrolysis (Satir, 1968; Summers and Gibbons, 1971). During this process, the dynein arms of the axoneme become phosphorylated and the dynein ATPase are activated, driving the hydrolysis of ATP and converting it into mechanical force (Tash, 1989). The dynein arms then transiently interact with their adjacent microtubular doublets and generate a power stroke, thus causing the microtubules to slide past one another (Satir, 1968; Summers and Gibbons, 1971; Brokaw, 1972) resulting in a bend movement along the flagellum. Calmodulin-dependent protein phosphatase calcineurin is one of the enzymes responsible for the reversion of this process through dynein dephosphorylation (Tash *et al.*, 1988).

It is important to note that dynein produces a unidirectional force (Sale and Satir, 1977). Thus, the generation of a normal axonemal bend requires that phosphorylation/ dephosphorylation events and concomitant activation/inactivation of the dynein arms, occur in an asynchronous manner along the length of the axoneme (Fig. 1.5) (Wargo and Smith, 2003). Each dynein arm interacts with its adjacent doublet, generates a stroke to force that doublet to bend and releases the doublet, so that the axoneme can return to its starting position and bend again in the opposite direction.

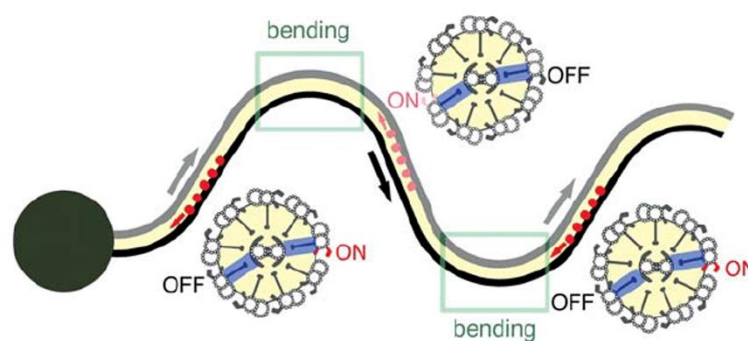


**Figure 1.5 – A possible model for the oscillatory mechanism of flagellar bending.**

Dyneins on two sides on the plane of the central pair (CP) apparatus (red and pink) are regulated by signals of the radial spokes (RS)/CP apparatus (blue), resulting in the formation of a planar wave. The axonemes are fixed at the basal body near the sperm head. The base or tip of the flagellum points toward the minus or plus end of doublet microtubules, respectively. Dyneins are minus-ended motors (red and pink arrows), sliding adjacent microtubules to the plus end (black and grey arrows). The bending provides feedback and switches active dyneins, resulting in the sliding of opposite microtubules across the bend. (Reproduced from (Inaba, 2011))

#### **1.1.4.1 Molecular mechanisms behind motility: cAMP and $\text{Ca}_2^+$ signalling**

The large majority of cellular and biochemical processes start as a response to extrinsic stimuli that trigger a specific receptor to initiate a signal transduction cascade. This typical pathway for stimulus-induced activation of a cellular process involves changes in conformation, phosphorylation, and/or localization of proteins, which results in the turn on/off of cellular processes. Sperm motility seems not to be an exception. Albeit some of the key factors involved in the initiation and regulation of sperm progressive motility are well known (including calcium ions ( $\text{Ca}_2^+$ ), bicarbonate ( $\text{HCO}_3^-$ ) and cyclic adenosine monophosphate (cAMP)), there are probably many others that remain to be identified (Eddy, 2006; Turner, 2006).

While the exact process by which sperm motility is initiated remains unclear, there are two major hypotheses: one suggests that it occurs as a result of the release of the sperm cells from the influence of an inhibitor factor, such as specific glycoproteins, present in the epididymal fluid (Usselman and Cone, 1983; Carr and Acott, 1984); the other one proposes that it happens by the activation of receptors located in the surface of the sperm cell (e.g. olfactory and GABA receptors), which could trigger a signalling response culminating in the activation of the motility (Calogero *et al.*, 1996; Fukuda *et al.*, 2004; Spehr *et al.*, 2004; McKnight *et al.*, 2014).

More recently, different strategies have been applied to study sperm motility, from diverse points of view. These include, for instance, the use of patch-clamp and mathematical modeling to decipher flagellar calcium signalling (Kirichok and Lishko, 2011; Olson *et al.*, 2011), the use of imaging and fluid mechanics simulation of sperm swimming to reveal the influence of media viscosity in sperm motility (Kirkman-Brown and Smith, 2011), the use of protein-protein interaction detection tools to study the role of specific proteins in sperm movement (Fardilha *et al.*, 2011), among others (Publicover and Barratt, 2011).

Inside the cell, the previously mentioned factors ( $\text{Ca}_2^+$ ,  $\text{HCO}_3^-$  and cAMP), seem to play important roles in signalling pathways that have also been assumed to be involved in mammalian sperm motility regulation: cAMP/protein kinase A (PKA) pathway and calcium signalling (Tash and Means, 1982; Tash and Bracho, 1994; Ho *et al.*, 2002; Turner, 2006). In addition, there are other signalling cascades less well characterised in mature sperm that may likely play roles in sperm motility, such as heterotrimeric and small G-protein-mediated pathways and pH changes (Fig. 1.6) (Nakamura *et al.*, 1999; Fujita *et al.*, 2000; Mannowetz *et al.*, 2012; Nishigaki *et al.*, 2014). Furthermore, data from knockout mouse models have made clear that several proteins are required for proper sperm flagellum functioning (Escalier, 2006; Inaba, 2011).



### ***Cyclic adenosine monophosphate (cAMP)***

Cyclic adenosine monophosphate (cAMP) is a key second messenger in the regulation of sperm motility and the cAMP-dependent phosphorylation of flagellar proteins through the activation of PKA, is at least partially responsible for the initiation and maintenance of activated sperm motility in mammals (Tash and Means, 1982, 1983; Tash and Bracho, 1994). Upon ejaculation, an increase in intracellular cAMP levels occurs due to the activation of the sperm soluble adenylyl cyclase (sACY; responsible for the conversion of ATP into cAMP) by the action of bicarbonate, which is present in higher concentration in the seminal plasma and female reproductive tract than in the epididymal fluid (Okamura *et al.*, 1985; Chen *et al.*, 2000). This results in the activation of PKA that phosphorylates downstream proteins in serine/threonine residues (e.g. axonemal dynein) triggering a cascade of protein phosphorylation events and activation of tyrosine kinases, which culminates mainly in the phosphorylation of several proteins in tyrosine residues (Tash, 1989; Leclerc *et al.*, 1996; Si and Okuno, 1999; Nolan *et al.*, 2004). This mechanism is probably balanced by the action of phosphatases, specifically serine/threonine and tyrosine phosphatases, and the resulting net amount of protein phosphorylation seems to be correlated with sperm motility status (Tash and Bracho, 1994; Smith *et al.*, 1996; Vijayaraghavan *et al.*, 1996).

It has also been shown that male mice deficient for sperm sACY (Esposito *et al.*, 2004; Hess *et al.*, 2005) and PKA (Nolan *et al.*, 2004) are infertile and have impaired sperm motility. Nevertheless, it is important to note that PKA and sACY do not seem to be required for the initiation of sperm motility, but rather for progressive motility improvement, by increasing the frequency of tail beating (Wennemuth *et al.*, 2003; Nolan *et al.*, 2004).

Furthermore, cAMP may also activate other signalling pathways in sperm by directly influencing the activity of some gated ion channels and/or cAMP-mediated guanine nucleotide exchange factors (Burton *et al.*, 1999; Ren *et al.*, 2001).

### ***Calcium***

Calcium is known to regulate both activated and hyperactivated motility in sperm cells (Suárez and Osman, 1987; Ho *et al.*, 2002). It is also known that an increase in intracellular calcium happens during capacitation (Baldi *et al.*, 1991), characterized by an extensive tyrosine phosphorylation of sperm proteins (Visconti and Kopf, 1998). Hence, besides the  $\text{HCO}_3^-$ , sACY is also

activated by  $\text{Ca}_2^+$  (Jaiswal and Conti, 2003), and the presence of  $\text{Ca}_2^+$  in the extracellular medium is required for sACY-dependent increase in the frequency of flagellar beat triggered by bicarbonate (Carlson *et al.*, 2007). Curiously, one of the facts that makes sACY so distinct from the transmembrane one, is its uniqueness activation by both bicarbonate and calcium (Chen *et al.*, 2000; Esposito *et al.*, 2004; Hess *et al.*, 2005).

Nevertheless, some data suggest that there are other calcium pathways independent from PKA that are also involved in mammalian sperm motility, namely via downstream action of the calmodulin (CaM). Some studies have reported that the inhibition of CaM decreases sperm motility (Si and Olds-Clarke, 2000). However, calcium/CaM cannot compensate the loss of sACY function, highlighting the importance of both pathways (Turner, 2006). The downstream target of CaM is calmodulin kinase (CaMK), with specific isoforms in the mammalian sperm flagellum, the inhibition of which also results in sperm motility reduction (Fig. 1.6) (Ignotz and Suarez, 2005; Marín-Briggiler *et al.*, 2005).

Another evidence that highlights the importance of calcium and calcium-regulated events in sperm is the presence of numerous membrane channels that permit and control the passage of extracellular calcium, namely CatSper, and possibly control sperm movement (Lishko *et al.*, 2012). In a recent study, Tamburrino and colleagues report that CatSper channel expression and function is associated with progressive motility in human sperm and may also be involved in the pathogenesis of asthenozoospermia (Tamburrino *et al.*, 2014). These observations were also strengthened by other recent published work in which the authors found that only sperm with intact CatSper domains, able to organize in a time-dependent manner followed by a specific protein tyrosine phosphorylation pattern, could successfully migrate (Chung *et al.*, 2014). Thus, bicarbonate, besides activating sACY resulting in an increase in cAMP and PKA activity (Chen *et al.*, 2000) also raises intracellular pH, which activates CatSper channels (Kirichok *et al.*, 2006).

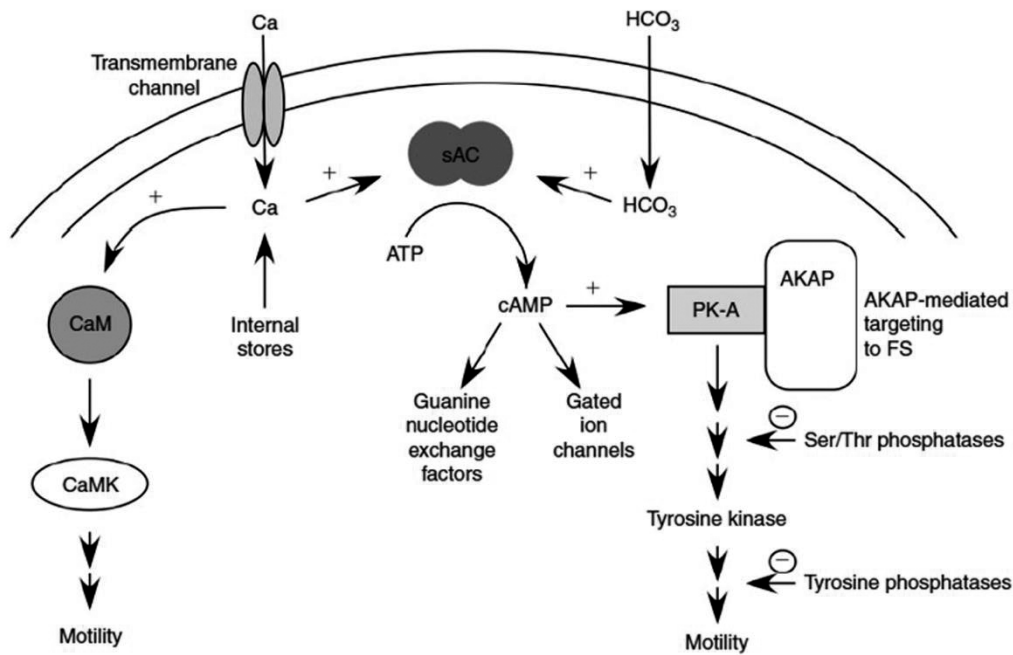


**Figure 1.6 – Schematic representation of the signalling pathways known or believed to be involved in the regulation of mammalian sperm motility.**

Abbreviations: Ca – calcium; CaM – calmodulin; CaMK – calmodulin kinase; HCO<sub>3</sub> – bicarbonate; sAC – soluble adenylate cyclase; ATP – adenosine triphosphate; cAMP – cyclic adenosine monophosphate; PK-A – protein kinase A; AKAP – cAMP-dependent protein kinase (PKA) anchoring proteins; FS – fibrous sheath (Reproduced from Turner, 2006).

#### **1.1.4.2 Motility fuel: the so-called energy debate**

The male gamete is a cell with very high energy demands: besides the obvious need of ATP to propel the cell forward, energy is required to achieve capacitation and perform the acrosome reaction, as well as for ordinary homeostasis (du Plessis *et al.*, 2014; Ferramosca and Zara, 2014). Indeed, when compared to other cell types (even with those known to need high levels of energy, such as skeletal muscle or heart cells), the rate of sperm ATP production is massive (Ruiz-Pesini *et al.*, 2007). Moreover, sperm motility is not only one of the most energetically expensive phenomena in sperm activity, but it also has the particular requirement of large amounts of ATP locally, along the tail, where the dynein proteins transduce the chemical energy of ATP hydrolysis into mechanical force.

As mentioned before, sperm cells have a mitochondrial sheath located in the midpiece, where the oxidative processes may take place, whereas glycolytic enzymes are mainly located in the principal piece of the tail, connected to the fibrous sheath (Eddy *et al.*, 2003; Miki *et al.*, 2004; Ford, 2006). This denotes a subcellular compartmentalization of the two main metabolic pathways

involved in energy production: glycolysis and oxidative phosphorylation (OXPHOS) (Mukai and Travis, 2012). The origin of the large amounts of ATP needed by sperm, especially to fuel motility, has been discussed for decades by scientists in the so-called “sperm energy debate” (Ford, 2006; Ruiz-Pesini *et al.*, 2007; Storey, 2008; Ramalho-Santos *et al.*, 2009; Amaral *et al.*, 2014a; du Plessis *et al.*, 2014).

On one hand, and when compared to glycolysis, mitochondrial respiration results in a more efficient ATP synthesis. On the other hand, and since mitochondria are confined to the midpiece, this compartmentalization may limit the diffusion of OXPHOS-derived ATP along the tail. This fact, together with the lack of information about the existence and importance of ATP shuttles along the tail of mammalian sperm (Ford, 2006) and the massive presence of glycolytic enzymes along the fibrous sheath of principal piece, led some scientists to suggest that glycolysis would be the main source of sperm ATP, even in aerobic conditions, as it happens in tumour cells and in fast axonemal transport (Zala *et al.*, 2013; Pereira *et al.*, 2014).

The relevance of glycolysis in ATP production in sperm was mainly shown by using gene targeting to knockout (KO) some of the glycolytic enzymes, and that resulted in male infertility or subfertility (Miki *et al.*, 2004; Odet *et al.*, 2008, 2011; Danshina *et al.*, 2010) due to impairment of sperm motility and low ATP levels. Furthermore, glycolysis in mouse sperm seems to also contribute to a pH-dependent flagellar beat frequency regulation (Mannowetz *et al.*, 2012).

In human sperm, the presence of glycolyzable substrates promotes sperm motility and ATP content maintenance, which declines rapidly in its absence, even in the presence of oxidizable substrates (Peterson and Freund, 1970; Bone *et al.*, 2000; Williams and Ford, 2001). Moreover, human sperm seem to convert exogenous labelled pyruvate into lactate, with no trace of oxidation in the tricarboxylic acid cycle (TCA), which indicates the prevalence of glycolysis (Hereng *et al.*, 2011).

However, and despite the fact that KO mice for the testicular isoform of cytochrome c, an essential protein for mitochondrial respiration, were fertile, their sperm were less motile and contained lower levels of ATP than controls (Narisawa *et al.*, 2002). It has also been shown that the incubation of human sperm with different mitochondrial electron transport chain (ETC) inhibitors in media containing glucose resulted in a rapid reduction of sperm motility (Ruiz-Pesini *et al.*, 2000; St John *et al.*, 2005). Moreover, the occurrence of a mitochondrial DNA (mtDNA) point mutation that affects the activity of ETC complex I is linked to low-motility sperm that can be rescued through

succinate (subtract for ETC complex II) supplementation (Folgerø *et al.*, 1993). Additionally, functional mitochondria seem to correlate with a better fertilization potential of human sperm (Ruiz-Pesini *et al.*, 1998; Espinoza *et al.*, 2009; Sousa *et al.*, 2011).

Interestingly, the results of experiments using mouse epididymal sperm seem to imply that both glycolysis and OXPHOS are able to sustain sperm motility, although with a glycolysis in a predominant role (Mukai and Okuno, 2004). In fact, glycolysis and OXPHOS are not isolated and independent metabolic pathways inside the sperm; and similarly to what occurs in somatic cells, glycolysis may be a preparative pathway that continuously supplies carbon units to mitochondria, where complete oxidation occurs (Mukai and Travis, 2012). Moreover, despite the controversial results of different studies that has fuelled this debate during all these decades, one thing seems to became clear: we have to be very careful concerning the interpretation and generalization of data, because there are species-specific discrepancies (Ford, 2006; Ramalho-Santos *et al.*, 2009), even when different mouse strains are used, i.e., the severity of phenotypes seems to be different (Odet *et al.*, 2013). It is also important to keep in mind that the majority of studies to functionally address this question and study sperm motility and ATP levels was performed in a classical way, *in vitro*, incubating sperm in media supplemented with different substrates, in the presence or absence of inhibitors; and these conditions, as well as, times of incubation, temperatures and substrates and inhibitor concentrations, vary from study to study. One thing is now clear, sperm energy metabolism seems to be very versatile, easily adaptable to the exogenous substrates available, and the energy pathway used may vary among species, also depending on the substrate composition of oviductal fluids (Ford, 2006; Ruiz-Pesini *et al.*, 2007; Ramalho-Santos *et al.*, 2009).

Recently, the publication of the human sperm tail proteome by Amaral and co-workers, added some more players to the energy debate. These data suggest that other carbohydrate pathways might operate in human sperm, including those involved in galactose and glycogen metabolism (Amaral *et al.*, 2013a). Also the compilation and analysis of the most complete human sperm proteome suggests that human sperm have functional Pentose Phosphate Pathway (PPP) (Amaral *et al.*, 2014a), which seems to be important for mouse sperm fertility (Urner and Sakkas, 1999, 2005). Remarkably, 24% of the sperm metabolic human sperm tail proteome includes proteins involved in both catabolic and anabolic lipid metabolism (such as fatty acid oxidation, carnitine shuttle, acycarnitine transport, ketone body catabolism, glycerol degradation, and phospholipid and triglyceride biosynthesis) and the inhibition of fatty acid oxidation with etomoxir, in the absence of exogenous substrates, severely affects sperm motility (Amaral *et al.*, 2013a). These results were in accordance with previous studies that report the importance of beta-

oxidation of free fatty acids to sperm function (Lenzi *et al.*; Jeulin and Lewin, 1996). Additionally, it was also reported that motility can be supported by ketone bodies in mouse sperm, suggesting that the loss of sperm function by a defect in the glycolytic pathway could be improved by the supplementation of ketone bodies as an energy source, using enzymes such as the testicular isoform of succinyl CoA transferase (SCOT-t), as a bypass enzyme for energy supplementation external to glycolysis (Tanaka *et al.*, 2004b). Glycogen is also a possible endogenous source of energy in mammalian sperm. It was shown that dog sperm is capable not only to use endogenous glycogen as an energy source, but also to synthesize new glycogen in the presence of exogenous glucose (Ballester *et al.*, 2000; Palomo *et al.*, 2003). In dog sperm, glycogen is also important in the achievement of capacitation in medium without glucose (Albarracín *et al.*, 2004). These could contribute for the long-term maintenance of human sperm motility in the absence of exogenous substrates (Amaral *et al.*, 2011). However this hypothesis needs further investigation.

Taken together, these cumulative reports seem to demonstrate that in the few days that mammalian sperm can spend in the female reproductive tract, they might be able to utilize both glycolysis and OXPHOS, and also other metabolic pathways to produce ATP for different purposes (Ramalho-Santos *et al.*, 2009; Amaral *et al.*, 2013a, 2014a). The balance between all the metabolic pathways may vary between species, according to the substrates available during sperm's travel (Ford, 2006; Ruiz-Pesini *et al.*, 2007). All these evidences highlight the urgent need to design and perform more molecular studies in order to better understand sperm physiology and their molecular basis.

### **1.1.5 Male infertility**

Infertility, commonly defined as the inability to conceive after at least 1 year of regular and unprotected intercourse, affects 10-15% of the population and it is estimated that approximately 40% is due to male etiology and poor sperm quality (Schulte *et al.*, 2010; Dada *et al.*, 2011; Hwang *et al.*, 2011). Nowadays, male infertility diagnosis relies on the microscopic assessment of standard semen parameters, mainly sperm concentration, motility and morphology, in the native sample based on the World Health Organization (WHO) guidelines and reference values ((WHO, 2010); Table I). Based on that, a sperm sample is considered normal (normozoospermic) if it contains  $\geq 15$  millions of spermatozoa *per ml* of semen,  $\geq 32\%$  of sperm with progressive motility and  $\geq 4\%$  of morphologically normal forms (WHO, 2010). If one of these parameters is below the reference

value, the sample is considered abnormal and dubbed oligozoospermic, asthenozoospermic or teratozoospermic, (low values of concentration, motility and morphology, respectively) (WHO, 2010).

**Table 1.1 – Reference values for the evaluation of human sperm quality (WHO, 2010).**

<b>Parameter</b>	<b>Reference value (WHO, 2010)</b>
Ejaculate volume	≥ 1.5 ml
Ejaculate pH	≥ 7.2
Total sperm number	≥ 39 million sperm/ejaculate
<b>Sperm concentration</b>	<b>≥ 15 million sperm/ml ejaculate</b>
<b>Sperm progressive motility</b>	<b>≥ 32 % total motile sperm</b>
<b>Sperm morphology*</b>	<b>≥ 4 % normal forms</b>
Sperm vitality	≥ 58 % live sperm

\*According to the strict criteria (Kruger et al., 1986).

## **1.2 Human sperm proteomics**

By definition, proteomics is the systematic analysis of all the proteins in a cell, tissue or organism, under a particular set of conditions and in a specific moment (Domon and Aebersold, 2006; Cox and Mann, 2007). Proteins are vital parts of living organisms, with important structural functions and they are the main components of the physiological metabolic pathways of cells. Moreover, the role of the proteomics field, coupled to the constant improvement of the systems used to its study, namely mass spectrometry (MS) techniques, and the generation of enormous databases with peptides and proteins information, as well as the development of bioinformatics tools, are making possible to perform meta-analysis using large volume of data. Altogether, these have been leading scientists to better know and characterize cells, tissues and organisms, and also diseases or specific pathways, at the molecular level. Although the high-throughput proteomics is a recent field, during the last decades the number of proteomic studies increased abruptly and the refinement and improvement of the techniques used to identify and characterize large number of proteins occurs at high velocity, probably due to the large number of researchers that uses proteomics in different subjects and areas to a wide range of purposes (Ahrens *et al.*, 2010).

The human sperm cell proteomics field is a good example of this evolution. Few decades ago no more than 100 different proteins had been described in the human male gametes. Nowadays, and thanks to the proteomics technological advances and study-designed

improvements, thousands of proteins have been described as part of human sperm. The most complete catalogue of human sperm proteins, which compiled the outputs of 30 proteomic studies, resulted in a list of 6198 different proteins (Amaral *et al.*, 2014a). In this elegant work the authors have considered the literature until 2012, and have selected the studies that accomplish some confidence requirements for the identification of proteins by liquid chromatography coupled to tandem mass spectrometry (LC-MS/MS), as a false discovery rate (FDR) < 5% and two peptides per protein or a FDR < 1% (Amaral *et al.*, 2014a). Currently, this catalogue is certainly bigger, with more proteins that were not previously described in human sperm. For example, two recently published works, conducted by Azpiazu *et al.* (2014) and Castillo *et al.* (2014), that performed proteomics in human sperm added “new” proteins to this list (Azpiazu *et al.*, 2014; Castillo *et al.*, 2014a). This compilation work had also huge importance, since it turned possible and performed large-scale bioinformatics analysis, using bioinformatics platforms in order to understand which metabolic pathways are likely active in human sperm (Amaral *et al.*, 2014a).

In fact, human sperm is a very suitable cell for proteomic studies since it is an accessible cell that can be easily purified and analysed (Oliva *et al.*, 2008, 2009; Amaral *et al.*, 2014a). Moreover, as mentioned before, sperm cells are believed to be transcriptionally and translationally silent, at least from nuclear encoded genes (Miller *et al.*, 2010; Baker, 2011; Amaral and Ramalho-Santos, 2013). This means that, at the end of the differentiation and maturation processes, the sperm cells have to contain all the proteins they need to be functional and accomplish their final objective, reach and fertilize an oocyte. The question is: are all proteins present in sperm cells functional proteins (either for sperm or for the oocyte and first steps of embryonic development) or are they mere leftovers of the spermiogenesis? Probably this question will be more easily answered after the complete characterization of the human sperm proteome. Then, will be easier to know if all the players of a specific pathway are present, which will allow researcher to focus on specific protein/pathway functionality, studying not only if these pathways are active but also their importance in sperm function. Therefore, during the last decades, many studies have been focused on the description of the human sperm proteome, starting mainly with whole cell proteomic analyses (Johnston *et al.*, 2005; Martínez-Heredia *et al.*, 2006; Baker *et al.*, 2007; de Mateo *et al.*, 2007; Li *et al.*, 2007; Wang *et al.*, 2013). Furthermore, the proteomic analysis of subcellular fractions of sperm cell (i.e. samples enriched in heads, tails or nucleus) was also a strategy that has been contributing to the identification of “new” sperm proteins, as it enriches the samples in minority proteins (proteins present in low amount in the cell), allowing their identification and improving the throughput (de Mateo *et al.*, 2011; Amaral *et al.*, 2013a; Baker *et al.*, 2013; Castillo *et al.*, 2014a, 2014b).



Considering sperm proteomics approaches, the first critical step is to ensure the purity of the samples, as the ejaculate has more than sperm cells (i.e. leucocytes, epithelial cells also known as round cells), and minor contaminations could lead to false positive results. For that, a normal procedure in human sperm proteomic studies is to select sperm cells, either by swim-up techniques, density gradient centrifugation or magnetic cell sorting (Fig. 1.7). After protein extraction, normally there are two technical strategies used in human sperm proteomic studies. The first one uses the initial protein separation (by one- or two-dimensional polyacrylamide gel electrophoresis (1D-PAGE, 2D-PAGE), followed by protein excision from the gel and digestion with enzymes (usually trypsin) into peptides. The second one performs the direct digestion of sperm proteins into peptides, with no previous separation. The peptides are further injected into mass spectrometer or separated using one- or two-dimensional liquid chromatography (1D-LC, 2D-LC) or isoelectric focusing (IEF) and then analysed by mass spectrometry (either by matrix-assisted laser desorption/ionization (MALDI)-MS or MS/MS) and identified using software to by search a peptide/protein databases (Fig 1.7) (Amaral *et al.*, 2014a).

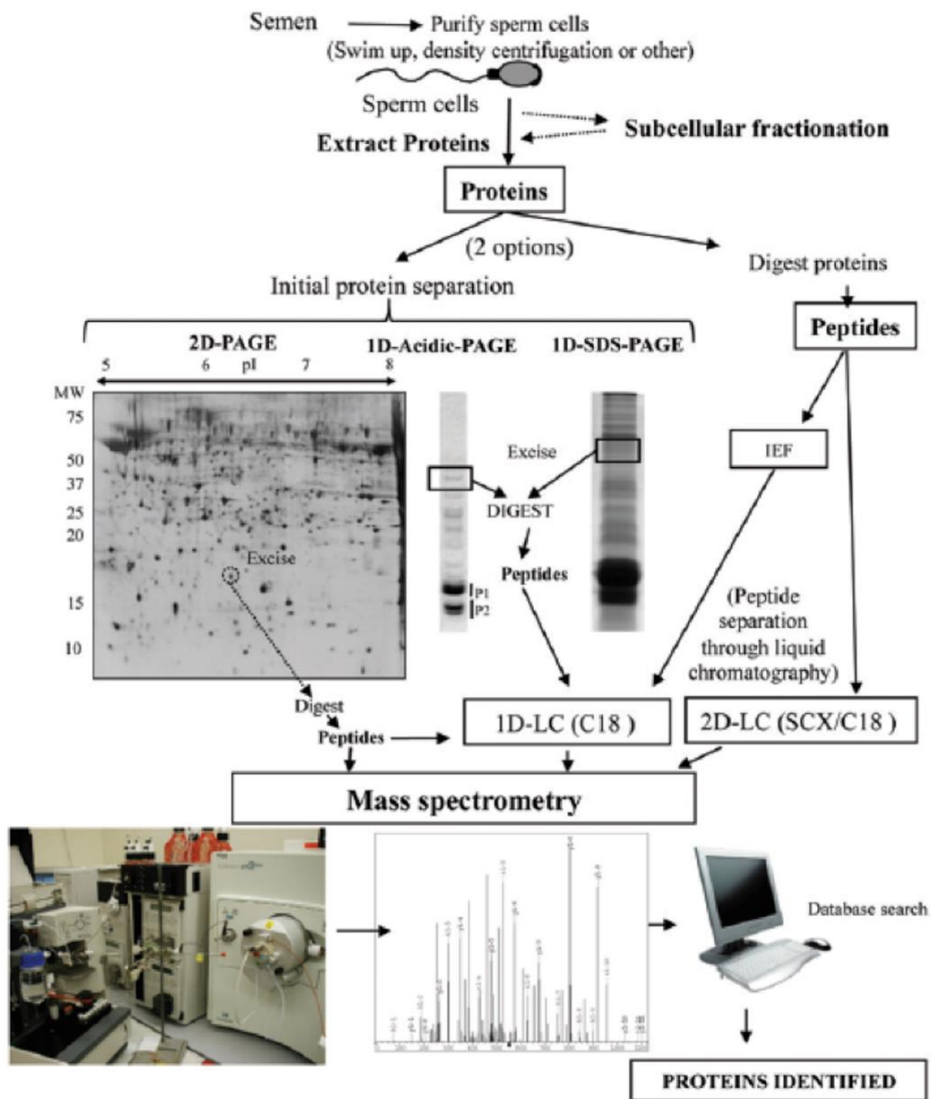


**Figure 1.7 – Human sperm proteomics strategies.**

This initial step in any sperm proteomics study consists on the isolation of sperm cells (from both the seminal plasma and other cells coexisting in semen). Sperm proteins are then extracted from either the whole cell or from specific subcellular compartments (in this case subcellular fractionation is performed beforehand). Once proteins are extracted, there are two technical options: (1) proteins are separated either by 1- or 2-dimensional polyacrylamide gel electrophoresis (1D-PAGE, 2D-PAGE), excised from the gels and digested (usually with trypsin) to generate peptides; 1D-acidic-PAGE may be used to resolve sperm nuclear proteins (mainly protamines: P1, P2), which cannot be resolved in a conventional SDS-PAGE; (2) proteins are digested without previous separation. Finally, peptides are analysed by mass spectroscopy (either MALDI-MS or MS/MS) and identified by searching a protein database. In order to improve the throughput, peptides can first be separated by 1- or 2-dimensional liquid chromatography (1D-LC or 2D-LC) or by isoelectric focusing (IEF). (Reproduced from Amaral et al., 2014).

The previous separation of the proteins (1D-PAGE) and peptides (1D- or 2D-LC, IEF) noticeably increases the quality of the obtained results, since it reduces the complexity of the mixture of proteins. It is also important to note that the initial analyses of sperm proteins were normally carried out using 2D-PAGE and MALDI-time of flight (TOF) MS and the number of

identified proteins were around 100 proteins (de Mateo *et al.*, 2007; Li *et al.*, 2007; Martínez-Heredia *et al.*, 2008). Nowadays, and using LC-MS/MS, the recently published results, include the identification of thousands of human sperm proteins, confirming the higher efficiency and throughput of this methods (Baker *et al.*, 2007, 2013; Amaral *et al.*, 2013a; Wang *et al.*, 2013).

### 1.2.1 Comparative human sperm proteomics

As stated before, all the technological improvements and the creation of a catalogue of proteins present in human sperm cell (Amaral *et al.*, 2014a), has been leading us to an increase of knowledge about the human male gametes gene products, that would be trivial to understand the molecular basis of their (dys)function and physiology and to address some (in)fertility questions, allowing the more confident search for novel putative biomarkers.

Therefore, the comparative and functional sperm proteomics has assumed an important role in the identification of differentially abundant proteins between distinct quality sperm or pathological conditions. In this field the most commonly used proteomic approach combined the 2D-PAGE, with in-gel protein digestion and the identification of the peptides by MS (Fig. 1.7) (Holland and Ohlendieck, 2014).

Hitherto the comparative sperm proteomics has been applied to compare different quality samples, such as sperm samples from patients with failed fertilization versus fertilization after *in vitro fertilization* (IVF) (Pixton *et al.*, 2004; Frapsauce *et al.*, 2009; Azpiazu *et al.*, 2014) or after artificial insemination (Xu *et al.*, 2012), teratozoospermic versus normozoospermic sperm samples (Liao *et al.*, 2009), diabetic patients sperm samples with non-diabetic obese patients and healthy donors (Paasch *et al.*, 2010; Liu *et al.*, 2014), or asthenozoospermic versus normozoospermic samples (Zhao *et al.*, 2007; Martínez-Heredia *et al.*, 2008; Chan *et al.*, 2009; Siva *et al.*, 2010; Parte *et al.*, 2012; Amaral *et al.*, 2014b). It has also been used to perform functional proteomics and compare, for example, capacitated versus non-capacitated sperm (Ficarro *et al.*, 2003; Secciani *et al.*, 2009). Therefore, this is an important area of research, and currently there are many other proteomics strategies with larger high-throughput capacity that can be more applied to study human sperm differential proteomes (Amaral *et al.*, 2014b; Azpiazu *et al.*, 2014).

### **1.2.1.1 Comparative human sperm proteomics focused on sperm motility**

Asthenozoospermia is one of the main seminal pathologies underlying male infertility, with a prevalence of up to 81 % (Thonneau *et al.*, 1991; Curi *et al.*, 2003). Moreover the concentration of progressively motile sperm seems to be the most predictive sperm parameter of both natural and assisted pregnancy outcomes (Tomlinson *et al.*, 2013). However and despite its importance, we still do not have a comprehensive model of the myriad of molecular mechanisms controlling sperm motility.

Thus, being proteomic technologies really efficient tools to help reveal molecular regulatory mechanisms, sperm motility is not an exception (Oliva *et al.*, 2008, 2009). In fact, as mentioned above, various groups have used mass spectrometry approaches to compare the proteome of sperm from asthenozoospermic individuals with that of normozoospermic controls (Zhao *et al.*, 2007; Martínez-Heredia *et al.*, 2008; Chan *et al.*, 2009; Siva *et al.*, 2010; Parte *et al.*, 2012).

In 2007 Zhao and co-workers compared the proteomic profile of sperm from 8 asthenozoospermic patients and 8 normozoospermic fertile donors by 2D electrophoresis and MALDI-TOF, which resulted in the identification of 10 differentially expressed proteins (Zhao *et al.*, 2007). One year later Martínez-Heredia and colleagues used a similar approach with larger number of samples (20 asthenozoospermic patients and 10 fertile controls) and identified 17 differentially expressed proteins (7 proteins less-abundant and 10 proteins more-abundant in asthenozoospermic samples). In 2010, seven more proteins were identified as differentially expressed in asthenozoospermic samples, using similar approach to compare proteins from 17 asthenozoospermic with 20 normozoospermic samples (Siva *et al.*, 2010).

Taking into account the important role of protein phosphorylation on sperm physiology, namely on motility, some studies have focused on performing differential phosphoproteomics to compare asthenozoospermic samples with normozoospermic ones, either by using conventional 2D electrophoresis (Chan *et al.*, 2009) or by performing immobilized metal affinity chromatography (IMAC) (Parte *et al.*, 2012) before MS analysis. The first study resulted in 12 differentially phosphorylated proteins after comparing 20 asthenozoospermic patients with 20 fertile controls (Chan *et al.*, 2009). The comparative human sperm phosphoproteome of 4 severe asthenozoospermic patients with 4 normozoospermic samples resulted in 68 phosphoproteins up- and down-regulated in asthenozoospermic samples (Parte *et al.*, 2012).

Merging the outcomes obtained in the aforementioned references, Amaral and co-workers have recently described that so far 109 specific proteins have been detected at altered levels in sperm samples with low motility (Amaral *et al.*, 2014a). Worth mentioning, most of the differential proteins belong to the cytoskeleton or have metabolic functions. However, and although these outcomes are pertinent, it should be stressed that these studies relied on the use of relatively low-sensitive proteomic techniques, when compared to more recent approaches. Moreover, in some of the studies the protein identification criteria were not indicated and therefore the possibility of false-positive identifications cannot be excluded.

Higher throughput techniques, with greater detection power, are currently available. Indeed, the use of liquid chromatography tandem mass spectrometry (LC-MS/MS) in descriptive proteomic studies has revealed that the human sperm proteome is much more complex than previously anticipated (Baker *et al.*, 2007, 2013; de Mateo *et al.*, 2011, 2013; Amaral *et al.*, 2013a, 2014a; Wang *et al.*, 2013; Castillo *et al.*, 2014b). The field of quantitative proteomics is also in constant progress, and the use of isobaric labelling strategies (such as isobaric tandem mass tags; TMTs) have been applied to study proteome alterations in distinct somatic cells (Thompson *et al.*, 2003; Dayon *et al.*, 2010; Sinclair and Timms, 2011; Raso *et al.*, 2012; Everley *et al.*, 2013).

The TMT reagents are isobaric chemical tags that enable simultaneous identification and quantitation of proteins in different samples using MS/MS. (Thompson *et al.*, 2003; Sinclair and Timms, 2011). The tags are composed of a primary amine reactive group and an isotopic reporter group linked by an isotopic balancer group for the normalization of the total mass of the tags. Shortly, the amine-reactive (NHS)-ester-activated compounds covalently attach, with high efficiency, to the peptide amino terminus and free amino termini of lysine residues of peptides and proteins, labeling all the proteins (or peptides) in a sample. Furthermore, as the tags are isotopomers (share identical structure and mass) and they use C and N isotopes instead of H isotopes, these permits the coelution of the labelled peptides during LC separation and co-isolation during MS/MS analysis, resulting in fewer missing peptide identifications among samples. During MS/MS analysis each isobaric tag is also fragmented, producing a unique reporter ion mass that is used for sample identification and quantitation. Thus, the protein quantitation is accomplished by the comparison of the six reporter ions relative intensities in the MS/MS spectra (Thompson *et al.*, 2003).

Recently, by using 2-plex TMT protein labelling and LC-MS/MS, Azpiazu and colleagues were able to efficiently identified several sperm proteins that are likely to be required for normal

embryo development (Azpiazu *et al.*, 2014). Nowadays, the 6-plex TMTs have simpler structure and smaller mass, comparing to the first generation of 2-plex TMTs, with the clear objective to promote enhanced cleavage of the reporter groups. In this way, the reporter groups are released in a “pseudo-quiet region” of the MS/MS spectra, allowing high-quantification performance and the best tracking of more individual samples (Dayon *et al.*, 2010).

### 1.3 Reproductive metabolomics

In recent years, the concept of biological fingerprint has emerged and comprehensive “omics” approaches (transcriptomics, proteomics, and metabolomics) have become a new but simultaneously an increasingly used way of addressing life complexity. Metabolomics is defined as the study of small, low molecular weight molecules and reflect downstream events of gene expression, thus it is considered to be closer to the actual phenotype than either proteomics or genomics (Kuile and Westerhoff, 2001; Nicholson and Lindon, 2008; Patti *et al.*, 2012; Kovac *et al.*, 2013). In fact, comprehensive “omic” approaches have substantially allowed very detailed characterizations of the complex molecular composition of distinct cells, tissues and organisms (Smith *et al.*, 2014).

The identification of the metabolites and proteins as main determinants of the expression of the genomes and transcriptomes as also influenced by environmental cues, represents a first step to understand the normal composition and physiology of cells and tissues and their dysfunction associated to pathological states (Jodar *et al.*, 2012; Wishart *et al.*, 2013; Castillo *et al.*, 2014a, 2014b). In the case of the human spermatozoon, as mentioned before over 6000 proteins have been identified using mass spectrometry (MS), representing about 80% of the estimated proteome of this cell (Oliva *et al.*, 2008, 2009; Amaral *et al.*, 2013a, 2014a; Baker *et al.*, 2013; Azpiazu *et al.*, 2014). However, and in contrast to the substantial proportion of proteins identified, so far a relatively small number of around 20 metabolites have been identified in sperm cells of different model species (Oliva *et al.*, 1982; Patel *et al.*, 1999; Dreanno *et al.*, 2000; Jones and Bubb, 2000; Marin *et al.*, 2003; Hung *et al.*, 2009; Lin *et al.*, 2009). This smaller number of metabolites is in part due to the fact that the number of metabolites in cells is much lower than that of proteins (Kouskoumvekaki and Panagiotou, 2011; Wishart *et al.*, 2013). But it is also due to the fact that the full potential of current “omic” techniques has not yet been fully applied to the study of the sperm metabolome (Kovac *et al.*, 2013).

The most widely used technique for metabolomic purposes has been nuclear magnetic resonance (NMR), mainly for historical reasons (Nicholson *et al.*, 2002; Courant *et al.*, 2013). However, more recently, MS-based methods have also proved to be extremely useful in metabolites identification and to have some advantages over NMR in terms of sensitivity (Theodoridis *et al.*, 2008; Alexandre-Gouabau *et al.*, 2011; Courant *et al.*, 2013). Nevertheless, and in order to obtain broad metabolomic descriptions, both approaches (NMR and MS) seem to complement each other (Fancy *et al.*, 2006; Patti *et al.*, 2012; Zhang *et al.*, 2012a).

Metabolomic studies have been performed in sperm cells from different species, such as goat (Patel *et al.*, 1998, 1999), boar (Jones and Bubb, 2000; Marin *et al.*, 2003), turbot (Dreanno *et al.*, 2000) and rhesus macaque (Hung *et al.*, 2009; Lin *et al.*, 2009). Rat testicular tissue (Griffin *et al.*, 2000) and human seminal plasma have also been subjected to metabolomic analyses (Hamamah *et al.*, 1993; Gupta *et al.*, 2011a, 2011b, 2013). However, there are no published reports on the application of these two metabolomics techniques (NMR and MS) to the study of human sperm metabolites. Nevertheless, the characterization of the normal sperm metabolome would therefore represent an important first step towards a better understanding of the function of this cell and its dysfunction associated to male infertility or subfertility. As it happens with human sperm proteomics, it would be important to perform comparative metabolomics to better understand human sperm (dys)function and physiology. This, coupled to the use of systems biology and the bioinformatics tools available, will certainly be an excellent and valuable way to characterize human sperm cells and associated pathologies, and consequently will promote the discovery of new (in)fertility biomarkers.

#### **1.4 Objectives**

The first objective of this work was to define the roots for human sperm motility deficiencies at the protein level, by using high throughput TMT protein labelling and LC-MS/MS protein identification and quantification. For that we have compared the proteome of sperm samples differing in motility, asthenozoospermic *versus* normozoospermic samples (sub-chapter 3.1). We have also compared our results with previous studies performed by others using less efficient proteomic approaches, in order to better understand human sperm motility (sub-chapter 3.1.5).

Another objective of this work was to identify and report, for the first time and through two complementary untargeted metabolomics approaches (NMR and MS), the initial catalogue of the human sperm cell endogenous metabolites (sub-chapter 3.2). We also aimed to explore the relationship between the identified metabolites and the previously reported human sperm proteome (sub-chapter 3.3).

The last objective was to compare for the first time, the metabolomics fingerprints of extracts from human sperm with different progressive motility, asthenozoospermic versus normozoospermic samples (sub-chapter 3.4).



## **CHAPTER II. MATERIALS AND METHODS**



## **CHAPTER II. MATERIALS AND METHODS**

### **2.1 Chemicals**

All reagents were supplied from Sigma Chemical Company (St. Louis, MO, USA) unless stated otherwise.

### **2.2 Biological Material**

Human semen samples were obtained from patients undergoing routine semen analysis at the Fertility Clinic (Clinic Hospital, Barcelona, Spain). All patients signed informed consent forms and all human material was used in accordance with the appropriate ethical and Internal Review Board guidelines. Semen samples were collected by masturbation into specific sterile containers after 3-5 days of sexual abstinence. Routine seminal analyses were performed according to the World Health Organization guidelines (WHO, 2010).

### **2.3 Differential Proteomics**

#### **2.3.1 Preparation and selection of sperm samples**

All semen samples were washed using Ham's F-10 nutrient mixture (Life Technologies™, Paisley, UK) supplemented with 0.6 % (w/v) bovine serum albumin (BSA) and 26 mM bicarbonate (NaHCO<sub>3</sub>) at 37 °C. Thenceforth, a density gradient centrifugation was performed for each sample, using 80 % (v/v) and 40 % Percoll™ (GE Healthcare, Sweden) for 30 min at 400 g, at room temperature, following the WHO recommendations (WHO, 2010). The purity of all sperm samples was checked using phase contrast microscopy. Sperm motility and vitality (assessed using 0.5 % (w/v) Eosin Y) of all sperm samples were determined, according to the WHO recommendations (WHO, 2010).

Only samples containing solely sperm cells after processing (i.e., without contaminating cells) were used for proteomic analyses. The selection of the sperm samples (5 asthenozoospermic and 5 normozoospermic) was further based on the outcomes of sperm motility and vitality. The

rationale was to compare groups of samples differing in progressive motility, but having similar % of live sperm. In the end and as expected, the asthenozoospermic group had a significantly lower motility (but similar vitality) compared to the normozoospermic group. Additional analysis were performed to compare the protamine 1 to protamine 2 (P1/P2) ratio, ensuring there were no differences between the P1/P2 ratio of the two groups of samples selected for the comparative proteomic analyses, with the objective to focus as much as possible in the motility parameter, excluding possible other factors. In order to corroborate our results, another strategy was applied using of normozoospermic samples fractionated into two fractions (higher and lower motility sperm) by swim-up technique (WHO, 2010), but these results are not part of this dissertation (Amaral *et al.*, 2014b).

### **2.3.2 Protein solubilization**

Sperm cells were washed with PBS and protein solubilization was independently performed for each sample, as described previously (Amaral *et al.*, 2013a; de Mateo *et al.*, 2013; Azpiazu *et al.*, 2014). Briefly, samples were incubated in Lysis Buffer [7 M urea, 2 M thiurea, 1% (w/v) 3-[[3-Cholamidopropyl) dimethylammonio]-1-propanesulfonate (CHAPS), 1% (w/v) N-Octilglucopyranoside, 18 mM dithiothreitol (DTT) and 2.4 mM phenylmethylsulfonyl fluoride (PMSF)] for 1 h at 4 °C, with constant shaking. Protein concentrations were determined using the Quick Start Bradford Protein Assay (BioRad, Hercules, CA, USA) following the manufacturer's instructions.

### **2.3.3 Protein labeling with isobaric tags (TMT 6-Plex)**

In addition to the 5 asthenozoospermic samples (A1 to A5) and the 5 normozoospermic samples (N1 to N5), internal controls (CT) were also included for normalization purposes. These controls consisted on a mixture of equal amounts of all the samples.

For labeling, Tandem Mass Tag (TMT) six-Plex™ Isotopic Label Reagent Set (Thermo Scientific, Rockford, IL, USA) was used. Twenty five µg of each sperm sample/internal control were precipitated with 80% (v/v) cold acetone and separately labeled according to the manufacturer's recommendations. Succinctly, proteins were incubated in 45 mM triethylammonium hydrogen carbonate buffer (TEAB) with 0.1% (v/v) sodium dodecyl sulfate (SDS), reduced in 9.5 mM tris (2-

carboxyethyl) phosphine (TCEP) for 1 h at 55 °C and alkylated with 17 mM iodoacetamide for 30 min, at room temperature, in the dark. Protein TMT labelling was used instead of TMT peptide labelling because we already had this approach set up in our unit. Also a pilot labelling experiment performed with TMT0 resulted in a sufficient number of peptide identifications to be able to reach our goals. TMT label reagents (0.8 mg each) were equilibrated to room temperature, dissolved in 24 µL anhydrous DMSO and added to the reduced and alkylated proteins (Fig. 2.1). After 1 h, the reaction was quenched with 8 µL of 0.5% hydroxylamine for 15 min, under shaking. Labelled samples were then mixed in equal amounts in such a way that two pools of samples were obtained for each of the experiments (each consisting of 5 different samples plus the respective internal control; Fig. 2.1). After pooling, proteins were precipitated as described previously.

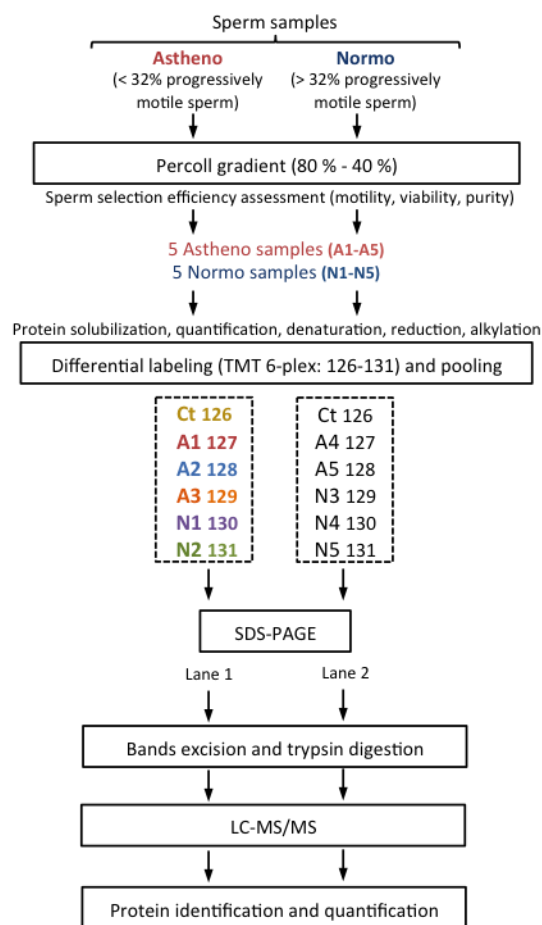


**Figure 2.1 – Overall strategy used for the identification of proteomic alterations in sperm with low motility.**

Comparative analysis was performed using asthenozoospermic (A1 to A5) versus normozoospermic (N1 to N5) samples. After 80%-40% Percoll purification, routine sperm quality was assessed (sperm viability, motility and purity) and based on the results 5 astheno and 5 normozoospermic samples were selected, considering statistical significant differences on motility (P value < 0.01) and no differences on the percentage of live sperm (P value > 0.05; bars graph: blue – normozoospermic and red – asthenozoospermic samples). The soluble proteins were extracted, digested, reduced, alkylated and labeled with TMT-6plex (126, 127, 128, 129, 130, 131) isobaric tags. Equal amounts of the different samples plus an internal control (CT) were then

combined as shown in the dotted boxes and run on SDS-PAGE. Each dotted box represents the independent multiplexed pools processed. Pools resulting from the astenozoospermic versus normozoospermic comparative analysis were run in a gel (2 lanes). Each lane was then excised into very small fragments, which were digested with trypsin. Tryptic peptides were further separated by LC and proteins were identified and quantified through MS/MS.

#### **2.3.4 Sodium dodecyl sulphate-polyacrylamide gel electrophoresis (SDS-PAGE)**

Precipitated proteins were dissolved in Laemmli buffer (60 mM Tris-HCl pH 6.8, 2.2% (w/v) SDS, 5% (v/v) glycerol, 0.1 M DTT) and incubated for 10 min at 90 °C. After cooling, a total of 50 µg of labelled proteins were separated by SDS-PAGE (12 % acrylamide gel with a 3.9 % acrylamide stacking gel). The gels were fixed with 50 % methanol 10 % acetic acid and stained with EZBlue™ Gel staining reagent for 5 min (until a protein smear was slightly visible).

#### **2.3.5 Liquid Chromatography and Tandem Mass Spectrometry (LC-MS/MS)**

Gel lanes (Fig 2.1) were carefully cut into very small pieces ( $\approx 1 \text{ mm}^3$ ) that were then processed for mass spectrometry analysis (Amaral *et al.*, 2013a; Azpiazu *et al.*, 2014). Gel slices were digested overnight with 100 to 150 ng trypsin (Promega, Madison, WI, USA) at 37 °C. Tryptic peptides were separated by means of nano liquid chromatography using a Proxeon EASY-nLC (Thermo Fisher Scientific, Waltham, MA, USA) with a flow rate of 400 nL/min, an EASY C18 trap column (5 µm, 120 Å, 100 µm inner diameter × 2 cm in length), and an EASY C18 analytical column (3 µm, 120 Å, 75 µm inner diameter × 10 cm in length). The following linear gradient, using Solvent B (97 % ACN, 0.1 % formic acid) and Solvent A (3 % ACN, 0.1 % formic acid), was employed: 5 % – 30 % buffer B (90 min). MS/MS analysis was performed using an LTQ Orbitrap Velos (Thermo Fisher Scientific) with a nanoelectrospray ion source with precursor ion selection in the Orbitrap at 30000 of resolution, selecting the 15 most intense precursor ions in positive ion mode. MS/MS data acquisition was completed using Xcalibur 2.1 (Thermo Fisher Scientific). For identification of TMT labelled peptides, higher energy collisional dissociation (HCD) with 40 % fixed collision energy (CE) was the fragmentation method used.

### 2.3.6 Protein identification and quantification

Data were processed using Proteome Discoverer 1.4.1.14 (Thermo Fisher Scientific). For database searching, raw mass spectrometry files were submitted to the in-house *Homo sapiens* UniProtKB/Swiss-Prot database (released February 2014; 20240 protein entries) using SEQUEST version 28.0 (Thermo Fisher Scientific). The Percolator search node, a machine-learning supplement to the SEQUEST search algorithm that increases the sensitivity and specificity of peptide identifications, was also used (Käll *et al.*, 2007). Searches were performed using the following settings: 4 maximum miss cleavage for trypsin; TMT-labelled lysine (+229.163 Da) and methionine oxidation (+15.995 Da) as dynamic modifications; cysteine carbamidomethylation (+57.021 Da) as static modification; 25 ppm precursor mass tolerance; 20 mmu fragment mass tolerance; 20 ppm peak integration tolerance; and most confident centroid peak integration method. The criteria used to accept identification included a minimum of 2 peptides matched per protein, with a false discovery rate (FDR) of 1 %.

Quantitative analysis of the TMT experiments was performed simultaneously to protein identification using Proteome Discoverer software. Reporter ion quantification of HCD MS2 spectra was enabled and TMT-6 plex was set as quantification method. The quantification values were extracted from the reporter ions intensities ( $i_n$ ; where n represents the reporter ions ranging from m/z 126.1 to m/z 131.1) and were corrected according to the isotopic purities of the reporter ions provided by the manufacturer. The reporter ions variability before normalization are indicated in supplementary table S3. Of note, over 90% of reporter ions had less than 20 % variability. In order to determine the relative abundance of each reporter, a normalization of the reporter intensities by the sum of all the reporter intensities was made (e.g.,  $i_{126}/i_{126}+i_{127}+i_{128}+i_{129}+i_{130}+i_{131}$ ). Quantification values were rejected whenever any quantification channel was missing. For protein quantification purposes, only unique peptides were considered and protein ratios were normalized to protein median. Normalized values for each protein were exported to Microsoft Excel (v14.0.0) and only those proteins with quantification values for all the samples (i.e., 10 samples and 2 internal controls) were considered for further analysis. Seeing that 2 lanes of the gel were used the values of each sample were further normalized by the respective internal control sample. In order to settle if any of the quantified proteins was differentially expressed between the two groups (asthenozoospermic *versus* normozoospermic), statistical analysis was performed (see below) and a final list of differential expressed proteins was generated for each experiment. Additionally, and in order to validate the results obtained, the MS spectra of all differential proteins detected were manually checked.

### **2.3.7 Differential protein annotation and bioinformatics analyses**

Proteins identified in different amounts in each of the two experiments were classified according to subcellular localization and biological function(s) using the information available at the UniProt Knowledgebase (UniProtKB/Swiss-Prot) website (<http://www.uniprot.org>). The lists of differential proteins were also analyzed using the bioinformatics tool DAVID v6.7 (Database for Annotation, Visualization and Integrated Discovery; <http://david.abcc.ncifcrf.gov/>) in order to identify both overrepresented Gene Ontology Biological Process terms and putative active biological pathways (Huang *et al.*, 2009a, 2009b). The significance of gene-enrichment analysis was expressed by an EASE Score, corresponding to a modified Fisher Exact *P* value (*P* values < 0.05 were considered significant).

### **2.3.8 Clustering analysis**

Hierarchical clustering analysis of the quantitative data of the differential proteins was performed using PermutMatrix software v.1.9.3 (<http://www.lirmm.fr/~caraux/PermutMatrix/>), a software originally developed for gene expression analysis (Caraux and Pinloche, 2005), but that has also been validated for proteomics (Meunier *et al.*, 2007). The protein intensity values of each sample/subpopulation were logarithmized and exported into PermutMatrix. Hierarchical clustering analysis was performed using the Pearson correlation and Ward's minimum variance methods for data distance and aggregation (Meunier *et al.*, 2007). Dendograms with samples on the *x* axis and protein name on the *y* axis were obtained.

### **2.3.9 Determination of protamine 1 (P1)/protamine 2 (P2) ratio**

In order to monitor the protamination status of the individual sperm samples as a way to assess overall sperm chromatin packing and protection, the P1/P2 ratio was also determined. Towards this goal, the insoluble fractions of the ten samples (5 astheno and 5 normozoospermic samples) were processed as described previously (Castillo *et al.*, 2011). Basically, extracted protamines, along with external standards of known protamine concentrations, were run on acid-urea polyacrylamide gels (acid-urea PAGE). Band intensities were quantified using Quantity One software (Bio-Rad Laboratories, Hercules, CA, USA) and used to determine the amounts of P1 and



P2 in each of the samples. Quantification calculations were based on a regression curve constructed with the protamine standards.

### **2.3.10 Western blotting**

The expression of two differential proteins, Tektin 1 (TEKT1) and WD repeat-containing protein 16 (WDR16) was determined in independent astheno and normozoospermic samples through western blotting. Fifteen  $\mu\text{g}$  of extracted proteins were run on SDS-PAGE, as described above, and transferred on ice to nitrocellulose membranes (NYTRAN Plus, Schleicher & Schuell BioScience GmbH, Dassel, Germany) in transferring buffer (25 mM tris, 0.2 M glycine and 15% (v/v) methanol), for 1 h 15 min at 100 mA. Membranes were washed in Tris-buffered saline with 0.1% (v/v) Tween 20 (TBST) for 15 min and blocked in TBST with 5% (w/v) skim milk (Nestlé, Vevey, Switzerland) for 1 h at room temperature. For immunostaining, rabbit anti-TEKT1 (ab182777; Abcam, Cambridge, UK) and rabbit anti-WDR16 (ab170937; Abcam, Cambridge, UK) antibodies (diluted 1:1000 in TBST) were used. Membranes were incubated with primary antibodies for 1 h at room temperature and then washed thrice with TBST (10 min each). The secondary antibody (Amersham™ ECL™ Anti-Rabbit IgG, Horseadish Peroxidase-linked whole antibody; GE Healthcare Life Science, Buckinghamshire, UK) was applied to the membranes diluted 1:2500 in blocking solution for 1h at room temperature. For detection, the WesternBright™ ECL Western Blotting Detection Kit (Advansta, Menlo Park, CA, USA), and a LAS-3000 imaging system (Fujifilm, Tokyo, Japan) were used. Band intensities were quantified using Quantity One software (Bio-Rad Laboratories, Hercules, CA, USA) and the ratio between band intensities of the two groups (asthenozoospermic to normozoospermic – Ast/Nor) was calculated.

### **2.3.11 Statistical analyses**

Statistical analysis was carried out using SPSS for Mac OS (version 20.0, Chicago, IL, USA). All variables were checked for normal distribution using the one-sample Kolmogorov-Smirnov test and for variance homogeneity using Levene's test. Comparison between groups (i.e., asthenozoospermic *versus* normozoospermic samples) was performed using Student's T-test in all the comparisons: 1) differential proteomic intensities results; 2) P1/P2 ratio between the two groups of sperm samples. *P* values < 0.05 were considered significant.

## **2.4 Metabolomics**

### **2.4.1 Biological material**

Semen samples collection followed the same criteria described above (subchapter 2.2). In this study a total of 15 samples with a normal sperm count, normal sperm morphology and free from other contaminating cells (after processing) were used: 9 for proton nuclear magnetic resonance ( $^1\text{H-NMR}$ ) analysis and 6 for Gas Chromatography (GC) Time of Flight (TOF) / Mass Spectrometry (MS) analysis. For  $^1\text{H-NMR}$  3 pools of samples were made (each one with 150 million sperm): 2 normozoospermic (n=2 in one pool and n=3 in the other pool) and 1 asthenozoospermic pool (n=4). For the GC-TOF/MS analysis 6 individual samples were used (each one with 15 million sperm): 3 normozoospermic and 3 asthenozoospermic samples. These samples were processed and classified following the WHO criteria (WHO, 2010).

### **2.4.2 Sperm samples preparation and purification**

All semen samples were washed and purified following the same criteria methods previously described (subchapter 2.3.1). The purity of all sperm samples was checked using phase contrast microscopy and only samples with no detectable contamination with non-sperm cells after processing were used for metabolomics analyses.

Sperm cells were then washed three times with cold PBS and, depending on the metabolomics technique used, cells were frozen with liquid nitrogen and stored at  $-80\text{ }^\circ\text{C}$  for further metabolite extraction (for GC-TOF/MS analysis) or metabolites were directly extracted and lyophilized (for  $^1\text{H-NMR}$ ), Fig. 2.2).

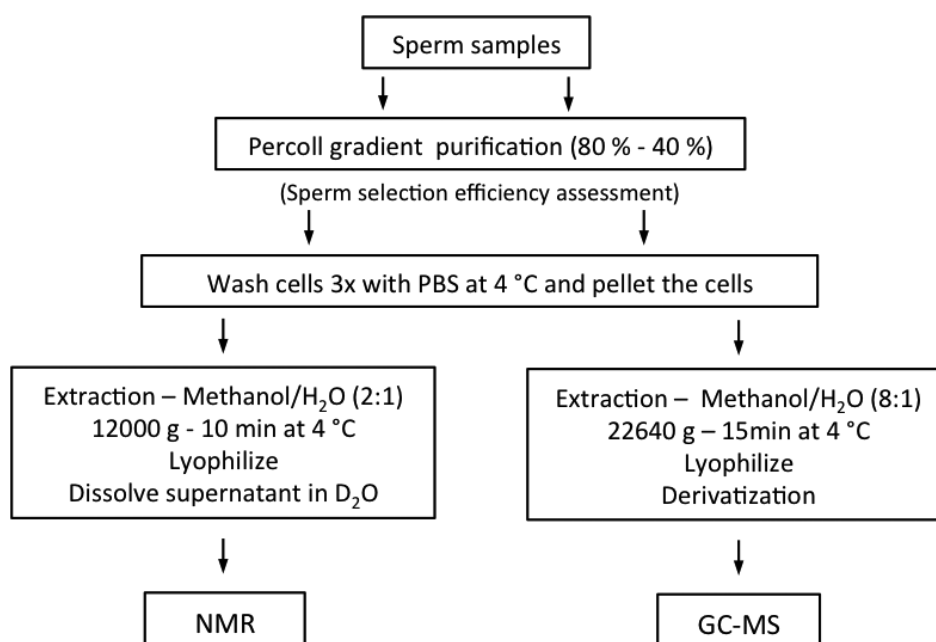


**Figure 2.2 – Overall untargeted metabolomics strategy used for the identification of metabolites in human sperm.**

After purification the sperm samples were washed and the metabolites extracted with methanol/water (H<sub>2</sub>O) at a ratio of 2:1 (v/v) for NMR spectroscopy analysis and at a ratio of 8:1 (v/v) for GC-TOF/MS analysis.

### 2.4.3 Sperm sample selection and metabolite extraction for <sup>1</sup>H-NMR

Only samples containing solely sperm cells after percoll selection (i.e., without contaminating cells) were used for metabolomic analyses. Due to the relatively low sensitivity of NMR, a high amount of cells (150 million) were needed to extract enough metabolites for each <sup>1</sup>H-NMR spectroscopy experiment. Three different pools of samples with identical phenotypes were prepared: 2 normozoospermic pools (one with n=2 and another with n=3) and 1 asthenozoospermic pool (n=4). The extracts of the first normozoospermic pool (n=2) were used to set the NMR spectrometer parameters and acquire the first <sup>1</sup>H-NMR spectra. The extracts of the other normozoospermic pool were used to perform the 1D and 2D NMR experiments for the identification of human sperm metabolites.

Simultaneously to the identification of human sperm endogenous metabolites, and in order to further explore, as a preliminary assay, if the human sperm signatures changed between different sperm sample quality, two pools of samples with 150 million sperm each one were used for <sup>1</sup>H-NMR analysis based on different motilities: one with 4 asthenozoospermic samples and the other one with 3 normozoospermic samples (percentage of motile sperm mean±SEM = 30.17±4.58 and 69.67±1.86, respectively). The third normozoospermic pool was used to setup the NMR machine and also to acquire 1D spectra for analysis (percentage of motile sperm 59.00±8.49).

Extraction of low molecular weight metabolites was performed following a previously published procedure (Lin *et al.*, 2007). Briefly, metabolites were extracted by re-suspending sperm pellets and precipitating proteins with 1 mL of cold methanol/water (2:1 v/v) solvent. After vortexing (15 sec, 3x with 15 sec incubation on ice in between each vortex), the samples were centrifuged at 12,000 g for 10 min at 4 °C. The supernatants (900 µL) were lyophilized and stored at – 80 °C.

#### 2.4.4 NMR analyses

Lyophilized extracts of 150 million sperm were resuspended in 700 µL of deuterium oxide (D<sub>2</sub>O, 99% D) containing 0.28 µg/µL of 3-(Trimethylsilyl) propionic-2,2,3,3-d<sub>4</sub> acid sodium salt (TSP; 98 atom % D) as an internal standard (0.0 ppm). After homogenization, samples were placed into 5 mm NMR tubes (Wilmad® NMR tubes 5 mm diam. precision). <sup>1</sup>H NMR spectra were recorded at 300 K on an Avance III Ultrashield Magnet 600 MHz spectrometer (Bruker, Rheinstetten, Germany) with 5 mm TCI Cryoprobe 1H[13C/15N], operating at a proton frequency of 600.20 MHz. One-dimensional <sup>1</sup>H pulse experiments were carried out using the “zgcppr” sequence with presaturation, using composite pulse to suppress the residual water peak. Solvent presaturation with irradiation power of 50 Hz was applied during recycling delay (RD = 2 s). The 90° pulse length was calibrated and was 9 ms. The spectral width was 7 kHz (12 ppm) and a total of 128 transients were collected into 36 k data points for each <sup>1</sup>H spectrum. The exponential line broadening applied before Fourier transformation was of 0.3 Hz. The frequency domain spectra were phased and baseline-corrected using TopSpin software (version 2.1, Bruker).

2D <sup>1</sup>H-<sup>1</sup>H homonuclear correlation spectroscopy (COSY) and 2D <sup>1</sup>H-<sup>13</sup>C heteronuclear single-quantum correlation (HSQC) spectroscopy were conducted to assist metabolite assignments. The acquired <sup>1</sup>H NMR spectra were phased, baseline-corrected, and referenced to the chemical shift of TSP signal at 0.0 ppm. References of pure compounds from the metabolic profiling AMIX spectra database (Bruker), Human Metabolome Database (HMDB; (Wishart *et al.*, 2007, 2013)), and Chenomx database, from Chenomx NMR Suite 7.0 (Chenomx Inc., Edmonton, Alberta, Canada) were used for metabolite identification. In addition, we assigned metabolites by COSY (<sup>1</sup>H-<sup>1</sup>H) and HSQC (<sup>1</sup>H-<sup>13</sup>C) 2D NMR experiments and by correlation with pure compounds run in-house. After baseline correction, specific <sup>1</sup>H NMR regions identified in the spectra were integrated using the AMIX 3.9 software package.

#### **2.4.5 Metabolite extraction and derivatization for GC-TOF/MS**

Seeing that the amount of sperm cells necessary to perform GC-MS is low (15 millions), individual samples (3 normozoospermic and 3 asthenozoospermic samples) were analysed. Sperm pellets were resuspended in 500 µL of cold methanol/water (8:1 v/v), followed by a quick liquid sonication (5 min) and an incubation at 4 °C during 10 min for protein precipitation. After that the samples were centrifuged at 22,640 g for 15 min at 4 °C. The supernatants were lyophilized, derivatized with methoxyamine hydrochloride, pyridine and N-methyl-N-(trimethylsilyl)trifluoroacetamide and enriched with FAMES (C8:0 to C30:0, NuChekPrep) as internal standard.

#### **2.4.6 GC-TOF/MS analysis**

Samples were automatically injected into a GC-MS system (Pegasus® 4D GCxGC-MS/TOF; LECO Corporation, St. Joseph, MI, USA). The chromatographic column was a J&W Scientific DB 5-MS stationary phase column (30 m x 0.25 mm i.d., 0.25 µm film) (Agilent Technologies, Sta. Clara, CA, USA). Mobile phase was helium. Injected sample volume was of 10 µL. Injection mode was splitless and flow rate was 1 mL/min. Injector temperature was 250 °C. Temperature gradient was held at 70 °C for 1 min, then increased to 325 °C at a rate of 10 °C/min and held at 325 °C for 9.5 min. Total time of the analysis was 36 min. Ionization performed was electron impact (EI) at 70eV. Acquisition was carried out in scan mode (mass scanning range of 35 to 700 m/z). Data analyses were performed using XCMS on-line.

#### **2.4.7 Metabolites annotation and bioinformatics analysis**

The metabolites identified with the two metabolomics techniques (<sup>1</sup>H-NMR and GC-TOF/MS) were classified according to their super class using the information available at the Human Metabolome Database version 3.6 (HMDB) website (<http://www.hmdb.ca>) (Wishart *et al.*, 2007, 2013) and PubChem Compound (<http://www.ncbi.nlm.nih.gov/pccompound>) website. The total list of metabolites was also analysed using the bioinformatic tool Metabolites Biological Role (MBRole; <http://csbg.cnb.csic.es/mbrole/>) in order to identify overrepresented or enriched biological pathways that could be putatively active (P-values < 0.05 were considered significant) (Chagoyen

and Pazos, 2011). These pathway results were based on the Small Molecule Pathway Database (SMPDB; <http://smpdb.ca>) (Frolkis *et al.*, 2010; Jewison *et al.*, 2014).

Combined analyses of protein and metabolite datasets were also performed to integrate the human sperm metabolomics data described here with the recently compiled human sperm proteome (Amaral *et al.*, 2014a), in order to investigate significantly represented pathways. Towards this goal the web based Integrated Molecular Pathway-Level Analysis (IMPALA; <http://impala.molgen.mpg.de> (Kamburov *et al.*, 2011)) was used. IMPALA combines the analysis using a comprehensive basis of biochemical pathways currently taken from 11 publicly available resources. The joint P-values (integrated with Fisher's method) and joint Q-values (the False Discovery Rate (FDR) which results from correcting the P-values for multiple testing using Benjamini and Hochberg correction) were considered significant if less than 0.01. In order to reduce the list of pathways, we restricted the results to those based on *Reactome* (Milacic *et al.*, 2012; Croft *et al.*, 2014).

#### **2.4.8 Statistical analysis**

Statistical analysis was carried out using SPSS for Mac OS (version 20.0, Chicago, IL, USA). All variables were checked for normal distribution using the one-sample Kolmogorov-Smirnov test and for variance homogeneity using Levene's test. Comparison of motility and vitality between samples (i.e., asthenozoospermic *versus* normozoospermic samples) was performed using Student's T-test. *P* values < 0.05 were considered significant.

## **CHAPTER III. RESULTS**





## CHAPTER III. RESULTS

### 3.1 Human Sperm Differential Proteomics

#### 3.1.1 Motility, vitality and P1/P2 ratio of the selected samples

As previously stated (subchapter 2.3.3), the selection of five asthenozoospermic and 5 normozoospermic samples was based on some parameters with the objective to focus as much as possible on the investigation of human sperm motility (Fig 3.1).

Therefore, the percentage of progressive motile sperm was significantly lower in asthenozoospermic samples (mean  $\pm$  SDM =  $18.7 \pm 4.33\%$ ) than in normozoospermic ones ( $70.4 \pm 0.81\%$ ;  $p = 0.008$ ), with no statistical differences in the percentage of live sperm ( $p = 0.093$ ; Fig 3.1 A). The analysis of the protamination levels of the selected samples through P1/P2 ratio, also reveal no statistical differences between asthenozoospermic (mean  $\pm$  SDM =  $1.69 \pm 0.33$ ) and normozoospermic ( $1.63 \pm 0.36$ ) samples ( $p = 0.776$ ; Fig 3.1 B).

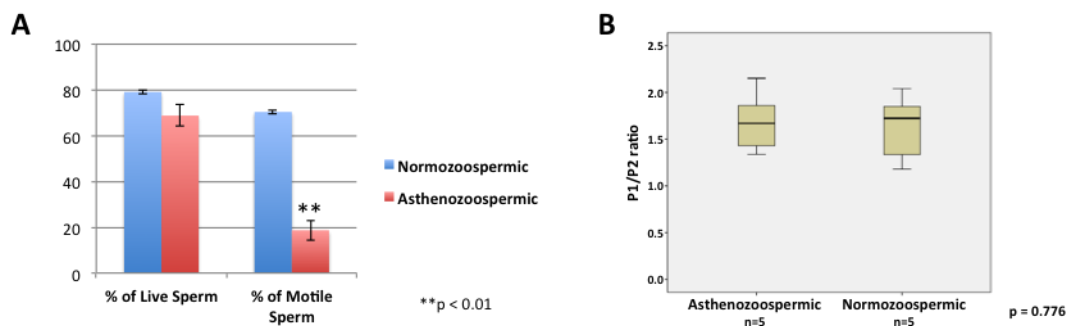


**Figure 3.1 – Motility, vitality and Protamine 1 to Protamine 2 (P1/P2) ratio of the selected samples for differential proteomic analysis.**

**(A)** 5 normozoospermic and 5 asthenozoospermic samples were selected, considering statistical significant differences on motility ( $P$  value  $< 0.01$ ) and no differences on the percentage of live sperm ( $P$  value  $> 0.05$ ; bars graph: blue – normozoospermic and red – asthenozoospermic samples). **(B)** Protamine 1 to protamine 2 (P1/P2) ratio of the 5 asthenozoospermic and 5 normozoospermic samples was also examined and no differences were found ( $p = 0.776$ ).

#### 3.1.2 Protein identification and quantification

With the aim of determining the molecular basis of human sperm motility deficiencies at the protein level, we have performed the quantitative proteomic comparison between sperm samples differing in motility, asthenozoospermic samples versus normozoospermic samples (Fig.

3.2). Noteworthy, and to the best of our knowledge, the high throughput quantitative proteomics approach employed (protein labelling using TMT 6-plex coupled to LC-MS/MS analyses) was used here for the first time to study sperm motility. LC-MS/MS resulted in the identification of a total of 1157 proteins in the pooled sperm samples (supplementary table S1) of which 29 proteins not previously described in human sperm cells comparing with the most complete proteomic lists published until date using LC-MS/MS (Baker *et al.*, 2007, 2013; de Mateo *et al.*, 2011, 2013; Amaral *et al.*, 2013a, 2014a; Wang *et al.*, 2013; Azpiazu *et al.*, 2014; Castillo *et al.*, 2014b).

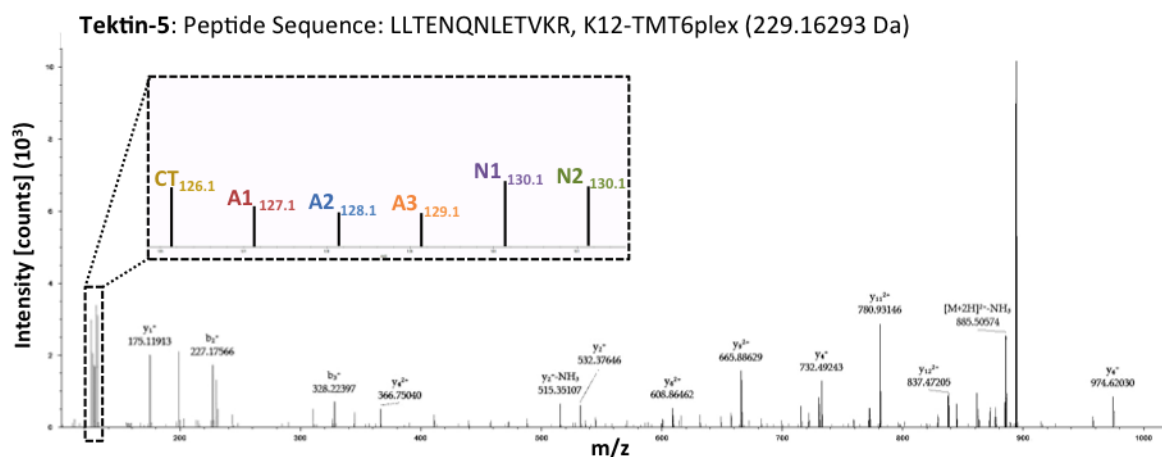


**Figure 3.2 – Representative example of a MS/MS spectrum of one peptide derived from one of the detected differential proteins (tektin-5).**

The dotted rectangle show the reporter ions region in greater detail: the intensity of each reporter ion indicates the relative proportion of the peptide in the different samples.

### 3.1.3 Differentially abundant proteins in asthenozoospermic samples

Comparison of the proteomes of asthenozoospermic and normozoospermic samples resulted in the identification of 80 differentially expressed proteins (the ratios of the protein levels of asthenozoospermics to normozoospermics - Asthenos/Normos - ranged from 0.537 to 2.491; Table 3.1). The quantification values (means  $\pm$  standard deviation) of each differential protein, together with the associated *P* values for the comparative analyses are listed in supplementary material (Supplementary table S2). Moreover, the peptides used for identification/quantification of each differential protein, along with their FDR, are also reported (Supplementary table S3).

**Table 3.1 – List of proteins detected at significantly different amounts in asthenozoospermic and normozoospermic samples.**

Results are expressed as ratios of protein levels of asthenozoospermics to normozoospermics.

<b>UniprotKB/ Swiss-Prot accession number</b>	<b>Protein name</b>	<b>Gene names</b>	<b>Ratio Asthenos/ Normos</b>
Q9P2T0	Testicular haploid expressed gene protein	THEG	0.537
Q13642	Four and a half LIM domains protein 1	FHL1; SLIM1	0.573
O95831	Apoptosis-inducing factor 1, mitochondrial	AIFM1; AIF; PDCD8	0.635
Q6UWQ5	Lysozyme-like protein 1	LYZL1; LYC2; UNQ648/PRO1278	0.656
P55060	Exportin-2	CSE1L; CAS; XPO2	0.670
Q96M32	Adenylate kinase 7	AK7	0.673
P10253	Lysosomal alpha-glucosidase	GAA	0.678
Q92526	T-complex protein 1 subunit zeta-2	CCT6B	0.688
P48047	ATP synthase subunit O, mitochondrial	ATP5O; ATPO	0.695
Q3ZCQ8	Mitochondrial import inner membrane translocase subunit TIM50	TIMM50; TIM50; PRO1512	0.703
Q96KX0	Lysozyme-like protein 4	LYZL4; LYC4	0.705
Q99798	Aconitate hydratase, mitochondrial	ACO2	0.712
P55786	Puromycin-sensitive aminopeptidase	NPEPPS; PSA	0.719
Q9H4K1	RIB43A-like with coiled-coils protein 2	RIBC2; C22orf11	0.725
Q15172	Serine/threonine-protein phosphatase 2A 56 kDa regulatory subunit alpha isoform	PPP2R5A	0.726
Q9NR28	Diablo homolog, mitochondrial	DIABLO; SMAC	0.731
P13667	Protein disulfide-isomerase A4	PDIA4; ERP70; ERP72	0.740
Q8N7U6	EF-hand domain-containing family member B	EFHB	0.741
P36776	Lon protease homolog, mitochondrial	LONP1; PRSS15	0.743
P06744	Glucose-6-phosphate isomerase	GPI	0.744
P06576	ATP synthase subunit beta, mitochondrial	ATP5B; ATPMB; ATPSB	0.748
Q96M91	Coiled-coil domain-containing protein 11	CCDC11	0.749
Q96MR6	WD repeat-containing protein 65	WDR65	0.757
P10515	Dihydrolipoyllysine-residue acetyltransferase component of pyruvate dehydrogenase complex, mitochondrial	DLAT; DLTA	0.758
Q5T655	Coiled-coil domain-containing protein 147	CCDC147; C10orf80	0.770
P36957	Dihydrolipoyllysine-residue succinyltransferase component of 2-oxoglutarate dehydrogenase complex, mitochondrial	DLST; DLTS	0.778
O75190	DnaJ homolog subfamily B member 6	DNAJB6; HSJ2; MRJ; MSJ1	0.786
Q5JVL4	EF-hand domain-containing protein 1	EFHC1	0.789
P49841	Glycogen synthase kinase-3 beta	GSK3B	0.791
Q86VP6	Cullin-associated NEDD8-dissociated protein 1	CAND1; KIAA0829; TIP120; TIP120A	0.791

Q4G0X9	Coiled-coil domain-containing protein 40	CCDC40; KIAA1640	0.792
Q9BRQ6	Coiled-coil-helix-coiled-coil-helix domain-containing protein 6, mitochondrial	CHCHD6; CHCM1	0.792
Q86Y39	NADH dehydrogenase [ubiquinone] 1 alpha subcomplex subunit 11	NDUFA11	0.793
P40939	Trifunctional enzyme subunit alpha, mitochondrial	HADHA; HADH	0.796
P41250	Glycine--tRNA ligase	GARS	0.797
P14314	Glucosidase 2 subunit beta	PRKCSH; G19P1	0.800
Q969V4	Tektin-1	TEKT1	0.812
Q14697	Neutral alpha-glucosidase AB	GANAB; G2AN; KIAA0088	0.822
Q6BCY4	NADH-cytochrome b5 reductase 2	CYB5R2	0.824
P46459	Vesicle-fusing ATPase	NSF	0.837
P11177	Pyruvate dehydrogenase E1 component subunit beta, mitochondrial	PDHB; PHE1B	0.846
Q14203	Dynactin subunit 1	DCTN1	0.846
Q93009	Ubiquitin carboxyl-terminal hydrolase 7	USP7; HAUSP	0.847
Q9NSE4	Isoleucine--tRNA ligase, mitochondrial	IARS2	0.847
Q9Y371	Endophilin-B1	SH3GLB1; KIAA0491; CGI-61	0.849
O00330	Pyruvate dehydrogenase protein X component, mitochondrial	PDHX; PDX1	0.858
Q8N1V2	WD repeat-containing protein 16	WDR16; WDRPUH	0.863
P22234	Multifunctional protein ADE2	PAICS; ADE2; AIRC; PAIS	0.867
Q15631	Translin	TSN	0.884
Q96M29	Tektin-5	TEKT5	0.892
P29218	Inositol monophosphatase 1	IMPA1; IMPA	1.107
Q9GZT6	Coiled-coil domain-containing protein 90B, mitochondrial	CCDC90B; CUA003; MDS011; MDS025	1.152
P67870	Casein kinase II subunit beta	CSNK2B; CK2N; G5A	1.199
P10606	Cytochrome c oxidase subunit 5B, mitochondrial	COX5B	1.204
Q96DE0	U8 snoRNA-decapping enzyme	NUDT16	1.211
P54652	Heat shock-related 70 kDa protein 2	HSPA2	1.219
P80303	Nucleobindin-2	NUCB2; NEFA	1.225
P20933	N(4)-(beta-N-acetylglucosaminyl)-L-asparaginase	AGA	1.249
P57105	Synaptojanin-2-binding protein	SYNJ2BP; OMP25	1.278
P30041	Peroxiredoxin-6	PRDX6; AOP2; KIAA0106	1.330
P60174	Triosephosphate isomerase	TPI1; TPI	1.333
Q8N0U8	Vitamin K epoxide reductase complex subunit 1-like protein 1	VKORC1L1	1.344
Q8NA82	Probable E3 ubiquitin-protein ligase MARCH10	MARCH10; RNF190	1.354
Q8NBU5	ATPase family AAA domain-containing protein 1	ATAD1; FNP001	1.390
P28070	Proteasome subunit beta type-4	PSMB4; PROS26	1.397
Q96AJ9	Vesicle transport through interaction with t-SNAREs homolog 1A	VT11A	1.417

Q9H4Y5	Glutathione S-transferase omega-2	GSTO2	1.449
Q8IZS6	Tctex1 domain-containing protein 3	TCTE3; TCTEX1D3	1.482
Q6UW68	Transmembrane protein 205 OS=Homo sapiens	TMEM205; UNQ501/PRO1018	1.496
P01034	Cystatin-C	CST3	1.496
P60981	Destrin	DSTN; ACTDP; DSN	1.500
P24666	Low molecular weight phosphotyrosine protein phosphatase	ACP1	1.508
Q9P0L0	Vesicle-associated membrane protein-associated protein A	VAPA; VAP33	1.515
O43674	NADH dehydrogenase [ubiquinone] 1 beta subcomplex subunit 5, mitochondrial	NDUFB5	1.566
P26885	Peptidyl-prolyl cis-trans isomerase FKBP2	FKBP2; FKBP13	1.606
Q8WY22	BRI3-binding protein	BRI3BP; KG19	1.645
P32119	Peroxiredoxin-2	PRDX2; NKEFB; TDPX1	1.875
P02649	Apolipoprotein E	APOE	1.900
P61088	Ubiquitin-conjugating enzyme E2 N	UBE2N; BLU	1.935
P15309	Prostatic acid phosphatase	ACPP	2.491

In order to obtain a comparative visualization of the levels of the differentially expressed proteins in each individual sample, results were displayed in a heat map (Fig. 3.2). Of note and with a few exceptions, similar trends for each differential protein were detected in the 5 asthenozoospermic samples when compared to the 5 normozoospermic samples, and two patterns of protein expression levels are perfectly distinguishable in the heat map. Moreover, almost all asthenozoospermic samples clustered together, forming a group distinct from that formed by normozoospermic samples (Fig. 3.3).

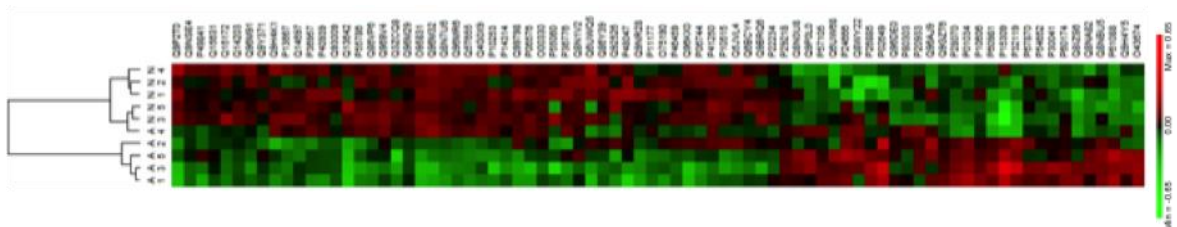


**Figure 3.3 – Heat maps of the levels of the differentially expressed proteins detected in each individual sample.**

Comparison between asthenozoospermic and normozoospermic samples. Hierarchical clustering analysis was performed according to the Pearson distance and Ward's minimum variance aggregation method.

### 3.1.4 UniProt classification of the differentially abundant proteins in asthenozoospermic samples

The categorization of the 80 differential proteins according to the information available at the Uniprot Knowledgebase concerning cellular localization (Fig. 3.4 - pie graph) revealed that the most represented groups of proteins were those localized to the *mitochondrion* (29%) and the *cytoplasm* (20%). Looking to the abundance of proteins on each cellular localization (Fig. 3.4 – bars graph), the trend between the different cellular locations was almost always the same (with exception *Cell membrane / Secreted* proteins), with a higher number of proteins in less-abundance in asthenozoospermic samples compared to normozoospermic samples.

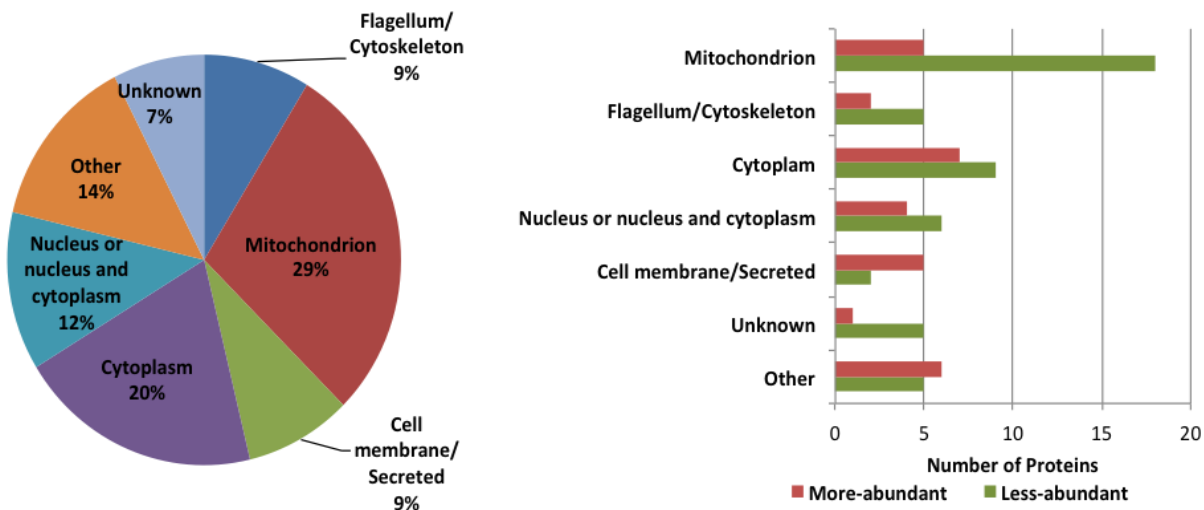


**Figure 3.4 – Classification of the differential proteins according to their subcellular localization using the information available at the UniProtKB/Swiss-Prot web site.**

The pie graph represents the percentage of deregulated proteins in asthenozoospermic samples in comparison with normozoospermic samples concerning the subcellular localization. The bars graph represents the number of deregulated proteins in asthenozoospermic samples in comparison with normozoospermic samples, which were less (green) or more (red)-abundant in asthenozoospermic samples, in each subcellular localization.

As for the main cellular functions (Fig. 3.5), a great proportion of the differential proteins have roles in *metabolism and energy production* (26% - pie graph). Besides that, some of the deregulated proteins in low motility sperm were found to be involved in functions as *sperm tail structure and motility* (6%), *signaling* (8%) and *mitochondrial maintenance* (5%; Fig. 3.5). Again, looking to the abundance of proteins on each particular function group (Fig. 3.4 – bars graph), the trend between the different cellular locations was almost always the same, with a higher number

of proteins in less-abundance in asthenozoospermic samples compared to normozoospermic samples. Interestingly, all the proteins associated with *mitochondrial maintenance* were less-abundant in asthenozoospermic samples (Fig 3.5).

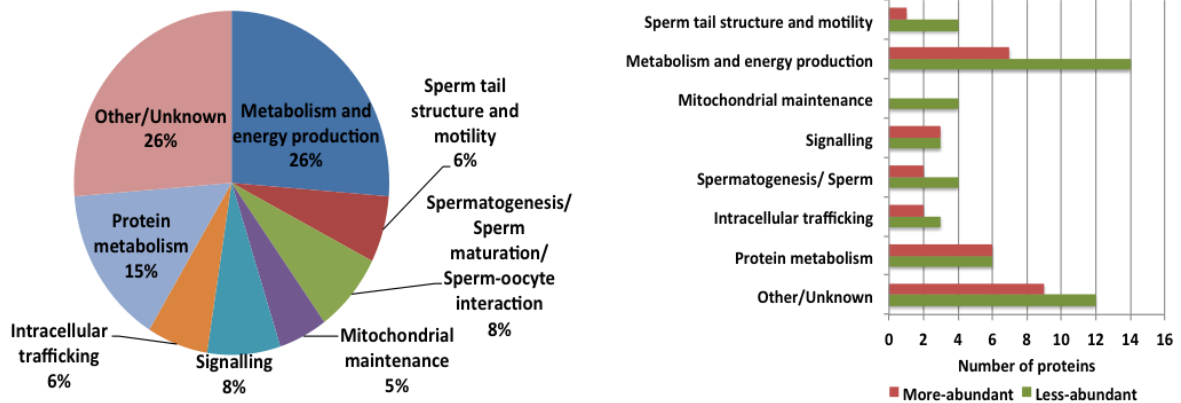


**Figure 3.5 – Classification of the differential proteins according to their main cellular function using the information available at the UniProtKB/Swiss-Prot web site.**

The pie graph represents the percentage of deregulated proteins in asthenozoospermic samples in comparison with normozoospermic samples concerning their main cellular function. The bars graph represents the number of deregulated proteins in asthenozoospermic samples in comparison with normozoospermic samples, which were less (green) or more (red)-abundant in asthenozoospermic samples, in each main cellular function.

### 3.1.5 Gene ontology terms analysis and cellular pathways enrichment analyses

The Gene Ontology (GO) terms and cellular pathways enrichment analyses confirmed that the most detected enriched GO terms related to cellular component were associated with the mitochondrion (Table 3.2; adjusted *P* values after Benjamini correction < 0.05). Concerning GO biological process terms enrichment and *Reactome* pathways analysis, almost all significant terms were related to energy metabolism, including pathways as pyruvate metabolism and TCA cycle.

**Table 3.2 – Enriched Gene Ontology terms and cellular pathways altered in low motility sperm.**

Data from asthenozoospermic *versus* normozoospermic samples were analyzed using DAVID software. *P*-values < 0.05 after Benjamini correction were considered significant.

Category	Term/Pathway	Identifier	Adjusted p-value (Benjamini correction)
<b>Gene Ontology Term Cellular Component (GOTERM_CC_FAT)</b>	Mitochondrial part	GO:0044429	3.55E-08
	Mitochondrion	GO:0005739	1.37E-06
	Mitochondrial lumen	GO:0031980	7.16E-05
	Mitochondrial matrix	GO:0005759	7.16E-05
	Mitochondrial envelope	GO:0005740	1.20E-03
	Organelle envelope	GO:0031967	1.13E-03
	Envelope	GO:0031975	9.75E-04
	Mitochondrial membrane	GO:0031966	1.36E-02
<b>Gene Ontology Term Biological Process (GO_BP_FAT)</b>	Generation of precursor metabolites and energy	GO:0006091	5.13E-05
	Pyruvate metabolic process	GO:0006090	1.18E-02
	Cell redox homeostasis	GO:0045454	3.85E-02
<b>Reactome Pathway</b>	Integration of energy metabolism	REACT_1505	1.62E-06
	Pyruvate metabolism and TCA cycle	REACT_1046	2.21E-04
	Metabolism of carbohydrates	REACT_474	2.08E-02

### 3.1.6 Western blot analysis: Tektin 1 and WDR 16

Through western blot analysis the presence of two differentially expressed proteins, tektin 1 (Tekt 1 – 55 kDa) and WD repeat-containing protein 16 (WDR 16 – 46 kDa), was also confirmed in protein extracts from independent samples: four normozoospermic (N1-N4) and four asthenozoospermic (A1-A4) samples (Fig 3.6). Moreover, the comparison of the ratios of protein level of asthenozoospermic to normozoospermic (ratio Ast/Nor) resulted in similar values tendency of those obtained by differential proteomics (ratio Ast/Nor: Tek1 = 0.908; WDR16 = 0.690).

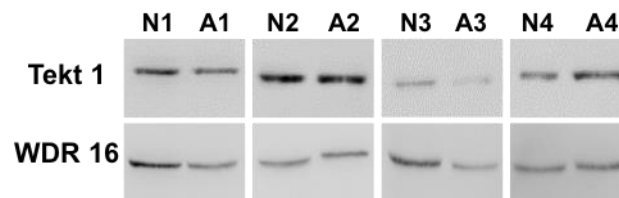


**Figure 3.6 – Immunoblotting detection of tektin 1 (Tekt 1 – 55 kDa) and WD repeat-containing protein 16 (WDR 16 – 46 kDa).**

The presence of two differentially expressed proteins were detected in protein extracts from four normozoospermic samples (N1-N4) and four asthenozoospermic samples (A1-A4).



### 3.1.7 Compiled list of differentially abundant proteins in asthenozoospermic samples

Comparing the list of the deregulated proteins indicated in table 3.1, with the compiled 109 proteins described in previous comparative proteomic studies as being differentially abundant in asthenozoospermic samples (Zhao *et al.*, 2007; Martínez-Heredia *et al.*, 2008; Chan *et al.*, 2009; Siva *et al.*, 2010; Parte *et al.*, 2012), just five proteins were common: tektin-1, inositol monophosphatase 1, heat shock-related 70 kDa protein 2, triosephosphate isomerase and prostatic acid phosphatase. This considerably increases the total list to a total of 184 deregulated proteins in asthenozoospermic samples (Supplementary table S4).

Concerning their main functions, not surprisingly the biggest percentage of deregulated proteins remain to the *metabolism and energy production* (22%) group, followed by *protein metabolism* (21%), *sperm tail structure and motility* related proteins (18%) and by the group of proteins evolved in the *spermatogenesis / sperm maturation / seminal plasma / sperm-oocyte interaction* (11%) (Fig 3.7).

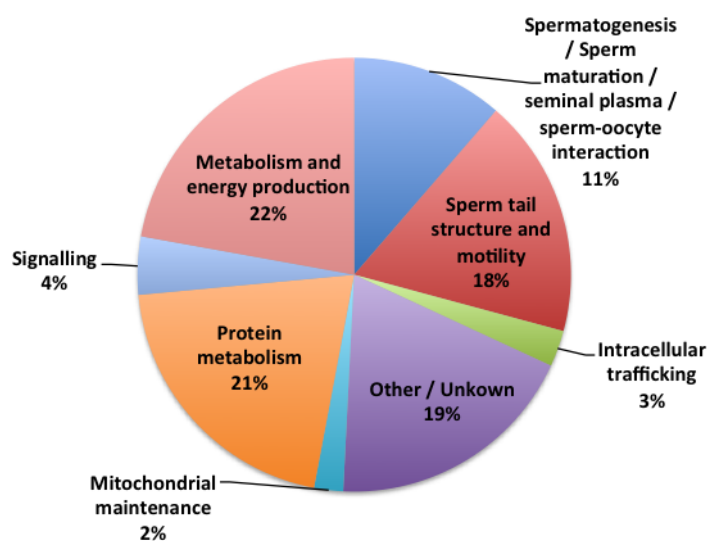


**Figure 3.7 – Classification of the compiled list of 185 differentially abundant proteins in asthenozoospermic samples according to their main cellular function using the information available at the UniProtKB/Swiss-Prot web site.**

The pie graph represents the percentage of the 185 deregulated proteins in asthenozoospermic samples in comparison with normozoospermic samples grouped according to their main cellular function.

## 3.2 Human Sperm Metabolomics

By performing two complementary untargeted metabolomics techniques, nuclear magnetic resonance (NMR) spectroscopy and gas chromatography mass spectrometry (GC/MS), we were

able to identify a total of 69 metabolites with absolute certainty, in human sperm extracts. Using NMR, 42 metabolites were identified with the information of names and structures. Additionally, evidence for 30 other potential metabolites was detected, but with insufficient spectral information to unequivocally identify them. In the case of GC-MS, 27 metabolites were identified. Evidence for additional 120 putative metabolites was also obtained, but with insufficient information to confirm their identity. These two strategies resulted in an overlap of four metabolites only (Fig 3.8).

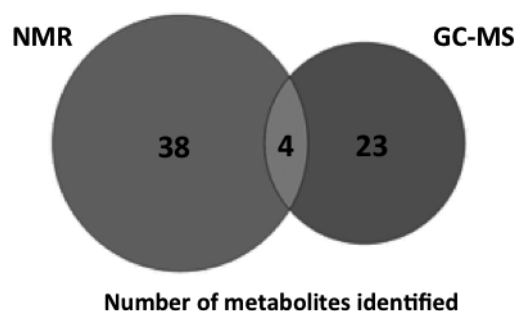


**Figure 3.8 – Total number of metabolites identified using the two untargeted metabolomics strategies (NMR and GC-MS).**

The Venn diagram represents the total number of identified metabolites using both techniques as well as the intersection between them with 4 metabolites in common.

All the metabolites identified, either by NMR or GC-MS, were identified in the two sets of samples (normozoospermic and asthenozoospermic samples).

### 3.2.1 Metabolites identified by nuclear magnetic resonance (NMR) spectroscopy

A representative  $^1\text{H}$  NMR spectrum showing the metabolic fingerprint of human sperm extracts is represented in Fig. 3.9. Glycerophosphocholine, acetylcarnitine and trimethylamine N-oxide were dominant in all human sperm extracts spectra obtained (Fig 3.9A). With this technique we were able to identify a total of 42 low weight molecules (Table 3.3).

The identity of some of these metabolites was further confirmed by 2D NMR experiments:  $^1\text{H}$ - $^1\text{H}$  homonuclear correlation spectroscopy (COSY; Fig. 3.9B) and by  $^1\text{H}$ - $^{13}\text{C}$  heteronuclear single-quantum correlation spectroscopy (HSQC; Fig. 3.9C).

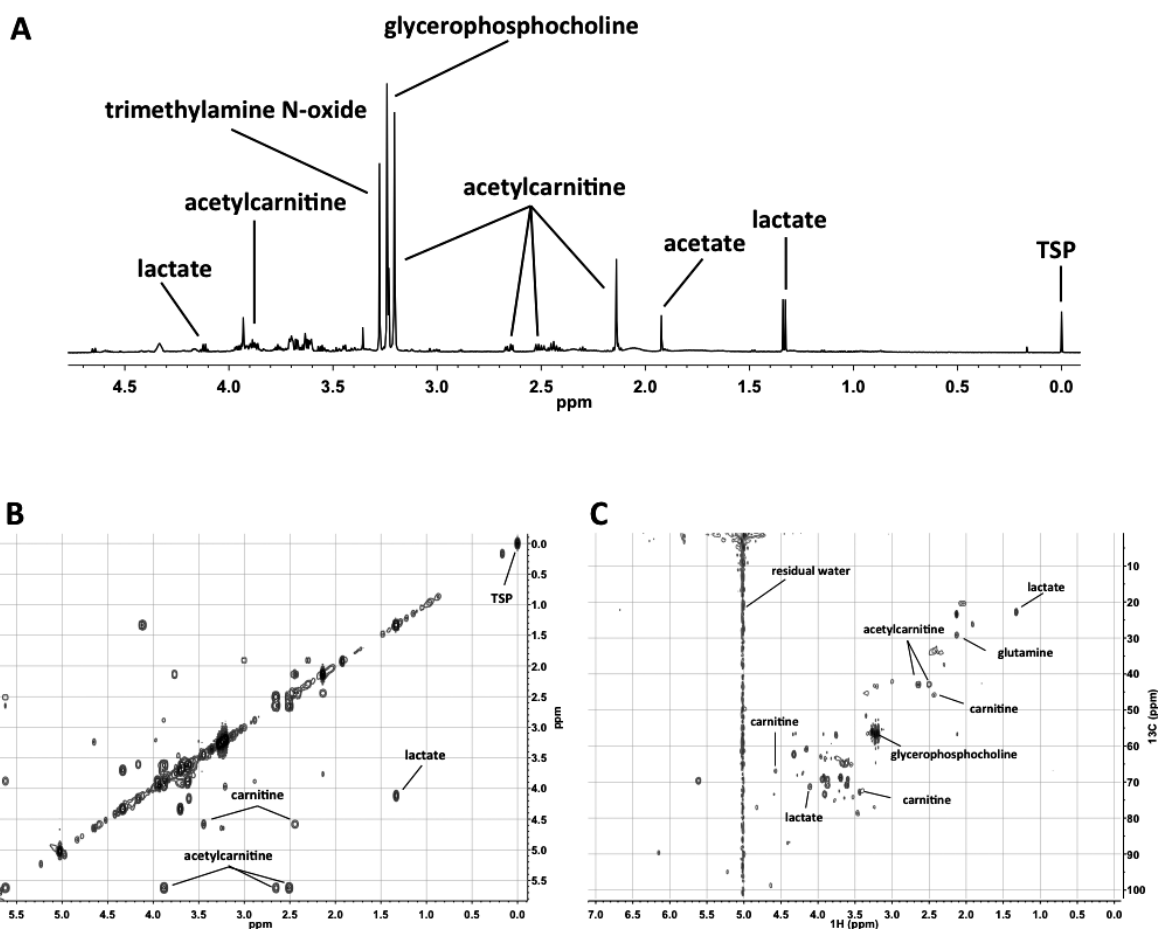


**Figure 3.9 – Representative NMR spectra (600 MHz) of extracts from human sperm cells.**

**(A)** Representative  $^1\text{H}$  NMR spectrum of extracts from a normozoospermic pool of samples. Some of the identified metabolites are indicated. **(B)** Representative 2D NMR spectra -  $^1\text{H}$ - $^1\text{H}$  homonuclear correlation spectroscopy (COSY) – of human sperm extracts from a pool of normozoospermic samples used for the confirmation of some of the metabolites assignment. **(C)** Representative 2D NMR spectra –  $^1\text{H}$ - $^{13}\text{C}$  heteronuclear single-quantum correlation (HSQC) spectroscopy – of human sperm extracts from a pool of samples, as a representative 2D HSQC NMR spectra, used for the confirmation of some of the metabolites assignment.

The classification of the metabolites identified according to their super class revealed that the majority of them belong to the *Amino acids, peptides and analogues* super class (i.e. alanine, arginine, creatine, glutamine, N-acetyltyrosine, tyrosine, valine), followed by the *Lipids* super class (acetylcarnitine, glycerophosphocholine, butyrate, caprate, caprylate, 2-methyl glutarate and 2-hydroxy-3-methylvalerate). Moreover, several *Organic acids and derivatives* (i.e. lactate, acetate, formate, glycolate, isobutyrate, azelate, 3-hydroxyisobutyrate, 2-oxoglutarate; 3-hydroxybutyrate) as well as *Aliphatic acyclic compounds* (i.e. phosphocholine, putrescine, creatinine, trimethylamine N-oxide) were identified, among others (see Table 3.3).

**Table 3.3 – Metabolites identified in human sperm extracts by NMR spectroscopy (1D and 2D).**

All of the identified metabolites were organized by super class (based on HMDB and PubChem website information). The respective HMDB ID is also present in the second column followed by the detailed information of the molecule assignments and proton (<sup>1</sup>H) and/or carbon (<sup>13</sup>C) resonances (ppm). The last column presents the type of spectra used to identify the metabolite.

Metabolites	HMDB ID	Assignment	<sup>1</sup> H		<sup>13</sup> C		Experiment
			Resonance (ppm)	Resonance (ppm)	Resonance (ppm)	Resonance (ppm)	
<b>Aliphatic Acyclic Compounds</b>							
<b>Carnitine</b>	HMDB00062	-CH <sub>2</sub> -COOH	2.43	45.68	1H, COSY, HSQC		
		-CHOH-CH <sub>2</sub>	4.58	66.78	1H, COSY, HSQC		
		(CH <sub>3</sub> ) <sub>3</sub> -N-CH <sub>2</sub>	3.42	72.82	1H, HSQC		
		-N-(CH <sub>3</sub> ) <sub>3</sub>	3.20	56.79	1H, HSQC		
<b>Methanol</b>	HMDB01875	CH <sub>3</sub> OH	3.35	51.57	1H, HSQC		
<b>O-Phosphocholine</b>	HMDB01565	HO <sub>3</sub> PO-CH-CH <sub>2</sub>	4.16	-	1H, COSY		
		(CH <sub>3</sub> ) <sub>3</sub> -N-CH <sub>2</sub>	3.60	-	1H, COSY		
		-N-(CH <sub>3</sub> ) <sub>3</sub>	3.22	-	1H, COSY		
<b>Propylene glycol</b>	HMDB01881	CH <sub>2</sub> OH-CHOH-CH <sub>3</sub>	3.49	-	1H, COSY		
<b>Putrescine</b>	HMDB01414	CH <sub>2</sub> OH-CHOH-CH <sub>3</sub>	3.87	-	1H, COSY		
		CH <sub>2</sub> OH-CHOH-CH <sub>3</sub>	1.14	-	1H		
		H <sub>2</sub> N-CH <sub>2</sub> -CH <sub>2</sub> -CH <sub>2</sub> -CH <sub>2</sub> -NH <sub>2</sub>	3.05	-	1H		
<b>Trimethylamine N-oxide</b>	HMDB00925	H <sub>2</sub> N-CH <sub>2</sub> -CH <sub>2</sub> -CH <sub>2</sub> -NH <sub>2</sub>	1.76	-	1H		
		(CH <sub>3</sub> ) <sub>3</sub> -NO <sup>+</sup>	3.27	-	1H		
<b>Creatinine</b>	HMDB00562	-C(=O)-CH <sub>2</sub> -N-	4.05	-	1H		
		CH <sub>3</sub> -N-	3.03	-	1H		
<b>Amino Acids, Peptides and Analogues</b>							
<b>2-Aminoadipate</b>	HMDB00510	HOOC-CHNH <sub>2</sub> -CH <sub>2</sub> -CH <sub>2</sub> -COOH	3.73	-	1H		
		HOOC-CHNH <sub>2</sub> -CH <sub>2</sub> -CH <sub>2</sub> -COOH	1.85	-	1H		
		HOOC-CHNH <sub>2</sub> -CH <sub>2</sub> -CH <sub>2</sub> -COOH	1.63	-	1H		
		HOOC-CHNH <sub>2</sub> -CH <sub>2</sub> -CH <sub>2</sub> -COOH	2.24	-	1H		

<b>3-Aminoisobutyrate</b>	HMDB03911	HOOC-C(CH <sub>3</sub> )HNH <sub>2</sub> -CH <sub>2</sub> -NH <sub>2</sub>	3.07	-	1H
		HOOC-C(CH <sub>3</sub> )NH <sub>2</sub> -CH <sub>2</sub> -NH <sub>2</sub>	2.59	-	1H
		HOOC-C(CH <sub>3</sub> )HNH <sub>2</sub> -CH <sub>2</sub> -NH <sub>2</sub>	1.18	-	1H
<b>4-Aminobutyrate</b>	HMDB00112	HOOC-CH <sub>2</sub> -CH <sub>2</sub> -CH <sub>2</sub> -NH <sub>2</sub>	2.99	-	1H, COSY
		HOOC-CH <sub>2</sub> -CH <sub>2</sub> -CH <sub>2</sub> -NH <sub>2</sub>	1.90	-	1H, COSY
		HOOC-CH <sub>2</sub> -CH <sub>2</sub> -CH <sub>2</sub> -NH <sub>2</sub>	2.29	-	1H
<b>Alanine</b>	HMDB00161	HOOC-C(CH <sub>3</sub> )HNH <sub>2</sub>	3.78	-	1H, COSY
		HOOC-C(CH <sub>3</sub> )HNH <sub>2</sub>	1.47	-	1H
<b>Arginine</b>	HMDB00517	HOOC-CHNH <sub>2</sub> -CH <sub>2</sub> -CH <sub>2</sub> -CH <sub>2</sub> -NH-C(=NH)-NH <sub>2</sub>	3.76	-	1H, COSY
		HOOC-CHNH <sub>2</sub> -CH <sub>2</sub> -CH <sub>2</sub> -CH <sub>2</sub> -NH-C(=NH)-NH <sub>2</sub>	1.90	-	1H, COSY
		HOOC-CHNH <sub>2</sub> -CH <sub>2</sub> -CH <sub>2</sub> -CH <sub>2</sub> -NH-C(=NH)-NH <sub>2</sub>	1.68	-	1H, COSY
		HOOC-CHNH <sub>2</sub> -CH <sub>2</sub> -CH <sub>2</sub> -CH <sub>2</sub> -NH-C(=NH)-NH <sub>2</sub>	3.24	-	1H
		HOOC-CHNH <sub>2</sub> -CH <sub>2</sub> -CH <sub>2</sub> -CH <sub>2</sub> -NH-C(=NH)-NH <sub>2</sub>	7.22	-	1H
<b>Creatine</b>	HMDB00064	HOOC-CH <sub>2</sub> -N(CH <sub>3</sub> )-C(=NH)-NH <sub>2</sub>	3.92	-	1H
		HOOC-CH <sub>2</sub> -N(CH <sub>3</sub> )-C(=NH)-NH <sub>2</sub>	3.03	-	1H
<b>Creatine phosphate</b>	HMDB01511	HOOC-CH <sub>2</sub> -N(CH <sub>3</sub> )-C(=NH)-NH-PO <sub>3</sub> H <sub>2</sub>	3.95	-	1H
		HOOC-CH <sub>2</sub> -N(CH <sub>3</sub> )-C(=NH)-NH-PO <sub>3</sub> H <sub>2</sub>	3.03	-	1H
		HOOC-CHNH <sub>2</sub> -CH <sub>2</sub> -CH <sub>2</sub> -CONH <sub>2</sub>	6.87	-	1H
<b>Glutamine</b>	HMDB00641	HOOC-CHNH <sub>2</sub> -CH <sub>2</sub> -CH <sub>2</sub> -CONH <sub>2</sub>	3.76	56.82	1H, COSY, HSQC
		HOOC-CHNH <sub>2</sub> -CH <sub>2</sub> -CH <sub>2</sub> -CONH <sub>2</sub>	2.13	28.94	1H, COSY, HSQC
		HOOC-CHNH <sub>2</sub> -CH <sub>2</sub> -CH <sub>2</sub> -CONH <sub>2</sub>	2.44	33.52	1H, HSQC
		HOOC-CHNH <sub>2</sub> -CH <sub>2</sub> -CH <sub>2</sub> -CONH <sub>2</sub>	7.59	-	1H
<b>Isoleucine</b>	HMDB00172	HOOC-CHNH <sub>2</sub> -CH-(CH <sub>3</sub> )-CH <sub>2</sub> -CH <sub>2</sub>	3.66	-	1H
		HOOC-CHNH <sub>2</sub> -CH-(CH <sub>3</sub> )-CH <sub>2</sub> -CH <sub>2</sub>	1.97	-	1H
		HOOC-CHNH <sub>2</sub> -CH-(CH <sub>3</sub> )-CH <sub>2</sub> -CH <sub>2</sub>	0.98	-	1H
		HOOC-CHNH <sub>2</sub> -CH-(CH <sub>3</sub> )-CH <sub>2</sub> -CH <sub>2</sub>	1.35	-	1H
		HOOC-CHNH <sub>2</sub> -CH-(CH <sub>3</sub> )-CH <sub>2</sub> -CH <sub>2</sub>	0.94	-	1H

<b>Leucine</b>	HMDB00687	HOOC-CHNH <sub>2</sub> -CH <sub>2</sub> -CH-(CH <sub>3</sub> )-CH <sub>3</sub>	3.73	-	1H
		HOOC-CHNH <sub>2</sub> -CH <sub>2</sub> -CH-(CH <sub>3</sub> )-CH <sub>3</sub>	1.70	-	1H
		HOOC-CHNH <sub>2</sub> -CH <sub>2</sub> -CH-(CH <sub>3</sub> )-CH <sub>3</sub>	1.71	-	1H
		HOOC-CHNH <sub>2</sub> -CH <sub>2</sub> -CH-(CH <sub>3</sub> )-CH <sub>3</sub>	0.94	-	1H
		HOOC-CHNH <sub>2</sub> -CH <sub>2</sub> -CH-(CH <sub>3</sub> )-CH <sub>3</sub>	0.96	-	1H
<b>N-Acetytyrosine</b>	HMDB00866	HO-Ar-CH <sub>2</sub> -CH(NHAc)-COOH	1.91	-	1H
		HO-Ar-CH <sub>2</sub> -CH(NHAc)-COOH	7.72	-	1H
		HO-Ar-CH <sub>2</sub> -CH(NHAc)-COOH	4.37	-	1H
		HO-Ar-CH <sub>2</sub> -CH(NHAc)-COOH	2.96	-	1H
		HO-Ar-CH <sub>2</sub> -CH(NHAc)-COOH Ortho-Ar	7.17	-	1H
		HO-Ar-CH <sub>2</sub> -CH(NHAc)-COOH Meta-Ar	6.84	-	1H
<b>Threonine</b>	HMDB00167	HOOC-CHNH <sub>2</sub> -CH(OH)-CH <sub>3</sub>	3.59	-	1H
		HOOC-CHNH <sub>2</sub> -CH(OH)-CH <sub>3</sub>	4.26	-	1H
		HOOC-CHNH <sub>2</sub> -CH(OH)-CH <sub>3</sub>	1.32	-	1H
<b>Tyrosine</b>	HMDB00158	HO-Ar-CH <sub>2</sub> -CH(NH <sub>2</sub> )-COOH	3.93	-	1H
		HO-Ar-CH <sub>2</sub> -CH(NH <sub>2</sub> )-COOH	3.11	-	1H
		HO-Ar-CH <sub>2</sub> -CH(NH <sub>2</sub> )-COOH Ortho-Ar	7.17	-	1H
		HO-Ar-CH <sub>2</sub> -CH(NH <sub>2</sub> )-COOH Meta-Ar	6.84	-	1H
<b>Valine</b>	HMDB00883	HOOC-CHNH <sub>2</sub> -CH-(CH <sub>3</sub> )-(CH <sub>3</sub> )	3.60	-	1H
		HOOC-CHNH <sub>2</sub> -CH-(CH <sub>3</sub> )-(CH <sub>3</sub> )	2.26	-	1H
		HOOC-CHNH <sub>2</sub> -CH-(CH <sub>3</sub> )-(CH <sub>3</sub> )	0.98	-	1H
		HOOC-CHNH <sub>2</sub> -CH-(CH <sub>3</sub> )-(CH <sub>3</sub> )	1.04	-	1H

### Carbohydrates and Carbohydrate Conjugates

<b>Glucose</b>	HMDB00122	a-O-CHOH-CHOH-CHOH-CHOH-CHO-CH <sub>2</sub> OH a-H1	5.22	-	1H
		b-O-CHOH-CHOH-CHOH-CHOH-CHO-CH <sub>2</sub> OH b-H1	4.63	-	1H
		a-O-CHOH-CHOH-CHOH-CHOH-CHO-CH <sub>2</sub> OH a-H2	3.52	74.2	1H, HSQC
		b-O-CHOH-CHOH-CHOH-CHOH-CHO-CH <sub>2</sub> OH b-H2	3.24	-	1H

	a-O-CHOH-CHOH-CHOH-CHOH-CHO-CH <sub>2</sub> OH a-H3	3.70	75.64	1H, HSQC
	b-O-CHOH-CHOH-CHOH-CHOH-CHO-CH <sub>2</sub> OH b-H3	3.47	-	1H
	a,b-O-CHOH-CHOH-CHOH-CHOH-CHO- a,b-H4	3.83	63.41	1H, HSQC
	a-O-CHOH-CHOH-CHOH-CHOH-CHO-CH <sub>2</sub> OH a-H5	3.81	-	1H
	a-O-CHOH-CHOH-CHOH-CHOH-CHO-CH <sub>2</sub> OH b-H5	3.47	-	1H
	a-O-CHOH-CHOH-CHOH-CHOH-CHO-CH <sub>2</sub> OH a-H6	3.83	63.41	1H, HSQC
	b-O-CHOH-CHOH-CHOH-CHOH-CHO-CH <sub>2</sub> OH b-H6	3.89	-	1H
	b-O-CHOH-CHOH-CHOH-CHOH-CHO-CH <sub>2</sub> OH b-H6'	3.74	-	1H
<b>Glycerol</b>	HMDB00131			
	CH <sub>2</sub> OH-CHOH-CH <sub>2</sub> OH	3.78	-	1H, COSY
	CH <sub>2</sub> OH-CHOH-CH <sub>2</sub> OH	3.65	-	1H, COSY
	CH <sub>2</sub> OH-CHOH-CH <sub>2</sub> OH	3.56	-	1H, COSY
<b>Lipids</b>				
<b>2-Methylglutarate</b>	HMDB00422			
	HOOC-CH(CH <sub>3</sub> )-CH <sub>2</sub> -CH <sub>2</sub> -COOH	1.06	-	1H
	HOOC-CH(CH <sub>3</sub> )-CH <sub>2</sub> -CH <sub>2</sub> -COOH	2.24	-	1H
	HOOC-CH(CH <sub>3</sub> )-CH <sub>2</sub> -CH <sub>2</sub> -COOH	1.74	-	1H
	HOOC-CH(CH <sub>3</sub> )-CH <sub>2</sub> -CH <sub>2</sub> -COOH	1.60	-	1H
	HOOC-CH(CH <sub>3</sub> )-CH <sub>2</sub> -CH <sub>2</sub> -COOH	2.16	-	1H
<b>2-hydroxy-3-methylvalerate</b>	HMDB00317			
	HOOC-CHOH-CH(CH <sub>3</sub> )-CH <sub>2</sub> -CH <sub>3</sub>	3.87	-	1H
	HOOC-CHOH-CH(CH <sub>3</sub> )-CH <sub>2</sub> -CH <sub>3</sub>	1.75	-	1H
	HOOC-CHOH-CH(CH <sub>3</sub> )-CH <sub>2</sub> -CH <sub>3</sub>	0.94	-	1H
	HOOC-CHOH-CH(CH <sub>3</sub> )-CH <sub>2</sub> -CH <sub>3</sub>	1.14	-	1H
	HOOC-CHOH-CH(CH <sub>3</sub> )-CH <sub>2</sub> -CH <sub>3</sub>	1.35	-	1H
	HOOC-CHOH-CH(CH <sub>3</sub> )-CH <sub>2</sub> -CH <sub>3</sub>	0.87	-	1H

<b>Butyrate</b>	HMDB00039	HOOC-CH <sub>2</sub> -CH <sub>2</sub> -CH <sub>3</sub>	2.15	-	1H
		HOOC-CH <sub>2</sub> -CH <sub>2</sub> -CH <sub>3</sub>	1.55	-	1H
		HOOC-CH <sub>2</sub> -CH <sub>2</sub> -CH <sub>3</sub>	0.88	-	1H
<b>Caprate</b>	HMDB00511	HOOC-CH <sub>2</sub> -CH <sub>2</sub> -CH <sub>2</sub> -CH <sub>2</sub> -CH <sub>2</sub> -CH <sub>2</sub> -CH <sub>2</sub> -CH <sub>2</sub> -CH <sub>2</sub> -CH <sub>2</sub> -CH <sub>3</sub>	0.89	-	1H
		HOOC-CH <sub>2</sub> -CH <sub>2</sub> -CH <sub>2</sub> -CH <sub>2</sub> -CH <sub>2</sub> -CH <sub>2</sub> -CH <sub>2</sub> -CH <sub>2</sub> -CH <sub>2</sub> -CH <sub>2</sub> -CH <sub>2</sub> -CH <sub>3</sub>	1.281	-	1H
		HOOC-CH <sub>2</sub> -CH <sub>2</sub> -CH <sub>2</sub> -CH <sub>2</sub> -CH <sub>2</sub> -CH <sub>2</sub> -CH <sub>2</sub> -CH <sub>2</sub> -CH <sub>2</sub> -CH <sub>2</sub> -CH <sub>3</sub>	1.260	-	1H
		HOOC-CH <sub>2</sub> -CH <sub>2</sub> -CH <sub>2</sub> -CH <sub>2</sub> -CH <sub>2</sub> -CH <sub>2</sub> -CH <sub>2</sub> -CH <sub>2</sub> -CH <sub>2</sub> -CH <sub>2</sub> -CH <sub>3</sub>	1.278	-	1H
		HOOC-CH <sub>2</sub> -CH <sub>2</sub> -CH <sub>2</sub> -CH <sub>2</sub> -CH <sub>2</sub> -CH <sub>2</sub> -CH <sub>2</sub> -CH <sub>2</sub> -CH <sub>2</sub> -CH <sub>2</sub> -CH <sub>3</sub>	1.326	-	1H
		HOOC-CH <sub>2</sub> -CH <sub>2</sub> -CH <sub>2</sub> -CH <sub>2</sub> -CH <sub>2</sub> -CH <sub>2</sub> -CH <sub>2</sub> -CH <sub>2</sub> -CH <sub>2</sub> -CH <sub>2</sub> -CH <sub>3</sub>	1.638	-	1H
		HOOC-CH <sub>2</sub> -CH <sub>2</sub> -CH <sub>2</sub> -CH <sub>2</sub> -CH <sub>2</sub> -CH <sub>2</sub> -CH <sub>2</sub> -CH <sub>2</sub> -CH <sub>2</sub> -CH <sub>2</sub> -CH <sub>3</sub>	2.357	-	1H
<b>Caprylate</b>	HMDB00482	HOOC-CH <sub>2</sub> -CH <sub>2</sub> -CH <sub>2</sub> -CH <sub>2</sub> -CH <sub>2</sub> -CH <sub>2</sub> -CH <sub>2</sub> -CH <sub>2</sub> -CH <sub>3</sub>	0.860	-	1H
		HOOC-CH <sub>2</sub> -CH <sub>2</sub> -CH <sub>2</sub> -CH <sub>2</sub> -CH <sub>2</sub> -CH <sub>2</sub> -CH <sub>2</sub> -CH <sub>2</sub> -CH <sub>3</sub>	1.308	-	1H
		HOOC-CH <sub>2</sub> -CH <sub>2</sub> -CH <sub>2</sub> -CH <sub>2</sub> -CH <sub>2</sub> -CH <sub>2</sub> -CH <sub>2</sub> -CH <sub>2</sub> -CH <sub>3</sub>	1.289	-	1H
		HOOC-CH <sub>2</sub> -CH <sub>2</sub> -CH <sub>2</sub> -CH <sub>2</sub> -CH <sub>2</sub> -CH <sub>2</sub> -CH <sub>2</sub> -CH <sub>2</sub> -CH <sub>3</sub>	1.318	-	1H
		HOOC-CH <sub>2</sub> -CH <sub>2</sub> -CH <sub>2</sub> -CH <sub>2</sub> -CH <sub>2</sub> -CH <sub>2</sub> -CH <sub>2</sub> -CH <sub>2</sub> -CH <sub>3</sub>	1.591	-	1H
		HOOC-CH <sub>2</sub> -CH <sub>2</sub> -CH <sub>2</sub> -CH <sub>2</sub> -CH <sub>2</sub> -CH <sub>2</sub> -CH <sub>2</sub> -CH <sub>2</sub> -CH <sub>3</sub>	2.144	-	1H
<b>O-Acetylcarnitine</b>	HMDB00201	HOOC-CH <sub>2</sub> -CHOAc-CH <sub>2</sub> -N <sup>+</sup> (CH <sub>3</sub> ) <sub>3</sub>	3.18	56.44	1H, HSQC
		HOOC-CH <sub>2</sub> -CHOAc-CH <sub>2</sub> -N <sup>+</sup> (CH <sub>3</sub> ) <sub>3</sub>	3.84	70.72	1H, HSQC
		HOOC-CH <sub>2</sub> -CHOAc-CH <sub>2</sub> -N <sup>+</sup> (CH <sub>3</sub> ) <sub>3</sub>	3.59	70.72	1H, HSQC
		HOOC-CH <sub>2</sub> -CHOAc-CH <sub>2</sub> -N <sup>+</sup> (CH <sub>3</sub> ) <sub>3</sub>	5.59	-	1H
		HOOC-CH <sub>2</sub> -CHOAc-CH <sub>2</sub> -N <sup>+</sup> (CH <sub>3</sub> ) <sub>3</sub>	2.50	43.84	1H, HSQC
		HOOC-CH <sub>2</sub> -CHOAc-CH <sub>2</sub> -N <sup>+</sup> (CH <sub>3</sub> ) <sub>3</sub>	2.63	43.84	1H, HSQC
		HOOC-CH <sub>2</sub> -CHOAc-CH <sub>2</sub> -N <sup>+</sup> (CH <sub>3</sub> ) <sub>3</sub>	2.13	23.24	1H, HSQC
		HOOC-CH <sub>2</sub> -CHOAc-CH <sub>2</sub> -N <sup>+</sup> (CH <sub>3</sub> ) <sub>3</sub>	3.21	56.74	1H, COSY, HSQC
<b>sn-Glycero-3-phosphocholine</b>	HMDB00086	GlyPO-CH <sub>2</sub> -CH <sub>2</sub> -N <sup>+</sup> (CH <sub>3</sub> ) <sub>3</sub>	3.66	64.67	1H, COSY, HSQC
		CH <sub>2</sub> OH-CHOH-CH <sub>2</sub> OPcho	3.90	73.51	1H, COSY, HSQC
		CH <sub>2</sub> OH-CHOH-CH <sub>2</sub> OPcho	3.87	69.14	1H, COSY, HSQC



GlyPO<sub>3</sub>-CH<sub>2</sub>-CH<sub>2</sub>-N<sup>+</sup>(CH<sub>3</sub>)<sub>3</sub> 4.32 62.35 1H, COSY, HSQC  
 GlyPO<sub>3</sub>-CH<sub>2</sub>-CH<sub>2</sub>-N<sup>+</sup>(CH<sub>3</sub>)<sub>3</sub> 3.67 68.57 1H, COSY, HSQC

### Nucleosides, Nucleotides, and Analogues

#### ADP

HMDB01341

H<sub>2</sub>OPO<sub>3</sub>-O<sub>3</sub>HPO-CH<sub>2</sub>-CHO-CHOH-CHOH-- 4.08 - 1H  
 H<sub>2</sub>OPO<sub>3</sub>-O<sub>3</sub>HPO-CH<sub>2</sub>-CHO-CHOH-CHOH-- 4.14 - 1H  
 H<sub>2</sub>OPO<sub>3</sub>-O<sub>3</sub>HPO-CH<sub>2</sub>-CHO-CHOH-CHOH- 4.12 - 1H  
 (H<sub>2</sub>O<sub>3</sub>P)<sub>2</sub>-CH<sub>2</sub>-CHO-CHOH-CHOH-CHO-N- 4.22 - 1H  
 (H<sub>2</sub>O<sub>3</sub>P)<sub>2</sub>-CH<sub>2</sub>-CHO-CHOH-CHOH-CHO-N-Ad 4.58 - 1H  
 (H<sub>2</sub>O<sub>3</sub>P)<sub>2</sub>-CH<sub>2</sub>-CHO-CHOH-CHOH-CHO-N-Ad 5.94 - 1H  
 Rib-Adenina H2 8.54 - 1H  
 Rib-Adenina H7 8.30 - 1H

#### AMP

HMDB00045

H<sub>2</sub>OPO<sub>3</sub>-CH<sub>2</sub>-CHO-CHOH-CHOH-- 4.04 - 1H  
 H<sub>2</sub>OPO<sub>3</sub>-CH<sub>2</sub>-CHO-CHOH-CHOH-- 4.37 - 1H  
 H<sub>2</sub>OPO<sub>3</sub>-CH<sub>2</sub>-CHO-CHOH-CHOH- 4.51 - 1H  
 H<sub>2</sub>OPO<sub>3</sub>-CH<sub>2</sub>-CHO-CHOH-CHOH-CHOH-N-Ad 4.77 - 1H  
 H<sub>2</sub>OPO<sub>3</sub>-CH<sub>2</sub>-CHO-CHOH-CHOH-CHOH-N-Ad 6.13 - 1H  
 Rib-Adenina H2 8.55 - 1H  
 Rib-Adenina H7 8.16 - 1H

#### IMP

HMDB00175

H<sub>2</sub>OPO<sub>3</sub>-CH<sub>2</sub>-CHO-CHOH-CHOH-- 4.02 - 1H  
 H<sub>2</sub>OPO<sub>3</sub>-CH<sub>2</sub>-CHO-CHOH-CHOH-- 4.36 - 1H  
 H<sub>2</sub>OPO<sub>3</sub>-CH<sub>2</sub>-CHO-CHOH-CHOH- 4.51 - 1H  
 H<sub>2</sub>OPO<sub>3</sub>-CH<sub>2</sub>-CHO-CHOH-CHOH-CHOH-N-  
 Inosine 4.78 - 1H  
 H<sub>2</sub>OPO<sub>3</sub>-CH<sub>2</sub>-CHO-CHOH-CHOH-CHOH-CHOH-N-  
 Inosine 6.12 - 1H  
 Rib-Inosine H2 8.54 - 1H  
 Rib-Adenina H7 8.14 - 1H

### Organic Acids and Derivatives

<b>3-Hydroxyisobutyrate</b>	HMDB00023	HO-CH <sub>2</sub> -CH(CH <sub>3</sub> )-COOH	1.05	-	1H
		HO-CH <sub>2</sub> -CH(CH <sub>3</sub> )-COOH	2.48	-	1H
		HO-CH <sub>2</sub> -CH(CH <sub>3</sub> )-COOH	3.61	-	1H
<b>2-Oxoglutarate</b>	HMDB00208	HOOC-CH <sub>2</sub> -CH <sub>2</sub> -C(=O)-COOH	2.44	-	1H
		HOOC-CH <sub>2</sub> -CH <sub>2</sub> -C(=O)-COOH	2.99	-	1H
<b>3-Hydroxybutyrate</b>	HMDB00357	HOOC-CH <sub>2</sub> -CHOH-CH <sub>3</sub>	2.29	-	1H
		HOOC-CH <sub>2</sub> -CHOH-CH <sub>4</sub>	2.40	-	1H
		HOOC-CH <sub>2</sub> -CHOH-CH <sub>4</sub>	4.14	-	1H
		HOOC-CH <sub>2</sub> -CHOH-CH <sub>5</sub>	1.19	-	1H
		CH <sub>3</sub> COO <sup>-</sup>	1.91	-	1H
<b>Azelate</b>	HMDB00784	HOOC-CH <sub>2</sub> -CH <sub>2</sub> -CH <sub>2</sub> -CH <sub>2</sub> -CH <sub>2</sub> -CH <sub>2</sub> -COOH	1.32	-	1H, COSY
		HOOC-CH <sub>2</sub> -CH <sub>2</sub> -CH <sub>2</sub> -CH <sub>2</sub> -CH <sub>2</sub> -CH <sub>2</sub> -COOH	1.56	-	1H, COSY
		HOOC-CH <sub>2</sub> -CH <sub>2</sub> -CH <sub>2</sub> -CH <sub>2</sub> -CH <sub>2</sub> -CH <sub>2</sub> -COOH	2.20	-	1H
<b>Formate</b>	HMDB00142	HO-C(=O)-H	8.45	-	1H
<b>Glycolate</b>	HMDB00115	HOOC-CH <sub>2</sub> -OH	3.93	64.00	1H, HSQC
<b>Isobutyrate</b>	HMDB01873	HOOC-CH(CH <sub>3</sub> )-CH <sub>3</sub>	1.05	-	1H, COSY
		HOOC-CH(CH <sub>3</sub> )-CH <sub>3</sub>	2.38	-	1H
<b>Lactate</b>	HMDB00190	HOOC-CH(CH <sub>3</sub> )-OH	1.32	22.90	1H, COSY, HSQC
		HOOC-CH(CH <sub>3</sub> )-OH	4.11	71.37	1H, HSQC

### **3.2.2 Metabolites identified by mass spectroscopy (MS)**

Using the GC-MS approach we were able to identify 27 metabolites in human sperm sample extracts (Table 3.4). Of these, only 4 were also identified by NMR: carnitine, L-threonine, gamma-aminobutyric acid and oxoglutaric acid). Importantly, by using MS, we were able to add two more amino acids (glycine and serine) to the list of sperm metabolites, making this class in the most represented overall from the total list of low weigh molecules described in human sperm extracts (see below). We have also detected five lipids (cholesterol, palmitoleic acid, demosterol, 2-monopalmitin, mercaptoacetic acid), which substantially increased the number of total lipids identified.

**Table 3.4 – Metabolites identified from human sperm extracts by GC-TOF/MS.**

The identified metabolites were organized by super classes (based on HMDB and PubChem website information). The CAS numbers were also included as well as the chemical formula of the identified compounds since they were valuable information on the classification of the metabolites. The matched name and HMDB ID are also indicated. The last columns show the retention time (R.T.) values and unique mass of the compounds identified by GC-TOF/MS.

Name	CAS Number	Formula	Match	HMDB ID	R.T.	Unique Mass
<b>Aliphatic Acyclic Compounds</b>						
Carnitine	541-15-1	C <sub>7</sub> H <sub>15</sub> NO <sub>3</sub>	L-Carnitine	HMDB00062	10.242	117
cyclohexane-1,2,3,4,5,6-hexol	6917-35-7	C <sub>6</sub> H <sub>12</sub> O <sub>6</sub>	Scyllitol	HMDB06088	18.773	318
2-aminoethan-1-ol	9007-33-4	C <sub>2</sub> H <sub>7</sub> NO	Ethanolamine	HMDB00149	10.137	174
<b>Amino Acids, Peptides, and Analogues</b>						
Serine	302-84-1	C <sub>3</sub> H <sub>7</sub> NO <sub>3</sub>	L-Serine	HMDB00187	10.615	116
L-Threonine	72-19-5	C <sub>4</sub> H <sub>9</sub> NO <sub>3</sub>	L-Threonine	HMDB00167	11.048	130
Glycine	56-40-6	C <sub>2</sub> H <sub>5</sub> NO <sub>2</sub>	Glycine	HMDB00123	11.222	174
4-aminobutanoic acid	56-12-2	C <sub>4</sub> H <sub>9</sub> NO <sub>2</sub>	Gamma-Aminobutyric acid	HMDB00112	14.008	174
<b>Carbohydrates and Carbohydrate Conjugates</b>						
d-Ribose	50-69-1	C <sub>5</sub> H <sub>10</sub> O <sub>5</sub>	D-Ribose	HMDB00283	15.718	217
Mannonic acid,delta-lactone	40600-45-1	C <sub>6</sub> H <sub>10</sub> O <sub>6</sub>	-	-	23.377	217
2,4,5,6-tetrahydroxy-3-oxohexanal	-	C <sub>6</sub> H <sub>10</sub> O <sub>6</sub>	Hexos-3-ulose	-	18.130	205
<b>Lipids</b>						
Cholesterol	57-88-5	C <sub>27</sub> H <sub>46</sub> O	Cholesterol	HMDB00067	28.295	129
Mercaptoacetic acid	68-11-1	CH <sub>4</sub> O <sub>2</sub> S	-	-	20.585	147
2-Monopalmitin	23470-00-0	C <sub>19</sub> H <sub>38</sub> O <sub>4</sub>	-	-	25.147	218
Demosterol	313-04-2	C <sub>27</sub> H <sub>44</sub> O	-	HMDB02719	28.607	129
Palmitoleic acid	373-49-9	C <sub>16</sub> H <sub>30</sub> O <sub>2</sub>	Palmitoleic acid	HMDB03229	34.475	129

Nucleosides, Nucleotides and Analogues						
uridine-5'-monophosphate	58-97-9	C <sub>9</sub> H <sub>13</sub> N <sub>2</sub> O <sub>9</sub> P	Uridine 5'-monophosphate	HMDB00288	27.368	169
Organic Acids and Derivatives						
2-Ketoglutaric acid	328-50-7	C <sub>5</sub> H <sub>6</sub> O <sub>5</sub>	Oxoglutaric acid	HMDB00208	17.540	173
Other / Unknown						
2-Hydroxyethyl disulfide	1892-29-1	C <sub>4</sub> H <sub>10</sub> O <sub>2</sub> S <sub>2</sub>	-	-	28.153	119
3-ethyl-3,5,5-trimethylcyclohex-1-en-1-ol	-	C <sub>11</sub> H <sub>20</sub> O	-	-	9.808	211
1-Phenyl-2-propylamine	96332-84-2	C <sub>9</sub> H <sub>13</sub> N	Amphetamine	HMDB14328	14.877	188
Phosphoric acid monomethyl ester	812-00-0	CH <sub>5</sub> O <sub>4</sub> P	methylphosphate	HMDB61711	9.702	241
Nonanamide	1120-07-6	C <sub>9</sub> H <sub>19</sub> NO	-	-	22.395	59
7-Chloro-1,3,4,10-tetrahydro-10-hydroxy-1-[2-[1-pyrrolidiny]ethyl]imino]-3-[3-(trifluoromethyl)phenyl]-9(2H)-acridinone	-	C <sub>26</sub> H <sub>25</sub> ClF <sub>3</sub> N <sub>3</sub> O <sub>2</sub>	-	-	13.702	84
4-[(E)-1-oxidanylpent-1-enyl]phenol	-	C <sub>11</sub> H <sub>14</sub> O <sub>2</sub>	-	-	19.092	293
b-(4-Hydroxyphenyl)lactic acid	306-23-0	C <sub>9</sub> H <sub>10</sub> O <sub>4</sub>	Hydroxyphenyllactic acid	HMDB00755	18.047	180
Phosphoric acid	7664-38-2	H <sub>3</sub> PO <sub>4</sub>	Phosphoric acid	HMDB02142	10.762	301
2-aminoethyl dihydrogen phosphate	1071-23-4	C <sub>2</sub> H <sub>8</sub> NO <sub>4</sub> P	O-Phosphoethanolamine	HMDB00224	16.878	174

### 3.2.3 Overall metabolite Super Class and enriched gene ontology term pathways

As already stated all metabolites identified by the two complementary techniques were categorized in super classes according to the information available in the HMDB and PubChem database (Fig. 3.10 and Tables 3.3 and 3.4). The more represented super classes of metabolites were the *Amino acids, peptides and analogues* with a total of 18 metabolites (14 by  $^1\text{H-NMR}$  and 4 by GC-MS) followed by *Lipids* super class with a total of 12 metabolites (7 by  $^1\text{H-NMR}$  and 5 by GC-MS). Some *Organic acids and derivatives* were also identified (8 by  $^1\text{H-NMR}$  and 1 by both techniques).

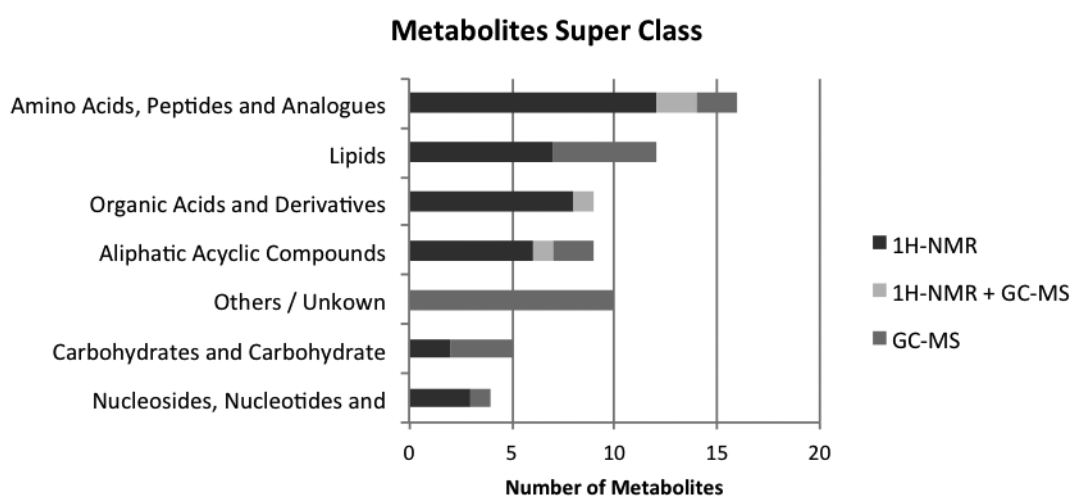


**Figure 3.10 – Number of metabolites identified per class with the two complementary techniques.**

A total of 69 metabolites were identified by  $^1\text{H-NMR}$  spectroscopy (dark gray), by GC-MS (middle gray) or by both techniques (light gray) and were classified according to their super class using the information available at the Human Metabolome Database (HMDB) and Pubchem websites.

Among other pathways the Gene Ontology (GO) terms and cellular pathways enrichment analyses performed with MBRole revealed the metabolism of some amino acids (such as alanine, glycine, serine, threonine), the glucose/alanine cycle, beta-oxidation of very long chain fatty acids and gluconeogenesis as important metabolic pathways for the human sperm processes (Table 3.5; P values < 0.05).

**Table 3.5 – Overrepresented pathways using the metabolites identified in human sperm extracts.**

All the metabolites identified, through the correspondent human metabolome database (HMDB) codes, were analysed using the bioinformatics tool MBRole to perform an overrepresentation analysis for the cellular pathways, based on the small molecule pathway database (SMPDB). P-values < 0.05 were considered significant.

SMPDB Pathway	P value	Compounds
Transcription/Translation	7.30E-08	HMDB00288 HMDB00641 HMDB00517 HMDB00161 HMDB00167 HMDB00158 HMDB00883 HMDB00172 HMDB00687 HMDB00045
Urea Cycle	1.36E-04	HMDB00641 HMDB00161 HMDB00517 HMDB00045 HMDB00208 HMDB01341
Ammonia Recycling	7.94E-04	HMDB00208 HMDB01341 HMDB00641 HMDB00123 HMDB00187
Beta Oxidation of Very Long Chain Fatty Acids	0.003	HMDB00511 HMDB00062 HMDB00482 HMDB00201
Glucose-Alanine Cycle	0.014	HMDB00122 HMDB00208 HMDB00161
Alanine Metabolism	0.027	HMDB00161 HMDB00208
Gluconeogenesis	0.029	HMDB00190 HMDB00122 HMDB01341 HMDB00208
Glycine, Serine and Threonine Metabolism	0.026	HMDB00123 HMDB00187 HMDB00064 HMDB00167
Glutamate Metabolism	0.043	HMDB00641 HMDB00208 HMDB00112

### 3.3 Combined analysis of the human sperm proteome and metabolites

The combined analysis of the metabolites identified in this work together with the recently compiled human sperm proteome (Amaral *et al.*, 2014a) (performed with IMPaLA) resulted in a very large number of enriched cellular pathways. Therefore, we decided to restrict the list to those having a joint false discovery rate value after Benjamini's correction < 1 % and at least two metabolites identified per pathway, and finally, by limiting the results only to the *Reactome* identified pathways. By doing so and as expected, *Metabolism* turned out to be the most significant pathway (Table 3.6; P=3.15E-49; Q=8.96E-46). The most significant subtypes of metabolism detected were: the metabolism of carbohydrates (Q=3.35E-14), the metabolism of lipids and lipoproteins (Q=1.62E-07), the citric acid (TCA) cycle and respiratory electron transport (Q=1.66E-27), the metabolism of nucleotides (Q=3.48E-08), the metabolism of amino acids and derivatives (Q=3.77E-12), and biological oxidations (Q=2.47E-05). There were also some other pathways significantly overrepresented (Table 3.6): transmembrane transport of small molecules (Q=3.6E-11), transport of glucose and other sugars, bile salts and organic acids, metal ions and amine compounds (1.08E-07), and signal transduction (Q=9.70E-05).

**Table 3.6 – Combined analysis of the human sperm proteome and the identified metabolites.**

A selection of some of the most statistically significant Reactome pathways derived from the analysis of the compiled list of human sperm proteins (Amaral et al., 2014) and the metabolites identified in the present work. P values (after Fisher's method) and Q values less than 0.01 were considered significant. The P and Q values are derived from the joint analysis (proteins and metabolites). The number of overlapping proteins and metabolites considered in each pathway are also indicated.

Reactome pathway	Number of overlapping proteins	Number of overlapping metabolites	P value (Fisher's method)	Q value (Benjamini's correction)
<b>METABOLISM</b>	<b>750</b>	<b>35</b>	<b>3.15E-49</b>	<b>8.96E-46</b>
<b>Metabolism of carbohydrates</b>	<b>154</b>	<b>6</b>	<b>4.59E-16</b>	<b>3.35E-14</b>
Glucose metabolism	55	5	2.94E-16	2.38E-14
Gluconeogenesis	27	4	6.79E-10	1.50E-08
Glycogen breakdown (glycogenolysis)	14	3	4.39E-07	5.11E-06
<b>Metabolism of lipids and lipoproteins</b>	<b>228</b>	<b>17</b>	<b>1.04E-08</b>	<b>1.62E-07</b>
Phospholipid metabolism	74	8	5.05E-09	8.15E-08
Glycerophospholipid biosynthesis	44	8	4.75E-07	5.51E-06
Peroxisomal lipid metabolism	16	5	1.08E-05	8.72E-05
Fatty acid, triacylglycerol and ketone body metabolism	51	5	6.83E-05	0.000455
Cholesterol biosynthesis	14	5	0.000161	0.000909
Triglyceride Biosynthesis	25	4	0.000173	0.000964
Lipid digestion, mobilization and transport	25	4	0.000463	0.00238
Beta-oxidation of very long chain fatty acids	6	2	0.000765	0.00368
Mitochondrial Fatty Acid Beta-Oxidation	12	2	0.00203	0.00825
<b>The citric acid (TCA) cycle and respiratory electron transport</b>	<b>112</b>	<b>5</b>	<b>1.75E-30</b>	<b>1.66E-27</b>
Pyruvate metabolism and Citric Acid (TCA) cycle	35	4	2.94E-11	9.60E-10
Citric acid cycle (TCA cycle)	19	3	2.06E-09	3.60E-08
Pyruvate metabolism	16	3	5.07E-06	4.53E-05
<b>Metabolism of nucleotides</b>	<b>54</b>	<b>8</b>	<b>1.97E-09</b>	<b>3.48E-08</b>
Purine metabolism	25	6	7.54E-07	8.37E-06
<b>Metabolism of amino acids and derivatives</b>	<b>80</b>	<b>20</b>	<b>7.70E-14</b>	<b>3.77E-12</b>
Creatine metabolism	4	7	1.13E-07	1.39E-06
Metabolism of polyamines	10	4	0.000406	0.00214
Urea cycle	6	4	0.000725	0.00352
<b>Biological oxidations</b>	<b>46</b>	<b>18</b>	<b>2.66E-06</b>	<b>2.47E-05</b>
<b>OTHERS</b>				
<b>Transmembrane transport of small molecules</b>	<b>205</b>	<b>23</b>	<b>8.58E-13</b>	<b>3.64E-11</b>



Transport of glucose and other sugars, bile salts and organic acids, metal ions and amine compounds	22	14	6.80E-09	1.08E-07
Signal Transduction	516	15	1.22E-05	9.70E-05

### 3.4 Comparison of metabolic signatures of normozoospermic and asthenozoospermic pool of samples

As preliminary analysis, the comparison of the metabolic fingerprint ( $^1\text{H-NMR}$  spectra) of a normozoospermic pool of samples (150 million sperm) and an asthenozoospermic pool of samples (150 million sperm) was done. The metabolic signatures of the different pools revealed to be similar, with the same majority metabolites. However, the concentrations (i.e. intensity of the picks) of some of the metabolites were different (Fig 3.11).

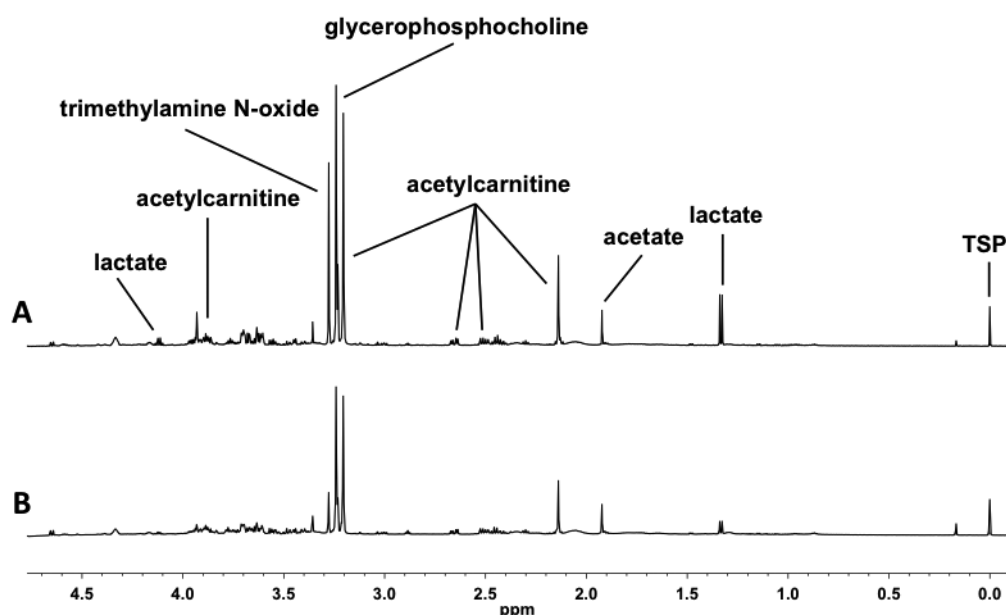


**Figure 3.11 – Representative  $^1\text{H-NMR}$  spectra (600 MHz) of extracts from human sperm cells.**

(A)  $^1\text{H-NMR}$  spectrum of extracts from normozoospermic pool of samples. (B)  $^1\text{H-NMR}$  spectrum of extracts from asthenozoospermic pool of samples. Some of the identified quantified metabolites are indicated. Both spectra have the same reference (3-(Trimethylsilyl) propionic-2,2,3,3- $\text{d}_4$  acid sodium salt - TSP) with the same peak intensity as the concentration added was the same in the two pools of samples.

In order to visualize which metabolites were present in different amount in asthenozoospermic pool compared to normozoospermic pool, the ratio of metabolite concentrations asthenozoospermic to normozoospermic was calculated and logarithmized ( $\text{Log}_{10}([\text{Astheno}]/[\text{Normo}])$ ) (Fig 3.12).

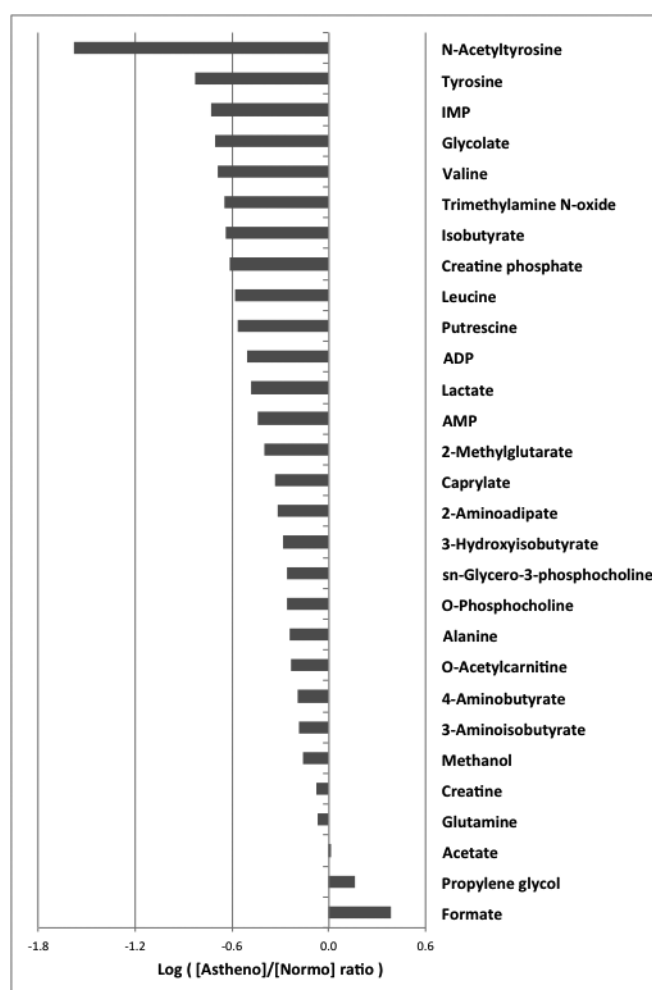


**Figure 3.12 – Metabolites identified in variable concentration in the asthenozoospermic pool of samples compared to the normozoospermic pool of samples.**

The graph represents the logarithmic concentrations ratio of metabolites quantified in asthenozoospermic to normozoospermic pools of samples ( $\text{Log}_{10} ([\text{Asthen}]/[\text{Normo}])$ ). The metabolites with ratio equal to zero were excluded from the graphic.

The N-Acetyltyrosine appeared as the metabolite less abundant in asthenozoospermic pool ( $\text{Log}_{10}$  ratio = -1.58) with the higher difference between the two pools of samples, followed by others such as, tyrosine, trimethylamine N-oxide, putrescine, sn-glycero-3-phosphocholine and O-acetylcarnitine (log ratios = -0.83; -0.65; -0.57; -0.26 and -0.26 respectively) ( $\text{Log}_{10}$  3.10). Not surprisingly, the majority of the quantified metabolites were present in lower concentration in the asthenozoospermic pool compared to the normozoospermic pool of samples (Fig 3.11 and 3.12), including the quantified IMP, AMP and ADP ( $\text{Log}_{10}$  ratios = -0.73; -0.44 and -0.51, respectively). On the other hand, acetate, propylene glycol and formate were detected in higher concentration in the asthenozoospermic pool extracts ( $\text{Log}_{10}$  ratios = 0.02; 0.16; 0.39, respectively) (Fig 3.12).

## **CHAPTER IV. DISCUSSION**



## CHAPTER IV. DISCUSSION

### 4.1 Human sperm differential proteomics – insights about human sperm motility

Determining what distinguishes motile from immotile sperm at the proteome level is a crucial approach to appreciate which proteins and cellular pathways play a role in male gamete motility regulation. In this study we have used, for the first time, protein TMT labelling coupled to LC-MS/MS to compare the proteome of sperm samples differing in motility. The results of this study were further confirmed by a complementary strategy (Amaral *et al.*, 2014b). Briefly, five normozoospermic samples were fractionated in two sperm subpopulations (one more motile and one less motile) using the swim-up technique, conventionally used in the clinic following the WHO recommendations (WHO, 2010). After that, protein extraction, TMT labelling and LC-MS/MS were identical to what was done in the experiments described here (sub-chapter 2.3).

It is important to note that the samples used for this experiment were carefully selected with the main objective of focus our study exclusively in human sperm motility. Keeping this in mind, we have tried to exclude the influence of other parameters, such as contamination with other cells, morphology, vitality and also P1/P2 ratio. The reasoning behind the investigation of this last parameter was the possible influence that different protamine levels can have in nuclear DNA conformation, interfering not only in DNA damage status but also in head shape, thus potentially disturbing sperm motility. In fact, on the literature we can find some studies indicating a possible correlation between altered levels of protamines and decreased sperm motility (Mengual *et al.*, 2003; Aoki *et al.*, 2006). However, in our selected samples there was no difference between the P1/P2 ratio of the asthenozoospermic and the normozoospermic ones groups.

Interestingly, the categorization of the 80 differential proteins according their cellular localization showed that many of the deregulated proteins (29%) are localized to mitochondria, and the majority of them were founded as less-abundant in asthenozoospermic samples. As expected, we have also found proteins related to flagellum/ cytoskeleton as deregulated and less-abundant in sperm with motility disruption. In fact, the involvement of structural proteins (i.e. tektins) in sperm motility is well documented and thus finding two members of this family in the list of differential proteins was unsurprising. Tektins are structural components of flagellar and ciliary microtubules, with a molecular structure very similar to that of intermediate filament proteins and lamins but that, unlike these proteins, associate with tubulins, contributing to microtubules stability (reviewed in (Amos, 2008)). Mammalian tektins 1 and 5 are almost exclusively testis-specific and may play a

role in flagellar formation during spermiogenesis (Xu *et al.*, 2001; Roy *et al.*, 2004; Cao *et al.*, 2011). Different tektins were shown to localize to the mammalian sperm flagellum (Wolkowicz *et al.*, 2002; Oiki *et al.*, 2014), where some may be linked with the outer dense fibers or with the mitochondria, instead of being associated with microtubules (Iida *et al.*, 2006; Murayama *et al.*, 2008). Whatever the case may be, tektin genes mutations and tektin disruption (in humans and mice models, respectively), seem to be associated with decreased sperm motility and male infertility or subfertility, without affecting females (Tanaka *et al.*, 2004a; Roy *et al.*, 2007, 2009; Zuccarello *et al.*, 2008). Interestingly, orthologues of both tektin-3 (identified as deregulated using the subpopulations strategy; data not shown) and coiled-coil domain-containing protein 11 (CCDC11; a protein that we have also detected at deregulated levels in low motility sperm) were shown to belong to the cilium of *Xenopus* epithelial cells (Hayes *et al.*, 2007). Although the exact function of CCDC11 is unknown, this protein seems to be an interacting partner of KIF3A motor protein (a heterotrimeric kinesin II subunit) in mice spermatogenesis (Lehti *et al.*, 2013). Seeing that KIF3A participates in axoneme formation both in somatic ciliated cells and sperm flagellum, it is tempting to hypothesize that CCDC11 is also involved in flagellum formation during mammalian spermiogenesis.

Additionally, our outcomes point to the idea that the majority of proteins deregulated in sperm samples with motility defects are those with roles in metabolism and energy production. Indeed, most of the GO biological process terms and *Reactome* pathways detected by *David* were related to energy metabolism. ATP is obviously needed to fuel sperm motility and thus the levels of any enzymes participating in ATP-producing cellular pathways contributing to flagellar movement need to be tightly regulated in the male gamete. What is not totally clear is what the actual contribution of the distinct ATP-producing pathways to the generation of the energy that enables sperm to move forward is. As discussed previously (subchapter 1.1.4.2), the energy debate usually disputes mainly glycolysis and mitochondrial oxidative phosphorylation (OXPHOS), with the majority of data pointing to glycolysis as the main pathway fuelling sperm motility in mice and humans (Ramalho-Santos *et al.*, 2009; Amaral *et al.*, 2011, 2013b). But in fact an increasing body of data is suggesting that other pathways may also be involved (Amaral *et al.*, 2013a, 2014a).

Our outcomes support the idea that several metabolic pathways contribute to sperm motility regulation. It was indeed interesting to determine that low motility sperm have altered levels of so many post-glycolytic enzymes, which clearly suggests that glycolysis may not be the sole player in this process. Pyruvate metabolism and tricarboxylic acid cycle link glycolysis to other pathways, such as OXPHOS and beta-oxidation of fatty acids. OXPHOS relies on the activity of the

mitochondrial electron transfer chain (ETC) complexes and on the maintenance of a mitochondrial membrane potential (MMP) across the inner mitochondrial membrane. Importantly low levels of several ETC proteins (complexes I, IV and V) were detected in low motility sperm, suggesting that the whole ETC may be deregulated. In agreement, both MMP and the levels of other complex IV subunits were positively correlated with human sperm motility (Amaral *et al.*, 2007; Amaral and Ramalho-Santos, 2010). Interesting, in a patient harbouring a mitochondrial DNA point mutation causing reduced activity of the ETC complex I, and whose sperm presented low motility, the presence of succinate (a substrate for complex II) in the culture medium was enough to restore the ability of sperm to move (Folgerø *et al.*, 1993). Furthermore, the incubation of human sperm with different ETC complexes inhibitors in the presence of glucose (thus in conditions supporting glycolysis) resulted in a rapid drop of sperm motility (Ruiz-Pesini *et al.*, 2000; St John *et al.*, 2005). On the other hand, and also in accordance with the proteomic data obtained in the present study, Amaral and co-workers have recently shown that inhibition of mitochondrial beta-oxidation impairs human sperm motility (without affecting sperm viability) in a concentration- and time-dependent manner, at least in the absence of exogenous substrates (Amaral *et al.*, 2013a). Furthermore and in addition to catabolic pathways, fatty acids anabolic pathways may also be relevant for sperm function (Amaral *et al.*, 2014a), in particular for sperm motility (current study). That condensing mouse spermatids are capable of synthesizing fatty acids were previously shown by others (Grogan and Lam, 1982). The same may be true for human sperm, which may have the capacity to synthesize fatty acids and use them to obtain some of the energy needed to fuel motility. Furthermore, and although the literature suggests that glycolysis plays the preponderant role in mammalian sperm motility (and in fact enzymes involved in all glycolytic steps were detected and quantified), it is nevertheless interesting that very few enzymes directly implicated in this pathway were identified as differentially expressed between samples with distinct motility, obtained with two different strategies, while other pathways involved in energy metabolism seem more represented. Taken together, these data strongly suggest that the correct functioning of other metabolic pathways apart from glycolysis is critical for the ability of sperm to move.

Remarkably, the two lists of differential proteins that result from both strategies (asthenozoospermic vs normozoospermic samples and more- and less-motile subpopulations) have a lot in common. First of all, the categorization of proteins according to both cellular localization and function resulted in very similar distributions, suggesting, for instance, that proteins involved in metabolism and energy production, and notably mitochondrial proteins, are typically deregulated in non-motile sperm. Excitingly, a number of protein families and of proteins participating in specific cellular pathways were also commonly detected in both comparisons (Amaral *et al.*,

2014b). These include cytoskeletal proteins and proteins involved in energy metabolism, protein metabolism and vesicle trafficking. Noteworthy, the detection of similar proteomic alterations in the two complementary technical approaches provides a substantial confirmation that these protein families/cellular pathways might indeed be involved in sperm motility regulation.

Moreover and as also described in previous proteomics studies investigating deregulated proteins in less motile sperm, we have detected proteins with functions in protein metabolism (specifically in protein folding and degradation) as differentially abundant proteins. Heat shock proteins, together with other chaperones, mediate protein folding and prevent protein aggregation. This is the case of human heat shock-related 70 kDa protein 2 (HSPA2), detected as differential protein in both our study and studies from others (Martínez-Heredia *et al.*, 2008; Siva *et al.*, 2010; Parte *et al.*, 2012). This protein is constitutively expressed at low levels in most tissues, but at higher levels in the testis (Bonnycastle *et al.*, 1994; Son *et al.*, 1999). Targeted disruption of this protein in mice models resulted in germ cell apoptosis and male infertility, with failed meiosis in HSPA2 homozygous knockout male mice (Dix *et al.*, 1996), providing evidence of its importance for normal spermatogenesis. As a matter of fact, HSPA2 expression seems to be lower in men with abnormal spermatogenesis (Huszar *et al.*, 2000; Son *et al.*, 2000). Our data add further evidence that HSPA2 levels are correlated with human sperm motility. Interestingly, one of the binding partners of HSP70s seems to be the product of a testis-specific transcript of WD repeat-containing protein 16 (WDR16; (Silva *et al.*, 2005)) that we also have detected at lower levels in low motile sperm.

The proteasome is a proteinase complex with ATP-dependent proteolytic activity that mediates protein turnover, and the implication of the ubiquitin-proteasome pathway in sperm function is very well documented (Sutovsky, 2011; Hou and Yang, 2013). Proteasome alpha subunit proteins were previously reported to have a role in sperm capacitation (Arcelay *et al.*, 2008) and motility (Siva *et al.*, 2010) and here we show that altered levels of proteasome beta subunit proteins are also associated with reduced sperm motility phenotype. Moreover, we have also found cullin-associated neddylation/NEDD8-dissociated protein 1 (CAND1) at reduced levels in asthenozoospermic samples. CAND1 is a cullin 1 binding protein that regulates the formation of the “Skp, cullin, F-box containing complex” (SCF) ubiquitin E3 ligase complex, controlling the protein levels of many regulatory proteins (Liu *et al.*, 2002; Zheng *et al.*, 2002), and may also participate in centrosome duplication regulation and prostate cancer development (Korzeniewski *et al.*, 2012).



Furthermore, proteins involved in vesicle trafficking were also found at altered levels in sperm with impaired motility. The occurrence of membrane trafficking events during spermiogenesis has been clearly established, specifically in the biogenesis of the acrosome (reviewed in (Amaral *et al.*, 2014a)). Vesicle trafficking proteins also participate in sperm fusion events and indeed the vesicle-fusing ATPase (NSF) detected here to be under expressed in low motility samples was suggested to be useful to predict stallion fertility (Gamboa and Ramalho-Santos, 2005). Nevertheless, the altered levels of these proteins in sperm with motility defects may simply mirror a defective spermiogenesis process.

Additionally, and not surprisingly, proteins implicated in signalling pathways appeared deregulated in asthenozoospermic samples. As discussed, there are several signalling pathways presumably involved in sperm motility acquisition and maintenance. Even so, further studies are needed to better decipher many of these pathways and their actual meanings in human sperm function. One of these proteins, also found in lower amounts in asthenozoospermic samples, was glycogen synthase kinase 3B (GSK3B). The GSK3 is a serine/threonine protein kinase, which has two isoforms (GSK3A and GSK3B) and works as a key component of many cellular processes, not only in glucose regulation but also in immune responses, cell proliferation, migration and apoptosis (Jope and Johnson, 2004; Kaidanovich-Beilin and Woodgett, 2011; Beurel *et al.*, 2014). Furthermore, it seems to be involved in sperm motility (Vijayaraghavan *et al.*, 1996, 2000; Smith *et al.*, 1999; Aparicio *et al.*, 2007). It was previously reported that immotile caput sperm contain six-fold higher GSK3 activity than motile caudal sperm (Somanath *et al.*, 2004). More recently, a targeted KO approach for GSK3a resulted in infertile mice with compromised sperm motility, which undoubtedly shows their implication in this mechanism (Bhattacharjee *et al.*, 2015). Although more studies are needed to investigate the specific function of GSK3B, our results are in accordance with the literature showing the GSK3 might be an important player in human sperm motility regulation.

The low number of deregulated proteins in common between our study and the previous ones (Zhao *et al.*, 2007; Martínez-Heredia *et al.*, 2008; Chan *et al.*, 2009; Siva *et al.*, 2010; Parte *et al.*, 2012) (only 5 proteins) was probably due to the different techniques and parameters used to perform the analyses. Our work was based in a high-throughput proteomic technique coupled to the use of a high sensitive way to label and quantify proteins in independent samples. However, it is also interesting to analyse the compiled list of 185 proteins detected as deregulated in asthenozoospermic samples. Not surprisingly, when characterized by their main function, the majority of these proteins have roles in metabolism and energy production. Looking in more detail to the pathways in which these deregulated proteins are involved in, we can find some related to

glycolysis and mitochondrial OXPHOS, and also many others involved in pyruvate metabolism, TCA cycle, lipid metabolism, fatty acids beta-oxidation, mitochondrial ETC, amino acid metabolism, among others. These evidences reinforce the idea that many metabolic pathways are involved in the regulation of human sperm metabolism.

Interestingly, triosephosphate isomerase (TPI) is commonly detected as a deregulated protein in low-motile sperm (Zhao *et al.*, 2007; Siva *et al.*, 2010; Parte *et al.*, 2012; Amaral *et al.*, 2014b). TPI is a very important glycolytic enzyme that is required to convert dihydroxyacetone phosphate to glyceraldehyde 3-phosphate. This conversion is highly efficient and very reversible taking part in the gluconeogenesis process too (Orosz *et al.*, 2006). Moreover, this enzyme (TPI1) has been studied in human, mice and rat male germ lines and seemed to be important during the spermatogenic process (Russell and Kim, 1996; Auer *et al.*, 2004; Ijiri *et al.*, 2013). Thus, although more studies will be needed to investigate the real role of TPI in sperm function, it seems to have an important role in the regulation of human sperm motility.

Another important group of proteins is the one related to sperm tail structure and motility. In this specific case the advantage of compiling the list of deregulated proteins described in the different studies is evident, with an increase of proteins involved in these functions from 6% (in our study) to 18% (in the compiled list). The majority of proteins included in this group were described by Parte and colleagues and are mainly tubulins. As main components of the microtubules, tubulins assume an important role in sperm flagellum structure and movement (Mohri, 1968). It is also known that both  $\alpha$ - and  $\beta$ -tubulins undergo several posttranslational modifications such as tyrosylation/detyrosylation, and acetylation/deacetylation (Hammond *et al.*, 2008). Moreover, an association between low levels of acetylated  $\alpha$ -tubulin and asthenozoospermia was recently described, suggesting an important role of tubulin acetylation on sperm motility (Bhagwat *et al.*, 2014).

The compilation of all the proteins described on the literature as being disrupted in asthenozoospermic patients is an excellent exercise through the clarification of the molecular mechanisms behind human sperm motility. In this way, we are trying to join all the already known pieces of the puzzle to see, in the future, the whole picture. Overall, our data suggest that proteins involved in cytoskeleton, energy metabolism, protein folding and degradation and vesicle trafficking are, with a few exceptions, consistently altered in low motility sperm. The exception (one asthenozoospermic sample that clustered with the normozoospermic samples) might indicate that in addition to alterations in protein levels, low motility sperm might also be typified by other molecular deregulations, most probably at the metabolome level. Indeed, our results strongly

support the emerging idea that several bioenergetics metabolic pathways (including glycolysis, the tricarboxylic acid cycle, mitochondrial OXPHOS and fatty acids beta-oxidation) contribute to sperm motility (de)regulation. In the future, it will be interesting to further explore the potential use of the detected proteins and pathways towards their potential diagnostic and prognostic use and perhaps to pinpoint novel therapeutic targets.

#### **4.2 Human sperm endogenous metabolites – the first little step towards human sperm metabolome**

As already mentioned, the use of genomic, transcriptomic and proteomic technologies are significantly contributing to characterize and better understand the human sperm at the molecular level (Jodar *et al.*, 2012; Kovac *et al.*, 2013; Amaral *et al.*, 2014a). However, metabolomics, the study of small and low molecular weight molecules that are products of metabolism, has not been greatly applied in the study and characterization of human sperm cells (Kovac *et al.*, 2013). Furthermore, as metabolomics reflects downstream events of gene expression, it is also considered to be more closely related to the actual phenotype than either transcriptomics or proteomics (Nicholson and Lindon, 2008; Patti *et al.*, 2012), as it can be used to directly monitor biochemical activity.

Thus, to the best of our knowledge, this was the first time that untargeted metabolomics techniques have been performed using human sperm cells extracts to identify their endogenous metabolites. Importantly, in the present study, we applied two complementary techniques normally used for untargeted metabolomics: nuclear magnetic resonance (NMR) and mass spectrometry (MS) (Nicholson and Lindon, 2008; Patti *et al.*, 2012). Using these two strategies we were able to identify a total of 69 metabolites, most of them not previously described in human sperm. Of note, only 4 metabolites were identified with both techniques, thus highlighting the importance of the use of complementary approaches to ultimately complete a metabolic characterization of human sperm cells.

Although some studies previously used  $^1\text{H}$  NMR technologies to examine human seminal plasma (Gupta *et al.*, 2011a, 2011b, 2013) or circulating plasma metabolic changes (Courant *et al.*, 2013), in an attempt to correlate metabolites with seminal quality, none of them focussed on the mature human sperm cell metabolome. Therefore, this is the first work that describes a metabolic fingerprint of human sperm extracts. Interestingly, when compared to the metabolic fingerprint of

the rhesus macaque sperm extracts, the major metabolites identified in human were similar, namely lactate and acetylcarnitine (Hung *et al.*, 2009; Lin *et al.*, 2009).

It is important to note that while the presence of lactate suggests that sperm has active glycolysis, carnitine and acetylcarnitine are metabolites usually associated with fatty acid oxidation. Acetylcarnitine is an acetic acid ester of carnitine that facilitates the import of acetyl CoA into the matrices of mammalian mitochondria, modulating the transfer of fatty acids and acetyl groups into mitochondria for beta-oxidation (Rosca *et al.*, 2009). This is in accordance not only with the results of overrepresented pathways analysis (using the 69 metabolites described) but also with our proteomic results (sub-chapter 4.1) and other previous proteomic and functional analyses (Amaral *et al.*, 2014a). In fact, earlier studies have also shown that the levels of carnitine and acetylcarnitine in the epididymis, seminal plasma and spermatozoa are much higher when compared with those found in circulating plasma (Jeulin and Lewin, 1996). This suggests a possible role of these molecules not only in human sperm maturation but also in sperm function, directly in energetic metabolism, and possibly as anti-apoptotic and antioxidant factors (Jeulin and Lewin, 1996; Ng *et al.*, 2004). The role of lipid metabolism in the production of energy to supply human sperm function was already suggested in previous studies (Amaral *et al.*, 2014a, 2014b) and, accordingly, the incubation of these cells with a fatty acid oxidation inhibitor (etomoxir) drastically affected human sperm motility, highlighting the importance of mitochondrial fatty acid metabolism to fuel human sperm (Amaral *et al.*, 2013a).

Furthermore, we identified larger number of metabolites belonging to the “amino acids, peptides and analogues” super class. In goat a high content of free amino acids was found in the ejaculate and the epididymal fluid, where these molecules could serve as chelating agents, in particular for toxic metals, and/or as oxidizable substrates for sperm (Patel *et al.*, 1998, 1999). In human sperm cells, amino acids could also serve as endogenous substrates, whereas their presence in human semen (Hervann *et al.*, 1986) could be related to functions similar to those described in goat semen. However, further studies would be needed to validate this assumption.

Concerning the application of both untargeted metabolomics techniques it is important to note that, in general, both have advantages and disadvantages (Patti *et al.*, 2012). For example, in order to obtain good NMR spectra, with defined resonances and intensities for peak assignment and metabolite identification, in the 1D (<sup>1</sup>H-NMR) and 2D (COSY and HSQC), a high amount of cells was required (150 million) driving us to the need of using pools of samples. On the other hand, the GC-TOF/MS revealed to be more sensitive and therefore a lower amount of cells (15 million) were

needed, allowing the analysis of independent sperm samples. Nevertheless, the GC-TOF/MS resulted in the identification of less but different types of small molecules, which confirms the advantage of using of both techniques, even taking into account the major limitations of each one. Hence, the application of these two complementary techniques seems to constitute a promising strategy to investigate human sperm metabolism and to better understand the physiology (and pathophysiology) of the male gamete. Moreover and while it is certainly premature to try to make an estimation of the number of human sperm endogenous metabolites at this stage, the comprehensive list of sperm metabolites might be considerably larger than the one described here. The use of other complementary techniques in future studies, such as liquid chromatography (LC)-MS, as well as of different extraction methods, could contribute to the identification of more metabolites towards further completing the human sperm metabolome. It would also be interesting to investigate whether there are differences in the relative abundance of the different metabolites in sperm cells from human samples with distinct phenotypes (e.g., differing in motility and/or in fertilization ability) or collected from individuals at different ages or with different diets. Moreover, it would be also interesting to follow the integration of exogenous metabolites, using tracers (i.e. labeled substrates, as glucose or fatty acids) as it has been performed using boar sperm (Marin *et al.*, 2003).

Furthermore, as metabolomics is also one of the emerging “omic” sciences, and new approaches are in constant evolution, metabolomics might be applied to address different questions in biology of reproduction, in particular to better understand the molecular bases of human sperm physiology and (dys)functionality.

#### **4.3 Combined analysis of human sperm endogenous metabolites and the human sperm compiled proteome – the importance of the integration of metabolomics and proteomics analysis**

The pathway-level analysis is a powerful method enabling interpretation of post-genomic data (i.e. proteins and metabolites) at a higher level than that of individual biomolecules. Taking this into account, many scientists are currently developing numerous bioinformatics tools to let this kind of analysis be possible and feasible, with an increasing confidence, using curated databases and applying statistical methods to restrict the results and increase their significance (Henry *et al.*, 2014). The *Integrated Molecular Pathway Level Analysis* (IMPALA) is a web tool for the joint pathway analysis of transcriptomics or proteomics and metabolomics data that performs over-

representation or enrichment analysis with user-specified lists of metabolites and genes or proteins, using over 3000 pre-annotated pathways from 11 databases (Kamburov *et al.*, 2011).

In the present work and using IMPALA, we performed the combined analysis of the 69 metabolites identified by untargeted metabolomics approaches and the recently compiled human sperm proteome (Amaral *et al.*, 2014a). This resulted in a very large number of enriched cellular pathways, which, after selection, resulted in the most probable significant ones. Not surprisingly, *Metabolism* turned out to be the most significant pathway. Moreover, these results contribute to reinforce the importance not only of the metabolism of lipids and lipoproteins but also the possible significance of pathways like the citric acid (TCA) cycle, respiratory electron transport, the metabolism of nucleotides, as well as the metabolism of amino acids and derivatives and biological oxidations for the correct human sperm functionality. Inside the category of metabolism of carbohydrates, it was particularly interesting to detect glycogen metabolism as a putative pathway operating in human sperm, since despite the lack of experiments in humans, this was previously showed to be active in dog sperm (Ballester *et al.*, 2000; Palomo *et al.*, 2003; Albarracín *et al.*, 2004).

However, and since the human sperm metabolome is certainly much more extensive than the list described here, this would be very interesting to perform more descriptive and comparative studies to amplify this list and increase the statistical power of this kind of analysis. For instance, the integrated analysis of differential proteome and metabolome of less- and more-motile sperm cells and also the respective analysis of their interactomes will most probably contribute to a more detailed knowledge of the molecular basis of human sperm motility, as well as to define novel therapeutic targets.

#### **4.4 The comparison between the metabolic signatures of extracts of normozoospermic and asthenozoospermic pool of samples – a preliminary look to possible important metabolites to human sperm motility**

As preliminary analysis, in the present work we have performed the comparison between the metabolic fingerprints of extracts of two pools of samples with different motility using NMR. Interestingly, the metabolic signatures of the two pools revealed to be similar, with the same majority metabolites. However, the concentrations (i.e. intensity of the picks) of some of these were different.

The majority of the identified and quantified metabolites appeared in less quantity in the asthenozoospermic pool extracts. Acetyltyrosine (a side chain reaction of tyrosine) and tyrosine were the metabolites that appeared as more differently abundant in the extracts of asthenozoospermic pool, with lower quantity when compared to normozoospermic ones. Interestingly, tyrosine is an essential amino acid that readily crosses barriers (i.e. blood-brain barrier) since it is a precursor for neurotransmitters as dopamine, norepinephrine and epinephrine (also known as adrenalin). This could suggest a possible involvement of this metabolite in the synthesis of some transmitters, as dopamine and epinephrine, that could be involved in sperm motility mechanism, as it seems to happen in stallion sperm (Urta *et al.*, 2014).

Another metabolite detected in lower abundance in asthenozoospermic samples was trimethylamine N-oxide, an oxidation product of trimethylamine that could derive from choline, which in turn can be derived from dietary phosphatidylcholines or carnitine. Trimethylamine N-oxide is known to act as an osmolyte that counteracts the effects of increased concentrations of other molecules (i.e. urea in the kidneys) (Meersman *et al.*, 2009). This could suggest a similar function in sperm cells, as a protection of external environment, but further experiments are needed to test this hypothesis.

Interestingly, putrescine was also found in lower concentration in asthenozoospermic samples. The presence of this polyamine and others (as spermidine and spermine, of which putrescine is a precursor) in semen and sperm and their abundance during spermatogenesis, is well documented (Oliva *et al.*, 1982; Lefèvre *et al.*, 2011). Putrescine also appears to be a growth factor necessary for cell division and embryogenesis (Lefèvre *et al.*, 2011). Moreover, polyamines seem to have a direct role in sperm motility, since the addition of polyamines or L-arginine to human spermatozoa with reduced or no motility increases sperm motility (Morales *et al.*, 2003).

Furthermore, and not surprisingly, acetylcarnitine also appeared in lower concentration in the extracts of less motile human sperm. Since the inner mitochondrial membrane is not permeable to long-chain fatty acids or acyl-coenzyme A (CoA) derivatives, acetylcarnitine esters transport these fatty acyl groups across the inner mitochondrial membrane. Thus, as already mentioned, acetylcarnitine plays a critical role in the regulation of  $\beta$ -oxidation (Jeulin and Lewin, 1996). This seems to be in accordance with the earlier discussed importance of lipid metabolism and fatty acids oxidation in human sperm function, namely in human sperm motility (Jeulin and Lewin, 1996; Amaral *et al.*, 2013a). In fact, the outcomes of the differential proteomics studies using asthenozoospermic samples (ours included) also point out to a deregulation of mitochondrial

proteins and proteins involved in fatty acids oxidation and lipid metabolism (sub-chapter 4.1). Additionally, previous studies already showed a significant increase on the percentage of human sperm motility after adding acetyl-L-carnitine to the incubation medium (Jeulin and Lewin, 1996). Based on that, the oral supplementation of asthenozoospermic patients with carnitine to increase sperm motility was proposed (Garolla *et al.*, 2005). In conclusion, acetyl-L-carnitine seems to be a very important metabolite involved in the regulation of human sperm motility (Jeulin and Lewin, 1996). Thus, in future studies, it would be interesting to further clarify the molecular mechanisms in which this metabolite is involved, as well as to study the possibility of using this and other metabolites as biomarkers of sperm (dys)function and hopefully to develop efficient therapies.

Also without surprise, the nucleosides IMP, AMP and ADP revealed to be present in lower concentration in the extracts of asthenozoospermic pool of samples when compared to normozoospermic one. The lower availability of the ATP precursors may indicate an imbalance in the energetic state of the cell, which possibly correlates with the impairment of sperm motility.

On the other hand, formate was found to be in higher concentration in asthenozoospermic extracts. Formate is an intermediate in normal metabolism taking part in the metabolism of one-carbon compounds (Reda *et al.*, 2008). It is typically produced as a by-product in the production of acetate, another metabolite present in higher amount in less motile sperm. Of note, this metabolite is responsible for both metabolic acidosis and disrupting mitochondrial electron transport and energy production by cytochrome oxidase inhibition, which results in ATP depletion and drives the cells to death (Nicholls, 1976). Moreover, the inhibition of cytochrome oxidase by formate may also cause cell death by increasing the production of cytotoxic reactive oxygen species (ROS). All these effects could be involved in mitochondrial disruption and subsequently have an effect on sperm motility, as previously discussed.

Nevertheless, all of these results are really preliminary and further investigations are absolutely needed. Hereafter it would be very interesting to look to the metabolomic signatures of different human sperm pathologies, particularly asthenozoospermia, using more samples and methods, to describe and quantify metabolites. Those strategies will certainly go through the performance of differential metabolomics, using higher number of samples in order to increase the statistical power of the study and also to decrease the variability between independent samples. This will lead to a better understanding of the metabolomic basis of human sperm motility.



## **CHAPTER V. CONCLUSIONS**



## CHAPTER V. CONCLUSIONS

In conclusion, we have applied for the first time a high-throughput differential proteomic strategy to identify proteins involved in sperm motility (de)regulation and we have detected 80 differentially abundant proteins in asthenozoospermic samples compared to normozoospermic samples. Our data suggest that proteins involved in cytoskeleton, energy metabolism, protein folding and degradation and vesicle trafficking are, with a few exceptions, consistently altered in low-motile sperm. Furthermore, our results strongly support the emerging idea that several bioenergetics metabolic pathways, including glycolysis, the tricarboxylic acid cycle, mitochondrial OXPHOS and fatty acids beta-oxidation, contribute to sperm motility (de)regulation. In the future, it will be interesting to further explore the potential use of the detected proteins and pathways towards their potential diagnostic and prognostic use and perhaps to pinpoint novel therapeutic targets.

On the other hand, and to the best of our knowledge, here we have described for the first time a list of 69 endogenous metabolites of human sperm extracts, applying two complementary techniques normally used for untargeted metabolomics: nuclear magnetic resonance (NMR) and mass spectrometry (MS). Here we presented for the first time a metabolic fingerprint of human sperm extracts in NMR spectra. Of note, only 4 metabolites were identified with both techniques, which highlights the importance of the use of complementary approaches to ultimately complete a metabolic characterization of sperm cells.

We have also performed a first metabo-proteomic analysis, combining the 69 described metabolites and the previously compiled sperm proteome (Amaral *et al.*, 2014a). This analysis reinforces the importance of metabolic pathways as fatty acids beta-oxidation and lipid metabolism for the correct human sperm functionality. However, and taking into account that sperm metabolome is certainly much more extensive than we described here, it will be very important to perform more descriptive and comparative studies to amplify these lists and increase the statistical power of this kind of analysis.

Lastly, and as preliminary results, we presented some different concentrated metabolites in extracts of asthenozoospermic samples compared to normozoospermic samples. Here, the majority of the metabolites revealed to be in lower concentration in less motile sperm, pointing out to some possibilities and hypothesis of metabolic disruptions in sperm motility, that certainly need further

investigation. The use of more samples and complementary technique (as GC- and LC-MS) will be important to metabolically characterize sperm pathologies, as asthenozoospermia, and better understand molecular mechanisms, in a physiological point of view. Furthermore, the integrated analysis of differential proteome and metabolome of asthenozoospermic and normozoospermic samples coupled to the analysis of their interactomes will probably contribute for to the unrevealing of the molecular basis of human sperm motility, as well as novel therapeutic targets. With this knowledge we will be in the future to easily modulate sperm metabolism and function, using for instance suitable mediums or supplementation to improve sperm performance in infertile patients.

Although clearly still in its infancy, the application of metabolomics to the study of human spermatozoa has a huge potential, and its application as a phenotypic readout can be an important key to understand fundamental biological processes acting in human sperm cells. Another challenging area it will be the application of metabo-proteomics strategies to the study of human sperm. For that propose, the use of high-throughput technologies (either in proteomics as in metabolomics field) coupled to the constantly improved bioinformatics tools, will definitely lead us to better comprehend distinct male reproductive pathologies, including molecular basis of motility, and perhaps to discover new (in)fertility biomarkers. Here, we have just taken the first step.

## **CHAPTER VI. BIBLIOGRAPHY**



## CHAPTER VI. BIBLIOGRAPHY

- Abou-haila A, Tulsiani DRP. Signal transduction pathways that regulate sperm capacitation and the acrosome reaction. *Arch Biochem Biophys* 2009;**485**:72–81. Elsevier Inc.
- Ahrens CH, Brunner E, Qeli E, Basler K, Aebersold R. Generating and navigating proteome maps using mass spectrometry. *Nat Rev Mol Cell Biol* 2010;**11**:789–801.
- Albarracín JL, Fernández-Novell JM, Ballester J, Rauch MC, Quintero-Moreno A, Peña A, Mogas T, Rigau T, Yañez A, Guinovart JJ, *et al.* Gluconeogenesis-linked glycogen metabolism is important in the achievement of in vitro capacitation of dog spermatozoa in a medium without glucose. *Biol Reprod* 2004;**71**:1437–1445.
- Alexandre-Gouabau M-C, Courant F, Gall G Le, Moyon T, Darmaun D, Parnet P, Coupé B, Antignac J-P. Offspring metabolomic response to maternal protein restriction in a rat model of intrauterine growth restriction (IUGR). *J Proteome Res* 2011;**10**:3292–3302.
- Amann RP, Howards SS. Daily spermatozoal production and epididymal spermatozoal reserves of the human male. *J Urol* 1980;**124**:211–215.
- Amaral A, Castillo J, Estanyol JM, Ballescà JL, Ramalho-Santos J, Oliva R. Human sperm tail proteome suggests new endogenous metabolic pathways. *Mol Cell Proteomics* 2013a;**12**:330–342.
- Amaral A, Castillo J, Ramalho-Santos J, Oliva R. The combined human sperm proteome: cellular pathways and implications for basic and clinical science. *Hum Reprod Update* 2014a;**20**:40–62.
- Amaral A, Lourenço B, Marques M, Ramalho-Santos J. Mitochondria functionality and sperm quality. *Reproduction* 2013b;**146**:R163–R174.
- Amaral A, Paiva C, Attardo Parrinello C, Estanyol JM, Ballescà JL, Ramalho-Santos J, Oliva R. Identification of Proteins Involved in Human Sperm Motility Using High-Throughput Differential Proteomics. *J Proteome Res* 2014b;.
- Amaral A, Paiva C, Baptista M, Sousa AP, Ramalho-Santos J. Exogenous glucose improves long-standing human sperm motility, viability, and mitochondrial function. *Fertil Steril* 2011;**96**:848–850.
- Amaral A, Ramalho-Santos J, St John JC. The expression of polymerase gamma and mitochondrial transcription factor A and the regulation of mitochondrial DNA content in mature human sperm. *Hum Reprod* 2007;**22**:1585–1596.
- Amaral A, Ramalho-Santos J. Assessment of mitochondrial potential: implications for the correct monitoring of human sperm function. *Int J Androl* 2010;**33**:e180–e186.
- Amaral A, Ramalho-Santos J. The male gamete is not a somatic cell--the possible meaning of varying sperm RNA levels. *Antioxid Redox Signal* 2013;**18**:179–180.
- Amaral S. Diabetes, age and male reproductive function. 2009; PhD Thesis. University of Coimbra.

- Amos LA. The tektin family of microtubule-stabilizing proteins. *Genome Biol* 2008;**9**:229.
- Aoki VW, Liu L, Carrell DT. A novel mechanism of protamine expression deregulation highlighted by abnormal protamine transcript retention in infertile human males with sperm protamine deficiency. *Mol Hum Reprod* 2006;**12**:41–50.
- Aparicio IM, Bragado MJ, Gil MC, Garcia-Herreros M, Gonzalez-Fernandez L, Tapia JA., Garcia-Marin LJ. Porcine sperm motility is regulated by serine phosphorylation of the glycogen synthase kinase-3a. *Reproduction* 2007;**134**:435–444.
- Arcelay E, Salicioni AM, Wertheimer E, Visconti PE. Identification of proteins undergoing tyrosine phosphorylation during mouse sperm capacitation. *Int J Dev Biol* 2008;**52**:463–472.
- Auer J, Camoin L, Courtot A-M, Hotellier F, Almeida M De. Evidence that P36, a human sperm acrosomal antigen involved in the fertilization process is triosephosphate isomerase. *Mol Reprod Dev* 2004;**68**:515–523.
- Azpiazu R, Amaral A, Castillo J, Estanyol JM, Guimerà M, Ballescà JL, Balasch J, Oliva R. High-throughput sperm differential proteomics suggests that epigenetic alterations contribute to failed assisted reproduction. *Hum Reprod* 2014;**29**:1225–1237.
- Baker M a, Naumovski N, Hetherington L, Weinberg A, Velkov T, Aitken RJ. Head and flagella subcompartmental proteomic analysis of human spermatozoa. *Proteomics* 2013;**13**:61–74.
- Baker M a, Reeves G, Hetherington L, Müller J, Baur I, Aitken RJ. Identification of gene products present in Triton X-100 soluble and insoluble fractions of human spermatozoa lysates using LC-MS/MS analysis. *Proteomics Clin Appl* 2007;**1**:524–532.
- Baker M a. The 'omics revolution and our understanding of sperm cell biology. *Asian J Androl* 2011;**13**:6–10.
- Baldi E, Casano R, Falsetti C, Krausz C, Maggi M, Forti G. Intracellular calcium accumulation and responsiveness to progesterone in capacitating human spermatozoa. *J Androl* 1991;**12**:323–330.
- Ballester J, Fernández-Novell JM, Rutllant J, García-Rocha M, Jesús Palomo M, Mogas T, Peña A, Rigau T, Guinovart JJ, Rodríguez-Gil JE. Evidence for a functional glycogen metabolism in mature mammalian spermatozoa. *Mol Reprod Dev* 2000;**56**:207–219.
- Balsamo M, Guidi L, Pierboni L, Marotta R, Todaro MA, Ferraguti M. Living without mitochondria: spermatozoa and spermatogenesis in two species of Urodasya (Gastrotricha, Macrotrichida) from dysoxic sediments. *Invertebr Biol* 2007;**126**:1–9.
- Bench GS, Friz AM, Corzett MH, Morse DH, Balhorn R. DNA and total protamine masses in individual sperm from fertile mammalian subjects. *Cytometry* 1996;**23**:263–271.
- Beurel E, Grieco SF, Jope RS. Glycogen synthase kinase-3 (GSK3): Regulation, actions, and diseases. *Pharmacol Ther* 2014;



- Bhagwat S, Dalvi V, Chandrasekhar D, Matthew T, Acharya K, Gajbhiye R, Kulkarni V, Sonawane S, Ghosalkar M, Parte P. Acetylated  $\alpha$ -tubulin is reduced in individuals with poor sperm motility. *Fertil Steril* 2014;**101**:95–104.e3.
- Bhattacharjee R, Goswami S, Dudiki T, Popkie AP, Phiel CJ, Kline D, Vijayaraghavan S. Targeted Disruption of Glycogen Synthase Kinase 3a (Gsk3a) Affects Sperm Motility Resulting in Male Infertility. *Biol Reprod* 2015;
- Bianchi E, Doe B, Goulding D, Wright GJ. Juno is the egg Izumo receptor and is essential for mammalian fertilization. *Nature* 2014;**508**:483–487. Jan 7. pii: biolreprod.114.124495. [Epub ahead of print]
- Blanco A, Zinkham WH. Lactate Dehydrogenases in Human Testes. *Science* 1963;**139**:601–602.
- Bone W, Jones N, Kamp G, Yeung C, Cooper T. Effect of ornidazole on fertility of male rats: inhibition of a glycolysis-related motility pattern and zona binding required for fertilization in vitro. *Reproduction* 2000;**118**:127–135.
- Bonnycastle LL, Yu CE, Hunt CR, Trask BJ, Clancy KP, Weber JL, Patterson D, Schellenberg GD. Cloning, sequencing, and mapping of the human chromosome 14 heat shock protein gene (HSPA2). *Genomics* 1994;**23**:85–93.
- Brohmann H, Pinnecke S, Hoyer-Fender S. Identification and characterization of new cDNAs encoding outer dense fiber proteins of rat sperm. *J Biol Chem* 1997;**272**:10327–10332.
- Brokaw C. Computer simulation of flagellar movement: I. Demonstration of stable bend propagation and bend initiation by the sliding filament model. *Biophys J* 1972;**16**:122–127.
- Brown PR, Miki K, Harper DB, Eddy EM. A-kinase anchoring protein 4 binding proteins in the fibrous sheath of the sperm flagellum. *Biol Reprod* 2003;**68**:2241–2248.
- Brunner AM, Nanni P, Mansuy IM. Epigenetic marking of sperm by post-translational modification of histones and protamines. *Epigenetics Chromatin* 2014;**7**:2.
- Burgos C, Maldonado C, Gerez de Burgos NM, Aoki a, Blanco a. Intracellular localization of the testicular and sperm-specific lactate dehydrogenase isozyme C4 in mice. *Biol Reprod* 1995;**53**:84–92.
- Burton K a., Treash-Osio B, Muller CH, Dunphy EL, McKnight GS. Deletion of type IIalpha regulatory subunit delocalizes protein kinase A in mouse sperm without affecting motility or fertilization. *J Biol Chem* 1999;**274**:24131–24136.
- Calogero a E, Hall J, Fishel S, Green S, Hunter a, D'Agata R. Effects of gamma-aminobutyric acid on human sperm motility and hyperactivation. *Mol Hum Reprod* 1996;**2**:733–738.
- Calvin HI, Cooper GW, Wallace E. Evidence that selenium in rat sperm is associated with a cysteine-rich structural protein of the mitochondrial capsules. *Gamete Res* 1981;**4**:139–149.
- Cao W, Ijiri TW, Huang AP, Gerton GL. Characterization of a novel tektin member, TEKT5, in mouse sperm. *J Androl* 2011;**32**:55–69.

- Caraux G, Pinloche S. PermutMatrix: a graphical environment to arrange gene expression profiles in optimal linear order. *Bioinformatics* 2005;**21**:1280–1281.
- Carlson AE, Hille B, Babcock DF. External Ca<sup>2+</sup> acts upstream of adenylyl cyclase SACY in the bicarbonate signaled activation of sperm motility. *Dev Biol* 2007;**312**:183–192.
- Carone BR, Hung J-H, Hainer SJ, Chou M-T, Carone DM, Weng Z, Fazio TG, Rando OJ. High-Resolution Mapping of Chromatin Packaging in Mouse Embryonic Stem Cells and Sperm. *Dev Cell* 2014;**30**:11–22.
- Carone BR, Rando OJ. Rewriting the epigenome. *Cell* 2012;**149**:1422–1423.
- Carr DW, Acott TS. Inhibition of bovine spermatozoa by caudal epididymal fluid: I. Studies of a sperm motility quiescence factor. *Biol Reprod* 1984;**30**:913–925.
- Carrell DT, Hammoud SS. The human sperm epigenome and its potential role in embryonic development. *Mol Hum Reprod* 2010;**16**:37–47.
- Carrell DT, Liu L. Altered protamine 2 expression is uncommon in donors of known fertility, but common among men with poor fertilizing capacity, and may reflect other abnormalities of spermiogenesis. *J Androl* 2001;**22**:604–610.
- Carrera A, Gerton GL, Moss SB. The major fibrous sheath polypeptide of mouse sperm: structural and functional similarities to the A-kinase anchoring proteins. *Dev Biol* 1994;**165**:272–284.
- Castillo J, Amaral A, Azpiazu R, Vavouri T, Estanyol JM, Ballescà JL, Oliva R. Genomic and proteomic dissection and characterization of the human sperm chromatin. *Mol Hum Reprod* 2014a;**20**:1041–1053.
- Castillo J, Amaral A, Oliva R. Sperm nuclear proteome and its epigenetic potential. *Andrology* 2014b;**2**:326–338.
- Castillo J, Simon L, Mateo S de, Lewis S, Oliva R. Protamine/DNA ratios and DNA damage in native and density gradient centrifuged sperm from infertile patients. *J Androl* 2011;**32**:324–332.
- Chagoyen M, Pazos F. MBRole: enrichment analysis of metabolomic data. *Bioinformatics* 2011;**27**:730–731.
- Chan C-C, Shui H-A, Wu C-H, Wang C-Y, Sun G-H, Chen H-M, Wu G-J. Motility and protein phosphorylation in healthy and asthenozoospermic sperm. *J Proteome Res* 2009;**8**:5382–5386.
- Chang MC. Fertilizing capacity of spermatozoa deposited into the fallopian tubes. *Nature* 1951;**168**:697–698.
- Chen Y, Cann MJ, Litvin TN, Iourgenko V, Sinclair ML, Levin LR, Buck J. Soluble adenylyl cyclase as an evolutionarily conserved bicarbonate sensor. *Science* 2000;**289**:625–628.
- Cho C, Jung-Ha H, Willis WD, Goulding EH, Stein P, Xu Z, Schultz RM, Hecht NB, Eddy EM. Protamine 2 deficiency leads to sperm DNA damage and embryo death in mice. *Biol Reprod* 2003;**69**:211–217.

- Cho C, Willis WD, Goulding EH, Jung-Ha H, Choi YC, Hecht NB, Eddy EM. Haploinsufficiency of protamine-1 or -2 causes infertility in mice. *Nat Genet* 2001;**28**:82–86.
- Chung J-J, Shim S-H, Everley R a, Gygi SP, Zhuang X, Clapham DE. Structurally distinct Ca(2+) signaling domains of sperm flagella orchestrate tyrosine phosphorylation and motility. *Cell* 2014;**157**:808–822.
- Cohen R, Buttke DE, Asano A, Mukai C, Nelson JL, Ren D, Miller RJ, Cohen-Kutner M, Atlas D, Travis AJ. Lipid modulation of calcium flux through CaV2.3 regulates acrosome exocytosis and fertilization. *Dev Cell* 2014;**28**:310–321.
- Corzett M, Mazrimas J, Balhorn R. Protamine 1: protamine 2 stoichiometry in the sperm of eutherian mammals. *Mol Reprod Dev* 2002;**61**:519–527.
- Courant F, Antignac J, Monteau F, Bizec B Le. Metabolomics as a potential new approach for investigating human reproductive disorders. *J Proteome Res* 2013;**12**:2914–2920.
- Cox J, Mann M. Is proteomics the new genomics? *Cell* 2007;**130**:395–398.
- Croft D, Mundo AF, Haw R, Milacic M, Weiser J, Wu G, Caudy M, Garapati P, Gillespie M, Kamdar MR, et al. The Reactome pathway knowledgebase. *Nucleic Acids Res* 2014;**42**:D472–D477.
- Curi SM, Ariagno JI, Chenlo PH, Mendeluk GR, Pugliese MN, Sardi Segovia LM, Repetto HEH, Blanco AM. Asthenozoospermia: analysis of a large population. *Arch Androl* 2003;**49**:343–349.
- Dada R, Mahfouz RZ, Kumar R, Venkatesh S, Shamsi MB, Agarwal a, Talwar P, Sharma RK. A comprehensive work up for an asthenozoospermic man with repeated intracytoplasmic sperm injection (ICSI) failure. *Andrologia* 2011;**43**:368–372.
- Danshina P V, Geyer CB, Dai Q, Goulding EH, Willis WD, Kitto GB, McCarrey JR, Eddy EM, O'Brien D a. Phosphoglycerate kinase 2 (PGK2) is essential for sperm function and male fertility in mice. *Biol Reprod* 2010;**82**:136–145.
- Dayon L, Turck N, Scherl A, Hochstrasser DF, Burkhard PR, Sanchez J-C. From relative to absolute quantification of tryptic peptides with tandem mass tags: application to cerebrospinal fluid. *Chimia (Aarau)* 2010;**64**:132–135.
- Dix DJ, Allen JW, Collins BW, Mori C, Nakamura N, Poorman-Allen P, Goulding EH, Eddy EM. Targeted gene disruption of Hsp70-2 results in failed meiosis, germ cell apoptosis, and male infertility. *Proc Natl Acad Sci U S A* 1996;**93**:3264–3268.
- Domon B, Aebersold R. Mass spectrometry and protein analysis. *Science* 2006;**312**:212–217.
- Dreanno C, Seguin F, Cosson J, Suquet M, Billard R. 1H-NMR and (31)P-NMR analysis of energy metabolism of quiescent and motile turbot (*Psetta maxima*) spermatozoa. *J Exp Zool* 2000;**286**:513–522.
- Eddy EM, Toshimori K, O'Brien D a. Fibrous sheath of mammalian spermatozoa. *Microsc Res Tech* 2003;**61**:103–115.

- Eddy EM. Knobil and Neill's Physiology of Reproduction, Volume 1. In Knobil E, Neill JD, editors. 2006;, p. 3–54. Gulf Professional Publishing: United States of America.
- Eddy EM. The scaffold role of the fibrous sheath. *Soc Reprod Fertil Suppl* 2007;**65**:45–62.
- Escalier D. Knockout mouse models of sperm flagellum anomalies. *Hum Reprod Update* 2006;**12**:449–461.
- Espinoza JA, Schulz MA, Sánchez R, Villegas J V. Integrity of mitochondrial membrane potential reflects human sperm quality. *Andrologia* 2009;**41**:51–54.
- Espósito G, Jaiswal BS, Xie F, Krajnc-Franken M a M, Robben TJ a a, Strik AM, Kuil C, Philipsen RL a, Duin M van, Conti M, *et al.* Mice deficient for soluble adenylyl cyclase are infertile because of a severe sperm-motility defect. *Proc Natl Acad Sci U S A* 2004;**101**:2993–2998.
- Everley R a, Kunz RC, McAllister FE, Gygi SP. Increasing throughput in targeted proteomics assays: 54-plex quantitation in a single mass spectrometry run. *Anal Chem* 2013;**85**:5340–5346.
- Fancy S-A, Beckonert O, Darbon G, Yabsley W, Walley R, Baker D, Perkins GL, Pullen FS, Rumpel K. Gas chromatography/flame ionisation detection mass spectrometry for the detection of endogenous urine metabolites for metabonomic studies and its use as a complementary tool to nuclear magnetic resonance spectroscopy. *Rapid Commun Mass Spectrom* 2006;**20**:2271–2280.
- Fardilha M, Esteves SLC, Korrodi-Gregório L, Pelech S, Cruz E Silva OAB da, Cruz E Silva E da. Protein phosphatase 1 complexes modulate sperm motility and present novel targets for male infertility. *Mol Hum Reprod* 2011;**17**:466–477.
- Fawcett DW. The mammalian spermatozoon. *Dev Biol* 1975;**44**:394–436.
- Fenderson BA, Toshimori K, Muller CH, Lane TF, Eddy EM. Identification of a protein in the fibrous sheath of the sperm flagellum. *Biol Reprod* 1988;**38**:345–357.
- Ferramosca A, Zara V. Bioenergetics of mammalian sperm capacitation. *Biomed Res Int* 2014;**2014**:902953.
- Ficarro S, Chertihin O, Westbrook VA, White F, Jayes F, Kalab P, Marto J a, Shabanowitz J, Herr JC, Hunt DF, *et al.* Phosphoproteome analysis of capacitated human sperm. Evidence of tyrosine phosphorylation of a kinase-anchoring protein 3 and valosin-containing protein/p97 during capacitation. *J Biol Chem* 2003;**278**:11579–11589.
- Fiedler SE, Dudiki T, Vijayaraghavan S, Carr DW. Loss of R2D2 proteins ROPN1 and ROPN1L causes defects in murine sperm motility, phosphorylation, and fibrous sheath integrity. *Biol Reprod* 2013;**88**:41.
- Folgerø T, Bertheussen K, Lindal S, Torbergesen T, Oian P. Mitochondrial disease and reduced sperm motility. *Hum Reprod* 1993;**8**:1863–1868.
- Ford WCL. Glycolysis and sperm motility: does a spoonful of sugar help the flagellum go round? *Hum Reprod Update* 2006;**12**:269–274.

- Frapsauce C, Pionneau C, Bouley J, Larouzière V de, Berthaut I, Ravel C, Antoine J-M, Soubrier F, Mandelbaum J. [Unexpected in vitro fertilization failure in patients with normal sperm: a proteomic analysis]. *Gynécologie, Obs Fertil* 2009;**37**:796–802.
- Fraser LR. The “switching on” of mammalian spermatozoa: molecular events involved in promotion and regulation of capacitation. *Mol Reprod Dev* 2010;**77**:197–208.
- Frenette G, Girouard J, D’Amours O, Allard N, Tessier L, Sullivan R. Characterization of two distinct populations of epididymosomes collected in the intraluminal compartment of the bovine cauda epididymis. *Biol Reprod* 2010;**83**:473–480.
- Frolkis A, Knox C, Lim E, Jewison T, Law V, Hau DD, Liu P, Gautam B, Ly S, Guo AC, *et al.* SMPDB: The Small Molecule Pathway Database. *Nucleic Acids Res* 2010;**38**:D480–D487.
- Fujinoki M, Kawamura T, Toda T, Ohtake H, Ishimoda-Takagi T, Shimizu N, Yamaoka S, Okuno M. Identification of 36 kDa phosphoprotein in fibrous sheath of hamster spermatozoa. *Comp Biochem Physiol B Biochem Mol Biol* 2004;**137**:509–520.
- Fujita a, Nakamura K, Kato T, Watanabe N, Ishizaki T, Kimura K, Mizoguchi a, Narumiya S. Ropporin, a sperm-specific binding protein of rhophilin, that is localized in the fibrous sheath of sperm flagella. *J Cell Sci* 2000;**113**:103–112.
- Fukuda N, Yomogida K, Okabe M, Touhara K. Functional characterization of a mouse testicular olfactory receptor and its role in chemosensing and in regulation of sperm motility. *J Cell Sci* 2004;**117**:5835–5845.
- Fulcher KD, Mori C, Welch JE, O’Brien DA, Klapper DG, Eddy EM. Characterization of Fsc1 cDNA for a mouse sperm fibrous sheath component. *Biol Reprod* 1995a;**52**:41–49.
- Fulcher KD, Welch JE, Klapper DG, O’Brien DA, Eddy EM. Identification of a unique mu-class glutathione S-transferase in mouse spermatogenic cells. *Mol Reprod Dev* 1995b;**42**:415–424.
- Gamboa S, Ramalho-Santos J. SNARE proteins and caveolin-1 in stallion spermatozoa: possible implications for fertility. *Theriogenology* 2005;**64**:275–291.
- Garolla A, Maiorino M, Roverato A, Roveri A, Ursini F, Foresta C. Oral carnitine supplementation increases sperm motility in asthenozoospermic men with normal sperm phospholipid hydroperoxide glutathione peroxidase levels. *Fertil Steril* 2005;**83**:355–361.
- Gastmann O, Burfeind P, Günther E, Hameister H, Szpirer C, Hoyer-Fender S. Sequence, expression, and chromosomal assignment of a human sperm outer dense fiber gene. *Mol Reprod Dev* 1993;**36**:407–418.
- Gatewood JM, Cook GR, Balhorn R, Bradbury EM, Schmid CW. Sequence-specific packaging of DNA in human sperm chromatin. *Science* 1987;**236**:962–964.
- Goldberg E, Sberna D, Wheat T, Urbanski G, Margoliash E. Cytochrome c: immunofluorescent localization of the testis-specific form. *Science (80- )* 1977;**196**:1010–1012.

- Griffin JL, Troke J, Walker LA, Shore RF, Lindon JC, Nicholson JK. The biochemical profile of rat testicular tissue as measured by magic angle spinning  $^1\text{H}$  NMR spectroscopy. *FEBS Lett* 2000;**486**:225–229.
- Grogan WM, Lam JW. Fatty acid synthesis in isolated spermatocytes and spermatids of mouse testis. *Lipids* 1982;**17**:604–611.
- Gupta A, Mahdi AA, Ahmad MK, Shukla KK, Bansal N, Jaiswer SP, Shankhwar SN. A proton NMR study of the effect of *Mucuna pruriens* on seminal plasma metabolites of infertile males. *J Pharm Biomed Anal* 2011a;**55**:1060–1066. Elsevier B.V.
- Gupta A, Mahdi AA, Ahmad MK, Shukla KK, Jaiswer SP, Shankhwar SN.  $^1\text{H}$  NMR spectroscopic studies on human seminal plasma: a probative discriminant function analysis classification model. *J Pharm Biomed Anal* 2011b;**54**:106–113. Elsevier B.V.
- Gupta A, Mahdi AA, Shukla KK, Ahmad MK, Bansal N, Sankhwar P, Sankhwar SN. Efficacy of *Withania somnifera* on seminal plasma metabolites of infertile males: a proton NMR study at 800 MHz. *J Ethnopharmacol* 2013;**149**:208–214.
- Hamamah S, Seguin F, Barthelemy C, Akoka S, Pape A Le, Lansac J, Royere D.  $^1\text{H}$  nuclear magnetic resonance studies of seminal plasma from fertile and infertile men. *J Reprod Fertil* 1993;**97**:51–55.
- Hammond JW, Cai D, Verhey KJ. Tubulin modifications and their cellular functions. *Curr Opin Cell Biol* 2008;**20**:71–76.
- Hammoud SS, Nix D a, Zhang H, Purwar J, Carrell DT, Cairns BR. Distinctive chromatin in human sperm packages genes for embryo development. *Nature* 2009;**460**:473–478. Nature Publishing Group.
- Hayes JM, Kim SK, Abitua PB, Park TJ, Herrington ER, Kitayama A, Grow MW, Ueno N, Wallingford JB. Identification of novel ciliogenesis factors using a new in vivo model for mucociliary epithelial development. *Dev Biol* 2007;**312**:115–130.
- Henry VJ, Bandrowski a. E, Pepin a.-S, Gonzalez BJ, Desfeux a. OMICtools: an informative directory for multi-omic data analysis. *Database* 2014;**2014**:bau069–bau069.
- Hereng TH, Elgstøen KBP, Cederkvist FH, Eide L, Jahnsen T, Skålhegg BS, Rosendal KR. Exogenous pyruvate accelerates glycolysis and promotes capacitation in human spermatozoa. *Hum Reprod* 2011;**26**:3249–3263.
- Hervann A, Gonzales J, Troupel S, Galli A. Amino acid content of human semen in normal and infertility cases. *Andrologia* 1986;**18**:461–469.
- Hess KC, Jones BH, Marquez B, Chen Y, Ord TS, Kamenetsky M, Miyamoto C, Zippin JH, Kopf GS, Suarez SS, *et al.* The “soluble” adenylyl cyclase in sperm mediates multiple signaling events required for fertilization. *Dev Cell* 2005;**9**:249–259.
- Hess R a, Miller L a, Kirby JD, Margoliash E, Goldberg E. Immunoelectron microscopic localization of testicular and somatic cytochromes c in the seminiferous epithelium of the rat. *Biol Reprod* 1993;**48**:1299–1308.

- Ho H, Granish KA, Suarez SS. Hyperactivated motility of bull sperm is triggered at the axoneme by Ca<sup>2+</sup> and not cAMP. *Dev Biol* 2002;**250**:208–217.
- Ho H, Wey S. Three dimensional rendering of the mitochondrial sheath morphogenesis during mouse spermiogenesis. *Microsc Res Tech* 2007;**70**:719–723.
- Holdcraft RW, Braun RE. Hormonal regulation of spermatogenesis. *Int J Androl* 2004;**27**:335–342.
- Holland A, Ohlendieck K. Comparative profiling of the sperm proteome. *Proteomics* 2014;
- Holstein A-F, Schulze W, Davidoff M. Understanding spermatogenesis is a prerequisite for treatment. *Reprod Biol Endocrinol* 2003;**1**:107.
- Hou C-C, Yang W-X. New insights to the ubiquitin-proteasome pathway (UPP) mechanism during spermatogenesis. *Mol Biol Rep* 2013;**40**:3213–3230.
- Hoyer-Fender S, Burfeind P, Hameister H. Sequence of mouse Odf1 cDNA and its chromosomal localization: extension of the linkage group between human chromosome 8 and mouse chromosome 15. *Cytogenet Cell Genet* 1995;**70**:200–204.
- Huang DW, Sherman BT, Lempicki RA. Systematic and integrative analysis of large gene lists using DAVID bioinformatics resources. *Nat Protoc* 2009a;**4**:44–57.
- Huang DW, Sherman BT, Lempicki RA. Bioinformatics enrichment tools: paths toward the comprehensive functional analysis of large gene lists. *Nucleic Acids Res* 2009b;**37**:1–13.
- Hughes V. Epigenetics: The sins of the father. *Nature* 2014;**507**:22–24.
- Hung P-H, Froenicke L, Lin CY, Lyons L a, Miller MG, Pinkerton KE, VandeVoort C a. Effects of environmental tobacco smoke in vivo on rhesus monkey semen quality, sperm function, and sperm metabolism. *Reprod Toxicol* 2009;**27**:140–148.
- Huszar G, Stone K, Dix D, Vigue L. Putative creatine kinase M-isoform in human sperm is identified as the 70-kilodalton heat shock protein HspA2. *Biol Reprod* 2000;**63**:925–932.
- Hüttemann M, Jaradat S, Grossman LI. Cytochrome c oxidase of mammals contains a testes-specific isoform of subunit VIb--the counterpart to testes-specific cytochrome c? *Mol Reprod Dev* 2003;**66**:8–16.
- Hwang K, Walters RC, Lipshultz LI. Contemporary concepts in the evaluation and management of male infertility. *Nat Rev Urol* 2011;**8**:86–94. Nature Publishing Group.
- Ignotz GG, Suarez SS. Calcium/calmodulin and calmodulin kinase II stimulate hyperactivation in demembrated bovine sperm. *Biol Reprod* 2005;**73**:519–526.
- Iida H, Honda Y, Matsuyama T, Shibata Y, Inai T. Tektin 4 is located on outer dense fibers, not associated with axonemal tubulins of flagella in rodent spermatozoa. *Mol Reprod Dev* 2006;**73**:929–936.

- Ijiri TW, Vadnais ML, Lin AM, Huang AP, Cao W, Merdiushev T, Gerton GL. Male mice express spermatogenic cell-specific triosephosphate isomerase isozymes. *Mol Reprod Dev* 2013;**80**:862–870.
- Inaba K. Sperm flagella: comparative and phylogenetic perspectives of protein components. *Mol Hum Reprod* 2011;**17**:524–538.
- Inoue N, Ikawa M, Isotani A, Okabe M. The immunoglobulin superfamily protein Izumo is required for sperm to fuse with eggs. *Nature* 2005;**434**:234–238.
- Jaiswal BS, Conti M. Calcium regulation of the soluble adenylyl cyclase expressed in mammalian spermatozoa. *Proc Natl Acad Sci U S A* 2003;**100**:10676–10681.
- Jeulin C, Lewin LM. Role of free L-carnitine and acetyl-L-carnitine in post-gonadal maturation of mammalian spermatozoa. *Hum Reprod Update* 1996;**2**:87–102.
- Jewison T, Su Y, Disfany FM, Liang Y, Knox C, Maciejewski A, Poelzer J, Huynh J, Zhou Y, Arndt D, et al. SMPDB 2.0: big improvements to the Small Molecule Pathway Database. *Nucleic Acids Res* 2014;**42**:D478–D484.
- Jodar M, Kalko S, Castillo J, Ballescà JL, Oliva R. Differential RNAs in the sperm cells of asthenozoospermic patients. *Hum Reprod* 2012;**27**:1431–1438.
- Johnston DS, Wooters J, Kopf GS, Qiu Y, Roberts KP. Analysis of the human sperm proteome. *Ann N Y Acad Sci* 2005;**1061**:190–202.
- Jones AR, Bubb WA. Substrates for endogenous metabolism by mature boar spermatozoa. *J Reprod Fertil* 2000;**119**:129–135.
- Jope RS, Johnson GVW. The glamour and gloom of glycogen synthase kinase-3. *Trends Biochem Sci* 2004;**29**:95–102.
- Kaidanovich-Beilin O, Woodgett JR. GSK-3: Functional Insights from Cell Biology and Animal Models. *Front Mol Neurosci* 2011;**4**:40.
- Käll L, Canterbury JD, Weston J, Noble WS, MacCoss MJ. Semi-supervised learning for peptide identification from shotgun proteomics datasets. *Nat Methods* 2007;**4**:923–925.
- Kamburov A, Cavill R, Ebbels TMD, Herwig R, Keun HC. Integrated pathway-level analysis of transcriptomics and metabolomics data with IMPaLA. *Bioinformatics* 2011;**27**:2917–2918.
- Katz DF, Vanagimachi R. Movement characteristics of hamster spermatozoa within the oviduct. *Biol Reprod* 1980;**22**:759–764.
- Kierszenbaum AL, Rivkin E, Fefer-Sadler S, Mertz JR, Tres LL. Purification, partial characterization, and localization of Sak57, an acidic intermediate filament keratin present in rat spermatocytes, spermatids, and sperm. *Mol Reprod Dev* 1996;**44**:382–394.
- Kierszenbaum AL. Keratins: unraveling the coordinated construction of scaffolds in spermatogenic cells. *Mol Reprod Dev* 2002;**61**:1–2.



- Kirichok Y, Lishko P V. Rediscovering sperm ion channels with the patch-clamp technique. *Mol Hum Reprod* 2011;**17**:478–499.
- Kirichok Y, Navarro B, Clapham DE. Whole-cell patch-clamp measurements of spermatozoa reveal an alkaline-activated Ca<sup>2+</sup> channel. *Nature* 2006;**439**:737–740.
- Kirkman-Brown JC, Smith DJ. Sperm motility: is viscosity fundamental to progress? *Mol Hum Reprod* 2011;**17**:539–544.
- Korzeniewski N, Hohenfellner M, Duensing S. CAND1 promotes PLK4-mediated centriole overduplication and is frequently disrupted in prostate cancer. *Neoplasia* 2012;**14**:799–806.
- Kouskoumvekaki I, Panagiotou G. Navigating the human metabolome for biomarker identification and design of pharmaceutical molecules. *J Biomed Biotechnol* 2011;**2011**:
- Kovac JR, Pastuszak AW, Lamb DJ. The use of genomics, proteomics, and metabolomics in identifying biomarkers of male infertility. *Fertil Steril* 2013;**99**:998–1007.
- Kretser DM de, Loveland KL, Meinhardt a, Simorangkir D, Wreford N. Spermatogenesis. *Hum Reprod* 1998;**13 Suppl 1**:1–8.
- Krisfalusi M, Miki K, Magyar PL, O’Brien D a. Multiple glycolytic enzymes are tightly bound to the fibrous sheath of mouse spermatozoa. *Biol Reprod* 2006;**75**:270–278.
- Kuile BH, Westerhoff H V. Transcriptome meets metabolome: Hierarchical and metabolic regulation of the glycolytic pathway. *FEBS Lett* 2001;**500**:169–171.
- Leclerc P, Lamirande E de, Gagnon C. Cyclic adenosine 3’,5’monophosphate-dependent regulation of protein tyrosine phosphorylation in relation to human sperm capacitation and motility. *Biol Reprod* 1996;**55**:684–692.
- Lefèvre PLC, Palin M-F, Murphy BD. Polyamines on the reproductive landscape. *Endocr Rev* 2011;**32**:694–712.
- Lehti MS, Kotaja N, Sironen A. KIF3A is essential for sperm tail formation and manchette function. *Mol Cell Endocrinol* 2013;**377**:44–55.
- Lenzi A, Picardo M, Gandini L, Dondero F. Lipids of the sperm plasma membrane: from polyunsaturated fatty acids considered as markers of sperm function to possible scavenger therapy. *Hum Reprod Update***2**:246–256.
- Li L-W, Fan L-Q, Zhu W-B, Nien H-C, Sun B-L, Luo K-L, Liao T-T, Tang L, Lu G-X. Establishment of a high-resolution 2-D reference map of human spermatozoal proteins from 12 fertile sperm-bank donors. *Asian J Androl* 2007;**9**:321–329.
- Liao T-T, Xiang Z, Zhu W-B, Fan L-Q. Proteome analysis of round-headed and normal spermatozoa by 2-D fluorescence difference gel electrophoresis and mass spectrometry. *Asian J Androl* 2009;**11**:683–693.

- Lin C-Y, Hung P, VandeVoort C a, Miller MG. 1H NMR to investigate metabolism and energy supply in rhesus macaque sperm. *Reprod Toxicol* 2009;**28**:75–80.
- Lin CY, Wu H, Tjeerdema RS, Viant MR. Evaluation of metabolite extraction strategies from tissue samples using NMR metabolomics. *Metabolomics* 2007;**3**:55–67.
- Lin J, Okada K, Raytchev M, Smith MC, Nicastro D. Structural mechanism of the dynein power stroke. *Nat Cell Biol* 2014;**16**:479–485.
- Lishko P V, Botchkina IL, Kirichok Y. Progesterone activates the principal Ca<sup>2+</sup> channel of human sperm. *Nature* 2011;**471**:387–391.
- Lishko P V, Kirichok Y, Ren D, Navarro B, Chung J-J, Clapham DE. The control of male fertility by spermatozoan ion channels. *Annu Rev Physiol* 2012;**74**:453–475.
- Liu J, Furukawa M, Matsumoto T, Xiong Y. NEDD8 modification of CUL1 dissociates p120(CAND1), an inhibitor of CUL1-SKP1 binding and SCF ligases. *Mol Cell* 2002;**10**:1511–1518.
- Liu Y, Guo Y, Song N, Fan Y, Li K, Teng X, Guo Q, Ding Z. Proteomic pattern changes associated with obesity-induced asthenozoospermia. *Andrology* 2014;1–13.
- Mannowetz N, Wandernoth PM, Wennemuth G. Glucose is a pH-dependent motor for sperm beat frequency during early activation. *PLoS One* 2012;**7**:e41030.
- Marin S, Chiang K, Bassilian S, Lee W-NP, Boros LG, Fernández-Novell JM, Centelles JJ, Medrano A, Rodriguez-Gil JE, Cascante M. Metabolic strategy of boar spermatozoa revealed by a metabolomic characterization. *FEBS Lett* 2003;**554**:342–346.
- Marín-Briggiler CI, Jha KN, Chertihin O, Buffone MG, Herr JC, Vazquez-Levin MH, Visconti PE. Evidence of the presence of calcium/calmodulin-dependent protein kinase IV in human sperm and its involvement in motility regulation. *J Cell Sci* 2005;**118**:2013–2022.
- Martínez-Heredia J, Estanyol JM, Ballescà JL, Oliva R. Proteomic identification of human sperm proteins. *Proteomics* 2006;**6**:4356–4369.
- Martínez-Heredia J, Mateo S de, Vidal-Taboada JM, Ballescà JL, Oliva R. Identification of proteomic differences in asthenozoospermic sperm samples. *Hum Reprod* 2008;**23**:783–791.
- Mateo S de, Castillo J, Estanyol JM, Ballescà JL, Oliva R. Proteomic characterization of the human sperm nucleus. *Proteomics* 2011;**11**:2714–2726.
- Mateo S de, Estanyol JM, Oliva R. *Spermatogenesis*. In Carrell DT, Aston KI, editors. 2013;**927**:411–422. Humana Press: Totowa, NJ.
- Mateo S de, Martínez-Heredia J, Estanyol JM, Domínguez-Fandos D, Domínguez-Fandos D, Vidal-Taboada JM, Ballescà JL, Oliva R. Marked correlations in protein expression identified by proteomic analysis of human spermatozoa. *Proteomics* 2007;**7**:4264–4277.

- McKnight K, Hoang HD, Prasain JK, Brown N, Vibbert J, Hollister K a, Moore R, Ragains JR, Reese J, Miller M a. Neurosensory perception of environmental cues modulates sperm motility critical for fertilization. *Science* 2014;**344**:754–757.
- Meersman F, Bowron D, Soper AK, Koch MHJ. Counteraction of urea by trimethylamine N-oxide is due to direct interaction. *Biophys J* 2009;**97**:2559–2566.
- Mengual L, Ballescá JL, Ascaso C, Oliva R. Marked differences in protamine content and P1/P2 ratios in sperm cells from percoll fractions between patients and controls. *J Androl* 2003;**24**:438–447.
- Mercer TR, Mattick JS. Structure and function of long noncoding RNAs in epigenetic regulation. *Nat Struct Mol Biol* 2013;**20**:300–307.
- Meunier B, Dumas E, Piec I, Béchet D, Hébraud M, Hocquette J-F. Assessment of hierarchical clustering methodologies for proteomic data mining. *J Proteome Res* 2007;**6**:358–366.
- Miki K, Qu W, Goulding EH, Willis WD, Bunch DO, Strader LF, Perreault SD, Eddy EM, O'Brien DA. Glyceraldehyde 3-phosphate dehydrogenase-S, a sperm-specific glycolytic enzyme, is required for sperm motility and male fertility. *Proc Natl Acad Sci U S A* 2004;**101**:16501–16506.
- Milacic M, Haw R, Rothfels K, Wu G, Croft D, Hermjakob H, D'Eustachio P, Stein L. Annotating cancer variants and anti-cancer therapeutics in reactome. *Cancers (Basel)* 2012;**4**:1180–1211.
- Miller D, Brinkworth M, Iles D. Paternal DNA packaging in spermatozoa: more than the sum of its parts? DNA, histones, protamines and epigenetics. *Reproduction* 2010;**139**:287–301.
- Miranda-Vizueté A, Tsang K, Yu Y, Jiménez A, Pelto-Huikko M, Flickinger CJ, Sutovsky P, Oko R. Cloning and developmental analysis of murid spermatid-specific thioredoxin-2 (SPTRX-2), a novel sperm fibrous sheath protein and autoantigen. *J Biol Chem* 2003;**278**:44874–44885.
- Mohri H. Amino-acid composition of “Tubulin” constituting microtubules of sperm flagella. *Nature* 1968;**217**:1053–1054.
- Morales CR, Oko R, Clermont Y. Molecular cloning and developmental expression of an mRNA encoding the 27 kDa outer dense fiber protein of rat spermatozoa. *Mol Reprod Dev* 1994;**37**:229–240.
- Morales ME, Rico G, Bravo C, Tapia R, Alvarez C, Méndez JD. [Progressive motility increase caused by L-arginine and polyamines in sperm from patients with idiopathic and diabetic asthenozoospermia]. *Ginecol Obstet Mex* 2003;**71**:297–303.
- Mori C, Nakamura N, Welch JE, Gotoh H, Goulding EH, Fujioka M, Eddy EM. Mouse spermatogenic cell-specific type 1 hexokinase (mHk1-s) transcripts are expressed by alternative splicing from the mHk1 gene and the HK1-S protein is localized mainly in the sperm tail. *Mol Reprod Dev* 1998;**49**:374–385.
- Mori C, Welch JE, Fulcher KD, O'Brien D a, Eddy EM. Unique hexokinase messenger ribonucleic acids lacking the porin-binding domain are developmentally expressed in mouse spermatogenic cells. *Biol Reprod* 1993;**49**:191–203.

- Mukai C, Okuno M. Glycolysis plays a major role for adenosine triphosphate supplementation in mouse sperm flagellar movement. *Biol Reprod* 2004;**71**:540–547.
- Mukai C, Travis AJ. What sperm can teach us about energy production. *Reprod Domest Anim* 2012;**47 Suppl 4**:164–169.
- Murayama E, Yamamoto E, Kaneko T, Shibata Y, Inai T, Iida H. Tektin5, a new Tektin family member, is a component of the middle piece of flagella in rat spermatozoa. *Mol Reprod Dev* 2008;**75**:650–658.
- Nakamura K, Fujita a, Murata T, Watanabe G, Mori C, Fujita J, Watanabe N, Ishizaki T, Yoshida O, Narumiya S. Rhoophilin, a small GTPase Rho-binding protein, is abundantly expressed in the mouse testis and localized in the principal piece of the sperm tail. *FEBS Lett* 1999;**445**:9–13.
- Nakamura N, Dai Q, Williams J, Goulding EH, Willis WD, Brown PR, Eddy EM. Disruption of a spermatogenic cell-specific mouse enolase 4 (eno4) gene causes sperm structural defects and male infertility. *Biol Reprod* 2013;**88**:90.
- Nakamura N, Mori C, Eddy EM. Molecular complex of three testis-specific isozymes associated with the mouse sperm fibrous sheath: hexokinase 1, phosphofructokinase M, and glutathione S-transferase mu class 5. *Biol Reprod* 2010;**82**:504–515.
- Narisawa S, Hecht NB, Goldberg E, Boatright KM, Reed JC, Millán JL. Testis-specific cytochrome c-null mice produce functional sperm but undergo early testicular atrophy. *Mol Cell Biol* 2002;**22**:5554–5562.
- Navara CS, First NL, Schatten G. Microtubule organization in the cow during fertilization, polyspermy, parthenogenesis, and nuclear transfer: the role of the sperm aster. *Dev Biol* 1994;**162**:29–40.
- Ng CM, Blackman MR, Wang C, Swerdloff RS. The role of carnitine in the male reproductive system. *Ann N Y Acad Sci* 2004;**1033**:177–188.
- Nicholls P. The effect of formate on cytochrome aa3 and on electron transport in the intact respiratory chain. *Biochim Biophys Acta* 1976;**430**:13–29.
- Nicholson JK, Connelly J, Lindon JC, Holmes E. Metabonomics: a platform for studying drug toxicity and gene function. *Nat Rev Drug Discov* 2002;**1**:153–161.
- Nicholson JK, Lindon JC. Systems biology: Metabonomics. *Nature* 2008;**455**:1054–1056.
- Nishigaki T, José O, González-Cota AL, Romero F, Treviño CL, Darszon A. Intracellular pH in sperm physiology. *Biochem Biophys Res Commun* 2014;**450**:1149–1158. Elsevier Inc.
- Nolan M a, Babcock DF, Wennemuth G, Brown W, Burton K a, McKnight GS. Sperm-specific protein kinase A catalytic subunit Calpha2 orchestrates cAMP signaling for male fertility. *Proc Natl Acad Sci U S A* 2004;**101**:13483–13488.
- O'Bryan MK, Sebire K, Meinhardt A, Edgar K, Keah HH, Hearn MT, Kretser DM De. Tpx-1 is a component of the outer dense fibers and acrosome of rat spermatozoa. *Mol Reprod Dev* 2001;**58**:116–125.

- Odet F, Duan C, Willis WD, Goulding EH, Kung A, Eddy EM, Goldberg E. Expression of the gene for mouse lactate dehydrogenase C (Ldhc) is required for male fertility. *Biol Reprod* 2008;**79**:26–34.
- Odet F, Gabel S a, Williams J, London RE, Goldberg E, Eddy EM. Lactate dehydrogenase C and energy metabolism in mouse sperm. *Biol Reprod* 2011;**85**:556–564.
- Odet F, Gabel S, London RE, Goldberg E, Eddy EM. Glycolysis and mitochondrial respiration in mouse LDHC-null sperm. *Biol Reprod* 2013;**88**:95.
- Oiki S, Hiyama E, Gotoh T, Iida H. Localization of Tektin 1 at both acrosome and flagella of mouse and bull spermatozoa. *Zoolog Sci* 2014;**31**:101–107.
- Okabe M. The cell biology of mammalian fertilization. *Development* 2013;**140**:4471–4479.
- Okamura N, Tajima Y, Soejima a, Masuda H, Sugita Y. Sodium bicarbonate in seminal plasma stimulates the motility of mammalian spermatozoa through direct activation of adenylate cyclase. *J Biol Chem* 1985;**260**:9699–9705.
- Oliva R, Castillo J. Proteomics and the genetics of sperm chromatin condensation. *Asian J Androl* 2011;**13**:24–30.
- Oliva R, Dixon GH. Expression and processing of the rooster protamine mRNA. *Ann N Y Acad Sci* 1991;**637**:289–299.
- Oliva R, Martínez-Heredia J, Estanyol JM. Proteomics in the study of the sperm cell composition, differentiation and function. *Syst Biol Reprod Med* 2008;**54**:23–36.
- Oliva R, Mateo S de, Estanyol JM. Sperm cell proteomics. *Proteomics* 2009;**9**:1004–1017.
- Oliva R, Vidal S, Mezquita C. Cellular content and biosynthesis of polyamines during rooster spermatogenesis. *Biochem J* 1982;**116**:135–148.
- Oliva R. Protamines and male infertility. *Hum Reprod Update* 2006;**12**:417–435.
- Olson GE, Hamilton DW, Fawcett DW. Isolation and characterization of the fibrous sheath of rat epididymal spermatozoa. *Biol Reprod* 1976;**14**:517–530.
- Olson GE, Winfrey VP. Mitochondria-cytoskeleton interactions in the sperm midpiece. *J Struct Biol* 1990;**103**:13–22.
- Olson SD, Fauci LJ, Suarez SS. Mathematical modeling of calcium signaling during sperm hyperactivation. *Mol Hum Reprod* 2011;**17**:500–510.
- Orosz F, Oláh J, Ovádi J. Triosephosphate isomerase deficiency: facts and doubts. *IUBMB Life* 2006;**58**:703–715.
- Otani H, Tanaka O, Kasai K, Yoshioka T. Development of mitochondrial helical sheath in the middle piece of the mouse spermatid tail: regular dispositions and synchronized changes. *Anat Rec* 1988;**222**:26–33.

- Paasch U, Grunewald S, Kratzsch J, Glander H-J. Obesity and age affect male fertility potential. *Fertil Steril* 2010;**94**:2898–2901.
- Palomo MJ, FernAndez-Novell JM, Peña A, Guinovart JJ, Rigau T, Rodríguez-Gil JE. Glucose- and fructose-induced dog-sperm glycogen synthesis shows specific changes in the location of the sperm glycogen deposition. *Mol Reprod Dev* 2003;**64**:349–359.
- Parte PP, Rao P, Redij S, Lobo V, D'Souza SJ, Gajbhiye R, Kulkarni V. Sperm phosphoproteome profiling by ultra performance liquid chromatography followed by data independent analysis (LC-MS(E)) reveals altered proteomic signatures in asthenozoospermia. *J Proteomics* 2012;**75**:5861–5871.
- Patel a B, Srivastava S, Phadke RS, Govil G. Identification of low-molecular-weight compounds in goat epididymis using multinuclear nuclear magnetic resonance. *Anal Biochem* 1999;**266**:205–215.
- Patel AB, Srivastava S, Phadke RS, Govil G. Arginine activates glycolysis of goat epididymal spermatozoa: an NMR study. *Biophys J* 1998;**75**:1522–1528.
- Patti GJ, Yanes O, Siuzdak G. Innovation: Metabolomics: the apogee of the omics trilogy. *Nat Rev Mol Cell Biol* 2012;**13**:263–269.
- Pereira SL, Rodrigues AS, Sousa MI, Correia M, Perestrelo T, Ramalho-Santos J. From gametogenesis and stem cells to cancer: common metabolic themes. *Hum Reprod Update* 2014;**20**:924–943.
- Petersen C, Füzesi L, Hoyer-Fender S. Outer dense fibre proteins from human sperm tail: molecular cloning and expression analyses of two cDNA transcripts encoding proteins of approximately 70 kDa. *Mol Hum Reprod* 1999;**5**:627–635.
- Peterson RN, Freund M. ATP synthesis and oxidative metabolism in human spermatozoa. *Biol Reprod* 1970;**3**:47–54.
- Piomboni P, Focarelli R, Stendardi a, Ferramosca a, Zara V. The role of mitochondria in energy production for human sperm motility. *Int J Androl* 2012;**35**:109–124.
- Pixton KL, Deeks ED, Flesch FM, Moseley FLC, Björndahl L, Ashton PR, Barratt CLR, Brewis I a. Sperm proteome mapping of a patient who experienced failed fertilization at IVF reveals altered expression of at least 20 proteins compared with fertile donors: case report. *Hum Reprod* 2004;**19**:1438–1447.
- du Plessis SS, Agarwal A, Mohanty G, Linde M van der. Oxidative phosphorylation versus glycolysis: what fuel do spermatozoa use? *Asian J Androl* 2014; Nov 25. doi: 10.4103/1008-682X.135123. [Epub ahead of print]
- Porter ME, Sale WS. The 9 + 2 axoneme anchors multiple inner arm dyneins and a network of kinases and phosphatases that control motility. *J Cell Biol* 2000;**151**:F37–F42.
- Primakoff P, Myles DG. Penetration, adhesion, and fusion in mammalian sperm-egg interaction. *Science* 2002;**296**:2183–2185.

- Publicover SJ, Barratt CLR. Sperm motility: things are moving in the lab! *Mol Hum Reprod* 2011;**17**:453–456.
- Ramalho-Santos J, Amaral A, Sousa AP, Rodrigues AS, Martins L, Baptista M, Mota PC, Tavares R, Amaral S, Gamboa S. Probing the structure and function of mammalian sperm using optical and fluorescence microscopy. In Mendez-Vilas A, Diaz J, editors. *Mod Res Educ Top Microsc* 2007;**351**: p. 394–402.
- Ramalho-Santos J, Varum S, Amaral S, Mota PC, Sousa AP, Amaral A. Mitochondrial functionality in reproduction: from gonads and gametes to embryos and embryonic stem cells. *Hum Reprod Update* 2009;**15**:553–572.
- Rando OJ. Daddy issues: paternal effects on phenotype. *Cell* 2012;**151**:702–708.
- Raso C, Cosentino C, Gaspari M, Malara N, Han X, McClatchy D, Park SK, Renne M, Vadalà N, Prati U, et al. Characterization of breast cancer interstitial fluids by TmT labeling, LTQ-Orbitrap Velos mass spectrometry, and pathway analysis. *J Proteome Res* 2012;**11**:3199–3210.
- Reda T, Plugge CM, Abram NJ, Hirst J. Reversible interconversion of carbon dioxide and formate by an electroactive enzyme. *Proc Natl Acad Sci U S A* 2008;**105**:10654–10658.
- Ren D, Navarro B, Perez G, Jackson AC, Hsu S, Shi Q, Tilly JL, Clapham DE. A sperm ion channel required for sperm motility and male fertility. *Nature* 2001;**413**:603–609.
- Rivera CM, Ren B. Mapping human epigenomes. *Cell* 2013;**155**:39–55.
- Rosca MG, Lemieux H, Hoppel CL. Mitochondria in the elderly: Is acetylcarnitine a rejuvenator? *Adv Drug Deliv Rev* 2009;**61**:1332–1342.
- Roy A, Lin Y-N, Agno JE, DeMayo FJ, Matzuk MM. Absence of tektin 4 causes asthenozoospermia and subfertility in male mice. *FASEB J* 2007;**21**:1013–1025.
- Roy A, Lin Y-N, Agno JE, DeMayo FJ, Matzuk MM. Tektin 3 is required for progressive sperm motility in mice. *Mol Reprod Dev* 2009;**76**:453–459.
- Roy A, Yan W, Burns KH, Matzuk MM. Tektin3 encodes an evolutionarily conserved putative testicular microtubules-related protein expressed preferentially in male germ cells. *Mol Reprod Dev* 2004;**67**:295–302.
- Ruiz-Pesini E, Diez C, Lapeña AC, Pérez-Martos A, Montoya J, Alvarez E, Arenas J, López-Pérez MJ. Correlation of sperm motility with mitochondrial enzymatic activities. *Clin Chem* 1998;**44**:1616–1620.
- Ruiz-Pesini E, Díez-Sánchez C, López-Pérez MJ, Enríquez JA. The role of the mitochondrion in sperm function: is there a place for oxidative phosphorylation or is this a purely glycolytic process? *Curr Top Dev Biol* 2007;**77**:3–19.
- Ruiz-Pesini E, Lapeña a C, Díez-Sánchez C, Pérez-Martos a, Montoya J, Alvarez E, Díaz M, Urriés a, Montoro L, López-Pérez MJ, et al. Human mtDNA haplogroups associated with high or reduced spermatozoa motility. *Am J Hum Genet* 2000;**67**:682–696.

- Russell DL, Kim KH. Expression of triosephosphate isomerase transcripts in rat testis: evidence for retinol regulation and a novel germ cell transcript. *Biol Reprod* 1996;**55**:11–18.
- Sale WS, Satir P. Direction of active sliding of microtubules in Tetrahymena cilia. *Proc Natl Acad Sci U S A* 1977;**74**:2045–2049.
- Samans B, Yang Y, Krebs S, Sarode GV, Blum H, Reichenbach M, Wolf E, Steger K, Dansranjavin T, Schagdarsurengin U. Uniformity of Nucleosome Preservation Pattern in Mammalian Sperm and Its Connection to Repetitive DNA Elements. *Dev Cell* 2014;**30**:23–35.
- Satir P. Studies on cilia. 3. Further studies on the cilium tip and a “sliding filament” model of ciliary motility. *J Cell Biol* 1968;**39**:77–94.
- Schalles U, Shao X, Hoorn F a van der, Oko R. Developmental expression of the 84-kDa ODF sperm protein: localization to both the cortex and medulla of outer dense fibers and to the connecting piece. *Dev Biol* 1998;**199**:250–260.
- Schulte RT, Ohl D a, Sigman M, Smith GD. Sperm DNA damage in male infertility: etiologies, assays, and outcomes. *J Assist Reprod Genet* 2010;**27**:3–12.
- Secciani F, Bianchi L, Ermini L, Cianti R, Armini A, Sala GB La, Focarelli R, Bini L, Rosati F. Protein profile of capacitated versus ejaculated human sperm. *J Proteome Res* 2009;**8**:3377–3389.
- Shao X, Tarnasky H a., Schalles U, Oko R, Hoorn F a. van der. Interactional Cloning of the 84-kDa Major Outer Dense Fiber Protein Odf84: LEUCINE ZIPPER MEDIATED ASSOCIATIONS OF Odf84 AND Odf27. *J Biol Chem* 1997;**272**:6105–6113.
- Si Y, Okuno M. Role of tyrosine phosphorylation of flagellar proteins in hamster sperm hyperactivation. *Biol Reprod* 1999;**61**:240–246.
- Si Y, Olds-Clarke P. Evidence for the involvement of calmodulin in mouse sperm capacitation. *Biol Reprod* 2000;**62**:1231–1239.
- Silva FP, Hamamoto R, Nakamura Y, Furukawa Y. WDRPUH, A Novel WD-Repeat—Containing Protein, Is Highly Expressed in Human Hepatocellular Carcinoma and Involved in Cell Proliferation. *Neoplasia* 2005;**7**:348–355.
- Sinclair J, Timms JF. Quantitative profiling of serum samples using TMT protein labelling, fractionation and LC-MS/MS. *Methods* 2011;**54**:361–369.
- Siva AB, Kameshwari DB, Singh V, Pavani K, Sundaram CS, Rangaraj N, Deenadayal M, Shivaji S. Proteomics-based study on asthenozoospermia: differential expression of proteasome alpha complex. *Mol Hum Reprod* 2010;**16**:452–462.
- Smith GD, Wolf DP, Trautman KC, Cruz e Silva EF da, Greengard P, Vijayaraghavan S. Primate sperm contain protein phosphatase 1, a biochemical mediator of motility. *Biol Reprod* 1996;**54**:719–727.
- Smith GD, Wolf DP, Trautman KC, Vijayaraghavan S. Motility potential of macaque epididymal sperm: the role of protein phosphatase and glycogen synthase kinase-3 activities. *J Androl* 1999;**20**:47–53.



- Smith R, Mathis AD, Ventura D, Prince JT. Proteomics, lipidomics, metabolomics: a mass spectrometry tutorial from a computer scientist's point of view. *BMC Bioinformatics* 2014;**15** Suppl 7:S9.
- Somanath PR, Jack SL, Vijayaraghavan S. Changes in sperm glycogen synthase kinase-3 serine phosphorylation and activity accompany motility initiation and stimulation. *J Androl* 2004;**25**:605–617.
- Son WY, Han CT, Hwang SH, Lee JH, Kim S, Kim YC. Repression of hspA2 messenger RNA in human testes with abnormal spermatogenesis. *Fertil Steril* 2000;**73**:1138–1144.
- Son WY, Hwang SH, Han CT, Lee JH, Kim S, Kim YC. Specific expression of heat shock protein HspA2 in human male germ cells. *Mol Hum Reprod* 1999;**5**:1122–1126.
- Sousa AP, Amaral A, Baptista M, Tavares R, Caballero Campo P, Caballero Peregrín P, Freitas A, Paiva A, Almeida-Santos T, Ramalho-Santos J. Not all sperm are equal: functional mitochondria characterize a subpopulation of human sperm with better fertilization potential. *PLoS One* 2011;**6**:e18112.
- Spehr M, Schwane K, Riffell J a, Barbour J, Zimmer RK, Neuhaus EM, Hatt H. Particulate adenylate cyclase plays a key role in human sperm olfactory receptor-mediated chemotaxis. *J Biol Chem* 2004;**279**:40194–40203.
- St John JC, Jokhi RP, Barratt CLR. The impact of mitochondrial genetics on male infertility. *Int J Androl* 2005;**28**:65–73.
- Storey BT. Mammalian sperm metabolism: oxygen and sugar, friend and foe. *Int J Dev Biol* 2008;**52**:427–437.
- Strünker T, Goodwin N, Brenker C, Kashikar ND, Weyand I, Seifert R, Kaupp UB. The CatSper channel mediates progesterone-induced Ca<sup>2+</sup> influx in human sperm. *Nature* 2011;**471**:382–386.
- Suárez SS, Osman R a. Initiation of hyperactivated flagellar bending in mouse sperm within the female reproductive tract. *Biol Reprod* 1987;**36**:1191–1198.
- Suarez SS. Control of hyperactivation in sperm. *Hum Reprod Update* 2008;**14**:647–657.
- Summers KE, Gibbons IR. Adenosine triphosphate-induced sliding of tubules in trypsin-treated flagella of sea-urchin sperm. *Proc Natl Acad Sci U S A* 1971;**68**:3092–3096.
- Sutovsky P, Hewitson L, Simerly CR, Tengowski MW, Navara CS, Haavisto a, Schatten G. Intracytoplasmic sperm injection for Rhesus monkey fertilization results in unusual chromatin, cytoskeletal, and membrane events, but eventually leads to pronuclear development and sperm aster assembly. *Hum Reprod* 1996;**11**:1703–1712.
- Sutovsky P. Sperm proteasome and fertilization. *Reproduction* 2011;**142**:1–14.
- Tamburrino L, Marchiani S, Minetti F, Forti G, Muratori M, Baldi E. The CatSper calcium channel in human sperm: relation with motility and involvement in progesterone-induced acrosome reaction. *Hum Reprod* 2014;**29**:418–428.

- Tanaka H, Iguchi N, Toyama Y, Kitamura K, Takahashi T, Kaseda K, Maekawa M, Nishimune Y. Mice deficient in the axonemal protein Tektin-t exhibit male infertility and immotile-cilium syndrome due to impaired inner arm dynein function. *Mol Cell Biol* 2004a;**24**:7958–7964.
- Tanaka H, Takahashi T, Iguchi N, Kitamura K, Miyagawa Y, Tsujimura A, Matsumiya K, Okuyama A, Nishimune Y. Ketone bodies could support the motility but not the acrosome reaction of mouse sperm. *Int J Androl* 2004b;**27**:172–177.
- Tash JS, Bracho GE. Regulation of sperm motility: emerging evidence for a major role for protein phosphatases. *J Androl* 1994;**15**:505–509.
- Tash JS, Krinks M, Patel J, Means RL, Klee CB, Means a R. Identification, characterization, and functional correlation of calmodulin-dependent protein phosphatase in sperm. *J Cell Biol* 1988;**106**:1625–1633.
- Tash JS, Means AR. Regulation of protein phosphorylation and motility of sperm by cyclic adenosine monophosphate and calcium. *Biol Reprod* 1982;**26**:745–763.
- Tash JS, Means AR. Cyclic adenosine 3',5' monophosphate, calcium and protein phosphorylation in flagellar motility. *Biol Reprod* 1983;**28**:75–104.
- Tash JS. Protein phosphorylation: the second messenger signal transducer of flagellar motility. *Cell Motil Cytoskeleton* 1989;**14**:332–339.
- Terada Y, Simerly CR, Hewitson L, Schatten G. Sperm aster formation and pronuclear decondensation during rabbit fertilization and development of a functional assay for human sperm. *Biol Reprod* 2000;**62**:557–563.
- Theodoridis G, Gika HG, Wilson ID. LC-MS-based methodology for global metabolite profiling in metabonomics/metabolomics. *TrAC Trends Anal Chem* 2008;**27**:251–260.
- Thompson A, Schäfer J, Kuhn K, Kienle S, Schwarz J, Schmidt G, Neumann T, Johnstone R, Mohammed a K a, Hamon C. Tandem mass tags: a novel quantification strategy for comparative analysis of complex protein mixtures by MS/MS. *Anal Chem* 2003;**75**:1895–1904.
- Thonneau P, Marchand S, Tallec A, Ferial M-L, Ducot B, Lansac J, Lopes P, Tabaste J-M, Spira A. Incidence and main causes of infertility in a resident population (1 850 000) of three French regions (1988-1989)\*. *Hum Reprod* 1991;**6**:811–816.
- Tomlinson M, Lewis S, Morroll D. Sperm quality and its relationship to natural and assisted conception: British Fertility Society guidelines for practice. *Hum Fertil (Camb)* 2013;**16**:175–193.
- Torregrosa N, Domínguez-Fandos D, Camejo MI, Shirley CR, Meistrich ML, Ballescà JL, Oliva R. Protamine 2 precursors, protamine 1/protamine 2 ratio, DNA integrity and other sperm parameters in infertile patients. *Hum Reprod* 2006;**21**:2084–2089.
- Travis a J, Foster J a, Rosenbaum N a, Visconti PE, Gerton GL, Kopf GS, Moss SB. Targeting of a germ cell-specific type 1 hexokinase lacking a porin-binding domain to the mitochondria as well as to the head and fibrous sheath of murine spermatozoa. *Mol Biol Cell* 1998;**9**:263–276.

- Tres LL, Kierszenbaum AL. Sak57, an acidic keratin initially present in the spermatid manchette before becoming a component of paraaxonemal structures of the developing tail. *Mol Reprod Dev* 1996;**44**:395–407.
- Turner RM. Tales from the tail: what do we really know about sperm motility? *J Androl* 2003;**24**:790–803.
- Turner RM. Moving to the beat: a review of mammalian sperm motility regulation. *Reprod Fertil Dev* 2006;**18**:25–38.
- Urner F, Sakkas D. Characterization of glycolysis and pentose phosphate pathway activity during sperm entry into the mouse oocyte. *Biol Reprod* 1999;**60**:973–978.
- Urner F, Sakkas D. Involvement of the pentose phosphate pathway and redox regulation in fertilization in the mouse. *Mol Reprod Dev* 2005;**70**:494–503.
- Urra JA, Villaroel-Espíndola F, Covarrubias AA, Rodríguez-Gil JE, Ramírez-Reveco A, Concha II. Presence and function of dopamine transporter (DAT) in stallion sperm: dopamine modulates sperm motility and acrosomal integrity. *PLoS One* 2014;**9**:e112834.
- Ursini F, Heim S, Kiess M, Maiorino M, Roveri A, Wissing J, Flohé L. Dual function of the selenoprotein PHGPx during sperm maturation. *Science* 1999;**285**:1393–1396.
- Usselman MC, Cone RA. Rat sperm are mechanically immobilized in the caudal epididymis by “immobilin,” a high molecular weight glycoprotein. *Biol Reprod* 1983;**29**:1241–1253.
- Vadnais ML, Aghajanian HK, Lin A, Gerton GL. Signaling in sperm: toward a molecular understanding of the acquisition of sperm motility in the mouse epididymis. *Biol Reprod* 2013;**89**:127.
- Vijayaraghavan S, Mohan J, Gray H, Khatra B, Carr DW. A role for phosphorylation of glycogen synthase kinase-3 $\alpha$  in bovine sperm motility regulation. *Biol Reprod* 2000;**62**:1647–1654.
- Vijayaraghavan S, Stephens DT, Trautman K, Smith GD, Khatra B, Cruz e Silva EF da, Greengard P. Sperm motility development in the epididymis is associated with decreased glycogen synthase kinase-3 and protein phosphatase 1 activity. *Biol Reprod* 1996;**54**:709–718.
- Visconti PE, Kopf GS. Regulation of protein phosphorylation during sperm capacitation. *Biol Reprod* 1998;**59**:1–6.
- Wang G, Guo Y, Zhou T, Shi X, Yu J, Yang Y, Wu Y, Wang J, Liu M, Chen X, *et al.* In-depth proteomic analysis of the human sperm reveals complex protein compositions. *J Proteomics* 2013;**79**:114–122. Elsevier B.V.
- Wargo MJ, Smith EF. Asymmetry of the central apparatus defines the location of active microtubule sliding in *Chlamydomonas* flagella. *Proc Natl Acad Sci U S A* 2003;**100**:137–142.
- Wassarman PM. Reproductive biology: Sperm protein finds its mate. *Nature* 2014;**508**:466–467. Nature Publishing Group, a division of Macmillan Publishers Limited. All Rights Reserved.

- Welch JE, Schatte EC, O'Brien DA, Eddy EM. Expression of a glyceraldehyde 3-phosphate dehydrogenase gene specific to mouse spermatogenic cells. *Biol Reprod* 1992;**46**:869–878.
- Wennemuth G, Carlson AE, Harper AJ, Babcock DF. Bicarbonate actions on flagellar and Ca<sup>2+</sup> - channel responses: initial events in sperm activation. *Development* 2003;**130**:1317–1326.
- WHO. *WHO laboratory manual for the Examination and processing of human semen*. In World Health Organization, 5<sup>th</sup> edition. 2010. Geneva.
- Williams AC, Ford WC. The role of glucose in supporting motility and capacitation in human spermatozoa. *J Androl* 2001;**22**:680–695.
- Wishart DS, Jewison T, Guo AC, Wilson M, Knox C, Liu Y, Djoumbou Y, Mandal R, Aziat F, Dong E, *et al*. HMDB 3.0--The Human Metabolome Database in 2013. *Nucleic Acids Res* 2013;**41**:D801–D807.
- Wishart DS, Tzur D, Knox C, Eisner R, Guo AC, Young N, Cheng D, Jewell K, Arndt D, Sawhney S, *et al*. HMDB: the Human Metabolome Database. *Nucleic Acids Res* 2007;**35**:D521–D526.
- Wolkowicz MJ, Naaby-Hansen S, Gamble AR, Reddi PP, Flickinger CJ, Herr JC. Tektin B1 demonstrates flagellar localization in human sperm. *Biol Reprod* 2002;**66**:241–250.
- Xu M, Zhou Z, Cheng C, Zhao W, Tang R, Huang Y, Wang W, Xu J, Zeng L, Xie Y, *et al*. Cloning and characterization of a novel human TEKIN1 gene. *Int J Biochem Cell Biol* 2001;**33**:1172–1182.
- Xu W, Hu H, Wang Z, Chen X, Yang F, Zhu Z, Fang P, Dai J, Wang L, Shi H, *et al*. Proteomic characteristics of spermatozoa in normozoospermic patients with infertility. *J Proteomics* 2012;**75**:5426–5436.
- Yang K, Meinhardt A, Zhang B, Grzmil P, Adham IM, Hoyer-Fender S. The small heat shock protein ODF1/HSPB10 is essential for tight linkage of sperm head to tail and male fertility in mice. *Mol Cell Biol* 2012;**32**:216–225.
- Yu Y, Oko R, Miranda-Vizuete A. Developmental expression of spermatid-specific thioredoxin-1 protein: transient association to the longitudinal columns of the fibrous sheath during sperm tail formation. *Biol Reprod* 2002;**67**:1546–1554.
- Zala D, Hinckelmann M-V, Yu H, Lyra da Cunha MM, Liot G, Cordelières FP, Marco S, Saudou F. Vesicular glycolysis provides on-board energy for fast axonal transport. *Cell* 2013;**152**:479–491.
- Zarsky HA, Tarnasky HA, Cheng M, Hoorn FA van der. Novel RING finger protein OIP1 binds to conserved amino acid repeats in sperm tail protein ODF1. *Biol Reprod* 2003;**68**:543–552.
- Zhang A, Sun H, Wang P, Han Y, Wang X. Modern analytical techniques in metabolomics analysis. *Analyst* 2012a;**137**:293–300.
- Zhang Y, Ou Y, Cheng M, Saadi HS, Thundathil JC, Hoorn F a van der. KLC3 is involved in sperm tail midpiece formation and sperm function. *Dev Biol* 2012b;**366**:101–110. Elsevier.

- Zhao C, Huo R, Wang F-Q, Lin M, Zhou Z-M, Sha J-H. Identification of several proteins involved in regulation of sperm motility by proteomic analysis. *Fertil Steril* 2007;**87**:436–438.
- Zheng J, Yang X, Harrell JM, Ryzhikov S, Shim EH, Lykke-Andersen K, Wei N, Sun H, Kobayashi R, Zhang H. CAND1 binds to unneddylated CUL1 and regulates the formation of SCF ubiquitin E3 ligase complex. *Mol Cell* 2002;**10**:1519–1526.
- Zuccarello D, Ferlin A, Garolla A, Pati M a, Moretti A, Cazzadore C, Francavilla S, Foresta C. A possible association of a human tektin-t gene mutation (A229V) with isolated non-syndromic asthenozoospermia: case report. *Hum Reprod* 2008;**23**:996–1001.



## **SUPPLEMENTARY TABLES**





## SUPPLEMENTARY TABLES

### Supplementary Table S1 – Complete list of identified proteins (1157) in Asthenozoospermic vs. Normozoospermic samples differential proteomics experiment.

For all proteins shown in this table at least two peptides have been identified with a false discovery rate (FDR) < 1%. Asterisks (\*) note proteins not previously described in human sperm cells, comparing with the most complete proteomic lists published till date using LC-MS/MS (Baker et al, 2007; 2013; de Mateo et al, 2011; 2013; Amaral et al., 2013; 2014; Wang et al, 2013; Azpiazu et al., 2014; Castillo et al, 2014). Note: the table with all the MS details for each protein is available free of charge via <http://pubs.acs.org>. (<http://pubs.acs.org/doi/suppl/10.1021/pr500652y>)

UniprotKB/ SwissProt Accession Number	Protein Description	$\Sigma$ Protein Coverage (%)	MW [kDa]	calc. pI
O00233	26S proteasome non-ATPase regulatory subunit 9 *	21.97	24.70	6.95
P0CW22	40S ribosomal protein S17-like *	42.22	15.50	9.85
P18077	60S ribosomal protein L35a *	27.27	12.50	11.06
Q8NEV1	Casein kinase II subunit alpha 3 *	32.74	45.20	8.50
A6NHG4	D-dopachrome decarboxylase-like protein *	60.45	14.20	6.29
P47813	Eukaryotic translation initiation factor 1A, X-chromosomal *	18.06	16.50	5.24
O14602	Eukaryotic translation initiation factor 1A, Y-chromosomal *	18.06	16.40	5.24
B5ME19	Eukaryotic translation initiation factor 3 subunit C-like protein *	3.28	105.40	5.64
O94808	Glutamine--fructose-6-phosphate aminotransferase [isomerizing] 2 *	2.49	76.90	7.37
P48668	Keratin, type II cytoskeletal 6C *	50.71	60.00	8.00
Q5XKE5	Keratin, type II cytoskeletal 79 *	20.75	57.80	7.20
P31025	Lipocalin-1 *	23.86	19.20	5.58
P0DKB6	Mitochondrial pyruvate carrier 1-like protein *	63.97	15.10	9.94
A6NHN6	Nuclear pore complex-interacting protein family member B15 *	5.64	51.20	10.49
E9PJ23	Nuclear pore complex-interacting protein family member B6 *	5.88	49.10	10.36
O75200	Nuclear pore complex-interacting protein family member B7 *	6.04	47.70	10.33
E9PQR5	Nuclear pore complex-interacting protein family member B8 *	5.79	49.60	10.13
F8W1W9	Nuclear pore complex-interacting protein family member B9 *	5.83	49.20	10.43
P0CG47	Polyubiquitin-B *	58.95	25.70	7.43
O15212	Prefoldin subunit 6 *	17.05	14.60	8.88
Q7Z333	Probable helicase senataxin *	0.75	302.70	7.17
O14737	Programmed cell death protein 5 *	28.00	14.30	6.04
Q6NXS1	Protein phosphatase inhibitor 2-like protein 3 *	13.17	23.00	4.92

Q7Z2V1	Protein TNT *	18.89	23.10	6.92
P0DJD1	RANBP2-like and GRIP domain-containing protein 2 *	0.74	197.20	6.20
Q9NRW1	Ras-related protein Rab-6B *	27.88	23.40	5.53
Q8NFU3	Thiosulfate sulfurtransferase/rhodanese-like domain-containing protein 1 *	20.00	12.50	6.07
Q8N5N4	Uncharacterized protein C3orf22 *	16.31	15.70	9.85
P61421	V-type proton ATPase subunit d 1 *	5.41	40.30	5.00
Q15120	[Pyruvate dehydrogenase (acetyl-transferring)] kinase isozyme 3, mitochondrial	6.40	46.90	8.37
Q86YW0	1-phosphatidylinositol 4,5-bisphosphate phosphodiesterase zeta-1	4.61	70.40	9.04
P61604	10 kDa heat shock protein, mitochondrial	22.55	10.90	8.92
P62258	14-3-3 protein epsilon	22.35	29.20	4.74
P61981	14-3-3 protein gamma	24.29	28.30	4.89
P31947	14-3-3 protein sigma	25.00	27.80	4.74
P27348	14-3-3 protein theta	23.27	27.70	4.78
P63104	14-3-3 protein zeta/delta	35.10	27.70	4.79
Q9UJ83	2-hydroxyacyl-CoA lyase 1	3.81	63.70	7.36
Q6N063	2-oxoglutarate and iron-dependent oxygenase domain-containing protein 2	4.86	39.00	5.68
Q02218	2-oxoglutarate dehydrogenase, mitochondrial	23.56	115.90	6.86
P12694	2-oxoisovalerate dehydrogenase subunit alpha, mitochondrial	8.54	50.40	8.27
Q16698	2,4-dienoyl-CoA reductase, mitochondrial	13.73	36.00	9.28
P62333	26S protease regulatory subunit 10B	31.88	44.10	7.49
P62191	26S protease regulatory subunit 4	19.55	49.20	6.21
P17980	26S protease regulatory subunit 6A	18.45	49.20	5.24
P43686	26S protease regulatory subunit 6B	13.88	47.30	5.21
P35998	26S protease regulatory subunit 7	24.02	48.60	5.95
P62195	26S protease regulatory subunit 8	25.86	45.60	7.55
Q99460	26S proteasome non-ATPase regulatory subunit 1	8.92	105.80	5.39
O00231	26S proteasome non-ATPase regulatory subunit 11	18.72	47.40	6.48
O00232	26S proteasome non-ATPase regulatory subunit 12	14.91	52.90	7.65
Q9UNM6	26S proteasome non-ATPase regulatory subunit 13	33.51	42.90	5.81
O00487	26S proteasome non-ATPase regulatory subunit 14	17.74	34.60	6.52
Q13200	26S proteasome non-ATPase regulatory subunit 2	18.50	100.10	5.20
Q16401	26S proteasome non-ATPase regulatory subunit 5	4.96	56.20	5.48
Q15008	26S proteasome non-ATPase regulatory subunit 6	15.17	45.50	5.62
P51665	26S proteasome non-ATPase regulatory subunit 7	14.81	37.00	6.77
P48556	26S proteasome non-ATPase regulatory subunit 8	16.86	39.60	9.70
P82909	28S ribosomal protein S36, mitochondrial	36.89	11.50	9.99
Q99714	3-hydroxyacyl-CoA dehydrogenase type-2	28.35	26.90	7.78
P42765	3-ketoacyl-CoA thiolase, mitochondrial	11.59	41.90	8.09
P25325	3-mercaptopyruvate sulfurtransferase	40.74	33.20	6.60
O95861	3'(2'),5'-bisphosphate nucleotidase 1	14.29	33.40	5.69
P49189	4-trimethylaminobutyraldehyde dehydrogenase	14.37	53.80	5.87

P62263	40S ribosomal protein S14	17.22	16.30	10.05
P62244	40S ribosomal protein S15a	53.85	14.80	10.13
P62269	40S ribosomal protein S18	13.16	17.70	10.99
P39019	40S ribosomal protein S19	13.79	16.10	10.32
P60866	40S ribosomal protein S20	34.45	13.40	9.94
P63220	40S ribosomal protein S21	32.53	9.10	8.50
P62857	40S ribosomal protein S28	21.74	7.80	10.70
P23396	40S ribosomal protein S3	30.45	26.70	9.66
P22090	40S ribosomal protein S4, Y isoform 1	6.08	29.40	10.24
P62081	40S ribosomal protein S7	15.46	22.10	10.10
P46781	40S ribosomal protein S9	24.23	22.60	10.65
P08865	40S ribosomal protein SA	10.17	32.80	4.87
O14841	5-oxoprolinase	12.11	137.40	6.58
P54619	5'-AMP-activated protein kinase subunit gamma-1	14.20	37.60	6.92
Q8TCD5	5'(3')-deoxyribonucleotidase, cytosolic type	30.85	23.40	6.64
Q01813	6-phosphofructokinase type C	27.81	85.50	7.55
P08237	6-phosphofructokinase, muscle type	7.05	85.10	7.99
P52209	6-phosphogluconate dehydrogenase, decarboxylating	9.11	53.10	7.23
O95336	6-phosphogluconolactonase	49.61	27.50	6.05
P10809	60 kDa heat shock protein, mitochondrial	19.55	61.00	5.87
P05388	60S acidic ribosomal protein P0	14.51	34.30	5.97
P62913	60S ribosomal protein L11	36.52	20.20	9.60
P30050	60S ribosomal protein L12	56.36	17.80	9.42
Q02543	60S ribosomal protein L18a	10.80	20.70	10.71
P35268	60S ribosomal protein L22	21.88	14.80	9.19
P62888	60S ribosomal protein L30	36.52	12.80	9.63
P11021	78 kDa glucose-regulated protein	25.99	72.30	5.16
O60733	85/88 kDa calcium-independent phospholipase A2	2.73	89.80	7.27
O75969	A-kinase anchor protein 3	34.11	94.70	6.18
Q5JQC9	A-kinase anchor protein 4	40.63	94.40	6.96
Q9BWD1	Acetyl-CoA acetyltransferase, cytosolic	28.97	41.30	6.92
P24752	Acetyl-CoA acetyltransferase, mitochondrial	4.92	45.20	8.85
O43427	Acidic fibroblast growth factor intracellular-binding protein	6.04	41.90	6.48
Q99798	Aconitate hydratase, mitochondrial	19.74	85.40	7.61
P10323	Acrosin	46.08	45.80	9.07
Q8NEB7	Acrosin-binding protein	40.88	61.30	5.16
P26436	Acrosomal protein SP-10	5.66	28.10	4.69
Q5JWF8	Actin-like protein 10	8.16	26.70	9.32
Q9Y615	Actin-like protein 7A	17.24	48.60	7.09
Q8TC94	Actin-like protein 9	24.04	45.60	7.08
Q9NZ32	Actin-related protein 10	5.04	46.30	7.37
P61160	Actin-related protein 2	11.17	44.70	6.74
P59998	Actin-related protein 2/3 complex subunit 4	28.57	19.70	8.43
Q9BPX5	Actin-related protein 2/3 complex subunit 5-like protein	26.14	16.90	6.60
Q8TDY3	Actin-related protein T2	18.57	41.70	5.47

Q9BYD9	Actin-related protein T3	20.16	41.00	5.82
Q9H845	Acyl-CoA dehydrogenase family member 9, mitochondrial	4.35	68.70	7.96
Q9NPJ3	Acyl-coenzyme A thioesterase 13	12.14	15.00	9.14
O14734	Acyl-coenzyme A thioesterase 8	14.73	35.90	7.56
O75608	Acyl-protein thioesterase 1	17.39	24.70	6.77
O95372	Acyl-protein thioesterase 2	9.96	24.70	7.23
P13798	Acylamino-acid-releasing enzyme	6.01	81.20	5.48
P07741	Adenine phosphoribosyltransferase	30.00	19.60	6.02
P54819	Adenylate kinase 2, mitochondrial	42.26	26.50	7.81
Q96M32	Adenylate kinase 7	7.88	82.60	4.74
Q96MA6	Adenylate kinase 8	15.03	54.90	6.15
Q5TCS8	Adenylate kinase 9	3.45	221.30	5.01
P00568	Adenylate kinase isoenzyme 1	65.46	21.60	8.63
Q9Y3D8	Adenylate kinase isoenzyme 6	10.47	20.00	4.58
Q9HDC9	Adipocyte plasma membrane-associated protein	17.79	46.50	6.16
P84077	ADP-ribosylation factor 1	33.15	20.70	6.80
P61204	ADP-ribosylation factor 3	33.15	20.60	7.43
P40616	ADP-ribosylation factor-like protein 1	19.34	20.40	5.72
P36404	ADP-ribosylation factor-like protein 2	27.72	20.90	6.34
Q9NVJ2	ADP-ribosylation factor-like protein 8B	32.26	21.50	8.43
P12235	ADP/ATP translocase 1	23.15	33.00	9.76
P05141	ADP/ATP translocase 2	27.52	32.80	9.69
P12236	ADP/ATP translocase 3	21.81	32.80	9.74
Q9HOC2	ADP/ATP translocase 4	42.54	35.00	9.89
O00253	Agouti-related protein	43.94	14.40	7.44
O00468	Agrin	5.27	217.10	6.39
O00170	AH receptor-interacting protein	6.67	37.60	6.29
Q9NRG9	Aladin	7.51	59.50	7.50
P49588	Alanine--tRNA ligase, cytoplasmic	1.65	106.70	5.53
Q9BTE6	Alanyl-tRNA editing protein Aarsd1	34.22	45.50	6.42
P11766	Alcohol dehydrogenase class-3	7.22	39.70	7.49
P15121	Aldose reductase	23.10	35.80	6.98
P12814	Alpha-actinin-1	4.60	103.00	5.41
P61163	Alpha-centractin	16.49	42.60	6.64
P02511	Alpha-crystallin B chain	17.71	20.10	7.33
P06733	Alpha-enolase	29.72	47.10	7.39
Q9BT30	Alpha-ketoglutarate-dependent dioxygenase alkB homolog 7, mitochondrial	24.89	24.50	7.11
Q9NTJ4	Alpha-mannosidase 2C1	25.58	115.80	6.57
Q96IU4	Alpha/beta hydrolase domain-containing protein 14B	11.43	22.30	6.40
Q8TCU4	Alstrom syndrome protein 1	2.26	460.70	6.28
Q12904	Aminoacyl tRNA synthase complex-interacting multifunctional protein 1	18.27	34.30	8.43
Q13155	Aminoacyl tRNA synthase complex-interacting multifunctional protein 2	15.00	35.30	8.22

P12821	Angiotensin-converting enzyme	13.63	149.60	6.39
Q9NU02	Ankyrin repeat and EF-hand domain-containing protein 1	2.84	86.60	8.28
P04083	Annexin A1	12.14	38.70	7.02
P07355	Annexin A2	5.90	38.60	7.75
P12429	Annexin A3	16.41	36.40	5.92
P08758	Annexin A5	34.38	35.90	5.05
P03973	Antileukoproteinase	28.79	14.30	8.75
Q10567	AP-1 complex subunit beta-1	4.21	104.60	5.06
O95782	AP-2 complex subunit alpha-1	5.53	107.50	7.03
P53680	AP-2 complex subunit sigma	25.35	17.00	6.18
P02647	Apolipoprotein A-I	31.09	30.80	5.76
P05090	Apolipoprotein D	11.64	21.30	5.15
P02649	Apolipoprotein E	21.45	36.10	5.73
Q9BUR5	Apolipoprotein O	13.64	22.30	9.13
O95831	Apoptosis-inducing factor 1, mitochondrial	6.20	66.90	8.95
P55064	Aquaporin-5	13.96	28.30	8.62
P54136	Arginine--tRNA ligase, cytoplasmic	3.18	75.30	6.68
Q5T9G4	Armadillo repeat-containing protein 12	23.82	38.60	7.88
Q5W041	Armadillo repeat-containing protein 3	4.47	96.30	6.21
Q5T2S8	Armadillo repeat-containing protein 4	4.02	115.60	7.77
Q6NXE6	Armadillo repeat-containing protein 6	10.38	54.10	6.24
P15289	Arylsulfatase A	8.48	53.60	6.07
P17174	Aspartate aminotransferase, cytoplasmic	32.93	46.20	7.01
P00505	Aspartate aminotransferase, mitochondrial	28.60	47.50	9.01
P14868	Aspartate--tRNA ligase, cytoplasmic	14.37	57.10	6.55
Q6PI48	Aspartate--tRNA ligase, mitochondrial	3.10	73.50	8.02
Q9ULA0	Aspartyl aminopeptidase	18.95	52.40	7.42
Q6DD88	Atlastin-3	8.50	60.50	5.66
P24539	ATP synthase F(0) complex subunit B1, mitochondrial	10.94	28.90	9.36
P25705	ATP synthase subunit alpha, mitochondrial	45.21	59.70	9.13
P06576	ATP synthase subunit beta, mitochondrial	30.25	56.50	5.40
P56385	ATP synthase subunit e, mitochondrial	65.22	7.90	9.35
P56381	ATP synthase subunit epsilon, mitochondrial	35.29	5.80	9.92
P48047	ATP synthase subunit O, mitochondrial	25.82	23.30	9.96
Q99766	ATP synthase subunit s, mitochondrial	27.44	24.80	7.56
P53396	ATP-citrate synthase	14.44	120.80	7.33
Q8IW45	ATP-dependent (S)-NAD(P)H-hydrate dehydratase	18.73	36.60	8.06
O00148	ATP-dependent RNA helicase DDX39A	8.43	49.10	5.68
Q8NBU5	ATPase family AAA domain-containing protein 1	7.20	40.70	6.90
Q9NV17	ATPase family AAA domain-containing protein 3A	2.68	71.30	8.98
Q9UII2	ATPase inhibitor, mitochondrial	19.81	12.20	9.35
O75882	Attractin	4.27	158.40	7.31
O14645	Axonemal dynein light intermediate polypeptide 1	53.49	29.60	8.50
O95816	BAG family molecular chaperone regulator 2	15.64	23.80	6.70
Q9UL15	BAG family molecular chaperone regulator 5	34.90	51.20	6.05

O75531	Barrier-to-autointegration factor	75.28	10.10	6.09
P61769	Beta-2-microglobulin	21.01	13.70	6.52
Q8WTQ1	Beta-defensin 104	37.50	8.50	9.19
Q8NG35	Beta-defensin 105	26.92	8.90	8.32
Q9BYW3	Beta-defensin 126	20.72	12.20	9.31
Q6UWU2	Beta-galactosidase-1-like protein	9.79	74.10	8.92
P08236	Beta-glucuronidase	7.22	74.70	7.02
Q3LXA3	Bifunctional ATP-dependent dihydroxyacetone kinase/FAD-AMP lyase (cyclizing)	12.35	58.90	7.49
P07814	Bifunctional glutamate/proline--tRNA ligase	4.10	170.50	7.33
P50583	Bis(5'-nucleosyl)-tetraphosphatase [asymmetrical]	19.73	16.80	5.35
P07738	Bisphosphoglycerate mutase	24.32	30.00	6.54
Q13867	Bleomycin hydrolase	6.81	52.50	6.27
Q9H3K6	BolA-like protein 2	37.21	10.10	6.52
Q9BQP9	BPI fold-containing family A member 3	12.20	28.40	6.65
O15382	Branched-chain-amino-acid aminotransferase, mitochondrial	9.69	44.30	8.65
Q8WY22	BRI3-binding protein	6.77	27.80	9.44
Q7KYR7	Butyrophilin subfamily 2 member A1	4.36	59.60	6.48
Q96BS2	Calcineurin B homologous protein 3	14.02	24.70	4.93
Q9Y376	Calcium-binding protein 39	18.77	39.80	6.89
O75952	Calcium-binding tyrosine phosphorylation-regulated protein	11.76	52.70	4.55
Q9Y2V2	Calcium-regulated heat stable protein 1	18.37	15.90	8.21
Q16566	Calcium/calmodulin-dependent protein kinase type IV	5.92	51.90	5.82
Q13939	Calicin	18.54	66.50	8.18
Q96JQ2	Calmin	9.88	111.60	4.94
P62158	Calmodulin	36.24	16.80	4.22
P17612	cAMP-dependent protein kinase catalytic subunit alpha	29.06	40.60	8.79
P22612	cAMP-dependent protein kinase catalytic subunit gamma	27.64	40.40	8.59
P10644	cAMP-dependent protein kinase type I-alpha regulatory subunit	30.45	43.00	5.35
P13861	cAMP-dependent protein kinase type II-alpha regulatory subunit	53.22	45.50	5.07
P16152	Carbonyl reductase [NADPH] 1	32.85	30.40	8.32
Q8WXQ8	Carboxypeptidase A5	7.11	49.00	6.73
O75976	Carboxypeptidase D	14.86	152.80	6.05
P43155	Carnitine O-acetyltransferase	9.58	70.80	8.44
Q92523	Carnitine O-palmitoyltransferase 1, muscle isoform	17.49	87.70	8.62
P23786	Carnitine O-palmitoyltransferase 2, mitochondrial	20.82	73.70	8.18
P48729	Casein kinase I isoform alpha	8.31	38.90	9.57
Q9HCP0	Casein kinase I isoform gamma-1	4.74	48.50	9.01
P68400	Casein kinase II subunit alpha	42.97	45.10	7.74
P19784	Casein kinase II subunit alpha'	12.00	41.20	8.56
P67870	Casein kinase II subunit beta	25.58	24.90	5.55
P31944	Caspase-14	12.81	27.70	5.58

Q9BXW7	Cat eye syndrome critical region protein 5	8.98	46.30	8.13
P49913	Cathelicidin antimicrobial peptide	43.53	19.30	9.41
P07858	Cathepsin B	7.96	37.80	6.30
Q9UBX1	Cathepsin F	13.64	53.30	8.22
Q9NZ45	CDGSH iron-sulfur domain-containing protein 1	27.78	12.20	9.09
Q12798	Centrin-1	26.16	19.60	4.88
Q66GS9	Centrosomal protein of 135 kDa	16.75	133.40	6.21
Q5TA50	Ceramide-1-phosphate transfer protein	50.47	24.30	7.21
P23435	Cerebellin-1	30.05	21.10	7.28
Q9BWS9	Chitinase domain-containing protein 1	16.79	44.90	8.63
Q8NE62	Choline dehydrogenase, mitochondrial	7.58	65.30	8.28
Q8NCS7	Choline transporter-like protein 5	3.34	81.60	8.16
Q9Y259	Choline/ethanolamine kinase	7.09	45.20	5.49
O75390	Citrate synthase, mitochondrial	13.09	51.70	8.32
Q00610	Clathrin heavy chain 1	26.39	191.50	5.69
P09496	Clathrin light chain A	17.74	27.10	4.51
P10909	Clusterin	28.73	52.50	6.27
Q96T59	CMT1A duplicated region transcript 15 protein	39.36	20.60	8.05
Q96EY8	Cob(I)yrinic acid a,c-diamide adenosyltransferase, mitochondrial	12.40	27.40	8.60
Q16568	Cocaine- and amphetamine-regulated transcript protein	18.10	12.80	8.25
Q8IW40	Coiled-coil domain-containing protein 103	23.14	27.10	5.97
Q8IYK2	Coiled-coil domain-containing protein 105	14.43	56.90	9.86
Q6ZU64	Coiled-coil domain-containing protein 108	2.23	217.10	6.51
Q96M91	Coiled-coil domain-containing protein 11	23.15	61.80	8.90
Q9H0I3	Coiled-coil domain-containing protein 113	4.24	44.20	8.73
Q96M63	Coiled-coil domain-containing protein 114	3.28	75.00	6.28
Q8IYX3	Coiled-coil domain-containing protein 116	6.99	56.90	9.64
Q8IYE0	Coiled-coil domain-containing protein 146	6.60	112.70	8.48
Q5T655	Coiled-coil domain-containing protein 147	19.84	103.40	8.41
A5D8V7	Coiled-coil domain-containing protein 151	4.71	69.10	9.07
Q9UL16	Coiled-coil domain-containing protein 19, mitochondrial	31.40	65.70	8.90
Q9UFE4	Coiled-coil domain-containing protein 39	10.95	109.80	6.44
Q4G0X9	Coiled-coil domain-containing protein 40	11.47	130.00	5.29
Q4VC31	Coiled-coil domain-containing protein 58	27.08	16.60	7.81
Q6ZN84	Coiled-coil domain-containing protein 81	3.53	76.00	9.14
Q9GZT6	Coiled-coil domain-containing protein 90B, mitochondrial	8.66	29.50	7.55
Q2M329	Coiled-coil domain-containing protein 96	14.77	62.70	4.94
Q8IY82	Coiled-coil domain-containing protein lobo homolog	9.15	103.40	5.67
Q9NX63	Coiled-coil-helix-coiled-coil-helix domain-containing protein 3, mitochondrial	59.03	26.10	8.28
Q9BRQ6	Coiled-coil-helix-coiled-coil-helix domain-containing protein 6, mitochondrial	46.81	26.40	8.85
P38432	Coilin	6.42	62.60	9.07
P39060	Collagen alpha-1(XVIII) chain	1.20	178.10	6.01

P08174	Complement decay-accelerating factor	13.12	41.40	7.59
Q5U5X0	Complex III assembly factor LYRM7	38.46	11.90	9.66
Q9BT78	COP9 signalosome complex subunit 4	9.61	46.20	5.83
Q9NTM9	Copper homeostasis protein cutC homolog	48.35	29.30	8.18
P12277	Creatine kinase B-type	19.16	42.60	5.59
Q13618	Cullin-3	9.77	88.90	8.48
Q86VP6	Cullin-associated NEDD8-dissociated protein 1	13.25	136.30	5.78
P35663	Cylicin-1	4.92	74.20	9.67
P01034	Cystatin-C	52.74	15.80	8.75
Q9Y697	Cysteine desulfurase, mitochondrial	13.57	50.20	8.31
P49589	Cysteine--tRNA ligase, cytoplasmic	6.15	85.40	6.76
P54107	Cysteine-rich secretory protein 1	25.30	28.50	5.91
P16562	Cysteine-rich secretory protein 2	20.58	27.20	6.49
P31930	Cytochrome b-c1 complex subunit 1, mitochondrial	25.62	52.60	6.37
P22695	Cytochrome b-c1 complex subunit 2, mitochondrial	25.17	48.40	8.63
P07919	Cytochrome b-c1 complex subunit 6, mitochondrial	34.07	10.70	4.44
P14927	Cytochrome b-c1 complex subunit 7	42.34	13.50	8.78
O14949	Cytochrome b-c1 complex subunit 8	54.88	9.90	10.08
P47985	Cytochrome b-c1 complex subunit Rieske, mitochondrial	21.53	29.60	8.32
Q6P9G0	Cytochrome b5 domain-containing protein 1	32.02	26.70	5.60
O43169	Cytochrome b5 type B	15.07	16.30	4.97
Q5RI15	Cytochrome c oxidase protein 20 homolog	36.44	13.30	8.76
P00403	Cytochrome c oxidase subunit 2	19.38	25.50	4.82
P20674	Cytochrome c oxidase subunit 5A, mitochondrial	32.67	16.80	6.79
P10606	Cytochrome c oxidase subunit 5B, mitochondrial	75.19	13.70	8.81
P14854	Cytochrome c oxidase subunit 6B1	43.02	10.20	7.05
P09669	Cytochrome c oxidase subunit 6C	66.67	8.80	10.39
P08574	Cytochrome c1, heme protein, mitochondrial	19.38	35.40	9.00
P28838	Cytosol aminopeptidase	17.34	56.10	7.93
Q96P26	Cytosolic 5'-nucleotidase 1B	12.46	68.80	8.82
O00154	Cytosolic acyl coenzyme A thioester hydrolase	9.21	41.80	8.54
P53384	Cytosolic Fe-S cluster assembly factor NUBP1	7.81	34.50	5.33
Q9Y5Y2	Cytosolic Fe-S cluster assembly factor NUBP2	10.70	28.80	5.83
O43175	D-3-phosphoglycerate dehydrogenase	6.75	56.60	6.71
P30046	D-dopachrome decarboxylase	68.64	12.70	7.30
Q96EP5	DAZ-associated protein 1	9.83	43.40	8.56
Q96GG9	DCN1-like protein 1	10.04	30.10	5.34
Q58WW2	DDB1- and CUL4-associated factor 6	2.21	96.20	5.27
Q6UWP2	Dehydrogenase/reductase SDR family member 11	31.15	28.30	6.64
P13716	Delta-aminolevulinic acid dehydratase	5.45	36.30	6.79
Q13011	Delta(3,5)-Delta(2,4)-dienoyl-CoA isomerase, mitochondrial	37.50	35.80	8.00
Q16854	Deoxyguanosine kinase, mitochondrial	18.77	32.00	8.66
P33316	Deoxyuridine 5'-triphosphate nucleotidohydrolase, mitochondrial	28.17	26.50	9.36
P81605	Dermcidin	22.73	11.30	6.54



O43323	Desert hedgehog protein	4.80	43.50	9.28
Q02413	Desmoglein-1	4.29	113.70	5.03
P15924	Desmoplakin	1.71	331.60	6.81
P60981	Destrin	20.00	18.50	7.85
Q9NR28	Diablo homolog, mitochondrial	33.47	27.10	5.90
P09622	Dihydrolipoyl dehydrogenase, mitochondrial	22.00	54.10	7.85
P10515	Dihydrolipoyllysine-residue acetyltransferase component of pyruvate dehydrogenase complex, mitochondrial	5.56	69.00	7.84
P36957	Dihydrolipoyllysine-residue succinyltransferase component of 2-oxoglutarate dehydrogenase complex, mitochondrial	7.73	48.70	8.95
Q02127	Dihydroorotate dehydrogenase (quinone), mitochondrial	5.57	42.80	9.67
Q9H4B8	Dipeptidase 3	12.91	53.70	7.96
Q9UHL4	Dipeptidyl peptidase 2	25.41	54.30	6.32
Q9NY33	Dipeptidyl peptidase 3	5.29	82.50	5.10
P27487	Dipeptidyl peptidase 4	1.83	88.20	6.04
O95989	Diphosphoinositol polyphosphate phosphohydrolase 1	22.09	19.50	6.34
Q9UKF5	Disintegrin and metalloproteinase domain-containing protein 29	3.29	92.70	7.40
Q9UKF2	Disintegrin and metalloproteinase domain-containing protein 30	7.97	88.90	7.61
Q8TC27	Disintegrin and metalloproteinase domain-containing protein 32	19.06	87.90	5.55
Q16531	DNA damage-binding protein 1	12.28	126.90	5.26
Q9NRW3	DNA dC->dU-editing enzyme APOBEC-3C	12.63	22.80	7.59
Q8WW22	DnaJ homolog subfamily A member 4	7.30	44.80	7.59
P25685	DnaJ homolog subfamily B member 1	24.12	38.00	8.63
Q9UBS4	DnaJ homolog subfamily B member 11	23.18	40.50	6.18
P59910	DnaJ homolog subfamily B member 13	36.08	36.10	7.87
Q9UDY4	DnaJ homolog subfamily B member 4	12.76	37.80	8.50
O75190	DnaJ homolog subfamily B member 6	19.94	36.10	9.16
Q8NHS0	DnaJ homolog subfamily B member 8	24.57	25.70	6.42
Q9UBS3	DnaJ homolog subfamily B member 9	14.80	25.50	8.27
Q9NVH1	DnaJ homolog subfamily C member 11	9.12	63.20	8.40
Q13217	DnaJ homolog subfamily C member 3	7.34	57.50	6.15
Q8WXX5	DnaJ homolog subfamily C member 9	22.69	29.90	5.73
P04843	Dolichyl-diphosphooligosaccharide--protein glycosyltransferase subunit 1	7.91	68.50	6.38
A8MYV0	Doublecortin domain-containing protein 2C	13.52	40.40	9.42
Q8WWB3	DPY30 domain-containing protein 1	62.15	20.90	4.67
P36507	Dual specificity mitogen-activated protein kinase kinase 2	6.75	44.40	6.55
Q14203	Dynactin subunit 1	16.74	141.60	5.81
O75935	Dynactin subunit 3	27.42	21.10	5.47
O60313	Dynamamin-like 120 kDa protein, mitochondrial	5.42	111.60	7.87
Q9P2D7	Dynein heavy chain 1, axonemal	2.12	493.60	5.94

Q8IVF4	Dynein heavy chain 10, axonemal	2.12	514.50	5.88
Q6ZR08	Dynein heavy chain 12, axonemal	1.75	356.70	6.19
Q9UFH2	Dynein heavy chain 17, axonemal	7.27	511.50	5.77
Q9P225	Dynein heavy chain 2, axonemal	0.77	507.40	6.37
Q8TD57	Dynein heavy chain 3, axonemal	1.97	470.50	6.43
Q9C0G6	Dynein heavy chain 6, axonemal	0.87	475.70	6.00
Q8WXX0	Dynein heavy chain 7, axonemal	6.06	460.90	6.00
Q96JB1	Dynein heavy chain 8, axonemal	6.12	514.30	6.32
Q9UI46	Dynein intermediate chain 1, axonemal	10.73	79.20	6.87
Q9GZS0	Dynein intermediate chain 2, axonemal	14.88	68.80	4.74
Q8TF09	Dynein light chain roadblock-type 2	34.38	10.80	7.50
O75928	E3 SUMO-protein ligase PIAS2	5.96	68.20	7.52
P62877	E3 ubiquitin-protein ligase RBX1	38.89	12.30	6.96
Q8WVD3	E3 ubiquitin-protein ligase RNF138	11.02	28.20	6.93
Q13508	Ecto-ADP-ribosyltransferase 3	10.03	43.90	6.06
Q9HAE3	EF-hand calcium-binding domain-containing protein 1	15.64	24.50	5.06
Q5VUJ9	EF-hand calcium-binding domain-containing protein 2	13.75	29.70	8.79
A4FU69	EF-hand calcium-binding domain-containing protein 5	1.06	173.30	5.82
Q5THR3	EF-hand calcium-binding domain-containing protein 6	6.13	172.80	8.40
Q8N7U6	EF-hand domain-containing family member B	16.33	93.70	7.58
Q5JST6	EF-hand domain-containing family member C2	9.35	87.30	7.37
Q5JVL4	EF-hand domain-containing protein 1	18.59	73.90	6.16
P13804	Electron transfer flavoprotein subunit alpha, mitochondrial	15.02	35.10	8.38
P38117	Electron transfer flavoprotein subunit beta	38.43	27.80	8.10
P68104	Elongation factor 1-alpha 1	10.39	50.10	9.01
P29692	Elongation factor 1-delta	24.56	31.10	5.01
P26641	Elongation factor 1-gamma	24.03	50.10	6.67
P13639	Elongation factor 2	25.06	95.30	6.83
P49411	Elongation factor Tu, mitochondrial	19.03	49.50	7.61
Q99963	Endophilin-A3	17.87	39.30	5.38
Q9Y371	Endophilin-B1	19.73	40.80	6.04
Q9BS26	Endoplasmic reticulum resident protein 44	25.12	46.90	5.26
Q9Y282	Endoplasmic reticulum-Golgi intermediate compartment protein 3	23.50	43.20	6.06
P14625	Endoplasmin	26.65	92.40	4.84
P42126	Enoyl-CoA delta isomerase 1, mitochondrial	37.09	32.80	8.54
O75521	Enoyl-CoA delta isomerase 2, mitochondrial	7.61	43.60	9.00
P30084	Enoyl-CoA hydratase, mitochondrial	11.72	31.40	8.07
Q14507	Epididymal secretory protein E3-alpha	38.10	17.60	8.35
P56851	Epididymal secretory protein E3-beta	14.29	17.60	6.99
Q96BH3	Epididymal sperm-binding protein 1	15.70	26.10	6.62
Q9NRG7	Epimerase family protein SDR39U1	9.09	34.70	9.77
O75477	Erlin-1	12.14	38.90	7.87
Q86YB8	ERO1-like protein beta	7.92	53.50	7.99
P30042	ES1 protein homolog, mitochondrial	14.55	28.20	8.27

Q92506	Estradiol 17-beta-dehydrogenase 8	16.48	27.00	6.54
Q99447	Ethanolamine-phosphate cytidyltransferase	30.33	43.80	6.92
P60842	Eukaryotic initiation factor 4A-I	11.58	46.10	5.48
Q14240	Eukaryotic initiation factor 4A-II	15.48	46.40	5.48
O43324	Eukaryotic translation elongation factor 1 epsilon-1	24.14	19.80	8.54
Q14152	Eukaryotic translation initiation factor 3 subunit A	1.30	166.50	6.79
P55884	Eukaryotic translation initiation factor 3 subunit B	3.56	92.40	5.00
Q99613	Eukaryotic translation initiation factor 3 subunit C	3.29	105.30	5.68
Q13347	Eukaryotic translation initiation factor 3 subunit I	6.46	36.50	5.64
P06730	Eukaryotic translation initiation factor 4E	11.98	25.10	6.15
P56537	Eukaryotic translation initiation factor 6	13.88	26.60	4.68
O14980	Exportin-1	5.98	123.30	6.06
P55060	Exportin-2	4.12	110.30	5.77
Q9UIA9	Exportin-7	20.70	123.80	6.32
P52907	F-actin-capping protein subunit alpha-1	23.78	32.90	5.69
Q96KX2	F-actin-capping protein subunit alpha-3	21.40	35.00	7.69
P47756	F-actin-capping protein subunit beta	35.38	31.30	5.59
P55789	FAD-linked sulfhydryl oxidase ALR	49.27	23.40	7.62
Q9UNN5	FAS-associated factor 1	2.77	73.90	4.88
Q9NQT6	Fascin-3	23.29	56.60	7.72
P49327	Fatty acid synthase	1.43	273.30	6.44
Q01469	Fatty acid-binding protein, epidermal	41.48	15.20	7.01
O00519	Fatty-acid amide hydrolase 1	8.98	63.00	7.66
P02794	Ferritin heavy chain	19.67	21.20	5.55
Q8N4E7	Ferritin, mitochondrial	26.86	27.50	7.27
P22830	Ferrochelatase, mitochondrial	4.02	47.80	8.73
Q08830	Fibrinogen-like protein 1	5.77	36.40	5.87
P02751	Fibronectin	5.99	262.50	5.71
Q8TC99	Fibronectin type III domain-containing protein 8	7.10	35.90	5.08
Q5CZC0	Fibrous sheath-interacting protein 2	2.30	780.10	6.71
Q5D862	Filaggrin-2	1.92	247.90	8.31
O75369	Filamin-B	1.77	278.00	5.73
P30043	Flavin reductase (NADPH)	17.96	22.10	7.65
O75955	Flotillin-1	3.75	47.30	7.49
Q13642	Four and a half LIM domains protein 1	7.12	36.20	8.97
Q8N0W7	Fragile X mental retardation 1 neighbor protein	27.06	29.20	8.94
Q9NQ88	Fructose-2,6-bisphosphatase TIGAR	12.59	30.00	7.69
P04075	Fructose-bisphosphate aldolase A	41.76	39.40	8.09
P07954	Fumarate hydratase, mitochondrial	13.33	54.60	8.76
Q9BWH2	FUN14 domain-containing protein 2	11.11	20.70	9.73
Q92820	Gamma-glutamyl hydrolase	16.98	35.90	7.11
Q9BVM4	Gamma-glutamylaminocyclotransferase	26.14	17.30	6.87
P20142	Gastricsin	6.44	42.40	4.46
Q6ZNW5	GDP-D-glucose phosphorylase 1	5.71	42.30	6.47
P57678	Gem-associated protein 4	1.61	120.00	6.04
O60763	General vesicular transport factor p115	3.22	107.80	4.91

Q2KHT4	Germ cell-specific gene 1 protein	6.30	39.20	7.99
Q4G1C9	GLIPR1-like protein 2	6.98	40.20	4.91
P11413	Glucose-6-phosphate 1-dehydrogenase	11.84	59.20	6.84
P06744	Glucose-6-phosphate isomerase	26.52	63.10	8.32
P14314	Glucosidase 2 subunit beta	13.26	59.40	4.41
P15104	Glutamine synthetase	34.58	42.00	6.89
Q06210	Glutamine--fructose-6-phosphate aminotransferase [isomerizing] 1	6.58	78.80	7.11
P47897	Glutamine--tRNA ligase	3.74	87.70	7.15
Q9H0J4	Glutamine-rich protein 2	7.46	180.70	6.73
P07203	Glutathione peroxidase 1	15.27	22.10	6.55
P21266	Glutathione S-transferase Mu 3	46.22	26.50	5.54
Q9H4Y5	Glutathione S-transferase omega-2	42.39	28.20	7.56
P48637	Glutathione synthetase	6.75	52.40	5.92
P04406	Glyceraldehyde-3-phosphate dehydrogenase	16.72	36.00	8.46
O14556	Glyceraldehyde-3-phosphate dehydrogenase, testis-specific	51.47	44.50	8.19
Q14410	Glycerol kinase 2	25.14	60.60	5.77
Q9NZC3	Glycerophosphodiester phosphodiesterase 1	14.20	37.70	6.71
Q8N9F7	Glycerophosphodiester phosphodiesterase domain-containing protein 1	15.61	36.10	8.47
P41250	Glycine--tRNA ligase	10.28	83.10	7.03
P11216	Glycogen phosphorylase, brain form	2.25	96.60	6.86
P49841	Glycogen synthase kinase-3 beta	9.52	46.70	8.78
Q9UBQ7	Glyoxylate reductase/hydroxypyruvate reductase	22.56	35.60	7.39
Q8N158	Glypican-2	10.54	62.80	8.00
Q92896	Golgi apparatus protein 1	1.61	134.50	6.90
O95995	Growth arrest-specific protein 8	29.08	56.30	7.94
P62826	GTP-binding nuclear protein Ran	40.74	24.40	7.49
Q9NR31	GTP-binding protein SAR1a	20.71	22.40	6.68
Q9Y6B6	GTP-binding protein SAR1b	15.66	22.40	6.11
P63244	Guanine nucleotide-binding protein subunit beta-2-like 1	15.14	35.10	7.69
Q9H0R4	Haloacid dehalogenase-like hydrolase domain-containing protein 2	35.14	28.50	6.24
Q7Z4H3	HD domain-containing protein 2	58.82	23.40	5.49
P34931	Heat shock 70 kDa protein 1-like	37.75	70.30	6.02
P08107	Heat shock 70 kDa protein 1A/1B	35.10	70.00	5.66
P34932	Heat shock 70 kDa protein 4	16.43	94.30	5.19
O95757	Heat shock 70 kDa protein 4L	21.45	94.50	5.88
P11142	Heat shock cognate 71 kDa protein	20.12	70.90	5.52
Q92598	Heat shock protein 105 kDa	12.59	96.80	5.39
Q12931	Heat shock protein 75 kDa, mitochondrial	5.54	80.10	8.21
P04792	Heat shock protein beta-1	33.17	22.80	6.40
P07900	Heat shock protein HSP 90-alpha	27.19	84.60	5.02
P08238	Heat shock protein HSP 90-beta	15.75	83.20	5.03
P54652	Heat shock-related 70 kDa protein 2	43.97	70.00	5.74

P30519	Heme oxygenase 2	42.72	36.00	5.41
P19367	Hexokinase-1	41.55	102.40	6.80
P49773	Histidine triad nucleotide-binding protein 1	29.37	13.80	6.95
Q9BX68	Histidine triad nucleotide-binding protein 2, mitochondrial	26.99	17.20	9.16
Q9NQE9	Histidine triad nucleotide-binding protein 3	25.82	20.30	6.60
Q96DB2	Histone deacetylase 11	5.76	39.20	7.65
Q96QV6	Histone H2A type 1-A	75.57	14.20	10.86
Q6F113	Histone H2A type 2-A	40.00	14.10	10.90
Q16777	Histone H2A type 2-C	40.31	14.00	10.90
P0C5Z0	Histone H2A-Bbd type 2/3	50.43	12.70	10.67
Q96A08	Histone H2B type 1-A	40.16	14.20	10.32
P84243	Histone H3.3	69.12	15.30	11.27
P62805	Histone H4	57.28	11.40	11.36
Q86YZ3	Hornerin	7.16	282.20	10.04
P50502	Hsc70-interacting protein	14.09	41.30	5.27
Q16543	Hsp90 co-chaperone Cdc37	18.52	44.40	5.25
O00291	Huntingtin-interacting protein 1	12.05	116.10	5.30
Q4G0P3	Hydrocephalus-inducing protein homolog	1.15	575.50	6.06
Q16836	Hydroxyacyl-coenzyme A dehydrogenase, mitochondrial	12.74	34.30	8.85
Q16775	Hydroxyacylglutathione hydrolase, mitochondrial	14.29	33.80	8.12
P35914	Hydroxymethylglutaryl-CoA lyase, mitochondrial	6.77	34.30	8.54
P00492	Hypoxanthine-guanine phosphoribosyltransferase	52.75	24.60	6.68
Q9Y4L1	Hypoxia up-regulated protein 1	15.42	111.30	5.22
P52292	Importin subunit alpha-1	15.50	57.80	5.40
O00629	Importin subunit alpha-3	9.21	57.90	4.96
O00505	Importin subunit alpha-4	10.75	57.80	4.94
O60684	Importin subunit alpha-7	11.19	60.00	4.98
Q14974	Importin subunit beta-1	11.99	97.10	4.78
Q8TEX9	Importin-4	17.02	118.60	4.96
O00410	Importin-5	5.56	123.50	4.94
Q8IV63	Inactive serine/threonine-protein kinase VRK3	9.07	52.80	9.04
P29218	Inositol monophosphatase 1	12.27	30.20	5.26
P49441	Inositol polyphosphate 1-phosphatase	6.27	44.00	5.26
Q9Y287	Integral membrane protein 2B	9.40	30.30	5.14
O75569	Interferon-inducible double-stranded RNA-dependent protein kinase activator A	13.10	34.40	8.41
Q6NXR0	Interferon-inducible GTPase 5	16.85	50.30	5.35
Q86XH1	IQ and AAA domain-containing protein 1	3.04	95.30	9.47
A8MTL0	IQ domain-containing protein F5	29.05	18.00	10.01
Q8N0W5	IQ domain-containing protein K	11.50	33.30	8.21
Q86U28	Iron-sulfur cluster assembly 2 homolog, mitochondrial	20.78	16.50	5.25
Q8IWL3	Iron-sulfur cluster co-chaperone protein HscB, mitochondrial	8.94	27.40	7.69
Q7L266	Isoaspartyl peptidase/L-asparaginase	23.38	32.00	6.24

Q96AB3	Isochorismatase domain-containing protein 2, mitochondrial	37.07	22.30	7.77
P50213	Isocitrate dehydrogenase [NAD] subunit alpha, mitochondrial	20.49	39.60	6.92
O43837	Isocitrate dehydrogenase [NAD] subunit beta, mitochondrial	20.78	42.20	8.46
P51553	Isocitrate dehydrogenase [NAD] subunit gamma, mitochondrial	24.17	42.80	8.50
O75874	Isocitrate dehydrogenase [NADP] cytoplasmic	9.66	46.60	7.01
P41252	Isoleucine--tRNA ligase, cytoplasmic	1.66	144.40	6.15
Q9NSE4	Isoleucine--tRNA ligase, mitochondrial	15.61	113.70	7.20
P26440	Isovaleryl-CoA dehydrogenase, mitochondrial	11.35	46.30	8.19
Q6UXV1	Izumo sperm-egg fusion protein 2	23.08	24.80	8.79
Q5VZ72	Izumo sperm-egg fusion protein 3	10.04	27.70	8.29
P14923	Junction plakoglobin	6.04	81.70	6.14
Q6JEL2	Kelch-like protein 10	9.38	68.90	5.68
P13645	Keratin, type I cytoskeletal 10	68.15	58.80	5.21
P19012	Keratin, type I cytoskeletal 15	16.67	49.20	4.77
P08779	Keratin, type I cytoskeletal 16	40.80	51.20	5.05
Q04695	Keratin, type I cytoskeletal 17	29.86	48.10	5.02
P35527	Keratin, type I cytoskeletal 9	63.24	62.00	5.24
P04264	Keratin, type II cytoskeletal 1	74.53	66.00	8.12
Q7Z794	Keratin, type II cytoskeletal 1b	25.43	61.90	5.99
P13647	Keratin, type II cytoskeletal 5	51.02	62.30	7.74
P02538	Keratin, type II cytoskeletal 6A	53.37	60.00	8.00
P04259	Keratin, type II cytoskeletal 6B	51.77	60.00	8.00
Q8N1N4	Keratin, type II cytoskeletal 78	15.96	56.80	6.02
P05787	Keratin, type II cytoskeletal 8	11.39	53.70	5.59
Q5T749	Keratinocyte proline-rich protein	2.76	64.10	8.27
Q9HAQ2	Kinesin-like protein KIF9	6.08	89.90	7.17
Q5H943	Kita-kyushu lung cancer antigen 1	32.74	12.80	10.20
P49223	Kunitz-type protease inhibitor 3	41.57	10.20	6.44
Q96RQ9	L-amino-acid oxidase	32.45	62.80	8.68
Q9NRN7	L-aminoadipate-semialdehyde dehydrogenase-phosphopantetheinyl transferase	38.83	35.80	6.80
P00338	L-lactate dehydrogenase A chain	10.54	36.70	8.27
P07864	L-lactate dehydrogenase C chain	21.08	36.30	7.46
Q7Z4W1	L-xylulose reductase	54.92	25.90	8.10
Q08431	Lactadherin	7.24	43.10	8.15
P02788	Lactotransferrin	34.37	78.10	8.12
Q04760	Lactoylglutathione lyase	16.85	20.80	5.31
O43813	LanC-like protein 1	7.77	45.30	7.75
P46379	Large proline-rich protein BAG6	10.16	119.30	5.60
O75610	Left-right determination factor 1	21.58	40.90	8.27
O95202	LETM1 and EF-hand domain-containing protein 1, mitochondrial	4.74	83.30	6.70
Q9UIC8	Leucine carboxyl methyltransferase 1	15.87	38.40	6.04

Q9NQ48	Leucine zipper transcription factor-like protein 1	16.39	34.60	5.36
Q9C099	Leucine-rich repeat and coiled-coil domain-containing protein 1	15.21	119.50	5.88
Q8N456	Leucine-rich repeat-containing protein 18	19.92	29.70	9.80
Q53EV4	Leucine-rich repeat-containing protein 23	17.78	39.70	4.65
A6NM11	Leucine-rich repeat-containing protein 37A2	6.53	188.30	5.50
O60309	Leucine-rich repeat-containing protein 37A3	5.39	180.50	5.31
Q96QE4	Leucine-rich repeat-containing protein 37B	11.30	105.50	4.91
Q96E66	Leucine-rich repeat-containing protein 51	19.27	22.20	9.35
Q6XZB0	Lipase member I	5.00	53.00	9.03
P06858	Lipoprotein lipase	6.53	53.10	8.15
P36776	Lon protease homolog, mitochondrial	7.82	106.40	6.39
P33121	Long-chain-fatty-acid--CoA ligase 1	17.48	77.90	7.15
Q9UKU0	Long-chain-fatty-acid--CoA ligase 6	8.32	77.70	7.43
P24666	Low molecular weight phosphotyrosine protein phosphatase	50.00	18.00	6.74
Q9P2M1	LRP2-binding protein	10.66	39.80	7.90
Q9HD34	LYR motif-containing protein 4	28.57	10.80	10.73
Q15046	Lysine--tRNA ligase	12.56	68.00	6.35
P10253	Lysosomal alpha-glucosidase	11.45	105.30	6.00
P42785	Lysosomal Pro-X carboxypeptidase	9.88	55.80	7.21
Q6UWQ5	Lysozyme-like protein 1	40.54	16.60	8.05
Q96KX0	Lysozyme-like protein 4	26.71	16.40	8.28
O75951	Lysozyme-like protein 6	16.89	16.90	6.14
Q8NDA8	Maestro heat-like repeat-containing protein family member 1	1.71	181.10	6.89
Q7Z745	Maestro heat-like repeat-containing protein family member 2B	2.40	180.70	6.28
Q68CQ1	Maestro heat-like repeat-containing protein family member 7	3.25	145.60	6.96
P40925	Malate dehydrogenase, cytoplasmic	7.49	36.40	7.36
P40926	Malate dehydrogenase, mitochondrial	12.72	35.50	8.68
O43708	Maleylacetoacetate isomerase	23.15	24.20	8.54
Q9NR99	Matrix-remodeling-associated protein 5	0.67	312.00	8.32
P11310	Medium-chain specific acyl-CoA dehydrogenase, mitochondrial	30.17	46.60	8.37
Q8NEH6	Meiosis-specific nuclear structural protein 1	13.74	60.50	7.12
Q495T6	Membrane metallo-endopeptidase-like 1	6.42	89.30	5.87
O00264	Membrane-associated progesterone receptor component 1	26.15	21.70	4.70
O15173	Membrane-associated progesterone receptor component 2	18.39	23.80	4.88
P55145	Mesencephalic astrocyte-derived neurotrophic factor	23.63	20.70	8.69
Q13505	Metaxin-1	4.72	51.40	9.79
P56192	Methionine--tRNA ligase, cytoplasmic	3.11	101.10	6.16
Q13825	Methylglutaconyl-CoA hydratase, mitochondrial	8.85	35.60	9.48
Q8IVH4	Methylmalonic aciduria type A protein, mitochondrial	6.46	46.50	9.29

Q9BQA1	Methylosome protein 50	5.85	36.70	5.17
Q9H492	Microtubule-associated proteins 1A/1B light chain 3A	17.36	14.30	8.68
Q8TC71	Mitochondria-eating protein	33.46	61.10	8.63
Q02978	Mitochondrial 2-oxoglutarate/malate carrier protein	21.66	34.00	9.91
Q96AQ8	Mitochondrial calcium uniporter regulator 1	8.08	39.70	9.63
O43772	Mitochondrial carnitine/acylcarnitine carrier protein	12.96	32.90	9.41
Q9Y6C9	Mitochondrial carrier homolog 2	33.00	33.30	7.97
Q9UBX3	Mitochondrial dicarboxylate carrier	22.65	31.30	9.54
Q9Y3D6	Mitochondrial fission 1 protein	31.58	16.90	8.79
Q3ZCQ8	Mitochondrial import inner membrane translocase subunit TIM50	6.80	39.60	8.37
Q9NS69	Mitochondrial import receptor subunit TOM22 homolog	21.13	15.50	4.34
Q15785	Mitochondrial import receptor subunit TOM34	23.95	34.50	8.98
O96008	Mitochondrial import receptor subunit TOM40 homolog	18.56	37.90	7.25
Q96LU5	Mitochondrial inner membrane protease subunit 1	20.48	18.50	8.09
Q96T52	Mitochondrial inner membrane protease subunit 2	16.00	19.70	9.36
Q16891	Mitochondrial inner membrane protein	20.05	83.60	6.48
Q9Y5U8	Mitochondrial pyruvate carrier 1	44.04	12.30	9.61
O95563	Mitochondrial pyruvate carrier 2	27.56	14.30	10.43
Q9HC21	Mitochondrial thiamine pyrophosphate carrier	12.81	35.50	9.55
Q6PF18	MORN repeat-containing protein 3	20.00	27.60	8.44
Q5VZ52	MORN repeat-containing protein 5	22.98	18.70	5.88
O75425	Motile sperm domain-containing protein 3	19.57	25.50	9.20
P78406	mRNA export factor	24.18	40.90	7.83
P22234	Multifunctional protein ADE2	19.29	47.00	7.23
Q9NUJ1	Mycophenolic acid acyl-glucuronide esterase, mitochondrial	17.65	33.90	8.57
P58340	Myeloid leukemia factor 1	32.46	30.60	9.45
Q96S97	Myeloid-associated differentiation marker	4.97	35.30	8.15
P05164	Myeloperoxidase	15.97	83.80	8.97
P14649	Myosin light chain 6B	16.35	22.70	5.73
P19105	Myosin regulatory light chain 12A	28.07	19.80	4.81
O14950	Myosin regulatory light chain 12B	27.91	19.80	4.84
P13533	Myosin-6	0.62	223.60	5.73
P12883	Myosin-7	0.88	223.00	5.80
Q9UJ70	N-acetyl-D-glucosamine kinase	16.86	37.40	6.24
P15586	N-acetylglucosamine-6-sulfatase	12.50	62.00	8.31
Q8NFW8	N-acylneuraminate cytidyltransferase	5.53	48.30	7.93
O95777	N-alpha-acetyltransferase 38, NatC auxiliary subunit	43.75	10.40	4.48
Q9BV86	N-terminal Xaa-Pro-Lys N-methyltransferase 1	12.11	25.40	5.52
P20933	N(4)-(beta-N-acetylglucosaminy)-L-asparaginase	6.94	37.20	6.28
O95865	N(G),N(G)-dimethylarginine dimethylaminohydrolase 2	8.42	29.60	6.01
Q4G0N4	NAD kinase 2, mitochondrial	6.33	49.40	8.18
P23368	NAD-dependent malic enzyme, mitochondrial	15.58	65.40	7.61
Q9NXA8	NAD-dependent protein deacylase sirtuin-5, mitochondrial	8.06	33.90	8.47



Q9BU61	NADH dehydrogenase [ubiquinone] 1 alpha subcomplex assembly factor 3	17.39	20.30	8.22
Q86Y39	NADH dehydrogenase [ubiquinone] 1 alpha subcomplex subunit 11	48.23	14.80	8.72
Q9UI09	NADH dehydrogenase [ubiquinone] 1 alpha subcomplex subunit 12	26.90	17.10	9.63
Q9P0J0	NADH dehydrogenase [ubiquinone] 1 alpha subcomplex subunit 13	24.31	16.70	8.43
O43678	NADH dehydrogenase [ubiquinone] 1 alpha subcomplex subunit 2	74.75	10.90	9.57
P56556	NADH dehydrogenase [ubiquinone] 1 alpha subcomplex subunit 6	22.73	17.90	10.14
O95182	NADH dehydrogenase [ubiquinone] 1 alpha subcomplex subunit 7	19.47	12.50	10.18
P51970	NADH dehydrogenase [ubiquinone] 1 alpha subcomplex subunit 8	13.37	20.10	7.65
O96000	NADH dehydrogenase [ubiquinone] 1 beta subcomplex subunit 10	23.26	20.80	8.48
O95168	NADH dehydrogenase [ubiquinone] 1 beta subcomplex subunit 4	31.01	15.20	9.85
O43674	NADH dehydrogenase [ubiquinone] 1 beta subcomplex subunit 5, mitochondrial	14.29	21.70	9.63
P17568	NADH dehydrogenase [ubiquinone] 1 beta subcomplex subunit 7	27.01	16.40	8.92
O95169	NADH dehydrogenase [ubiquinone] 1 beta subcomplex subunit 8, mitochondrial	23.12	21.80	6.80
Q9Y6M9	NADH dehydrogenase [ubiquinone] 1 beta subcomplex subunit 9	41.90	21.80	8.38
P49821	NADH dehydrogenase [ubiquinone] flavoprotein 1, mitochondrial	5.60	50.80	8.21
P19404	NADH dehydrogenase [ubiquinone] flavoprotein 2, mitochondrial	18.47	27.40	8.06
O75489	NADH dehydrogenase [ubiquinone] iron-sulfur protein 3, mitochondrial	51.14	30.20	7.50
O43920	NADH dehydrogenase [ubiquinone] iron-sulfur protein 5	23.58	12.50	9.14
O75251	NADH dehydrogenase [ubiquinone] iron-sulfur protein 7, mitochondrial	11.74	23.50	9.99
O00217	NADH dehydrogenase [ubiquinone] iron-sulfur protein 8, mitochondrial	21.43	23.70	6.34
Q6BCY4	NADH-cytochrome b5 reductase 2	27.17	31.40	8.50
P00387	NADH-cytochrome b5 reductase 3	11.30	34.20	7.59
P28331	NADH-ubiquinone oxidoreductase 75 kDa subunit, mitochondrial	20.91	79.40	6.23
P22570	NADPH:adrenodoxin oxidoreductase, mitochondrial	5.09	53.80	8.44
O43847	Nardilysin	8.26	131.50	5.00
Q13564	NEDD8-activating enzyme E1 regulatory subunit	4.87	60.20	5.40
P56730	Neurotrypsin	9.03	97.00	8.03
Q14697	Neutral alpha-glucosidase AB	27.22	106.80	6.14

Q86X76	Nitrilase homolog 1	35.17	35.90	7.74
Q9UNZ2	NSFL1 cofactor p47	17.03	40.50	5.10
O75694	Nuclear pore complex protein Nup155	25.95	155.10	6.16
Q12769	Nuclear pore complex protein Nup160	3.48	162.00	5.50
Q92621	Nuclear pore complex protein Nup205	12.52	227.80	6.19
Q9BW27	Nuclear pore complex protein Nup85	3.66	75.00	5.55
Q99567	Nuclear pore complex protein Nup88	13.50	83.50	5.69
Q8N1F7	Nuclear pore complex protein Nup93	21.73	93.40	5.72
P52948	Nuclear pore complex protein Nup98-Nup96	2.97	197.50	6.40
P37198	Nuclear pore glycoprotein p62	10.73	53.20	5.31
Q8TEM1	Nuclear pore membrane glycoprotein 210	5.41	205.00	6.81
Q5VU65	Nuclear pore membrane glycoprotein 210-like	14.67	210.50	7.50
Q8TAT6	Nuclear protein localization protein 4 homolog	3.13	68.10	6.38
P80303	Nucleobindin-2	9.29	50.20	5.12
Q5SRE5	Nucleoporin NUP188 homolog	10.86	195.90	6.73
Q8NFH3	Nucleoporin Nup43	6.58	42.10	5.63
Q8NFH5	Nucleoporin NUP53	25.15	34.80	9.09
Q7Z3B4	Nucleoporin p54	9.47	55.40	7.02
Q9BVL2	Nucleoporin p58/p45	7.68	60.90	9.33
Q96EE3	Nucleoporin SEH1	7.78	39.60	8.09
Q9Y5B8	Nucleoside diphosphate kinase 7	23.94	42.50	6.47
P15531	Nucleoside diphosphate kinase A	35.53	17.10	6.19
P22392	Nucleoside diphosphate kinase B	40.79	17.30	8.41
P56597	Nucleoside diphosphate kinase homolog 5	27.83	24.20	6.29
P55209	Nucleosome assembly protein 1-like 1	7.67	45.30	4.46
Q8WVJ2	NudC domain-containing protein 2	24.84	17.70	5.07
Q8IVD9	NudC domain-containing protein 3	6.37	40.80	5.25
Q9Y3B8	Oligoribonuclease, mitochondrial	18.99	26.80	6.87
Q9H6K4	Optic atrophy 3 protein	8.38	20.00	8.91
Q7L8S5	OTU domain-containing protein 6A	7.64	33.30	6.74
Q14990	Outer dense fiber protein 1	42.00	28.30	8.03
Q5BJF6	Outer dense fiber protein 2	30.76	95.30	7.62
Q96PU9	Outer dense fiber protein 3	31.10	27.70	9.89
Q8IXM7	Outer dense fiber protein 3-like protein 1	13.87	31.00	9.54
A8MYP8	Outer dense fiber protein 3B	46.25	27.30	10.42
Q9BUP3	Oxidoreductase HTATIP2	17.77	27.00	8.38
Q15645	Pachytene checkpoint protein 2 homolog	8.56	48.50	6.09
Q96M98	Parkin coregulated gene protein	11.82	33.30	8.21
P62937	Peptidyl-prolyl cis-trans isomerase A	40.61	18.00	7.81
P23284	Peptidyl-prolyl cis-trans isomerase B	20.83	23.70	9.41
P30405	Peptidyl-prolyl cis-trans isomerase F, mitochondrial	24.15	22.00	9.38
P26885	Peptidyl-prolyl cis-trans isomerase FKBP2	15.49	15.60	9.13
Q8IXY8	Peptidyl-prolyl cis-trans isomerase-like 6	9.65	35.20	7.02
O60664	Perilipin-3	6.22	47.00	5.44
Q06830	Peroxiredoxin-1	29.15	22.10	8.13
P32119	Peroxiredoxin-2	32.83	21.90	5.97

Q13162	Peroxiredoxin-4	36.90	30.50	6.29
P30044	Peroxiredoxin-5, mitochondrial	17.29	22.10	8.70
P30041	Peroxiredoxin-6	36.61	25.00	6.38
O96011	Peroxisomal membrane protein 11B	33.59	28.40	9.85
Q96HA9	Peroxisomal membrane protein 11C	20.75	26.60	9.13
P51659	Peroxisomal multifunctional enzyme type 2	3.94	79.60	8.84
Q9Y285	Phenylalanine--tRNA ligase alpha subunit	10.04	57.50	7.80
Q9NSD9	Phenylalanine--tRNA ligase beta subunit	19.02	66.10	6.84
Q00325	Phosphate carrier protein, mitochondrial	10.77	40.10	9.38
P30086	Phosphatidylethanolamine-binding protein 1	33.69	21.00	7.53
Q96S96	Phosphatidylethanolamine-binding protein 4	16.74	25.70	6.54
Q8WUK0	Phosphatidylglycerophosphatase and protein-tyrosine phosphatase 1	30.35	22.80	9.77
Q8TBX8	Phosphatidylinositol 5-phosphate 4-kinase type-2 gamma	4.51	47.30	6.84
Q8TCT1	Phosphoethanolamine/phosphocholine phosphatase	13.86	29.70	7.71
P00558	Phosphoglycerate kinase 1	13.67	44.60	8.10
P07205	Phosphoglycerate kinase 2	12.47	44.80	8.54
P18669	Phosphoglycerate mutase 1	59.45	28.80	7.18
P15259	Phosphoglycerate mutase 2	62.06	28.70	8.88
A6NDG6	Phosphoglycolate phosphatase	33.33	34.00	6.14
P14555	Phospholipase A2, membrane associated	43.75	16.10	9.23
P36969	Phospholipid hydroperoxide glutathione peroxidase, mitochondrial	30.46	22.20	8.37
O15305	Phosphomannomutase 2	14.63	28.10	6.77
Q15126	Phosphomevalonate kinase	16.15	22.00	5.73
Q9GZP4	PITH domain-containing protein 1	8.06	24.20	5.74
P23634	Plasma membrane calcium-transporting ATPase 4	8.86	137.80	6.60
P13796	Plastin-2	2.55	70.20	5.43
P43034	Platelet-activating factor acetylhydrolase IB subunit alpha	5.37	46.60	7.37
P68402	Platelet-activating factor acetylhydrolase IB subunit beta	9.61	25.60	5.92
Q15102	Platelet-activating factor acetylhydrolase IB subunit gamma	17.75	25.70	6.84
Q8TC44	POC1 centriolar protein homolog B	7.32	53.60	7.24
Q9NX46	Poly(ADP-ribose) glycohydrolase ARH3	16.25	38.90	5.07
Q8TBY8	Polyamine-modulated factor 1-binding protein 1	18.40	119.00	6.29
Q8TCS8	Polyribonucleotide nucleotidyltransferase 1, mitochondrial	9.20	85.90	7.77
P0CG48	Polyubiquitin-C	59.12	77.00	7.66
Q6ICG8	Postacrosomal sheath WW domain-binding protein	14.56	31.90	7.84
Q9UI14	Prenylated Rab acceptor protein 1	10.27	20.60	7.34
Q5JRX3	Presequence protease, mitochondrial	9.35	117.30	6.92
Q6NUT2	Probable C-mannosyltransferase DPY19L2	4.22	87.30	9.10
Q8NA82	Probable E3 ubiquitin-protein ligase MARCH10	4.70	90.50	6.71
Q8N9V2	Probable E3 ubiquitin-protein ligase TRIML1	21.79	53.00	5.49
Q9UKR5	Probable ergosterol biosynthetic protein 28	20.00	15.90	9.83

Q5GAN3	Probable inactive ribonuclease-like protein 13	22.44	17.80	8.59
A4D1T9	Probable inactive serine protease 37	22.13	26.40	8.87
P60673	Profilin-3	43.07	14.60	9.26
Q8WUM4	Programmed cell death 6-interacting protein	3.80	96.00	6.52
O75340	Programmed cell death protein 6	19.37	21.90	5.40
P35232	Prohibitin	43.75	29.80	5.76
Q99623	Prohibitin-2	64.88	33.30	9.83
P12273	Prolactin-inducible protein	27.40	16.60	8.05
Q9UQ80	Proliferation-associated protein 2G4	10.15	43.80	6.55
Q15185	Prostaglandin E synthase 3	13.75	18.70	4.54
Q8WXA2	Prostate and testis expressed protein 1	72.22	14.30	7.93
B3GLJ2	Prostate and testis expressed protein 3	40.82	11.70	8.97
P07288	Prostate-specific antigen	18.39	28.70	7.68
P15309	Prostatic acid phosphatase	8.55	44.50	6.24
Q16186	Proteasomal ubiquitin receptor ADRM1	16.46	42.10	5.07
Q14997	Proteasome activator complex subunit 4	13.08	211.20	6.90
Q969U7	Proteasome assembly chaperone 2	6.06	29.40	6.98
Q92530	Proteasome inhibitor PI31 subunit	23.25	29.80	5.74
P25786	Proteasome subunit alpha type-1	60.08	29.50	6.61
P25787	Proteasome subunit alpha type-2	26.07	25.90	7.43
P25788	Proteasome subunit alpha type-3	45.10	28.40	5.33
P25789	Proteasome subunit alpha type-4	15.71	29.50	7.72
P60900	Proteasome subunit alpha type-6	28.86	27.40	6.76
O14818	Proteasome subunit alpha type-7	40.73	27.90	8.46
Q8TAA3	Proteasome subunit alpha type-7-like	38.28	28.50	8.98
P20618	Proteasome subunit beta type-1	45.23	26.50	8.13
P49721	Proteasome subunit beta type-2	35.32	22.80	7.02
P49720	Proteasome subunit beta type-3	43.41	22.90	6.55
P28070	Proteasome subunit beta type-4	8.71	29.20	5.97
P28074	Proteasome subunit beta type-5	40.68	28.50	6.92
P28072	Proteasome subunit beta type-6	31.80	25.30	4.92
Q5VYK3	Proteasome-associated protein ECM29 homolog	1.25	204.20	7.12
O14744	Protein arginine N-methyltransferase 5	4.08	72.60	6.29
O43822	Protein C21orf2	34.38	28.30	7.34
Q9Y2B0	Protein canopy homolog 2	22.53	20.60	4.92
Q6TDU7	Protein CASC1	3.07	83.10	5.29
Q8WTU0	Protein DDI1 homolog 1	8.59	44.10	5.73
P07237	Protein disulfide-isomerase	12.80	57.10	4.87
P30101	Protein disulfide-isomerase A3	28.51	56.70	6.35
P13667	Protein disulfide-isomerase A4	13.49	72.90	5.07
Q15084	Protein disulfide-isomerase A6	23.86	48.10	5.08
Q99497	Protein DJ-1	46.03	19.90	6.79
Q9BVM2	Protein DPCD	20.20	23.20	9.03
Q9BPY3	Protein FAM118B	5.41	39.50	5.99
Q8IYX7	Protein FAM154A	37.34	54.60	8.37
Q96A26	Protein FAM162A	16.88	17.30	9.77

Q6J272	Protein FAM166A	45.43	36.10	7.81
A1A519	Protein FAM170A	18.48	37.10	5.03
Q6ZVS7	Protein FAM183B	37.78	16.20	8.43
Q6ZU69	Protein FAM205A	10.56	148.00	8.29
Q5JX71	Protein FAM209A	45.03	19.60	9.42
Q5JX69	Protein FAM209B	31.58	19.50	8.84
Q8IYT1	Protein FAM71A	17.34	63.10	9.64
Q8TC56	Protein FAM71B	16.20	64.70	9.48
Q8NEG0	Protein FAM71C	29.88	27.50	6.98
Q96LP2	Protein FAM81B	7.52	52.00	9.10
Q9BUN1	Protein MENT	65.98	36.70	8.59
Q9UFN0	Protein NipSnap homolog 3A	26.32	28.40	9.16
Q7Z5V6	Protein phosphatase 1 regulatory subunit 32	12.71	47.30	8.54
Q15435	Protein phosphatase 1 regulatory subunit 7	23.61	41.50	4.91
P35813	Protein phosphatase 1A	16.49	42.40	5.36
P41236	Protein phosphatase inhibitor 2	13.17	23.00	4.74
Q9Y570	Protein phosphatase methylesterase 1	9.59	42.30	5.97
P31151	Protein S100-A7	41.58	11.50	6.77
P05109	Protein S100-A8	29.03	10.80	7.03
P55735	Protein SEC13 homolog	9.63	35.50	5.48
P49221	Protein-glutamine gamma-glutamyltransferase 4	5.56	77.10	6.76
P22061	Protein-L-isoaspartate(D-aspartate) O-methyltransferase	32.16	24.60	7.21
P55786	Puromycin-sensitive aminopeptidase	21.11	103.20	5.72
Q5VTE0	Putative elongation factor 1-alpha-like 3	10.39	50.20	9.07
Q14409	Putative glycerol kinase 3	11.93	60.60	6.39
Q9GZT8	Putative GTP cyclohydrolase 1 type 2 NIF3L1	6.37	41.90	6.65
A6NK58	Putative lipoyltransferase 2, mitochondrial	22.08	25.20	8.27
Q8NHP8	Putative phospholipase B-like 2	6.45	65.40	6.80
Q7L7V1	Putative pre-mRNA-splicing factor ATP-dependent RNA helicase DHX32	2.29	84.40	4.97
Q8N5Q1	Putative protein FAM71E2	5.86	99.90	9.39
P0C874	Putative spermatogenesis-associated protein 31D3	4.91	102.40	8.07
Q6ZUB0	Putative spermatogenesis-associated protein 31D4	4.91	102.30	8.00
Q5T440	Putative transferase CAF17, mitochondrial	21.35	38.10	9.83
O00764	Pyridoxal kinase	9.94	35.10	6.13
Q53H96	Pyrraline-5-carboxylate reductase 3	9.49	28.60	7.50
P08559	Pyruvate dehydrogenase E1 component subunit alpha, somatic form, mitochondrial	17.95	43.30	8.06
P29803	Pyruvate dehydrogenase E1 component subunit alpha, testis-specific form, mitochondrial	41.75	42.90	8.46
P11177	Pyruvate dehydrogenase E1 component subunit beta, mitochondrial	16.99	39.20	6.65
O00330	Pyruvate dehydrogenase protein X component, mitochondrial	18.76	54.10	8.66
P14618	Pyruvate kinase PKM	45.20	57.90	7.84
P31150	Rab GDP dissociation inhibitor alpha	20.13	50.60	5.14

P50395	Rab GDP dissociation inhibitor beta	46.07	50.60	6.47
Q5HYI8	Rab-like protein 3	27.12	26.40	7.11
Q8WYR4	Radial spoke head 1 homolog	27.51	35.10	4.63
Q86UC2	Radial spoke head protein 3 homolog	10.89	63.60	5.69
Q9H0K4	Radial spoke head protein 6 homolog A	20.22	80.90	4.39
Q9H1X1	Radial spoke head protein 9 homolog	30.43	31.30	5.43
P35241	Radixin	4.46	68.50	6.37
P43487	Ran-specific GTPase-activating protein	14.43	23.30	5.29
P0DJD0	RANBP2-like and GRIP domain-containing protein 1	0.74	196.50	6.14
Q7Z3J3	RANBP2-like and GRIP domain-containing protein 4	0.74	197.20	6.27
Q99666	RANBP2-like and GRIP domain-containing protein 5/6	0.74	198.80	6.42
O14715	RANBP2-like and GRIP domain-containing protein 8	0.74	198.90	6.49
Q13576	Ras GTPase-activating-like protein IQGAP2	4.38	180.50	5.64
P63000	Ras-related C3 botulinum toxin substrate 1	15.63	21.40	8.50
P61026	Ras-related protein Rab-10	30.00	22.50	8.38
P62491	Ras-related protein Rab-11A	60.65	24.40	6.57
P61106	Ras-related protein Rab-14	36.74	23.90	6.21
Q9NP72	Ras-related protein Rab-18	18.93	23.00	5.24
P62820	Ras-related protein Rab-1A	24.39	22.70	6.21
Q9H0U4	Ras-related protein Rab-1B	24.88	22.20	5.73
P61019	Ras-related protein Rab-2A	47.64	23.50	6.54
Q8WUD1	Ras-related protein Rab-2B	46.76	24.20	7.83
P61018	Ras-related protein Rab-4B	16.43	23.60	6.06
P61020	Ras-related protein Rab-5B	14.42	23.70	8.13
P51148	Ras-related protein Rab-5C	19.91	23.50	8.41
P20340	Ras-related protein Rab-6A	34.62	23.60	5.54
P11233	Ras-related protein Ral-A	29.13	23.60	7.11
Q96HR9	Receptor expression-enhancing protein 6	36.96	20.70	8.56
P18754	Regulator of chromosome condensation	13.30	44.90	7.52
O94788	Retinal dehydrogenase 2	5.02	56.70	6.05
O43924	Retinal rod rhodopsin-sensitive cGMP 3',5'-cyclic phosphodiesterase subunit delta	16.00	17.40	5.67
P02753	Retinol-binding protein 4	11.44	23.00	6.07
Q9UHP6	Rhabdoid tumor deletion region protein 1	20.11	38.60	6.90
P52565	Rho GDP-dissociation inhibitor 1	36.76	23.20	5.11
Q8N443	RIB43A-like with coiled-coils protein 1	12.40	44.00	8.76
Q9H4K1	RIB43A-like with coiled-coils protein 2	20.39	37.00	9.54
P13489	Ribonuclease inhibitor	41.00	49.90	4.82
P60891	Ribose-phosphate pyrophosphokinase 1	6.92	34.80	6.98
Q9Y3A5	Ribosome maturation protein SBDS	13.60	28.70	8.75
P16083	Ribosylidihydronicotinamide dehydrogenase [quinone]	10.39	25.90	6.29
Q96AT9	Ribulose-phosphate 3-epimerase	7.46	24.90	5.58
Q96C74	Ropporin-1-like protein	35.22	26.10	7.72
Q9HAT0	Ropporin-1A	74.53	23.90	5.66
Q9BZX4	Ropporin-1B	75.47	23.90	5.15
Q9Y265	RuvB-like 1	24.56	50.20	6.42

Q9Y230	RuvB-like 2	39.96	51.10	5.64
P31153	S-adenosylmethionine synthase isoform type-2	5.82	43.60	6.48
P10768	S-formylglutathione hydrolase	19.15	31.40	7.02
P63208	S-phase kinase-associated protein 1	16.56	18.60	4.54
Q8NBX0	Saccharopine dehydrogenase-like oxidoreductase	17.25	47.10	9.14
Q49923	Schlafen-like protein 1	19.90	45.60	5.90
O15127	Secretory carrier-associated membrane protein 2	4.26	36.60	6.10
P04279	Semenogelin-1	52.38	52.10	9.29
Q02383	Semenogelin-2	18.73	65.40	9.07
Q9P0V9	Septin-10	6.61	52.60	6.80
Q8IYM1	Septin-12	15.64	40.70	7.11
O43236	Septin-4	12.97	55.10	6.11
P34896	Serine hydroxymethyltransferase, cytosolic	16.98	53.00	7.71
O43464	Serine protease HTRA2, mitochondrial	5.24	48.80	10.07
P20155	Serine protease inhibitor Kazal-type 2	54.76	9.30	9.00
Q07955	Serine/arginine-rich splicing factor 1	24.60	27.70	10.36
P84103	Serine/arginine-rich splicing factor 3	14.02	19.30	11.65
Q15172	Serine/threonine-protein phosphatase 2A 56 kDa regulatory subunit alpha isoform	4.73	56.20	6.71
P30153	Serine/threonine-protein phosphatase 2A 65 kDa regulatory subunit A alpha isoform	9.34	65.30	5.11
Q15257	Serine/threonine-protein phosphatase 2A activator	22.63	40.60	5.94
P67775	Serine/threonine-protein phosphatase 2A catalytic subunit alpha isoform	14.56	35.60	5.54
P62714	Serine/threonine-protein phosphatase 2A catalytic subunit beta isoform	14.56	35.60	5.43
P60510	Serine/threonine-protein phosphatase 4 catalytic subunit	15.31	35.10	5.06
Q8TF05	Serine/threonine-protein phosphatase 4 regulatory subunit 1	3.58	106.90	4.77
O00743	Serine/threonine-protein phosphatase 6 catalytic subunit	20.98	35.10	5.69
O15084	Serine/threonine-protein phosphatase 6 regulatory ankyrin repeat subunit A	2.94	112.90	6.25
Q96HS1	Serine/threonine-protein phosphatase PGAM5, mitochondrial	24.91	32.00	8.68
P62140	Serine/threonine-protein phosphatase PP1-beta catalytic subunit	35.78	37.20	6.19
P36873	Serine/threonine-protein phosphatase PP1-gamma catalytic subunit	50.15	37.00	6.54
Q96P63	Serpin B12	4.20	46.20	5.53
P35237	Serpin B6	24.73	42.60	5.27
P02768	Serum albumin	31.20	69.30	6.28
P02743	Serum amyloid P-component	34.08	25.40	6.54
P16219	Short-chain specific acyl-CoA dehydrogenase, mitochondrial	22.33	44.30	7.99
P67812	Signal peptidase complex catalytic subunit SEC11A	19.55	20.60	9.48
Q15005	Signal peptidase complex subunit 2	20.35	25.00	8.47

Q04837	Single-stranded DNA-binding protein, mitochondrial	81.08	17.20	9.60
O43805	Sjogren syndrome nuclear autoantigen 1	52.94	13.60	5.38
O60232	Sjogren syndrome/scleroderma autoantigen 1	29.15	21.50	5.24
O43765	Small glutamine-rich tetratricopeptide repeat-containing protein alpha	8.63	34.00	4.87
Q9UBC9	Small proline-rich protein 3	18.34	18.10	8.57
Q8NHG7	Small VCP/p97-interacting protein	27.27	8.40	8.91
P13637	Sodium/potassium-transporting ATPase subunit alpha-3	5.92	111.70	5.38
Q13733	Sodium/potassium-transporting ATPase subunit alpha-4	6.51	114.10	6.64
P54709	Sodium/potassium-transporting ATPase subunit beta-3	15.41	31.50	8.35
Q8TDB8	Solute carrier family 2, facilitated glucose transporter member 14	16.92	56.30	7.83
Q00796	Sorbitol dehydrogenase	34.17	38.30	7.97
Q9Y512	Sorting and assembly machinery component 50 homolog	7.68	51.90	6.90
O60493	Sorting nexin-3	19.75	18.80	8.66
Q9H3U7	SPARC-related modular calcium-binding protein 2	8.97	49.60	8.46
Q76KD6	Speriolin	5.25	62.40	8.19
Q9HBV2	Sperm acrosome membrane-associated protein 1	21.09	32.10	4.61
Q8IXA5	Sperm acrosome membrane-associated protein 3	26.98	23.40	7.94
Q8TDM5	Sperm acrosome membrane-associated protein 4	21.77	13.00	5.80
Q96QH8	Sperm acrosome-associated protein 5	16.35	17.90	6.42
Q6UW49	Sperm equatorial segment protein 1	18.00	38.90	5.73
Q9C093	Sperm flagellar protein 2	3.73	209.70	5.54
Q9NS25	Sperm protein associated with the nucleus on the X chromosome B/F	32.04	11.80	6.15
Q9BXN6	Sperm protein associated with the nucleus on the X chromosome D	48.45	11.00	6.11
Q8TAD1	Sperm protein associated with the nucleus on the X chromosome E	48.45	11.00	5.26
Q15506	Sperm surface protein Sp17	34.44	17.40	4.78
Q8N0X2	Sperm-associated antigen 16 protein	10.94	70.80	6.33
Q9NPE6	Sperm-associated antigen 4 protein	10.30	48.10	7.14
O75602	Sperm-associated antigen 6	14.54	55.40	6.83
Q8NCR6	Spermatid-specific manchette-related protein 1	51.15	30.10	8.40
Q7Z5L4	Spermatogenesis-associated protein 19, mitochondrial	58.68	19.20	6.96
Q8NHX4	Spermatogenesis-associated protein 3	9.84	19.90	10.17
Q6ZQQ2	Spermatogenesis-associated protein 31D1	4.89	175.50	8.85
Q96N06	Spermatogenesis-associated protein 33	27.34	15.50	9.22
Q9NWH7	Spermatogenesis-associated protein 6	4.10	56.00	8.48
Q9NXE4	Sphingomyelin phosphodiesterase 4	5.80	93.30	7.97
Q13838	Spliceosome RNA helicase DDX39B	8.41	49.00	5.67
Q5W111	SPRY domain-containing protein 7	11.22	21.70	6.70
P16949	Stathmin	18.12	17.30	5.97
Q9P1V8	Sterile alpha motif domain-containing protein 15	3.41	77.10	4.45
Q9UJZ1	Stomatin-like protein 2, mitochondrial	22.75	38.50	7.39
P38646	Stress-70 protein, mitochondrial	9.87	73.60	6.16



P31948	Stress-induced-phosphoprotein 1	11.79	62.60	6.80
Q9HCN8	Stromal cell-derived factor 2-like protein 1	17.65	23.60	7.03
P31040	Succinate dehydrogenase [ubiquinone] flavoprotein subunit, mitochondrial	25.45	72.60	7.39
P21912	Succinate dehydrogenase [ubiquinone] iron-sulfur subunit, mitochondrial	20.36	31.60	8.76
P51649	Succinate-semialdehyde dehydrogenase, mitochondrial	6.17	57.20	8.28
Q9P2R7	Succinyl-CoA ligase [ADP-forming] subunit beta, mitochondrial	10.80	50.30	7.42
P55809	Succinyl-CoA:3-ketoacid coenzyme A transferase 1, mitochondrial	13.08	56.10	7.46
Q9BYC2	Succinyl-CoA:3-ketoacid coenzyme A transferase 2, mitochondrial	4.84	56.10	7.14
Q8TC36	SUN domain-containing protein 5	10.03	43.10	8.31
P00441	Superoxide dismutase [Cu-Zn]	29.87	15.90	6.13
O95473	Synaptogyrin-4	6.84	25.80	7.75
P57105	Synaptojanin-2-binding protein	24.14	15.90	6.30
Q86Y82	Syntaxin-12	14.49	31.60	5.59
P17987	T-complex protein 1 subunit alpha	19.60	60.30	6.11
P78371	T-complex protein 1 subunit beta	29.53	57.50	6.46
P50991	T-complex protein 1 subunit delta	25.05	57.90	7.83
P48643	T-complex protein 1 subunit epsilon	14.97	59.60	5.66
Q99832	T-complex protein 1 subunit eta	25.05	59.30	7.65
P49368	T-complex protein 1 subunit gamma	30.09	60.50	6.49
P50990	T-complex protein 1 subunit theta	13.87	59.60	5.60
P40227	T-complex protein 1 subunit zeta	9.60	58.00	6.68
Q92526	T-complex protein 1 subunit zeta-2	12.45	57.80	7.24
Q8IYX1	TBC1 domain family member 21	8.33	39.20	6.19
Q8IZS6	Tctex1 domain-containing protein 3	18.69	23.20	9.33
Q969V4	Tektin-1	34.93	48.30	6.37
Q9UIF3	Tektin-2	47.91	49.60	5.55
Q9BXF9	Tektin-3	44.69	56.60	7.34
Q8WW24	Tektin-4	51.72	50.60	6.44
Q96M29	Tektin-5	44.33	56.30	7.14
Q9P2T0	Testicular haploid expressed gene protein	11.61	43.40	9.04
Q9BY14	Testis-expressed sequence 101 protein	16.47	26.60	4.94
O43247	Testis-expressed sequence 33 protein	8.21	30.70	7.99
Q5T0J7	Testis-expressed sequence 35 protein	10.30	26.50	9.11
Q96LM6	Testis-expressed sequence 37 protein	11.11	20.60	7.55
Q9BZW7	Testis-specific gene 10 protein	40.97	81.40	5.97
Q75WM6	Testis-specific H1 histone	25.49	28.10	11.78
Q9BXA7	Testis-specific serine/threonine-protein kinase 1	7.36	41.60	7.71
Q96PF2	Testis-specific serine/threonine-protein kinase 2	17.60	40.90	8.84
Q9BXA6	Testis-specific serine/threonine-protein kinase 6	20.88	30.30	9.11
Q6URK8	Testis, prostate and placenta-expressed protein	60.15	30.70	8.82
Q8NDW8	Tetratricopeptide repeat protein 21A	1.82	150.80	7.24

Q96NG3	Tetratricopeptide repeat protein 25	12.50	76.60	5.60
Q8N5M4	Tetratricopeptide repeat protein 9C	12.87	20.00	8.92
Q9BU02	Thiamine-triphosphatase	31.30	25.60	4.82
Q8N427	Thioredoxin domain-containing protein 3	4.59	67.20	4.97
Q9NNW7	Thioredoxin reductase 2, mitochondrial	13.74	56.50	7.50
Q9H1E5	Thioredoxin-related transmembrane protein 4	12.32	38.90	4.37
O00142	Thymidine kinase 2, mitochondrial	7.17	31.00	8.46
P23919	Thymidylate kinase	26.89	23.80	8.27
O43617	Trafficking protein particle complex subunit 3	26.11	20.30	4.96
Q9BV79	Trans-2-enoyl-CoA reductase, mitochondrial	7.24	40.40	8.76
P37837	Transaldolase	9.79	37.50	6.81
Q15369	Transcription elongation factor B polypeptide 1	43.75	12.50	4.78
Q00059	Transcription factor A, mitochondrial	41.06	29.10	9.72
Q00577	Transcriptional activator protein Pur-alpha	13.98	34.90	6.44
Q96QR8	Transcriptional activator protein Pur-beta	6.73	33.20	5.43
Q9Y4P3	Transducin beta-like protein 2	9.40	49.80	9.44
P55072	Transitional endoplasmic reticulum ATPase	50.74	89.30	5.26
Q14232	Translation initiation factor eIF-2B subunit alpha	6.23	33.70	7.33
P13693	Translationally-controlled tumor protein	19.19	19.60	4.93
Q15631	Translin	49.56	26.20	6.44
Q99598	Translin-associated protein X	31.38	33.10	6.55
P51571	Translocon-associated protein subunit delta	21.97	19.00	6.15
Q8N6Q1	Transmembrane and coiled-coil domain-containing protein 5A	21.88	34.20	6.05
P49755	Transmembrane emp24 domain-containing protein 10	24.66	25.00	7.44
Q7Z7H5	Transmembrane emp24 domain-containing protein 4	17.18	25.90	8.28
Q9BVK6	Transmembrane emp24 domain-containing protein 9	15.74	27.30	8.02
P17152	Transmembrane protein 11, mitochondrial	17.19	21.50	7.36
Q9H061	Transmembrane protein 126A	32.31	21.50	9.26
Q8WZ59	Transmembrane protein 190	43.50	19.40	5.24
Q6UW68	Transmembrane protein 205	37.04	21.20	8.62
Q96SK2	Transmembrane protein 209	4.10	62.90	8.63
A2RUT3	Transmembrane protein 89	64.15	17.60	10.01
Q5BJF2	Transmembrane protein 97	10.23	20.80	9.38
A6NFA0	Transmembrane protein ENSP00000340100	7.69	37.60	7.97
P40939	Trifunctional enzyme subunit alpha, mitochondrial	22.28	82.90	9.04
P55084	Trifunctional enzyme subunit beta, mitochondrial	19.20	51.30	9.41
P60174	Triosephosphate isomerase	26.22	30.80	5.92
P29144	Tripeptidyl-peptidase 2	9.21	138.30	6.32
P06753	Tropomyosin alpha-3 chain	7.02	32.90	4.72
P23381	Tryptophan--tRNA ligase, cytoplasmic	8.49	53.10	6.23
Q71U36	Tubulin alpha-1A chain	49.67	50.10	5.06
Q13748	Tubulin alpha-3C/D chain	58.89	49.90	5.10
Q9BVA1	Tubulin beta-2B chain	33.93	49.90	4.89
P68371	Tubulin beta-4B chain	38.43	49.80	4.89

P59282	Tubulin polymerization-promoting protein family member 2	26.47	18.50	9.00
Q99426	Tubulin-folding cofactor B	22.95	27.30	5.15
Q9BTW9	Tubulin-specific chaperone D	9.40	132.50	6.19
O15042	U2 snRNP-associated SURP motif-containing protein	1.94	118.20	8.47
Q9Y333	U6 snRNA-associated Sm-like protein LSm2	28.42	10.80	6.52
Q9UK45	U6 snRNA-associated Sm-like protein LSm7	31.07	11.60	5.27
Q96DE0	U8 snoRNA-decapping enzyme	18.97	21.30	6.89
P54578	Ubiquitin carboxyl-terminal hydrolase 14	5.26	56.00	5.30
P45974	Ubiquitin carboxyl-terminal hydrolase 5	5.01	95.70	5.03
Q93009	Ubiquitin carboxyl-terminal hydrolase 7	13.79	128.20	5.55
P09936	Ubiquitin carboxyl-terminal hydrolase isozyme L1	26.46	24.80	5.48
Q9Y5K5	Ubiquitin carboxyl-terminal hydrolase isozyme L5	5.17	37.60	5.33
Q14139	Ubiquitin conjugation factor E4 A	2.06	122.50	5.24
Q8WUN7	Ubiquitin domain-containing protein 2	11.11	26.20	5.67
Q92890	Ubiquitin fusion degradation protein 1 homolog	16.94	34.50	6.70
Q96FW1	Ubiquitin thioesterase OTUB1	19.93	31.30	4.94
Q96DC9	Ubiquitin thioesterase OTUB2	24.79	27.20	6.23
P62979	Ubiquitin-40S ribosomal protein S27a	28.85	18.00	9.64
P62987	Ubiquitin-60S ribosomal protein L40	35.16	14.70	9.83
P61077	Ubiquitin-conjugating enzyme E2 D3	19.73	16.70	7.80
P61086	Ubiquitin-conjugating enzyme E2 K	17.00	22.40	5.44
P61088	Ubiquitin-conjugating enzyme E2 N	38.16	17.10	6.57
Q13404	Ubiquitin-conjugating enzyme E2 variant 1	24.49	16.50	7.93
Q15819	Ubiquitin-conjugating enzyme E2 variant 2	35.86	16.40	8.09
Q9Y3C8	Ubiquitin-fold modifier-conjugating enzyme 1	23.95	19.40	7.40
P22314	Ubiquitin-like modifier-activating enzyme 1	8.98	117.80	5.76
A0AVT1	Ubiquitin-like modifier-activating enzyme 6	2.19	117.90	6.14
Q9BZV1	UBX domain-containing protein 6	10.43	49.70	6.89
Q14376	UDP-glucose 4-epimerase	6.32	38.30	6.73
Q9NYU2	UDP-glucose:glycoprotein glucosyltransferase 1	2.32	177.10	5.63
Q5T681	Uncharacterized protein C10orf62	13.90	25.10	7.59
Q8WW14	Uncharacterized protein C10orf82	12.61	25.90	8.47
Q6P656	Uncharacterized protein C15orf26	27.91	34.30	6.28
H3BRN8	Uncharacterized protein C15orf65	22.31	13.80	8.31
Q8NEP4	Uncharacterized protein C17orf47	8.42	63.10	9.20
A8MV24	Uncharacterized protein C17orf98	42.86	17.60	9.79
A6NCJ1	Uncharacterized protein C19orf71	86.12	24.20	8.95
Q5SVJ3	Uncharacterized protein C1orf100	25.17	17.60	9.61
Q8N1D5	Uncharacterized protein C1orf158	30.93	23.10	9.73
Q5T5A4	Uncharacterized protein C1orf194	55.03	19.30	9.28
Q9H1P6	Uncharacterized protein C20orf85	40.88	15.70	8.46
Q8N801	Uncharacterized protein C2orf61	10.48	27.80	9.58
Q96M34	Uncharacterized protein C3orf30	8.58	60.10	5.80
Q6V702	Uncharacterized protein C4orf22	25.32	26.90	5.44
Q6ZNM6	Uncharacterized protein C5orf48	46.27	15.40	9.16

A4QMS7	Uncharacterized protein C5orf49	58.50	17.00	7.59
Q5TEZ5	Uncharacterized protein C6orf163	10.64	38.50	6.96
Q8N865	Uncharacterized protein C7orf31	5.08	68.40	7.31
Q8IZ16	Uncharacterized protein C7orf61	14.56	23.80	10.40
A4D263	Uncharacterized protein C7orf72	24.89	49.60	8.48
Q5VTT2	Uncharacterized protein C9orf135	13.10	26.40	7.21
Q6ZQR2	Uncharacterized protein C9orf171	28.75	36.50	10.26
Q96E40	Uncharacterized protein C9orf9	42.79	25.10	9.13
Q9H0B3	Uncharacterized protein KIAA1683	17.80	127.60	10.23
Q9HB07	UPF0160 protein MYG1, mitochondrial	25.27	42.40	6.67
Q9H993	UPF0364 protein C6orf211	6.58	51.10	5.76
Q9Y6A4	UPF0468 protein C16orf80	39.90	22.80	9.76
A6NJV1	UPF0573 protein C2orf70	26.87	23.40	9.99
Q9NWW4	UPF0587 protein C1orf123	15.63	18.00	5.01
Q9H5F2	UPF0686 protein C11orf1	28.67	17.80	8.37
Q5BN46	UPF0691 protein C9orf116	64.71	15.30	8.81
Q537H7	UPF0732 protein C1orf227	45.92	11.30	10.07
Q16851	UTP--glucose-1-phosphate uridylyltransferase	11.22	56.90	8.15
P38606	V-type proton ATPase catalytic subunit A	9.56	68.30	5.52
P21281	V-type proton ATPase subunit B, brain isoform	7.44	56.50	5.81
Q96A05	V-type proton ATPase subunit E 2	31.42	26.10	8.76
Q16864	V-type proton ATPase subunit F	41.18	13.40	5.52
O75348	V-type proton ATPase subunit G 1	53.39	13.70	8.79
Q9UK41	Vacuolar protein sorting-associated protein 28 homolog	20.36	25.40	5.54
Q86WA6	Valacyclovir hydrolase	18.56	32.50	9.14
P26640	Valine--tRNA ligase	20.57	140.40	7.59
P49748	Very long-chain specific acyl-CoA dehydrogenase, mitochondrial	6.72	70.30	8.75
Q96AJ9	Vesicle transport through interaction with t-SNAREs homolog 1A	22.58	25.20	6.40
Q15836	Vesicle-associated membrane protein 3	55.00	11.30	8.79
O75379	Vesicle-associated membrane protein 4	25.53	16.40	7.34
Q9P0L0	Vesicle-associated membrane protein-associated protein A	23.29	27.90	8.62
O95292	Vesicle-associated membrane protein-associated protein B/C	21.81	27.20	7.30
P46459	Vesicle-fusing ATPase	15.46	82.50	6.95
O75396	Vesicle-trafficking protein SEC22b	17.21	24.60	6.92
Q8N0U8	Vitamin K epoxide reductase complex subunit 1-like protein 1	19.89	19.80	9.13
P45880	Voltage-dependent anion-selective channel protein 2	7.14	31.50	7.56
Q9NY47	Voltage-dependent calcium channel subunit alpha-2/delta-2	2.17	129.70	5.80
Q8IUA0	WAP four-disulfide core domain protein 8	38.59	27.80	8.02
Q8N1V2	WD repeat-containing protein 16	20.32	68.30	6.95
Q96MT7	WD repeat-containing protein 52	2.34	111.70	4.84
Q96MR6	WD repeat-containing protein 65	13.52	144.90	5.80

Q9UHR6	Zinc finger HIT domain-containing protein 2	11.41	42.90	5.99
Q9H0C1	Zinc finger MYND domain-containing protein 12	13.15	41.80	6.23
Q9BS86	Zona pellucida-binding protein 1	33.90	40.10	9.28
Q6X784	Zona pellucida-binding protein 2	14.20	38.60	7.78

---

**Supplementary Table S2 – Complete list of identified proteins (1157) in Asthenozoospermic (A) vs. Normozoospermic (N) samples differential proteomics experiment.**

Note: The table with all the MS details for each protein and peptide is available free of charge via <http://pubs.acs.org>. (<http://pubs.acs.org/doi/suppl/10.1021/pr500652y>)

UniprotKB/ Swiss-Prot accession number	Description	Σ# Unique Peptide	Identified Peptide Sequence	# PSMs	FDR	Modifications	MH+ [Da]	# Missed Cleavages	Unique Peptide	Used for quantifi cation	Reporter ion ratio variability between all A and N samples in both lanes (A and B)	
											All A samples Variability [%]	All N samples Variability [%]
P10606	Cytochrome c oxidase subunit 5B, mitochondrial	5	IVGCICEEDNTSVVWF LHKGEAQR	8	0	C4(Carbamidomethyl); C6(Carbamidomethyl); K20(TMT6plex)	3262.61	1	Yes	No	0.000	0.000
			EIMLAAKGLDPYNVLAPK GASGTR	2	0	K7(TMT6plex); K8(TMT6plex); K19(TMT6plex)	3287.92	3	Yes	Yes	0.000	0.000
			CGAHYKLPQQLAH	5	0	C1(Carbamidomethyl); K6(TMT6plex)	1850.99	1	Yes	Yes	13.951	16.374
			SMASGGVPTDEEQATGL ER	2	0	M2(Oxidation)	2007.89	0	Yes	No	0.000	0.000
			EDPNLVPSINR	19	0	K12(TMT6plex) M3(Oxidation);	1697.94	1	Yes	Yes	19.736	14.745
P01034	Cystatin-C	4	EIMLAAKGLDPYNVLAPK GASGTR	1	0	K7(TMT6plex); K8(TMT6plex); K19(TMT6plex)	3303.91	3	Yes	No	0.000	0.000
			KQIVAGVNYFLDVELGR	14	0	K1(TMT6plex)	2150.22	1	Yes	Yes	6.892	5.239
			ALDFAVGEYNKASNDMYH SR	4	0	K11(TMT6plex); M16(Oxidation)	2533.20	1	Yes	Yes	0.000	0.000
P24666	Low molecular	6	TTCTKTQPNLDNCPFHIDQ PHLKR	1	0	C3(Carbamidomethyl); K5(TMT6plex); C13(Carbamidomethyl); K22(TMT6plex)	3266.66	2	Yes	No	0.000	0.000
			LVGGPMDASVEEGR	1	0	M6(Oxidation)	1816.89	1	Yes	No	0.000	0.000
			KLVTDCNISENWR	7	0	K1(TMT6plex)	1831.99	1	Yes	Yes	11.254	9.363

Q15631	Translin	7	weight phosphotyrosine protein phosphatase	QITKEDFATFDYILCMDES NLR	2	0	0	C15(Carbamidomethyl); M16(Oxidation)	2954.41	1	Yes	Yes	0.000	0.000
				VDSAATSGYEIGNPPDYR	8	0	0		1911.87	0	Yes	No	0.000	0.000
				SPIAEAVFR	12	0	0		989.54	0	Yes	No	0.000	0.000
				AFLEKAH	4	0	0	K5(TMT6plex)	1044.61	1	Yes	Yes	0.000	0.000
				HGIPMSHVAR	1	0	0	M5(Oxidation)	1120.57	0	Yes	No	0.000	0.000
				YDGLKYDVKKVEEVVYDLSI R	4	0	0	K5(TMT6plex); K9(TMT6plex); K10(TMT6plex)	3218.83	3	Yes	No	0.000	0.000
				EKGFHLDVEDYLSGVILIAS ELSR	11	0	0	K2(TMT6plex)	2919.57	1	Yes	Yes	3.884	14.616
				EILTLQGVHQGAGFQDIP KR	9	0	0	K20(TMT6plex)	2549.44	1	Yes	Yes	0.000	0.000
				GFNKETAACVEK	14	0	0	C10(Carbamidomethyl); K13(TMT6plex)	1883.01	1	Yes	Yes	9.593	9.027
				KVVSLEQJAR	18	0	0	K1(TMT6plex)	1487.87	1	Yes	Yes	21.214	15.939
EAVTEILGIEPDR	3	0	0		1441.76	0	Yes	No	0.000	0.000				
LLNLKNDSLR	16	0	0	K5(TMT6plex)	1414.86	1	Yes	Yes	24.740	12.476				
Q86Y39	NADH dehydrogenase [ubiquinone] 1 alpha subcomplex subunit 11	4	weight phosphotyrosine protein phosphatase	LEGWEVFAKPKV	4	0	0	K9(TMT6plex); K11(TMT6plex)	1861.10	1	Yes	Yes	0.000	0.000
				QYWDIPDGTDCR	1	0	0	C11(Carbamidomethyl)	1662.70	0	Yes	No	0.000	0.000
				EKPDDPLNYFLGGCAGGLT LGAR	1	0	0	K2(TMT6plex); C14(Carbamidomethyl)	2650.35	0	Yes	No	0.000	0.000
KAYSTTSIASVAGLTAAYR	1	0	0	K1(TMT6plex)	2231.23	1	Yes	Yes	0.000	0.000				
Q9BRQ6	Coiled-coil-helix-coiled-coil-helix domain-	9	weight phosphotyrosine protein phosphatase	YEQEHAAIQDKLFQVAKR	3	0	0	K11(TMT6plex); K17(TMT6plex)	2632.46	2	Yes	Yes	0.000	0.000

containing protein 6, mitochondrial										
VVSGVDEEER	3	0	0	1166.53	0	Yes	No	0.000	0.000	0.000
APHKESTLPR	3	0	0	1364.78	1	Yes	Yes	13.541	8.016	0.000
DTFYKEQLER	5	0	0	1557.81	1	Yes	Yes	0.000	0.000	0.000
CVSAAHKG	3	0	0	1058.56	1	Yes	Yes	0.000	0.000	0.000
SGSSGGQQPSGMKEGVK R	3	0	0	2251.19	2	Yes	Yes	0.000	0.000	0.000
DRPHEVLLCSDLVKAYQR	2	0	0	2428.30	1	Yes	Yes	0.000	0.000	0.000
RVSFGVDEEER	1	0	0	1322.64	1	Yes	No	0.000	0.000	0.000
VEPVCSGLQAQIILHCYR	1	0	0	2030.00	0	Yes	No	0.000	0.000	0.000
DLEDKSSAQCIIDEKCFNLR	6	0	0	2786.38	2	Yes	No	0.000	0.000	0.000
RECAANEVNCPLQVALECLYHR	1	0	0	2815.33	1	Yes	No	0.000	0.000	0.000
LLQDKDQLTHQMREGTC R	3	0	0	2446.20	1	Yes	Yes	0.000	0.000	0.000
LECAANEVNCPLQVALECLYHR	1	0	0	2659.25	0	Yes	No	0.000	0.000	0.000
LLTENQNLTVKR	20	0	0	1787.02	1	Yes	Yes	19.854	15.266	0.000
DIPQLKLVNEVFTIDDTLQTLKLR	9	0	0	3270.92	2	Yes	No	0.000	0.000	0.000
YSPHIDWDSNQLQVLR	5	0	0	1872.86	0	Yes	No	0.000	0.000	0.000
LRETQDTLQLLVMTKCR	1	0	0	2334.29	2	Yes	No	0.000	0.000	0.000
LSDIGFWKSELSYELDR	3	0	0	2287.18	1	Yes	No	0.000	0.000	0.000
IGIDLVDHNVKELNLR	4	0	0	2077.20	1	Yes	No	0.000	0.000	0.000
ETQDTLQLLVMTKCR	1	0	0	2065.10	1	Yes	No	0.000	0.000	0.000

Q96M29

Tektin-5

17



P54652	Heat shock-related 70 kDa protein 2	14
SIMAKEGPKVAQTR	M3(Oxidation); K5(TMT6plex); K10(TMT6plex)	2 0 0 2103.24 2 Yes Yes 0.000 0.000
QFTDTNLAFNAR		4 0 0 1397.68 0 Yes No 0.000 0.000
SIMAKEGPKVAQTR	K5(TMT6plex); K10(TMT6plex)	3 0 0 2087.24 2 Yes Yes 19.081 6.008
KTFPCTPR	K1(TMT6plex); C5(Carbamidomethyl)	13 0.001 1235.68 1 Yes Yes 34.383 9.065
TRRPNMELCR	M6(Oxidation); C9(Carbamidomethyl)	1 0.002 1348.66 1 Yes No 0.000 0.000
DAQHVLER		1 0.002 967.50 0 Yes No 0.000 0.000
RPNMELCR	M4(Oxidation); C7(Carbamidomethyl)	1 0.005 1091.51 0 Yes No 0.000 0.000
LIGDAAKNQVAMNPTNTI FDAKR	K7(TMT6plex); M12(Oxidation); K22(TMT6plex)	32 0 0 2962.64 2 Yes Yes 26.848 12.371
KFEDATVQSDMKHWPFR	K1(TMT6plex); M11(Oxidation); K12(TMT6plex)	35 0 0 2596.34 2 Yes Yes 9.701 19.637
KFEDATVQSDMKHWPFR	K1(TMT6plex); K12(TMT6plex)	16 0 0 2580.38 2 Yes Yes 6.246 1.010
GPAIGIDLGTTSCVGVFQ HGKVEIANDQGNR	C14(Carbamidomethyl); K22(TMT6plex)	8 0 0 3715.92 1 Yes No 0.000 0.000
QATKDAGITGLNVLNLR	K4(TMT6plex)	87 0 0 1887.09 1 Yes Yes 25.025 23.650
DAKLDKGQIQEIVLVGGST R	K3(TMT6plex); K6(TMT6plex)	114 0 0 2585.51 2 Yes Yes 38.184 33.695
LIGDAAKNQVAMNPTNTI FDAKR	K7(TMT6plex); K22(TMT6plex)	9 0 0 2946.63 2 Yes Yes 33.400 9.548
ARFEELNADLFR		66 0 0 1480.76 1 No No 0.000 0.000
AMTKDNNLLGKFDLTGIPP APR	M2(Oxidation); K4(TMT6plex); K11(TMT6plex)	2 0 0 2843.59 2 Yes No 0.000 0.000
NTTIPTKQTQTFITYSDNQ SSVLVQVYEGER	K7(TMT6plex)	31 0 0 3764.89 1 Yes No 0.000 0.000
VAAKNALESYTYNIKQTVE DEKLR	K4(TMT6plex); K15(TMT6plex); K22(TMT6plex)	1 0 0 3470.95 3 Yes No 0.000 0.000
TTPSYVAFTDTER		61 0 0 1487.70 0 No No 0.000 0.000
FEELNADLFR		37 0 0 1253.62 0 No No 0.000 0.000

Q9H4V5	Glutathione S-transferase omega-2	8	MVSHLAEEFKR	20	0	K10(TMT6plex)	1575.85	1	Yes	Yes	27.277	11.980
			YKSEDEANR	99	0	K2(TMT6plex)	1340.66	1	Yes	Yes	27.825	16.158
			NQMAEKDEYEHKQKELER	3	0	K6(TMT6plex); K12(TMT6plex); K14(TMT6plex)	2992.58	3	Yes	Yes	0.000	0.000
			MVSHLAEEFKR	54	0	M1(Oxidation); K10(TMT6plex)	1591.85	1	Yes	Yes	31.151	29.639
			VEIANDQGNR	10	0		1228.63	0	No	No	0.000	0.000
			YKSEDEANRDR	74	0	K2(TMT6plex)	1611.79	2	Yes	Yes	32.405	21.238
			LSKDDIDR	163	0	K3(TMT6plex)	1190.66	1	Yes	Yes	20.417	15.594
			GTLEPVEKALR	79	0	K8(TMT6plex)	1441.86	1	No	No	0.000	0.000
			FDLTGIPAPR	2	0.001		1183.65	0	No	No	0.000	0.000
			KHKKDIGNKR	2	0.004	K1(TMT6plex); K3(TMT6plex); K4(TMT6plex); K10(TMT6plex)	2237.44	4	Yes	Yes	0.000	0.000
Q6UWQ5	Lysozyme-like protein 1	4	LDVYGILDCVSHTPALR	10	0	C9(Carbamidomethyl)	1929.00	0	Yes	No	0.000	0.000
			TLGKGSQPPGVPPEGLIR	13	0	K4(TMT6plex)	2032.18	1	Yes	Yes	10.311	24.466
			QKMILLEFCKVPHLTKECL VALR	1	0	C9(Carbamidomethyl); K10(TMT6plex); K16(TMT6plex); C18(Carbamidomethyl)	3514.06	3	Yes	No	0.000	0.000
			HEVYNINLR	5	0		1093.61	0	Yes	No	0.000	0.000
			ECTNLKAAALR	10	0	C2(Carbamidomethyl); K6(TMT6plex)	1404.79	1	Yes	Yes	19.761	15.488
			KLFPYDPYER	11	0	K1(TMT6plex)	1556.83	1	Yes	Yes	12.983	7.843
			FCPYSHR	2	0.001	C2(Carbamidomethyl)	966.42	0	Yes	No	0.000	0.000
			LVLKAKDIR	5	0.002	K4(TMT6plex); K6(TMT6plex)	1514.02	2	Yes	Yes	3.955	5.477
			GKLKENNHCHVACALITD DLTDAIICAR	2	0	K2(TMT6plex); K4(TMT6plex); C9(Carbamidomethyl); C13(Carbamidomethyl); C27(Carbamidomethyl)	3753.93	2	Yes	No	0.000	0.000
			CKLAKIFSR	74	0	C1(Carbamidomethyl); K2(TMT6plex);	1580.98	2	Yes	Yes	37.444	25.406

<b>P61088</b>	<b>Ubiquitin-conjugating enzyme E2 N</b>	<b>4</b>	KIVKETQGMNYYWQGWKK HCEGR	1	0	3680.03	4	Yes	No	0.000	0.000	
				LAKIFSR	1	0.002	1063.69	1	Yes	Yes	0.000	0.000
<b>Q6UW68</b>	<b>Transmembrane protein 205</b>	<b>4</b>	ICLDILKDKWSPALQIR	7	0	2527.50	2	Yes	Yes	0.000	0.000	
				LLAEPVPGIKAEPDESNA	3	0	2235.22	1	Yes	Yes	0.000	0.000
				IIKETQR	3	0	1116.70	1	Yes	Yes	0.000	0.000
				FMTKIYHPNVDKLGR	1	0	2293.29	2	Yes	No	0.000	0.000
				YHGLSSLCNLGCVLSNGLC LAGLALEIR	2	0	3060.55	0	Yes	No	0.000	0.000
				TTAAMWALQVTEKER	1	0	1964.05	1	Yes	Yes	0.000	0.000
<b>P30041</b>	<b>Peroxi-redoxin -6</b>	<b>6</b>	FHDFLGDSWGLFSHPR	4	0	1664.98	2	Yes	Yes	0.000	0.000	
				VVISLQLTAEKR	35	0	1585.99	1	Yes	Yes	18.217	15.008
				AAKLAPEFAKR	32	0	1660.03	2	Yes	Yes	16.816	19.680
				DFTPVCCTELGR	10	0	1395.66	0	Yes	No	0.000	0.000
				VVFVFGPDKKLKLILYPAT TGR	8	0	3236.98	3	Yes	Yes	9.278	23.764
				NFDEILR	10	0.001	906.47	0	Yes	No	0.000	0.000
<b>Q969V4</b>	<b>Tektin-1</b>	<b>11</b>	LKETLAQAQAEIKGLHR	9	0	2364.42	2	Yes	Yes	0.000	0.000	
				LMKEVQEITHNVAR	3	0	1913.05	1	Yes	Yes	8.890	9.921

<b>Q9NR28</b>	<b>Diablo homolog, mitochondrial</b>	<b>6</b>	TLEEASEQJR	3	0	1175.59	0	Yes	No	0.000	0.000	
			THRPNVELCR	2	0	C9(Carbamidomethyl)	1281.65	0	Yes	No	0.000	0.000
			NNSLMLKALVDR	2	0	M5(Oxidation); K7(TMT6plex)	1618.91	1	Yes	No	0.000	0.000
			LEKALETLKEPLHITETGLAYR	2	0	K3(TMT6plex); K9(TMT6plex); C18(Carbamidomethyl)	3086.73	2	Yes	Yes	0.000	0.000
			LVDEIEKTR	4	0	K7(TMT6plex)	1432.82	1	Yes	Yes	0.000	0.000
			ILSQTANDLR	2	0		1130.62	0	Yes	No	0.000	0.000
			KQCDVVDTAFKNLKDTKDAR	1	0	K1(TMT6plex); C3(Carbamidomethyl); K11(TMT6plex); K15(TMT6plex); K18(TMT6plex)	3325.87	4	Yes	No	0.000	0.000
			KSQSDVNMKLEQR	2	0.001	K1(TMT6plex); K8(TMT6plex); K9(TMT6plex)	2247.34	3	Yes	Yes	0.000	0.000
			YSENAVR	1	0.004		838.40	0	Yes	No	0.000	0.000
			NHIQLVKLQVEEVHQLSR	11	0	K7(TMT6plex)	2399.38	1	Yes	Yes	1.482	6.542
<b>P32119</b>	<b>Peroxioredoxin -2</b>	<b>4</b>	KAETKLAFAQIEELR	12	0	K1(TMT6plex); K5(TMT6plex)	2187.28	2	Yes	Yes	42.735	
			QKTQEEGER	17	0	K2(TMT6plex)	1462.73	1	Yes	Yes	58.690	
			QYTSLLGKMNSEEEDEVWQVIGAR	1	0	K8(TMT6plex)	3124.59	1	Yes	Yes	0.000	
			AESEQEAFLR	7	0		1195.56	0	Yes	No	0.000	
			AESEQEAFLRED	4	0		1439.63	1	Yes	No	0.000	
			KEGGLPLNIPLLADVTR	3	0	K1(TMT6plex)	2092.24	1	Yes	Yes	4.307	
			LSEDYGVLTDEGIAYR	3	0	K9(TMT6plex)	2158.13	1	Yes	Yes	11.724	
			QITVNDLPVGR	2	0		1211.68	0	No	No	0.000	
			GLFIDGKGVLR	8	0	K8(TMT6plex)	1516.94	1	Yes	Yes	29.106	
			SVDEALR	3	0.003		789.41	0	Yes	No	0.000	
<b>P06576</b>	<b>ATP synthase subunit beta, mitochondrial</b>	<b>10</b>	GQKLDGSAPIKIPVGPETLGR	27	0	K3(TMT6plex); K12(TMT6plex)	2690.60	2	Yes	Yes	9.848	
			IPSAVGYQPTLATDMGTMQER	6	0	M15(Oxidation); M18(Oxidation)	2298.08	0	Yes	No	0.000	

DOEQDVLFLIDNIFR	39	0		1921.97	0	Yes	No	0.000	0.000
IMDPNIVGSEHYDVAR	6	0	M2(Oxidation)	1831.87	0	Yes	No	0.000	0.000
VALTGLTVAEYFR	11	0		1439.79	0	Yes	No	0.000	0.000
AIAELGIYPAVDPLDSTSR	7	0		1988.04	0	Yes	No	0.000	0.000
LVLEVAQHLGESTVR	18	0		1650.92	0	Yes	No	0.000	0.000
IMDPNIVGSEHYDVAR	3	0		1815.88	0	Yes	No	0.000	0.000
IPSAVGYQPTLATDMGTM QER	1	0		2266.09	0	Yes	No	0.000	0.000
FTQAGSEVSALLGR	4	0		1435.75	0	Yes	No	0.000	0.000
IMNVIGEPIDER	7	0	M2(Oxidation)	1401.71	0	Yes	Yes	0.000	0.000
TIAMDGTEGLVR	10	0	M4(Oxidation)	1278.64	0	Yes	Yes	0.000	0.000
TIAMDGTEGLVR	2	0		1262.64	0	Yes	No	0.000	0.000
KPGINVASDWSIHRLR	4	0	K1(TMT6plex)	1922.08	0	Yes	Yes	0.000	0.000
FFSGNTLVSSADPEGHF ETPIWIER	2	0		3010.43	0	Yes	No	0.000	0.000
YSLLPFWYTLLYQAHR	2	0		2071.08	0	Yes	No	0.000	0.000
KLVAINDPHIKVDGYSYR	7	0	K1(TMT6plex); K11(TMT6plex)	2368.41	2	Yes	Yes	0.000	0.000
REPWLLPSQHNDIIR	3	0		1874.01	1	Yes	No	0.000	0.000
QYASLTGTQALPPLFSLGY HQSR	2	0		2535.30	0	Yes	No	0.000	0.000
LSFQHPETSIVLVR	3	0		1740.93	0	Yes	No	0.000	0.000
LKVTEGGEYSYR	8	0	K2(TMT6plex)	1477.82	1	Yes	Yes	13.192	10.783
VVIIGAGKPAAVVLQTKGS PESR	8	0	K8(TMT6plex); K17(TMT6plex)	2735.67	1	Yes	Yes	3.562	9.309
FRIDELEPR	2	0		1174.62	1	Yes	No	0.000	0.000
YRVPDVLVADPPIAR	1	0		1680.94	1	Yes	No	0.000	0.000
NLGLYVKTR	8	0	K7(TMT6plex)	1292.79	1	Yes	Yes	4.684	5.150
YFTWDPSR	2	0		1071.49	0	Yes	No	0.000	0.000
VSQSKDPAEGDGAQPEE TPR	1	0	K6(TMT6plex)	2384.15	1	Yes	No	0.000	0.000
SIRPGLSPYR	2	0.001		1145.64	0	Yes	No	0.000	0.000
AFFAGSQR	3	0.001		883.44	0	Yes	No	0.000	0.000
SLLSVNAR	2	0.001		972.58	0	Yes	No	0.000	0.000
QEFLLR	4	0.001		805.46	0	Yes	No	0.000	0.000

Neutral  
alpha-  
glucosidase  
AB

Q14697

18

<b>Q6BCY4</b>	<b>NADH-cytochrome b5 reductase 2</b>	<b>5</b>	VPDVLVADPPIAR	1	0.005	1361.78	0	Yes	No	0.000	0.000
			FGLPSPDHVGLGVPVGNVV QLLAKIDNELVVR	20	0	K23(TMT6plex)	1	Yes	Yes	10.662	13.336
<b>Q96KX0</b>	<b>Lysozyme-like protein 4</b>	<b>4</b>	MSLIFANQTEEDILVR	1	0	1878.97	0	Yes	No	0.000	0.000
			AYTPVSSDDDR	5	0	1225.53	0	Yes	No	0.000	0.000
			HITKDPDR	23	0	1297.71	1	Yes	Yes	21.050	11.937
			KELEEIAR	15	0	1216.71	1	Yes	Yes	11.202	16.702
			MSLIFANQTEEDILVR	2	0	1894.96	0	Yes	No	0.000	0.000
			YCOYSDTLAR	24	0	1276.56	0	Yes	No	0.000	0.000
			GSDWCGDHGR	9	0	1146.44	0	Yes	No	0.000	0.000
			WLDGCKL	12	0	1120.60	1	Yes	Yes	12.035	21.601
			EGYTGFLQMR	8	0	1421.65	0	Yes	No	0.000	0.000
			FNHFSLTINTNHGHILVDY SKNLVTEDEVMR	1	0	3743.92	1	Yes	Yes	0.000	0.000
<b>P06744</b>	<b>Glucose-6-phosphate isomerase</b>	<b>11</b>	KGLHHKILLANFLAQTEAL MR	2	0	2878.70	2	Yes	Yes	0.000	0.000
			KGLHHKILLANFLAQTEAL MR	3	0	2862.70	2	Yes	Yes	0.000	0.000
			KELQAAGKSPEDLER	28	0	2129.20	2	Yes	Yes	37.896	31.350
			FAAYFQQGDMESNGKYIT KSGTR	1	0	3057.55	2	Yes	No	0.000	0.000
			MFNGEKINYTEGR	2	0	1787.90	1	Yes	Yes	7.295	5.003
			MFNGEKINYTEGR	4	0	1803.89	1	Yes	Yes	0.000	0.000
			DPQFQKLQQWYR	14	0	1865.99	1	Yes	Yes	7.963	9.195
			AVLHVALR	2	0	878.56	0	Yes	No	0.000	0.000
			MLVDLAKSR	1	0	1261.76	1	Yes	Yes	0.000	0.000
			GKSTEEAR	20	0	1106.60	1	Yes	Yes	16.076	9.801
			MLVDLAKSR	8	0	1277.75	1	Yes	Yes	11.296	3.994
LFDANKDR	5	0	1207.67	1	Yes	Yes	9.488	5.753			

<b>P60174</b>	<b>Triosephosphate isomerase</b>	<b>6</b>	RLFDANKDR	1	0	0	K7(TMT6plex)	1363.76	2	Yes	No	0.000	0.000	
			GWLKSNVSDAVAQSTR	71	0	0	K4(TMT6plex)	1948.05	1	Yes	Yes	Yes	22.423	13.520
			LRADTDLQR	8	0	0		1087.59	1	Yes	Yes	No	0.000	0.000
			KFFVGGNWKMNGR	5	0	0	K1(TMT6plex); K9(TMT6plex); M10(Oxidation)	2015.11	2	Yes	Yes	Yes	5.223	7.026
			KFFVGGNWKMNGR	2	0	0	K1(TMT6plex); K9(TMT6plex)	1999.11	2	Yes	Yes	Yes	0.000	0.000
			LGSSAMAPSR	8	0	0	M6(Oxidation)	992.48	0	Yes	Yes	No	0.000	0.000
<b>P48047</b>	<b>ATP synthase subunit O, mitochondrial</b>	<b>3</b>	IIYGGSVTGATCK	3	0	0	C12(Carbamidomethyl); K13(TMT6plex)	1555.83	0	Yes	Yes	Yes	4.313	5.174
			EAGITEKVVFEQTK	1	0	0	K7(TMT6plex)	1808.00	1	Yes	Yes	No	0.000	0.000
			VAQILKEPKVAASVLPVW KR	4	0	0	K6(TMT6plex); K9(TMT6plex); K20(TMT6plex)	3010.88	3	Yes	Yes	Yes	0.000	0.000
			SIKVKSLNDITAKER	10	0	0	K3(TMT6plex); K5(TMT6plex); K13(TMT6plex)	2389.48	3	Yes	Yes	Yes	0.000	0.000
			LSNTQGVSAFSTMMSVH R	1	0	0	M14(Oxidation); M15(Oxidation)	2083.99	0	Yes	Yes	No	0.000	0.000
			GNEFFCEVDDEYIQDKFNL TGLNEQVPHYR	9	0	0	C6(Carbamidomethyl); K16(TMT6plex)	3905.85	1	Yes	Yes	No	0.000	0.000
<b>P67870</b>	<b>Casein kinase II subunit beta</b>	<b>3</b>	GIAQMLEKYQQGDFGYCP R	5	0	0	M5(Oxidation); K8(TMT6plex); C17(Carbamidomethyl)	2506.19	1	Yes	Yes	Yes	21.669	24.810
			GIAQMLEKYQQGDFGYCP R	4	0	0	K8(TMT6plex); C17(Carbamidomethyl)	2490.21	1	Yes	Yes	Yes	9.388	3.079
			YILTNR	3	0.008	0		779.44	0	Yes	Yes	No	0.000	0.000
			IKENGAAALDGR	19	0	0	K2(TMT6plex)	1443.81	1	Yes	Yes	Yes	23.600	15.767
<b>P57105</b>	<b>Synaptojanin-2-binding protein</b>	<b>3</b>	VDYLVTEEEINLTR NAGYAVSLR	5	0	0		1693.87	0	Yes	No	0.000	0.000	
				9	0	0		950.50	0	Yes	Yes	No	0.000	0.000
<b>Q9P010</b>	<b>Vesicle-associated membrane protein-</b>	<b>5</b>	KVAHSDKPGSTSTASFR	31	0	0	K1(TMT6plex); K7(TMT6plex)	2234.23	1	Yes	Yes	29.397	27.969	

	associated protein A											
		KVCFKVTAPR	20	0	C3(Carbamidomethyl); K1(TMT6plex); K5(TMT6plex); K7(TMT6plex)	2122.32	3	Yes	Yes	Yes	45.574	22.255
		LQGEMMKLSEENR	2	0	K7(TMT6plex)	1793.91	1	Yes	Yes	Yes	6.973	4.856
		HLRDEGLR	5	0		995.54	1	Yes	No	No	0.000	0.000
		KLMECKR	6	0	K1(TMT6plex); M3(Oxidation); C6(Carbamidomethyl); K7(TMT6plex)	1567.87	2	Yes	Yes	Yes	0.000	0.000
		LQGEMMKLSEENR	3	0	M5(Oxidation); M6(Oxidation); K7(TMT6plex)	1825.90	1	Yes	Yes	Yes	0.000	0.000
		EVKGPVIVR	1	0	K3(TMT6plex); K8(TMT6plex)	1880.21	2	Yes	No	No	0.000	0.000
		LGLNAQTSIKAQR	3	0	K11(TMT6plex)	1742.05	1	Yes	Yes	Yes	0.000	0.000
		EAKEQER	9	0	K3(TMT6plex)	1247.64	1	Yes	Yes	Yes	3.534	6.664
		VELLSHQKVCER	1	0	K9(TMT6plex); K10(TMT6plex); C12(Carbamidomethyl)	2326.33	2	Yes	No	No	0.000	0.000
		QATQLKEEAR	1	0	K7(TMT6plex)	1644.91	1	Yes	No	No	0.000	0.000
		KAQAFNEELSR	1	0	K1(TMT6plex)	1634.90	1	Yes	Yes	Yes	0.000	0.000
		KLVQEKLQR	1	0.001	K1(TMT6plex); K7(TMT6plex)	1728.09	2	Yes	No	No	0.000	0.000
		ALQDLQEEADKKQKR	1	0.002	K11(TMT6plex); K12(TMT6plex); K13(TMT6plex); K15(TMT6plex)	2844.71	4	Yes	No	No	0.000	0.000
		QDFVAEKLDQQFR	1	0.007	K7(TMT6plex)	1852.99	1	Yes	No	No	0.000	0.000
		LEKEAR	1	0.009	K3(TMT6plex)	974.58	1	Yes	Yes	Yes	0.000	0.000
		NELGGDGNSENQR	2	0		1647.72	0	Yes	No	No	0.000	0.000
<b>Q96M91</b>	<b>Coiled-coil domain-containing protein 11</b>			<b>10</b>								
<b>Q96A19</b>	<b>Vesicle transport through interaction with t-</b>			<b>4</b>								



P40939	Trifunctional enzyme subunit alpha, mitochondrial	10	SNAREs homolog 1A									
			ETDANLGKSSR	10	0	K8(TMT6plex)	1406.74	1	Yes	Yes	28.300	22.135
			SYQEMGKLETFKR	1	0	M6(Oxidation); K8(TMT6plex); K14(TMT6plex)	2563.42	3	Yes	No	0.000	0.000
			IAYSDEVK	2	0.001		952.48	0	Yes	No	0.000	0.000
			AKKMGVDQLVEPLGPKPEER	2	0	K2(TMT6plex); K3(TMT6plex); M4(Oxidation); K19(TMT6plex)	3304.94	2	Yes	No	0.000	0.000
			KTVLGTPEVLLGALPGAGG TQR	3	0	K1(TMT6plex)	2364.39	1	Yes	Yes	0.000	0.000
			THINYGKGDVAVVR	5	0	K8(TMT6plex)	1857.05	1	Yes	Yes	18.778	13.053
			FGGNPELLTQMVSQGLGR	2	0	K15(TMT6plex)	2337.26	1	Yes	No	0.000	0.000
			KSGKGFYQEGVQR	11	0	K1(TMT6plex); K4(TMT6plex); K14(TMT6plex)	2447.44	3	Yes	Yes	29.790	33.906
			FVDLYGAQKIVDR	15	0	K9(TMT6plex)	1752.98	1	Yes	Yes	24.314	17.435
			LPKMVGVPAALDMMLTGR	1	0	K3(TMT6plex); M4(Oxidation); M13(Oxidation); M14(Oxidation)	2177.18	1	Yes	Yes	0.000	0.000
			FGGNPELLTQMVSQGLGR	2	0	M12(Oxidation); K15(TMT6plex)	2353.25	1	Yes	No	0.000	0.000
			QQVYKKEEKVR	7	0	K5(TMT6plex); K6(TMT6plex); K10(TMT6plex)	2221.37	3	Yes	Yes	0.000	0.000
			TIEYLEEVAITFAKGLADKKI SPKR	1	0	K14(TMT6plex); K19(TMT6plex); K20(TMT6plex); K24(TMT6plex)	3737.25	4	Yes	No	0.000	0.000
			IATKDR	5	0.003	K4(TMT6plex)	932.57	1	Yes	Yes	2.582	3.717
			LDEVKEQVAEVR	7	0	K5(TMT6plex)	1643.92	1	Yes	Yes	4.924	9.836
P02649	Apolipoprotein E	6	LSKELQAAQAR	11	0	K3(TMT6plex)	1443.85	1	Yes	Yes	3.368	6.865

P55786	Puromycin-sensitive aminopeptidase	14	QQTEWQSGQR	3	0	1247.58	0	Yes	No	0.000	0.000
			AATVGSLAGPQER	2	0	1497.80	0	Yes	No	0.000	0.000
			AKLEEQAAQQR	1	0	1542.88	1	Yes	No	0.000	0.000
			LGPLVEQGR	1	0	968.55	0	Yes	No	0.000	0.000
			KAAWFKIKDNWEELYNR	2	0	2898.63	3	Yes	No	0.000	0.000
			LGWDPKPGEGHLDALLR	3	0	2103.16	0	Yes	Yes	8.688	13.368
			TIQQCCENILLNAAWLKR	4	0	2460.31	1	Yes	Yes	14.300	27.122
			LGLQNDLFLSLAR	3	0	1346.75	0	Yes	No	0.000	0.000
			ETALLIDPKNCSRSSR	3	0	2007.04	1	Yes	Yes	0.000	0.000
			YAAVTQFEATDAR	2	0	1442.69	0	Yes	No	0.000	0.000
			KPYPDENLVEVKFAR	7	0	2378.31	1	Yes	Yes	16.568	12.791
			SKDGVQVCR	6	0	1149.63	1	Yes	Yes	10.673	4.675
			FKDHVEGKQILSADLR	5	0	2314.33	2	Yes	Yes	16.539	6.795
			GLVLGKLGKAGHKATLEEAR	3	0	2735.69	3	Yes	Yes	0.000	0.000
DAESIHQYLLQR	3	0	1472.75	0	Yes	No	0.000	0.000			
SKYTTPSGEVR	1	0.001	1453.79	1	Yes	Yes	0.000	0.000			
DLSLPPVDR	2	0.001	1011.55	0	Yes	No	0.000	0.000			
YQGGFLISR	1	0.002	1040.55	0	Yes	No	0.000	0.000			
AEQKCAEALYTETR	4	0	1898.95	1	Yes	Yes	5.315	6.646			
LVQKQIQIEKLR	4	0	1969.23	2	Yes	Yes	0.000	0.000			
KKFQEEQNR	2	0	1664.95	2	Yes	Yes	0.000	0.000			
AINDFQSFQKPETR	2	0	2038.05	0	Yes	Yes	0.000	0.000			
ATLLFER	2	0.002	849.48	0	Yes	No	0.000	0.000			
Q9H4K1	RIB43A-like with coiled-coils protein 2	5									

<b>Q8N1VZ</b>	<b>WD repeat-containing protein 16</b>	<b>8</b>	LQEEKR	3	0.003	K5(TMT6plex)	1031.60	1	No	No	0.000	0.000
			IGVTAIATSDCKR	13	0	C12(Carbamidomethyl); K13(TMT6plex)	1721.94	1	Yes	Yes	11.544	16.737
			GEHQFLVGTTESHYR	5	0		1958.93	0	Yes	No	0.000	0.000
			TKLLTDVGPADKDFSLGVS AIR	3	0	K2(TMT6plex); K11(TMT6plex); K13(TMT6plex)	3003.83	3	Yes	No	0.000	0.000
			DGKSIISAWNDGKIR	10	0	K3(TMT6plex); K13(TMT6plex)	2118.21	2	Yes	Yes	4.758	12.726
			KIAYWEVFDGTVIR	3	0	K1(TMT6plex)	1926.07	1	Yes	Yes	8.534	17.476
			VISGGEGEVR	3	0		1059.54	0	Yes	No	0.000	0.000
			KIWPTECQTGQLKR	1	0	K1(TMT6plex); C7(Carbamidomethyl); K13(TMT6plex)	2203.24	2	Yes	Yes	0.000	0.000
			ISPGNQIVSVSADGAILR	1	0		1960.05	0	Yes	No	0.000	0.000
			YALYDASFETKESR	4	0	K11(TMT6plex)	1908.96	1	Yes	Yes	1.515	3.569
<b>P60981</b>	<b>Destrin</b>	<b>3</b>	KCSTPEEIKKR	4	0	C2(Carbamidomethyl); K9(TMT6plex); K10(TMT6plex)	2063.23	3	Yes	Yes	0.000	0.000
			IFYDMKVR	1	0.005	M5(Oxidation); K6(TMT6plex)	1316.73	1	Yes	Yes	0.000	0.000
			KFKQVAEAYEVLSDAKKR	13	0	K1(TMT6plex); K3(TMT6plex); K16(TMT6plex); K17(TMT6plex)	3026.82	4	Yes	Yes	17.114	17.778
			DPFSDFEFDFEFDFGNR	3	0		2375.00	0	Yes	No	0.000	0.000
			DPFSDFEFDFEFDFGNR R	1	0		2531.08	1	Yes	No	0.000	0.000
			HASPEDIKKAYR	12	0	K8(TMT6plex); K9(TMT6plex)	1873.07	2	Yes	Yes	16.012	25.111
			NPDDVFR	5	0.002		862.41	0	Yes	No	0.000	0.000
			IVENGQER	2	0.003		944.48	0	No	No	0.000	0.000
			LVLNLEAWKR	4	0	K9(TMT6plex)	1520.88	1	Yes	Yes	4.242	2.511
			<b>Q8N0U8</b>	<b>Vitamin K epoxide reductase complex subunit 1-like</b>	<b>3</b>							

protein 1	protein 1										
	QLQPKQD	6	0	0	K5(TMT6plex)	1085.62	1	Yes	Yes	5.188	9.782
Q5T655	ALCDLGPWVKCSAALASR	1	0	0	C3(Carbamidomethyl); K10(TMT6plex); C11(Carbamidomethyl)	2204.16	1	Yes	No	0.000	0.000
	QKKELDQVISED	5	0	0	K2(TMT6plex); K3(TMT6plex)	1931.14	2	Yes	Yes	0.000	0.000
	ESLAQTTEQQQETER	3	0	0		1777.82	0	Yes	No	0.000	0.000
	AAKELEQFQMR	1	0	0	K3(TMT6plex)	1579.85	1	Yes	No	0.000	0.000
	EVEASKKQAEIDR	5	0	0	K6(TMT6plex); K7(TMT6plex)	1961.11	2	Yes	Yes	2.325	5.588
	DQLLSEVVKLR	6	0	0	K9(TMT6plex)	1528.93	1	Yes	Yes	8.984	11.454
	DFQGVLEHLSGDKSLEKFR	2	0	0	K13(TMT6plex); K17(TMT6plex)	2663.46	2	Yes	Yes	0.000	0.000
	NLEGEIQNYKDEAQKQR	2	0	0	K10(TMT6plex); K15(TMT6plex)	2521.34	2	Yes	Yes	0.000	0.000
	LDIGKLNKIR	6	0	0	K5(TMT6plex); K8(TMT6plex)	1628.06	2	Yes	Yes	4.969	3.524
	FKEEVTKER	4	0	0	K2(TMT6plex); K7(TMT6plex)	1623.95	2	Yes	Yes	0.000	0.000
	KLEASDPNAVYELIQIHTLQ KR	1	0	0	K1(TMT6plex); K15(TMT6plex); K21(TMT6plex)	3282.92	3	Yes	No	0.000	0.000
	IEKEKETLKAELQKLR	1	0	0	K3(TMT6plex); K5(TMT6plex); K9(TMT6plex); K14(TMT6plex)	2872.80	4	Yes	No	0.000	0.000
QQALETKHFIKQEAEEER	1	0.001	0	K7(TMT6plex); K12(TMT6plex)	2672.45	2	Yes	No	0.000	0.000	
Q99798	GHLDNISNLLIGAINIENG KANSVR	3	0	0	K21(TMT6plex)	2975.64	1	Yes	Yes	0.000	0.000
	NAVTFQFGVPDPTAR	8	0	0		1601.79	0	Yes	No	0.000	0.000
	WVVIGDENYGEGR	2	0	0		1667.77	0	Yes	No	0.000	0.000
	VGLIGSCTNSSYEDMGR	2	0	0	C7(Carbamidomethyl); M15(Oxidation)	1861.81	0	Yes	No	0.000	0.000
LNRPLTSLSEKIVYGHLDPPA	3	0	0	K10(TMT6plex)	3222.73	1	Yes	Yes	0.000	0.000	



O00330	Pyruvate dehydrogenase protein X component, mitochondrial	6	VVAHFYAKR	2	0	0	K8(TMT6plex)	1319.78	1	Yes	Yes	0.000	0.000
			NILEKHSLDASQGTATGPR	1	0	0	K5(TMT6plex)	2224.19	1	Yes	Yes	0.000	0.000
			FLKSFKANLENPIR	7	0	0	K3(TMT6plex); K6(TMT6plex)	2135.28	2	Yes	Yes	3.360	6.303
			FRPVLKLTDEEGNAKLQQ R	1	0	0	K6(TMT6plex); K16(TMT6plex)	2829.60	2	Yes	No	0.000	0.000
			VDDDELATR	3	0	0		1017.52	0	Yes	No	0.000	0.000
			LTESKSTVPHAYATADCDL GAVLKVR	1	0	0	C17(Carbamidomethyl); K24(TMT6plex)	3260.77	2	Yes	No	0.000	0.000
			RVIAKR	2	0.002	0	K5(TMT6plex)	971.67	2	Yes	Yes	0.000	0.000
			GVKSSPIQTPNQTPQQAP VTPR	5	0	0	K3(TMT6plex)	2560.41	1	Yes	Yes	0.000	0.000
			RPSMFEKEAYTQILR	1	0	0	K7(TMT6plex)	2098.15	1	Yes	No	0.000	0.000
			YYKEKFGITDLP	10	0	0	K3(TMT6plex); K5(TMT6plex)	2088.19	2	Yes	No	0.000	0.000
Q8IZS6	Tctex1 domain-containing protein 3	2	YLAVLESPIPEDKDRR	8	0	0	K13(TMT6plex)	2130.18	2	Yes	No	0.000	0.000
			RPTVGIGGDR	2	0	0		1027.57	0	Yes	No	0.000	0.000
			YLAVLESPIPEDKDR	2	0	0	K13(TMT6plex)	1974.08	1	Yes	Yes	0.000	0.000
			EAFQYDKEASGYVDR	5	0	0	K8(TMT6plex)	2120.05	1	Yes	Yes	19.397	8.565
			GINITYGKTFR	6	0	0	K9(TMT6plex)	1611.94	1	Yes	Yes	25.437	11.965
			GDHYHWKDLNR	6	0	0	K7(TMT6plex)	1669.84	1	Yes	Yes	22.615	16.918
			MCSHGEGKINYYNFVR	1	0	0	C2(Carbamidomethyl); K8(TMT6plex)	2204.05	1	Yes	No	0.000	0.000
			NSGIIGGKYLGR	2	0	0	K8(TMT6plex)	1463.85	1	Yes	No	0.000	0.000
			RYYKEKFGITDLP	1	0	0	K4(TMT6plex); K6(TMT6plex)	2244.29	3	Yes	No	0.000	0.000
			TFFIYDCDPFTR	1	0	0	C7(Carbamidomethyl)	1581.71	0	Yes	No	0.000	0.000
P11177	Pyruvate dehydrogenase E1	4	DEKVFLLGEEVAQYDGYK VSR	6	0	0	K3(TMT6plex); K19(TMT6plex)	2974.60	2	Yes	Yes	18.320	5.821



ADDFRKEFQHKLGR	4	0	0	2406.39	3	Yes	No	0.000	0.000
IRPIYSGKFFDR	6	0	0	1727.98	1	Yes	Yes	0.000	0.000
AMAKSLYWLHELQMKR	1	0	0	2463.38	2	Yes	No	0.000	0.000
TPCWPSAGKVIPVGYR	1	0	0	2017.09	1	Yes	Yes	0.000	0.000
CGESPVVSNIKCEGR	1	0	0	1807.86	1	Yes	Yes	0.000	0.000
KYNPSSFHR	5	0	0	1364.73	1	Yes	Yes	11.798	7.241
IKCKTLM	2	0	0	1367.82	2	Yes	Yes	0.000	0.000
VATCLTEKLPR	2	0	0	1516.87	1	Yes	No	0.000	0.000
LPDEYLR	1	0.002	0	905.47	0	Yes	No	0.000	0.000
KGVFER	2	0.003	0	964.58	1	Yes	Yes	0.000	0.000
VGLGKEDSR	3	0.004	0	1189.67	1	Yes	Yes	1.911	11.203
SYKPVFWSPSSR	2	0	0	1669.90	0	Yes	No	0.000	0.000
RPYWCISR	2	0	0	1137.56	0	Yes	No	0.000	0.000
ELSNFYFSIIKDR	4	0	0	1861.01	1	Yes	No	0.000	0.000
CAEVVSGK	2	0	0	1078.58	0	Yes	Yes	0.000	0.000
LYCEKENDPKR	4	0	0	1910.02	2	Yes	Yes	10.530	1.892
SCQTALVEILDVIVR	3	0	0	1715.94	0	Yes	No	0.000	0.000
ADLYLEGKDLGGWFQSS LLTVAAR	1	0	0	3054.62	1	Yes	No	0.000	0.000
QQPDTELEIQKCGFSELY SWQR	1	0	0	3099.52	1	Yes	Yes	0.000	0.000
SFAKAAIEKQSAFIR	1	0	0	2482.51	3	Yes	No	0.000	0.000

**Q9NSE4**  
Isoleucine--  
tRNA ligase,  
mitochondrial



<b>P26885</b>	Peptidyl-prolyl cis-trans isomerase FKBP2	2	YRDTVLLPQTSFPMKLLGR	1	0.001	M14(Oxidation); K15(TMT6plex)	2480.40	2	Yes	No	0.000	0.000
			DDISKLR	1	0.008	K5(TMT6plex)	1075.63	1	Yes	Yes	0.000	0.000
<b>P46459</b>	Vesicle-fusing ATPase	9	KLVIPSELGYGER	4	0	K1(TMT6plex)	1689.98	1	Yes	Yes	4.171	2.005
			VDHCPKISR	7	0	C4(Carbamidomethyl); K7(TMT6plex)	1340.73	1	Yes	Yes	18.124	9.560
			FSNLVQLALLVLLKKAPPQGR	10	0	K14(TMT6plex); K15(TMT6plex)	2763.74	2	Yes	No	0.000	0.000
			KLLIIGTTSR	5	0	K1(TMT6plex)	1330.86	1	Yes	Yes	2.288	4.165
			LQLHIHTAR	11	0		1201.72	0	Yes	No	0.000	0.000
			KFLALLR	10	0	K1(TMT6plex)	1089.74	1	Yes	Yes	8.035	6.522
			KLFADAEEQR	3	0	K1(TMT6plex)	1564.82	1	Yes	Yes	6.163	3.497
			EPKVVNGPEILNKYVGESEANIR	1	0	K3(TMT6plex); K13(TMT6plex)	3013.68	2	Yes	No	0.000	0.000
			VLDDGELLVQQTKNSDR	1	0	K13(TMT6plex)	2159.15	1	Yes	No	0.000	0.000
			LEVKMEIGLPDEKGR	1	0	K4(TMT6plex); K13(TMT6plex)	2172.25	2	Yes	No	0.000	0.000
<b>O43674</b>	NADH dehydrogenase [ubiquinone] 1 beta subcomplex subunit 5, mitochondrial	2	NFYDSPEKIYER	3	0	K8(TMT6plex)	1789.90	1	Yes	Yes	0.000	0.000
			TMAVLQIEAEKAELR	1	0	M2(Oxidation); K11(TMT6plex)	1947.08	1	Yes	No	0.000	0.000
<b>Q93009</b>	Ubiquitin carboxyl-terminal hydrolase 7	11	YTYLEKAIKIHN	2	0	K6(TMT6plex); K9(TMT6plex)	1951.15	2	Yes	Yes	0.000	0.000
			VDFVFCDKTIPNDPGFVVTL SNR	2	0	C6(Carbamidomethyl); K8(TMT6plex)	2835.49	1	Yes	No	0.000	0.000
			DLIQFFKPR	9	0	K7(TMT6plex)	1392.82	0	Yes	Yes	12.291	11.848

Q96MR6	WD repeat-containing protein 65	14	CTKEEAIEHNYGGHDDLLS VR	1	0	C1(Carbamidomethyl); K3(TMT6plex)	2674.24	1	Yes	Yes	0.000	0.000
			SFKIWLNSQFR	1	0	K3(TMT6plex); C4(Carbamidomethyl)	1814.96	1	Yes	Yes	0.000	0.000
			SLNYGHIYTPISCKIR	1	0	C5(Carbamidomethyl); C14(Carbamidomethyl); K15(TMT6plex)	2311.19	1	Yes	No	0.000	0.000
			EEEEITLYPDKHGCVR	1	0	K10(TMT6plex); C13(Carbamidomethyl)	2075.04	1	Yes	Yes	0.000	0.000
			HNVEGTLR	1	0		989.48	0	Yes	No	0.000	0.000
			MNYFQVAKTVAQR	1	0.001	M1(Oxidation); K8(TMT6plex)	1800.96	1	Yes	No	0.000	0.000
			DDEKFSR	1	0.001	K4(TMT6plex)	1212.61	1	Yes	No	0.000	0.000
			IHQGEHFR	1	0.001		1023.51	0	Yes	No	0.000	0.000
			LQEEKR	3	0.003	K5(TMT6plex)	1031.60	1	No	No	0.000	0.000
			KPLIATCSLDR	6	0	K1(TMT6plex); C7(Carbamidomethyl)	1502.85	0	Yes	Yes	7.475	1.865
			VLLFEKMEKDFYR	2	0	K6(TMT6plex); M7(Oxidation); K10(TMT6plex)	2321.26	2	Yes	No	0.000	0.000
			DLEALVKR	5	0	K7(TMT6plex)	1172.72	1	Yes	Yes	5.015	5.562
			MQEYEQQLR	2	0	M1(Oxidation); K7(TMT6plex)	1598.81	1	Yes	Yes	0.000	0.000
			EFEETKKQIEEDDR	3	0	K6(TMT6plex); K7(TMT6plex)	2383.21	2	Yes	Yes	11.128	5.046
LRDQIQEQEQVTGFHTLA GVR	2	0		2425.25	1	Yes	No	0.000	0.000			
FKTDLHNCVAYIQEPR	3	0	K2(TMT6plex); C8(Carbamidomethyl)	2220.15	1	Yes	Yes	13.061	7.531			
FAEGLTKQTSFOR	5	0	K7(TMT6plex)	1741.94	1	Yes	Yes	8.049	5.900			
VEELKMENEYQLR	1	0	K5(TMT6plex); M6(Oxidation)	1925.99	1	Yes	Yes	0.000	0.000			
SFKEYSVR	1	0.001	K3(TMT6plex)	1244.69	1	Yes	No	0.000	0.000			
DEKESNLR	3	0.001	K3(TMT6plex)	1219.65	1	Yes	No	0.000	0.000			
GLFEKYVQR	3	0.001	K5(TMT6plex)	1368.78	1	Yes	Yes	2.421	3.998			
DETIQDKEKR	2	0.001	K7(TMT6plex); K9(TMT6plex)	1719.97	2	Yes	Yes	11.775	5.972			

<b>P13667</b>	<b>Protein disulfide-isomerase A4</b>	<b>7</b>	KKFSSLQKEIEER	2	0.002	K1(TMT6plex); K2(TMT6plex); K8(TMT6plex)	2309.38	3	Yes	Yes	5.233	10.389
			TQEEIVAKVR	10	0	K8(TMT6plex)	1401.83	1	Yes	Yes	7.849	9.072
<b>P14314</b>	<b>Glucosidase 2 subunit beta</b>	<b>6</b>	DLEHLSKFIEEHATKLSR	5	0	K7(TMT6plex); K15(TMT6plex)	2611.47	2	Yes	No	0.000	0.000
			FDVSGYPTLKIFR	7	0	K10(TMT6plex)	1772.00	1	Yes	Yes	9.861	1.908
			KGRPYDYNGPR	3	0	K1(TMT6plex)	1551.82	1	Yes	No	0.000	0.000
			SPPIPLAKVDATAETDLAKR	5	0	K8(TMT6plex); K19(TMT6plex)	2551.49	2	Yes	Yes	0.000	0.000
			KVSNDAKR	7	0	K1(TMT6plex); K7(TMT6plex)	1375.84	2	Yes	Yes	2.299	3.199
			AATQFWR	3	0.002		879.45	0	Yes	No	0.000	0.000
			LLCGKETMVTSTTEPSR	3	0	C3(Carbamidomethyl); K5(TMT6plex)	2139.10	1	Yes	Yes	12.629	16.030
			LLCGKETMVTSTTEPSR	7	0	C3(Carbamidomethyl); K5(TMT6plex); M8(Oxidation)	2155.09	1	Yes	Yes	28.128	21.187
			LKKILIEDWKKAR	6	0	K2(TMT6plex); K3(TMT6plex); K10(TMT6plex); K11(TMT6plex)	2557.68	4	Yes	Yes	11.821	14.199
			SLKDMEEISR	4	0	K3(TMT6plex); M5(Oxidation)	1452.76	1	Yes	Yes	0.000	0.000
			TVKEEAKEKPER	22	0	K3(TMT6plex); K8(TMT6plex)	1774.01	1	Yes	Yes	23.099	16.530
			NKFEAEAR	10	0	K2(TMT6plex)	1251.65	1	Yes	Yes	14.023	10.695
ESLQMAEVTR	1	0	M6(Oxidation)	1307.63	0	Yes	No	0.000	0.000			
ESLQMAEVTR	1	0		1291.63	0	Yes	No	0.000	0.000			
<b>Q86VP6</b>	<b>Cullin-associated NEDD8-dissociated protein 1</b>	<b>10</b>	ACPKEGPAVVGGFIQDVK NSR	8	0	C2(Carbamidomethyl); K4(TMT6plex); K18(TMT6plex)	2758.51	2	Yes	No	0.000	0.000
			AAAKCLDAVVSTR	14	0	K4(TMT6plex); C5(Carbamidomethyl)	1590.88	1	Yes	Yes	12.137	3.990
			VALVTFNSAAHNKPSLIR	12	0	K13(TMT6plex)	2167.26	0	Yes	Yes	19.535	40.640

<b>Q92526</b>	<b>T-complex protein 1 subunit zeta-2</b>	<b>3</b>	LKAADIDQEVKER	16	0	K2(TMT6plex); K11(TMT6plex)	1973.14	2	Yes	Yes	10.982	12.634
			LKGYLISGSSYAR	9	0	K2(TMT6plex)	1643.93	1	Yes	Yes	19.609	15.031
			DLLDVLPHLYNETKVR	6	0	K15(TMT6plex)	2255.26	1	Yes	Yes	0.000	0.000
			TYIQCIAISR	3	0	C5(Carbamidomethyl)	1295.68	0	Yes	No	0.000	0.000
			NVVAECLGKLTLDPEITLLP R	2	0	C6(Carbamidomethyl); K9(TMT6plex)	2580.47	1	Yes	No	0.000	0.000
			IGEYLEKIPLVVKFCNVDD DELK	1	0	K7(TMT6plex); K14(TMT6plex); C16(Carbamidomethyl)	3335.84	2	Yes	No	0.000	0.000
			LSTLCPSAVLQR	1	0	C5(Carbamidomethyl)	1344.73	0	Yes	No	0.000	0.000
			AALAVNICAAR	1	0	C8(Carbamidomethyl)	1129.61	0	Yes	No	0.000	0.000
			TSLQTKVHAEADVLTEVV VDSVLAVR	1	0	K6(TMT6plex)	3121.79	1	Yes	No	0.000	0.000
			KILLDVAR	4	0	K1(TMT6plex)	1156.77	1	Yes	Yes	7.728	4.516
KFIEDR	4	0.001	K1(TMT6plex)	1036.60	1	No	No	0.000	0.000			
HPDMMKRR	1	0.005	K5(TMT6plex); K6(TMT6plex)	1369.82	2	No	No	0.000	0.000			
AGMSSLK	1	0.006	M3(Oxidation); K7(TMT6plex)	938.52	0	No	No	0.000	0.000			
<b>P29218</b>	<b>Inositol monophosphatase 1</b>	<b>3</b>	MVLSNMEKLFICIPVHGIR	1	0	K8(TMT6plex); C11(Carbamidomethyl)	2373.28	1	Yes	No	0.000	0.000
			IAKEIQVIPLQR	27	0	K3(TMT6plex)	1637.03	1	Yes	Yes	10.281	8.749
			MVLSNMEKLFICIPVHGIR	2	0	M1(Oxidation); K8(TMT6plex); C11(Carbamidomethyl)	2389.28	1	Yes	No	0.000	0.000
			MVLSNMEKLFICIPVHGIR	1	0	M1(Oxidation); M6(Oxidation); K8(TMT6plex); C11(Carbamidomethyl)	2405.27	1	Yes	No	0.000	0.000
			IAKEIQVIPLQRDDED	1	0	K3(TMT6plex)	2111.16	2	Yes	Yes	0.000	0.000
<b>Q9P210</b>	<b>Testicular haploid expressed gene protein</b>	<b>4</b>	IISLAKPKVR	4	0	K6(TMT6plex); K8(TMT6plex)	1583.08	1	Yes	Yes	14.261	12.488

<b>Q4G0X9</b>	<b>Coiled-coil domain-containing protein 40</b>	<b>11</b>	WEVLDTKVKVVASPR	1	0	K8(TMT6plex); K9(TMT6plex)	2185.31	2	Yes	No	0.000	0.000
			KGLNEGDR	1	0	K1(TMT6plex)	1280.68	1	Yes	Yes	0.000	0.000
			LKELAAPKIR	3	0	K2(TMT6plex); K8(TMT6plex)	1597.06	2	Yes	No	0.000	0.000
			ALYTKTCAANEER	6	0	K5(TMT6plex); C7(Carbamidomethyl)	1826.92	1	Yes	Yes	17.848	12.398
			LALIATILDR	4	0		1098.69	0	Yes	No	0.000	0.000
			AIEKKKQDLVWQLTTR	1	0	K5(TMT6plex); K6(TMT6plex); K7(TMT6plex)	2865.68	3	Yes	No	0.000	0.000
			VTNEFVR	2	0		993.50	0	Yes	No	0.000	0.000
			KQGLINFLNKQLER	6	0	K1(TMT6plex); K10(TMT6plex)	2159.31	2	Yes	Yes	29.455	15.754
			FQAALKNYLNR	3	0	K6(TMT6plex)	1566.90	1	Yes	Yes	28.604	8.828
			QIEKLDLQELVVKQSR	1	0	K4(TMT6plex); K6(TMT6plex); K17(TMT6plex)	3026.86	3	Yes	No	0.000	0.000
<b>P10253</b>	<b>Lysosomal alpha-glucosidase</b>	<b>10</b>	QAIQGELELR	1	0		1156.63	0	Yes	No	0.000	0.000
			LKHLQAVKEGR	1	0	K2(TMT6plex); K8(TMT6plex)	1737.09	2	Yes	Yes	0.000	0.000
			SLKASER	2	0.002	K3(TMT6plex)	1019.60	1	Yes	Yes	0.000	0.000
			RKTDAAIR	2	0.008	K2(TMT6plex)	1159.71	2	Yes	No	0.000	0.000
			AGYIPLQGGPGLTTESR	1	0		1874.01	0	Yes	No	0.000	0.000
			AVPTQCDVPPNSR	4	0	C6(Carbamidomethyl)	1440.69	0	Yes	No	0.000	0.000
			WGYSSAIR	1	0		1141.57	0	Yes	No	0.000	0.000
			FDCAPDKAITQEQEAR	3	0	C3(Carbamidomethyl); K7(TMT6plex); C14(Carbamidomethyl)	2268.06	1	Yes	Yes	0.000	0.000
			LHFTIKDPANR	3	0.001	K6(TMT6plex)	1540.88	1	Yes	Yes	13.869	8.229
			GTRPFVISR	1	0.001		1032.59	0	Yes	No	0.000	0.000
DFTFNKDGFR	3	0.001	K6(TMT6plex)	1475.74	1	Yes	Yes	0.000	0.000			
RDFTFNKDGFR	1	0.001	K7(TMT6plex)	1631.85	2	Yes	No	0.000	0.000			
TTPTFFPKDILTLR	1	0.003	K8(TMT6plex)	1879.09	1	Yes	No	0.000	0.000			

	ITLWNR	1	0.007	802.46	0	Yes	No	0.000	0.000		
<b>P41250</b>	<b>Glycine-tRNA ligase</b>	<b>5</b>	VLEAKELALQPKDDIVDR	8	0	K5(TMT6plex); K12(TMT6plex)	2	Yes	Yes	0.000	0.000
			YPLFEGQETGKKEETIE	3	0	K11(TMT6plex); K12(TMT6plex)	2	Yes	Yes	3.605	5.923
			HGVSHKVDSSGSIQR	3	0	K6(TMT6plex)	1	Yes	Yes	20.925	11.380
			IYLYLTKVGISPKLR	4	0	K7(TMT6plex); K14(TMT6plex)	2	Yes	No	0.000	0.000
			AKMEDTLKR	1	0.002	K2(TMT6plex); M3(Oxidation); K8(TMT6plex)	2	Yes	No	0.000	0.000
<b>P49841</b>	<b>Glycogen synthase kinase-3 beta</b>	<b>2</b>	KLDHCNIVR	3	0	K1(TMT6plex); C5(Carbamidomethyl)	1	Yes	Yes	0.000	0.000
			IQAAASTPTNATAASDANT GDR	1	0		0	Yes	No	0.000	0.000
			LLEYPTAR	1	0.001		0	Yes	No	0.000	0.000
			LSKELDLVSHHVR	7	0	K3(TMT6plex)	1	Yes	No	0.000	0.000
<b>P80303</b>	<b>Nucleobindin-2</b>	<b>3</b>	EKLQKADIEEIKSQR	4	0	K2(TMT6plex); K5(TMT6plex); K12(TMT6plex)	3	Yes	No	0.000	0.000
			EYLKTLNEEKR	6	0	K4(TMT6plex); K10(TMT6plex)	2	Yes	Yes	7.573	3.508
			EYLEKQPVLSTEAR	46	0	K5(TMT6plex)	1	Yes	Yes	28.317	29.230
<b>P28070</b>	<b>Proteasome subunit beta type-4</b>	<b>2</b>	AHSWLTR	5	0		0	Yes	No	0.000	0.000
			RPVDITPLEQR	5	0		0	Yes	No	0.000	0.000
<b>Q9GZT6</b>	<b>Coiled-coil domain-containing protein 90B, mitochondrial</b>	<b>2</b>	ADNKLDINLER	3	0	K4(TMT6plex)	1	Yes	Yes	5.775	3.205
			LQGGVLVNEILNHMKR	2	0	K15(TMT6plex)	1	Yes	No	0.000	0.000
<b>P15309</b>	<b>Prostatic acid phosphatase</b>	<b>2</b>	FQLESETLKSEEFQKR	12	0	K10(TMT6plex); K16(TMT6plex)	2	Yes	Yes	25.119	13.258
			LAIKLIKEIGEPR	6	0	K4(TMT6plex);	2	Yes	No	0.000	0.000
<b>Q96M32</b>	<b>Adenylyate</b>	<b>4</b>									

<b>P36776</b>	<b>kinase 7</b>			NYGLTDEEKAEER	4	0	K8(TMT6plex)	1911.92	1	Yes	Yes	9.546	7.516
				ENAYLTKDLTQDCLDHLVV NLR	1	0	K7(TMT6plex); C13(Carbamidomethyl)	2873.50	1	Yes	No	0.000	0.000
				WEEWNKR	2	0.001	K6(TMT6plex)	1276.67	1	Yes	No	0.000	0.000
				GSTQGKILCFYGGPPGVGKT SIAR	2	0	K6(TMT6plex); C9(Carbamidomethyl); K18(TMT6plex)	2852.59	2	Yes	No	0.000	0.000
<b>P36957</b>	<b>Lon protease homolog, mitochondrial</b>	<b>6</b>		LAQPYVGVFLKR	1	0	K11(TMT6plex)	1619.99	1	Yes	No	0.000	0.000
				DIIALNPLYR	1	0		1187.68	0	Yes	No	0.000	0.000
				NLQKQVEKVLK	4	0.001	K4(TMT6plex); K8(TMT6plex)	1813.15	2	Yes	Yes	6.903	7.201
				GKKEAEDELSAR	1	0.002	K2(TMT6plex); K3(TMT6plex)	1791.00	2	Yes	Yes	0.000	0.000
				YLVPOAR	1	0.003		846.48	0	Yes	No	0.000	0.000
				KIKAAVEDPR	2	0	K1(TMT6plex); K3(TMT6plex)	1584.99	2	Yes	Yes	0.000	0.000
<b>Q8NBU5</b>	<b>Dihydrolipoyl lysine-residue succinyltransferase component of 2-oxoglutarate dehydrogenase complex, mitochondrial</b>	<b>4</b>		TITELGEKAR	2	0	K8(TMT6plex)	1346.78	1	Yes	Yes	0.000	0.000
				GLVVPVIR	2	0.002		852.57	0	Yes	No	0.000	0.000
				EAVTFLR	1	0.004		835.47	0	Yes	No	0.000	0.000
				EAILKILKLNENVDR	3	0	K5(TMT6plex); K9(TMT6plex)	2226.36	2	Yes	No	0.000	0.000
				FHINQPALKQR	5	0	K9(TMT6plex)	1580.92	1	Yes	Yes	16.769	15.431
<b>Q13642</b>	<b>ATPase family AAA domain-containing protein 1</b>	<b>2</b>		KPIGADSKVHYKNR	9	0	K1(TMT6plex); K8(TMT6plex); K13(TMT6plex)	2429.43	2	Yes	Yes	8.590	12.327
				FVHDTCFR	2	0	C6(Carbamidomethyl)	1168.50	0	Yes	No	0.000	0.000
<b>P20933</b>	<b>Four and a half LIM domains protein 1</b>	<b>3</b>		IKNAIGVAR	5	0	K2(TMT6plex)	1170.75	1	Yes	Yes	0.000	0.000





		M9(Oxidation)										
Q15172	Serine/threonine-protein phosphatase 2A 56 kDa regulatory subunit alpha isoform	1	DFLKTVLHR	1	0	K4(TMT6plex)	1357.82	1	Yes	Yes	0.000	0.000
			IYKFLGLR	3	0.001	K4(TMT6plex)	1295.81	1	Yes	No	0.000	0.000
			KELER	1	0.005	K1(TMT6plex)	903.56	1	No	No	0.000	0.000
Q8NA82	Probable E3 ubiquitin-protein ligase MARCH10	3	QKFFSDVQYLR	6	0	K2(TMT6plex)	1659.91	1	Yes	Yes	7.338	10.710
			DMQHKVDSEYQAQLR	3	0	M2(Oxidation); K5(TMT6plex); C13(Carbamidomethyl)	2125.00	1	Yes	Yes	0.000	0.000
			DQFWGQETSEFR	1	0		1529.67	0	Yes	No	0.000	0.000
P55060	Exportin-2	4	IVEDEPNKICEADR	5	0	K8(TMT6plex); C10(Carbamidomethyl)	1916.96	1	Yes	Yes	31.668	13.290
			LLQAFLEK	2	0		989.58	0	Yes	No	0.000	0.000
			KQIFILLFQR	1	0	K1(TMT6plex)	1534.97	1	Yes	No	0.000	0.000
			TAHSLFKR	3	0.002	K7(TMT6plex)	1188.71	1	Yes	Yes	0.000	0.000

**Supplementary Table S3 – Quantification values (means  $\pm$  standard deviation; Mean  $\pm$  SD) of each differential protein detected in Asthenozoospermic (Asthen) vs Normozoospermic (Normo) samples experiment, and associated P value.**

All the proteins shown in this table were statistically different (p-value<0.05).

UniprotKB/ Swiss-Prot accession number	Protein name	Asthen	Normo	P value
		samples Mean $\pm$ SD	samples Mean $\pm$ SD	
Q9P2T0	Testicular haploid expressed gene protein	0.701 $\pm$ 0.175	1.305 $\pm$ 0.202	0.001
Q13642	Four and a half LIM domains protein 1	0.648 $\pm$ 0.244	1.129 $\pm$ 0.243	0.014
O95831	Apoptosis-inducing factor 1, mitochondrial	0.790 $\pm$ 0.308	1.242 $\pm$ 0.083	0.013
Q6UWQ5	Lysozyme-like protein 1	0.792 $\pm$ 0.210	1.207 $\pm$ 0.315	0.040
P55060	Exportin-2	0.764 $\pm$ 0.196	1.140 $\pm$ 0.300	0.047
Q96M32	Adenylate kinase 7	0.852 $\pm$ 0.353	1.267 $\pm$ 0.085	0.034
P10253	Lysosomal alpha-glucosidase	0.805 $\pm$ 0.238	1.187 $\pm$ 0.176	0.020
Q92526	T-complex protein 1 subunit zeta-2	0.818 $\pm$ 0.199	1.189 $\pm$ 0.250	0.032
P48047	ATP synthase subunit O, mitochondrial	0.843 $\pm$ 0.258	1.213 $\pm$ 0.206	0.036
Q3ZCQ8	Mitochondrial import inner membrane translocase subunit TIM50	0.750 $\pm$ 0.226	1.067 $\pm$ 0.093	0.020
Q96KX0	Lysozyme-like protein 4	0.793 $\pm$ 0.256	1.125 $\pm$ 0.071	0.042
Q99798	Aconitate hydratase, mitochondrial	0.854 $\pm$ 0.265	1.200 $\pm$ 0.127	0.040
P55786	Puromycin-sensitive aminopeptidase	0.829 $\pm$ 0.201	1.153 $\pm$ 0.115	0.014
Q9H4K1	RIB43A-like with coiled-coils protein 2	0.856 $\pm$ 0.251	1.180 $\pm$ 0.179	0.047
Q15172	Serine/threonine-protein phosphatase 2A 56 kDa regulatory subunit alpha isoform	0.864 $\pm$ 0.096	1.190 $\pm$ 0.206	0.012
Q9NR28	Diablo homolog, mitochondrial	0.781 $\pm$ 0.132	1.069 $\pm$ 0.183	0.021
P13667	Protein disulfide-isomerase A4	0.826 $\pm$ 0.121	1.116 $\pm$ 0.159	0.012
Q8N7U6	EF-hand domain-containing family member B	0.864 $\pm$ 0.214	1.166 $\pm$ 0.059	0.016
P36776	Lon protease homolog, mitochondrial	0.872 $\pm$ 0.242	1.173 $\pm$ 0.136	0.041
P06744	Glucose-6-phosphate isomerase	0.856 $\pm$ 0.170	1.150 $\pm$ 0.092	0.009
P06576	ATP synthase subunit beta, mitochondrial	0.856 $\pm$ 0.256	1.144 $\pm$ 0.101	0.048
Q96M91	Coiled-coil domain-containing protein 11	0.856 $\pm$ 0.112	1.143 $\pm$ 0.137	0.007
Q96MR6	WD repeat-containing protein 65	0.862 $\pm$ 0.143	1.140 $\pm$ 0.079	0.005
P10515	Dihydrolipoyllysine-residue acetyltransferase component of pyruvate dehydrogenase complex, mitochondrial	0.875 $\pm$ 0.211	1.154 $\pm$ 0.114	0.032
Q5T655	Coiled-coil domain-containing protein 147	0.839 $\pm$ 0.179	1.089 $\pm$ 0.102	0.026
P36957	Dihydrolipoyllysine-residue succinyltransferase component of 2-oxoglutarate dehydrogenase complex, mitochondrial	0.896 $\pm$ 0.192	1.151 $\pm$ 0.091	0.027

O75190	DnaI homolog subfamily B member 6	0.856±0.133	1.089±0.153	0.033
Q5JVL4	EF-hand domain-containing protein 1	0.909±0.197	1.152±0.094	0.038
P49841	Glycogen synthase kinase-3 beta	0.831±0.169	1.050±0.079	0.030
Q86VP6	Cullin-associated NEDD8-dissociated protein 1	0.895±0.168	1.131±0.095	0.026
Q4G0X9	Coiled-coil domain-containing protein 40	0.900±0.210	1.137±0.064	0.042
Q9BRQ6	Coiled-coil-helix-coiled-coil-helix domain-containing protein 6, mitochondrial	0.883±0.153	1.115±0.160	0.047
Q86Y39	NADH dehydrogenase [ubiquinone] 1 alpha subcomplex subunit 11	0.891±0.086	1.123±0.114	0.007
P40939	Trifunctional enzyme subunit alpha, mitochondrial	0.893±0.144	1.122±0.147	0.038
P41250	Glycine--tRNA ligase	0.978±0.171	1.227±0.089	0.020
P14314	Glucosidase 2 subunit beta	0.854±0.111	1.068±0.066	0.006
Q969V4	Tektin-1	0.986±0.166	1.215±0.089	0.026
Q14697	Neutral alpha-glucosidase AB	0.908±0.123	1.105±0.140	0.046
Q6BCY4	NADH-cytochrome b5 reductase 2	0.927±0.101	1.125±0.138	0.032
P46459	Vesicle-fusing ATPase	0.912±0.107	1.089±0.091	0.022
P11177	Pyruvate dehydrogenase E1 component subunit beta, mitochondrial	0.882±0.108	1.043±0.111	0.049
Q14203	Dynactin subunit 1	0.934±0.036	1.104±0.097	0.014
Q93009	Ubiquitin carboxyl-terminal hydrolase 7	0.901±0.049	1.065±0.134	0.034
Q9NSE4	Isoleucine--tRNA ligase, mitochondrial	0.907±0.080	1.071±0.089	0.016
Q9Y371	Endophilin-B1	0.902±0.085	1.062±0.078	0.014
O00330	Pyruvate dehydrogenase protein X component, mitochondrial	0.950±0.118	1.108±0.030	0.039
Q8N1V2	WD repeat-containing protein 16	0.999±0.109	1.157±0.093	0.039
P22234	Multifunctional protein ADE2	0.932±0.086	1.074±0.080	0.027
Q15631	Translin	0.956±0.045	1.081±0.048	0.003
Q96M29	Tektin-5	0.963±0.076	1.080±0.050	0.020
P29218	Inositol monophosphatase 1	1.080±0.058	0.976±0.038	0.010
Q9GZT6	Coiled-coil domain-containing protein 90B, mitochondrial	1.074±0.117	0.932±0.055	0.040
P67870	Casein kinase II subunit beta	1.131±0.161	0.943±0.082	0.048
P10606	Cytochrome c oxidase subunit 5B, mitochondrial	1.134±0.154	0.942±0.095	0.045
Q96DE0	U8 snoRNA-decapping enzyme	1.005±0.064	0.830±0.101	0.011
P54652	Heat shock-related 70 kDa protein 2	1.091±0.162	0.895±0.079	0.041
P80303	Nucleobindin-2	1.030±0.137	0.841±0.072	0.026
P20933	N(4)-(beta-N-acetylglucosaminy)-L-asparaginase	1.134±0.161	0.907±0.112	0.033
P57105	Synaptojanin-2-binding protein	1.118±0.100	0.875±0.093	0.004

P30041	Peroxiredoxin-6	1.114±0.252	0.838±0.070	0.046
P60174	Triosephosphate isomerase	1.186±0.196	0.890±0.100	0.024
Q8N0U8	Vitamin K epoxide reductase complex subunit 1-like protein 1	1.130±0.184	0.841±0.154	0.027
Q8NA82	Probable E3 ubiquitin-protein ligase MARCH10	1.084±0.190	0.800±0.147	0.030
Q8NBU5	ATPase family AAA domain-containing protein 1	1.216±0.179	0.875±0.146	0.011
P28070	Proteasome subunit beta type-4	1.161±0.275	0.831±0.086	0.034
Q96AJ9	Vesicle transport through interaction with t-SNAREs homolog 1A	1.217±0.222	0.859±0.226	0.035
Q9H4Y5	Glutathione S-transferase omega-2	1.184±0.267	0.817±0.072	0.035
Q8IZS6	Tctex1 domain-containing protein 3	1.037±0.282	0.700±0.145	0.045
Q6UW68	Transmembrane protein 205 OS=Homo sapiens	1.097±0.238	0.733±0.225	0.038
P01034	Cystatin-C	1.263±0.365	0.844±0.059	0.035
P60981	Destrin	1.127±0.321	0.751±0.167	0.049
P24666	Low molecular weight phosphotyrosine protein phosphatase	1.330±0.178	0.882±0.216	0.007
Q9P0L0	Vesicle-associated membrane protein-associated protein A	1.213±0.215	0.801±0.068	0.010
O43674	NADH dehydrogenase [ubiquinone] 1 beta subcomplex subunit 5, mitochondrial	1.200±0.350	0.766±0.116	0.048
P26885	Peptidyl-prolyl cis-trans isomerase FKBP2	1.220±0.247	0.760±0.217	0.014
Q8WY22	BRI3-binding protein	1.195±0.231	0.726±0.297	0.024
P32119	Peroxiredoxin-2	1.325±0.550	0.706±0.138	0.041
P02649	Apolipoprotein E	1.583±0.497	0.833±0.285	0.019
P61088	Ubiquitin-conjugating enzyme E2 N	1.346±0.374	0.696±0.056	0.017
P15309	Prostatic acid phosphatase	1.576±0.793	0.633±0.382	0.043

**Supplementary Table S4 – Compiled list of proteins (185) differentially expressed in asthenozoospermic samples compared to normozoospermic samples.**

This list was obtained compiling our proteomic results with the results of other groups that perform comparative proteomics using asthenozoospermic vs normozoospermic samples (Zhao *et al.*, 2007; Martínez-Heredia *et al.*, 2008; Chan *et al.*, 2009; Siva *et al.*, 2010; Parte *et al.*, 2012)

UniProtKB/ Swiss-Prot accession number	Description	Reference
<b>SPERMATOGENESIS/ SPERM MATURATION/ SEMINAL PLASMA/ SPERM-OOCYTE INTERACTION</b>		
Q9P2T0	Testicular haploid expressed gene protein	Present study
Q6UWQ5	Lysozyme-like protein 1	Present study
Q92526	T-complex protein 1 subunit zeta-2	Present study
Q96KX0	Lysozyme-like protein 4	Present study
Q8IZS6	Tctex1 domain-containing protein 3	Present study
P54652	Heat shock-related 70 kDa protein 2	Present study; Martínez-Heredia <i>et al.</i> , 2008; Siva <i>et al.</i> , 2010; Parte <i>et al.</i> , 2012
Q9Y4C1	Lysine-specific demethylase 3A	Chan <i>et al.</i> , 2009
Q9Y265	RuvB-like 1	Chan <i>et al.</i> , 2009
Q9BXU0	Testis-expressed sequence 12 protein	Martínez-Heredia <i>et al.</i> , 2008
Q6S8J3	POTE ankyrin domain family member E	Parte <i>et al.</i> , 2012
P04279	Semenogelin-1	Zhao <i>et al.</i> , 2007; Martínez-Heredia <i>et al.</i> , 2008
P15309	Prostatic acid phosphatase	Present study; Parte <i>et al.</i> , 2012
P07288	Prostate specific antigen	Parte <i>et al.</i> , 2012
Q9NS25	Sperm protein associated with the nucleus on the X chromosome B F	Parte <i>et al.</i> , 2012
P36969	Phospholipid hydroperoxide glutathione peroxidase mitochondrial	Parte <i>et al.</i> , 2012
Q5JQC9	A kinase anchor protein 4	Parte <i>et al.</i> , 2012
P26436	Acrosomal protein SP 10	Parte <i>et al.</i> , 2012
Q8NEB7	Acrosin binding protein	Parte <i>et al.</i> , 2012
Q96BH3	Epididymal sperm binding protein 1	Chan <i>et al.</i> , 2009; Parte <i>et al.</i> , 2012
P09622	Dihydrolipoyl dehydrogenase, mitochondrial	Martínez-Heredia <i>et al.</i> , 2008
O75969	A kinase anchor protein 3	Parte <i>et al.</i> , 2012
<b>SPERM TAIL STRUCTURE AND MOTILITY</b>		
Q96M32	Adenylate kinase 7	Present study
Q4G0X9	Coiled-coil domain-containing protein 40	Present study
Q969V4	Tektin-1	Present study; Siva <i>et al.</i> , 2010
Q96M29	Tektin-5	Present study
P60981	Destrin	Present study
Q9BZX4	Ropporin 1B	Parte <i>et al.</i> , 2012
Q14990	Outer dense fiber protein 1	Parte <i>et al.</i> , 2012
P60709	Actin, cytoplasmic 1	Martínez-Heredia <i>et al.</i> , 2008; Parte <i>et al.</i> , 2012
Q562R1	Beta actin like protein 2	Parte <i>et al.</i> , 2012
P63267	Actin gamma enteric smooth muscle	Parte <i>et al.</i> , 2012
P68133	Actin alpha skeletal muscle	Parte <i>et al.</i> , 2012

P68032	Actin alpha cardiac muscle 1	Parte et al., 2012
P19105	Myosin regulatory light chain 12A	Parte et al., 2012
P63167	Dynein light chain 1 cytoplasmic	Parte et al., 2012
P13645	Keratin, type I cytoskeletal 10	Parte et al., 2012
P35527	Keratin type I cytoskeletal 9	Parte et al., 2012
P35908	Keratin, type II cytoskeletal 2 epidermal	Chan et al., 2009
P04264	Keratin type II cytoskeletal 1	Parte et al., 2012
P04264	Keratin, type II cytoskeletal 1	Chan et al., 2009
Q9BSJ2	Gamma-tubulin complex component 2	Chan et al., 2009
P68371	Tubulin beta-4B chain	Siva et al., 2010
P04350	Tubulin beta 4 chain	Parte et al., 2012
Q6PEY2	Tubulin alpha 3E chain	Parte et al., 2012
A6NKZ8	Putative tubulin beta chain like protein	Parte et al., 2012
Q3ZCM7	Tubulin beta 8 chain	Parte et al., 2012
Q13509	Tubulin beta 3 chain	Parte et al., 2012
P07437	Tubulin beta chain	Parte et al., 2012
P68366	Tubulin alpha 4A	Parte et al., 2012
Q9BUF5	Tubulin beta 6 chain	Parte et al., 2012
Q9NY65	Tubulin alpha 8 chain	Parte et al., 2012
Q13748	Tubulin alpha 3C D chain TUBA3C	Parte et al., 2012
P68363	Tubulin alpha 1B chain	Parte et al., 2012
P68371	Tubulin beta 2C chain TUBB2C	Parte et al., 2012
<b>INTRACELLULAR TRAFFICKING</b>		
P55060	Exportin-2	Present study
P46459	Vesicle-fusing ATPase	Present study
Q14203	Dynactin subunit 1	Present study
Q96AJ9	Vesicle transport through interaction with t-SNAREs homolog 1A	Present study
Q9P0L0	Vesicle-associated membrane protein-associated protein A	Present study
<b>METABOLISM AND ENERGY PRODUCTION</b>		
P10253	Lysosomal alpha-glucosidase	Present study
P48047	ATP synthase subunit O, mitochondrial	Present study
Q99798	Aconitate hydratase, mitochondrial	Present study
P06744	Glucose-6-phosphate isomerase	Present study
P06576	ATP synthase subunit beta, mitochondrial	Present study
P10515	Dihydrolipoyllysine-residue acetyltransferase component of pyruvate dehydrogenase complex, mitochondrial	Present study
P36957	Dihydrolipoyllysine-residue succinyltransferase component of 2-oxoglutarate dehydrogenase complex, mitochondrial	Present study
Q86Y39	NADH dehydrogenase [ubiquinone] 1 alpha subcomplex subunit 11	Present study
P40939	Trifunctional enzyme subunit alpha, mitochondrial	Present study
P14314	Glucosidase 2 subunit beta	Present study
Q6BCY4	NADH-cytochrome b5 reductase 2	Present study

<b>P11177</b>	Pyruvate dehydrogenase E1 component subunit beta, mitochondrial	Present study
<b>O00330</b>	Pyruvate dehydrogenase protein X component, mitochondrial	Present study
<b>P22234</b>	Multifunctional protein ADE2	Present study
<b>P10606</b>	Cytochrome c oxidase subunit 5B, mitochondrial	Present study
<b>P30041</b>	Peroxiredoxin-6	Present study
<b>P60174</b>	Triosephosphate isomerase	Present study; Zhao et al., 2007; Siva et al., 2010; Parte et al., 2012
<b>Q9H4Y5</b>	Glutathione S-transferase omega-2	Present study
<b>O43674</b>	NADH dehydrogenase [ubiquinone] 1 beta subcomplex subunit 5, mitochondrial	Present study
<b>P32119</b>	Peroxiredoxin-2	Present study
<b>P02649</b>	Apolipoprotein E	Present study
<b>P17174</b>	Aspartate aminotransferase, cytoplasmic	Zhao et al., 2007
<b>P15104</b>	Glutamine synthetase	Zhao et al., 2007
<b>P01275</b>	Glucagon	Chan et al., 2009
<b>P21266</b>	Glutathione S transferase Mu 3	Parte et al., 2012
<b>P21266</b>	Glutathione S-transferase Mu 3	Chan et al., 2009
<b>Q14410</b>	Glycerol kinase 2	Siva et al., 2010
<b>Q13011</b>	Delta(3,5)-Delta(2,4)-dienoyl-CoA isomerase, mitochondrial	Martínez-Heredia et al., 2008
<b>P55809</b>	Succinyl-CoA:3-ketoacid coenzyme A transferase 1, mitochondrial	Siva et al., 2010
<b>P15259</b>	Phosphoglycerate mutase 2	Zhao et al., 2007
<b>Q00796</b>	Sorbitol dehydrogenase	Parte et al., 2012
<b>O14556</b>	Glyceraldehyde 3 phosphate dehydrogenase testis specific	Parte et al., 2012
<b>P04075</b>	Fructose biphosphate aldolase A	Parte et al., 2012
<b>P50213</b>	Isocitrate dehydrogenase [NAD] subunit alpha, mitochondrial	Zhao et al., 2007
<b>P07954</b>	Fumarate hydratase, mitochondrial	Martínez-Heredia et al., 2008
<b>Q7L1R4</b>	Cytochrome c oxidase subunit 6B2	Martínez-Heredia et al., 2008
<b>P06576</b>	ATP synthase subunit beta mitochondrial	Parte et al., 2012
<b>P12277</b>	Creatine kinase B type	Parte et al., 2012
<b>Q8N8V2</b>	Guanylate-binding protein7	Chan et al., 2009
<b>P14555</b>	Phospholipase A2 membrane associated	Parte et al., 2012
<b>P25325</b>	3-mercaptopyruvate sulfurtransferase	Martínez-Heredia et al., 2008
<b>MITOCHONDRIAL MAINTENANCE</b>		
<b>Q3ZCQ8</b>	Mitochondrial import inner membrane translocase subunit TIM50	Present study
<b>P36776</b>	Lon protease homolog, mitochondrial	Present study
<b>Q9BRQ6</b>	Coiled-coil-helix-coiled-coil-helix domain-containing protein 6, mitochondrial	Present study
<b>Q9NSE4</b>	Isoleucine--tRNA ligase, mitochondrial	Present study
<b>PROTEIN METABOLISM</b>		
<b>P55786</b>	Puromycin-sensitive aminopeptidase	Present study
<b>P13667</b>	Protein disulfide-isomerase A4	Present study
<b>O75190</b>	DnaJ homolog subfamily B member 6	Present study

<b>Q86VP6</b>	Cullin-associated NEDD8-dissociated protein 1	Present study
<b>P41250</b>	Glycine--tRNA ligase	Present study
<b>Q14697</b>	Neutral alpha-glucosidase AB	Present study
<b>P20933</b>	N(4)-(beta-N-acetylglucosaminy)-L-asparaginase	Present study
<b>Q8NA82</b>	Probable E3 ubiquitin-protein ligase MARCH10	Present study
<b>P28070</b>	Proteasome subunit beta type-4	Present study
<b>P24666</b>	Low molecular weight phosphotyrosine protein phosphatase	Present study
<b>P26885</b>	Peptidyl-prolyl cis-trans isomerase FKBP2	Present study
<b>P61088</b>	Ubiquitin-conjugating enzyme E2 N	Present study
<b>P10909</b>	Clusterin	Martínez-Heredia et al., 2008; Parte et al., 2012
<b>P34931</b>	Heat shock 70 kDa protein 1 like	Parte et al., 2012
<b>P62988</b>	Ubiquitin	Parte et al., 2012
<b>P50502</b>	Hsc70 interacting protein	Parte et al., 2012
<b>P17066</b>	Heat shock 70 kDa protein 6	Parte et al., 2012
<b>P08107</b>	Heat shock 70 kDa protein 1A	Parte et al., 2012
<b>Q58FF7</b>	Putative heat shock protein HSP 90 beta 3	Parte et al., 2012
<b>Q58FF6</b>	Putative heat shock protein HSP 90 beta 4	Parte et al., 2012
<b>P14625</b>	Endoplasmic	Parte et al., 2012
<b>Q14568</b>	Putative heat shock protein HSP 90 alpha A2	Parte et al., 2012
<b>Q58FF8</b>	Putative heat shock protein HSP 90 beta 2	Parte et al., 2012
<b>P04792</b>	Heat shock protein beta 1	Parte et al., 2012
<b>P07900</b>	Heat shock protein HSP 90 alpha	Parte et al., 2012
<b>P08238</b>	Heat shock protein HSP 90 beta	Parte et al., 2012
<b>P11021</b>	78 kDa glucose regulated protein	Parte et al., 2012
<b>Q8TAT6</b>	Nuclear protein localization protein 4 homolog	Chan et al., 2009
<b>P35998</b>	26S protease regulatory subunit 7	Zhao et al., 2007
<b>P49720</b>	Proteasome subunit beta type-3	Martínez-Heredia et al., 2008
<b>P25788</b>	Proteasome subunit alpha type-3	Siva et al., 2010
<b>P05387</b>	60S acidic ribosomal protein P2	Parte et al., 2012
<b>P68104</b>	Elongation factor 1 alpha 1	Parte et al., 2012
<b>Q5VTE0</b>	Putative elongation factor 1 alpha like 3	Parte et al., 2012
<b>Q05639</b>	Elongation factor 1 alpha 2	Parte et al., 2012
<b>P26641</b>	Elongation factor 1 gamma	Parte et al., 2012
<b>Q8WUD1</b>	Ras related protein Rab 2B	Parte et al., 2012
<b>P61019</b>	Ras related protein Rab 2A	Parte et al., 2012
<b>SIGNALLING</b>		
<b>Q15172</b>	Serine/threonine-protein phosphatase 2A 56 kDa regulatory subunit alpha isoform	Present study
<b>Q5JVL4</b>	EF-hand domain-containing protein 1	Present study
<b>P49841</b>	Glycogen synthase kinase-3 beta	Present study
<b>P29218</b>	Inositol monophosphatase 1	Present study; Martínez-Heredia et al., 2008
<b>P67870</b>	Casein kinase II subunit beta	Present study
<b>P57105</b>	Synaptojanin-2-binding protein	Present study
<b>P63104</b>	14 3 3 protein zeta delta	Parte et al., 2012
<b>P52565</b>	Rho GDP dissociation inhibitor 1	Parte et al., 2012



---

**OTHER / UNKNOWN**

---

<b>Q13642</b>	Four and a half LIM domains protein 1	Present study
<b>O95831</b>	Apoptosis-inducing factor 1, mitochondrial	Present study
<b>Q9H4K1</b>	RIB43A-like with coiled-coils protein 2	Present study
<b>Q9NR28</b>	Diablo homolog, mitochondrial	Present study
<b>Q8N7U6</b>	EF-hand domain-containing family member B	Present study
<b>Q96M91</b>	Coiled-coil domain-containing protein 11	Present study
<b>Q96MR6</b>	WD repeat-containing protein 65	Present study
<b>Q5T655</b>	Coiled-coil domain-containing protein 147	Present study
<b>Q93009</b>	Ubiquitin carboxyl-terminal hydrolase 7	Present study
<b>Q9Y371</b>	Endophilin-B1	Present study
<b>Q8N1V2</b>	WD repeat-containing protein 16	Present study
<b>Q15631</b>	Translin	Present study
<b>Q9GZT6</b>	Coiled-coil domain-containing protein 90B, mitochondrial	Present study
<b>Q96DE0</b>	U8 snoRNA-decapping enzyme	Present study
<b>P80303</b>	Nucleobindin-2	Present study
<b>Q8N0U8</b>	Vitamin K epoxide reductase complex subunit 1- like protein 1	Present study
<b>Q8NBU5</b>	ATPase family AAA domain-containing protein 1	Present study
<b>Q6UW68</b>	Transmembrane protein 205 OS=Homo sapiens	Present study
<b>P01034</b>	Cystatin-C	Present study
<b>Q8WY22</b>	BRI3-binding protein	Present study
<b>P51398</b>	28S ribosomal protein S29, mitochondrial	Chan et al., 2009
<b>P00918</b>	Carbonic anhydrase 2	Zhao et al., 2007
<b>P58304</b>	Visual system homeobox 2	Chan et al., 2009
<b>P06702</b>	Protein S100-A9	Martínez-Heredia et al., 2008
<b>P49913</b>	Cathelicidin antimicrobial peptide	Parte et al., 2012
<b>P02788</b>	Lactotransferrin	Parte et al., 2012
<b>P59665</b>	Neutrophil defensin 1	Parte et al., 2012
<b>P11142</b>	Heat shock cognate 71 kDa protein	Parte et al., 2012
<b>P08758</b>	Annexin A5	Martínez-Heredia et al., 2008
<b>P61769</b>	Beta 2 microglobulin	Parte et al., 2012
<b>Q93077</b>	Histone H2A type 1-C	Martínez-Heredia et al., 2008
<b>Q96A08</b>	Histone H2B type 1 A	Parte et al., 2012
<b>Q96QV6</b>	Histone H2A type 1 A	Parte et al., 2012
<b>P12273</b>	Prolactin-inducible protein	Martínez-Heredia et al., 2008; Parte et al., 2012
<b>A5A3E0</b>	POTE ankyrin domain family member F	Parte et al., 2012

---

